EXPERIMENTAL INVESTIGATION INTO FLOW AROUND ISLAND

A THESIS

Submitted in partial fulfilment of the requirements for the award of the degree of

DOCTOR OF PHILOSOPHY

in

WATER RESOURCES DEVELOPMENT

By

UTPAL KUMAR MISRA

WATER RESOURCES DEVELOPMENT & MANAGEMENT
INDIAN INSTITUTE OF TECHNOLOGY ROORKEE
ROORKEE-247 667 (INDIA)

OCTOBER, 2005

6th Annual Convocation- 2006
Degree conferred on 11.11.2006

Supdt. (PGS&R)

INDIAN INSTITUTE OF TECHNOLOGY ROORKEE

ROORKEE

CANDIDATE'S DECLARATION

I hereby certify that the work which is being presented in the thesis entitled **"EXPERIMENTAL INVESTIGATION INTO FLOW AROUND ISLAND"** in partial fulfilment of the requirement for the award of the Degree of Doctor of Philosophy and submitted in the Department of Water Resources Development and Management, Indian Institute of Technology Roorkee, Roorkee, is an authentic record of my own work carried out during the period from January 2003 to October 2005 under the supervision of **Dr. Nayan Sharma**, Professor, department of Water Resources Development and Management, Indian Institute of Technology Roorkee and **Dr. C. S. P. Ojha**, Professor, Department of Civil Engineering, Indian Institute of Technology Roorkee.

The matter presented in this thesis has not been submitted by me for the award of any other degree of this or any other institute.

(UTPAL KUMAR MISRA)

This to certify that the above statement made by the candidate is correct to the best of our knowledge.

Dr. C. S. P. Ojha
Professor
Deptt. of Civil Engineering

Dr. Nayan Sharma
Professor
Water Resources Development and Management

Indian Institute of Technology Roorkee

Dated: October 13 , 2005

The Ph.D. Viva-Voce examination of **Utpal Kumar Misra**, Research Scholar, has been held on 5.6.2006

Signature of Supervisor(s)

Signature of External Examiner

ABSTRACT

Due to severe stream-induced erosion of the banks, large-sized islands like Majuli in the river Brahmaputra in the province of Assam, are facing imminent extinction. During high floods, these islands are subjected to debilitating erosion process and thus, protection of these islands has received a lot of attention. It has been found that there is lack of extensive study related to flow hydraulics around island. The present investigation basically attempts to fill this gap by undertaking study related to flow characteristics and scour pattern around island. Understanding of scour phenomenon is aimed at evolving flow control devices for protection of island.

In the present study, elaborate experimentations have been conducted to investigate flow division around islands having width to length ratio between 0.15 to 1.0 and placed at different eccentricities, varying from 0% to 40%. 45 experimental runs were carried out under rigid bed flow conditions and 24 experimental runs were carried out under mobile bed flow conditions and the Froude number ranged from 0.105 to 0.2. The relationship developed for flow division around island has been found to work well for both rigid bed and mobile bed flow conditions.

The scour pattern around islands having different width to length ratios has been studied for three Froude numbers, viz, 0.16, 0.19 and 0.2. The maximum scour around island has been found to increase with the increase in width to length ratio of island. The energy based theoretical model developed in the present study has also supported the above finding. The model indicates that islands with lesser value of width to length ratio are less vulnerable to scour.

The parameter moment of momentum per unit flow width (MOM/B) has been introduced to study the variation of strength of secondary current along the island. Based on 17 experimental runs at Froude numbers of 0.14, 0.16 and 0.19, the study has indicated a definite pattern of growth and decay of secondary flow along the island. The parameter MOM/B is generally observed to be more in the central region of the island. The effect of width to length ratio of island on the total MOM per unit length of island has been also investigated.

Based on the laboratory experiments, the usefulness of V-shaped deflector as a device for protection of island has been examined. The optimum location of V-shaped deflector with respect to the island has been also found out for two sizes of the deflector at Froude numbers of 0.16 and 0.19.

The present study has been carried out with the implicit focus on the Brahmaputra river, within which exists one of the largest river island in the world, namely Majuli. In the above backdrop, the experiments have been done for a sediment size of 0.225 mm. From analysis of sediment data of the river Brahmaputra, it has been observed that this sediment size is generally predominant in the reach of river Brahmaputra around Majuli island. The flow in Brahmaputra river is in sub-critical range and thus the work reported herein, is a novel attempt to explore simplified approaches for flow distribution and scour variation around islands, which is apparently non-existent in the literature.

ACKNOWLEDGEMENT

I take this opportunity to record my sincere gratitude and indebtedness to Dr. Nayan Sharma, Professor, Department of Water Resources Development and Management and Dr. C. S. P. Ojha, Professor, Department of Civil Engineering, I. I. T. Roorkee, for their expert guidance, constant encouragement, constructive criticism and very fruitful discussions at various stages of the research work presented in this thesis.

I am highly thankful to all faculty and staff of WRD&M Deptt. specially Prof. D. Das, Prof. S. K. Tripathy and Dr. Deepak Khare for their moral encouragement during this research work.

I am also thankful to Prof. K. G. Ranga Raju of Civil Engineering Deptt, I. I. T. Roorkee for his inspiring words and advise during the initial period of my research work.

The assistance rendered by Sri Beer Singh Chauhan, Sri Ram Dular, Sri Anurag Kumar, Sri Subhash Prasad and Sri Yogendra Sharma during the experimental investigations is thankfully acknowledged. Thanks are also due to all my friends who assisted me in one way or the other at times.

(UTPAL KUMAR MISRA)

CONTENTS

LIST OF TABLES

LIST OF FIGURES

LIST OF PLATES

INTRODUCTION

1.1 GENERAL

Rivers have fascinated humanity for centuries. Most prosperous cities around the world have been founded along rivers. But, rivers in alluvial plains are highly variable in their behaviour, due to which considerable damage occurs to the river banks as well as to the islands situated in the river, which in turn damages the property and human life. As an example, Majuli, the world's largest river island in the Brahmaputra river is facing gradual loss of land area due to severe bank erosion (Fig. 1.1 and Plate 1.1). This has posed an increasing threat to the island and the rich natural and cultural heritage it represents. This has very adversely affected the bio-diversity of the island, flora and fauna, socio cultural fabric and the demographic pattern of the population.

With time, large river islands like Majuli on the Brahmaputra have come to be used as habitat for sizeable population settlement. During floods, these islands are prone to erosion and thus, protection of these islands has received a lot of attention in the state of Assam, India. As the shape configuration of island can play an important role, it is necessary to understand the magnitude and the extent of scour around islands of varying shapes. Understanding of scour phenomenon can also provide insight into protection of these islands.

Thus, there is an imperative need to undertake research to investigate flow distribution and scour pattern around island to evolve appropriate device for protection

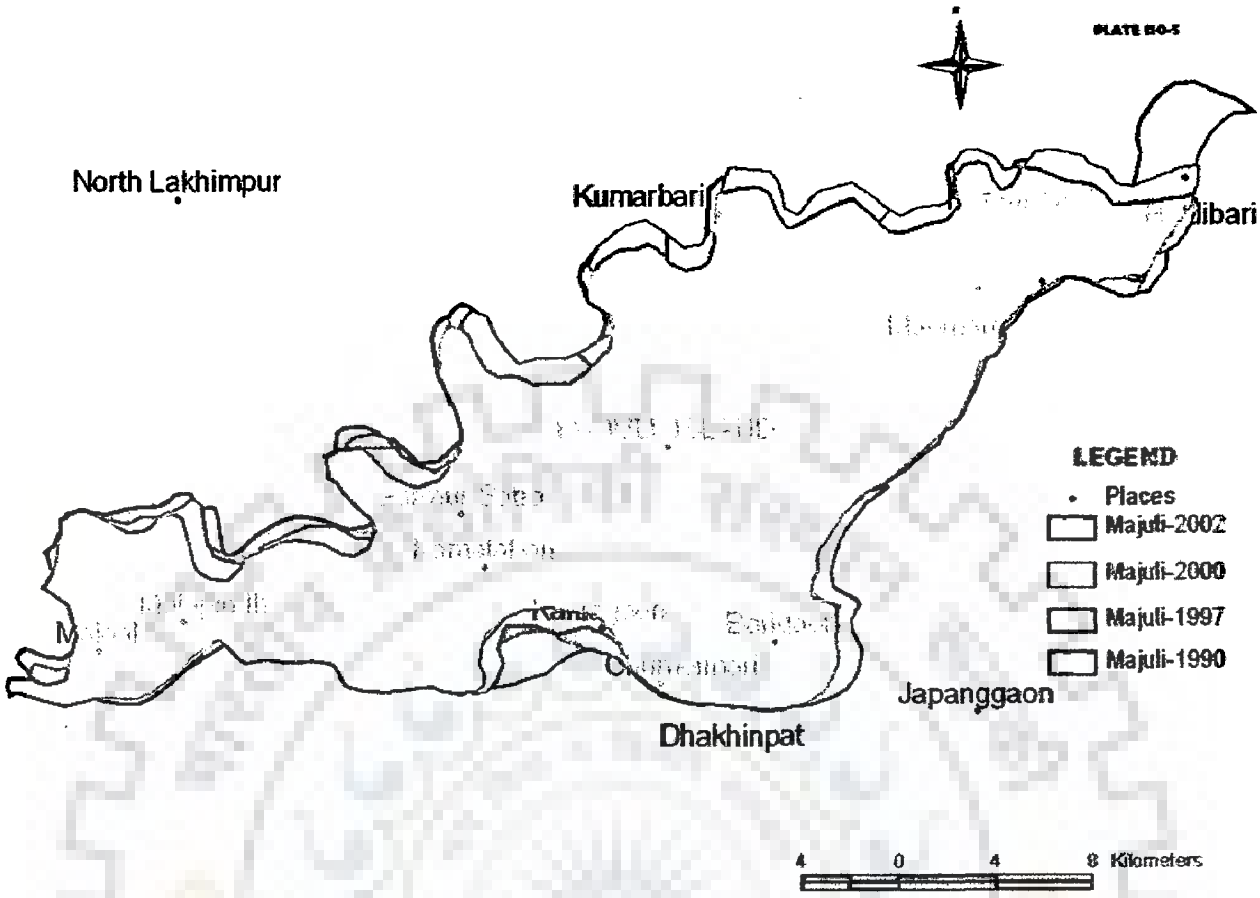

Fig. 1.1 Loss of land areas of Majuli island in different period of years

Plate 1.1 Erosion of bank near Kaniagaon situated in Majuli island

of island against erosion. From literature, it can be observed that there is lack of extensive study related to flow around island. With this in view, the following objectives have been set for the present research.

1.2 OBJECTIVES OF THE STUDY

(1) To perform experimental runs with elliptical model islands of different width to length ratio under rigid bed flow conditions and at different eccentricities.

(2) To develop simple approaches to quantify distribution of flow around islands and to evaluate the performance of such relationship against independent data.

(3) To investigate the scour pattern around islands of varying shape and under different flow conditions and to identify the condition when island is subjected to lesser scour.

(4) To study if there is any correlation between the energy expenditure across the island and its proneness to scour.

(5) To study the variation of strength of secondary current in terms of moment of momentum along the flow direction in the study domain around the island and to investigate how the growth of secondary flow affects the scour around island.

(6) To study the performance of certain deflectors as an alternative method for overall protection of island and to find the optimum location of such deflectors with respect to the island.

1.3 ORGANISATION OF THE THESIS

To meet the above objectives, the present study is organised as follows:

Chapter 1: It describes the introductory aspects of the topic of investigation, underlying objectives and the layout of the thesis.

Chapter 2: The literature review relevant to the topic is presented here.

Chapter 3: It provides the details of experimental programme for the present study.

Chapter 4: It presents a simple approach for determination of division of flow around islands with varying width to length ratios and placed at different eccentricities.

Chapter 5: It presents the pattern of scour and deposition around islands of different width to length ratio. It also includes the analysis of data to identify the width to length ratio of island for which the scour around island is minimum. The inter-relationship between energy expenditure and the scour is also explored.

Chapter 6: It includes the study related to the variation of strength of secondary current in the flow direction around island. Also the link between the strength of secondary current and the scour around island is explored in this chapter.

Chapter 7: It presents the role of V-shaped deflector for the protection of island. It also includes the optimization of location of deflector with respect to the island.

Chapter 8: It summarizes the result of present investigation and outlines the main findings and provides scope for future study.

REVIEW OF LITERATURE

2.1 GENERAL

Alluvial islands are important features in a braided stream. Although it is difficult to assess when a bar becomes an island, islands are different from bars in that they are stabilized by vegetation. The present chapter is devoted to the review of the relevant works as reported in the literature in the context of processes responsible for formation of island in alluvial stream. Additionally, the literature is reviewed regarding the formation of secondary flow structure in braided channels as well as around braid bar or island. Lastly, a brief discussion has been made covering scour around island and protection of island.

2.2 RIVERBED AGGRADATION AND FORMATION OF ISLAND

Channel aggradation refers to gradual stream bed-elevation increase that is due to bedload sedimentation. The formation of island can be best understood from Fig. 2.1. There is a tendency for the stream to widen and become very shallow with bars subjected to rapid changes in morphology. At high flows, braided streams have a low sinuosity and often appear to be straight. At low flows, numerous small channels weave through the exposed bars. Depending on the time the bar surface has been exposed above the seasonal low-water mark, the nature of the sediment surface exposed, the types of vegetation available for colonization, the sediment available to the river and the climate, freshly emergent unvegetated bars may become progressively vegetated as they accrete vertically and laterally (Fig. 2.1). During floods, vegetated islands trap sediment and aggrade (Julien, 2002).

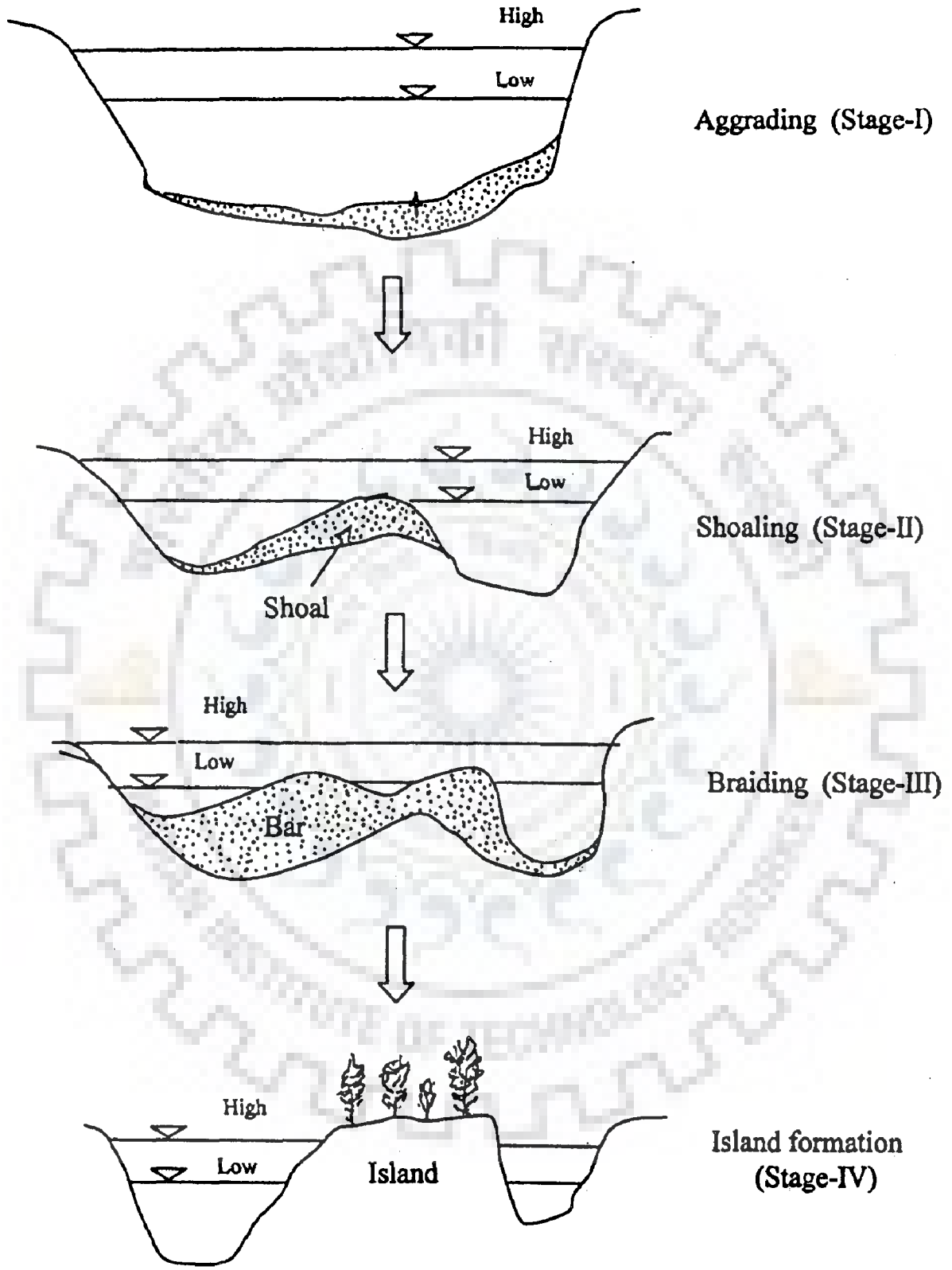

Fig. 2.1 Schematic features of river bed aggradation and formation of island

To realize the formation of island, it is necessary to understand the processes responsible for the occurrence of braiding. Worldwide earlier research (Leopold and Wolman, 1957; Lane, 1957; Brice, 1964; Schumm and Khan, 1972; Parker, 1976; Miall, 1977; Ashmore, 1982,1991; Bristow and Best, 1993; Bridge, 1993; Ashworth, 1996; Deng and Singh, 1999; Richardson and Thorne, 2001) on braided rivers has been devoted towards achieving this goal.

2.2.1 Braided Channel Patterns: Certain General Observations

Channel patterns and their associated flow and sedimentary processes form part of a continuum. This has been demonstrated in experimental studies of natural and laboratory channels (e.g. Leopold and Wolman, 1957; Ackers and Charlton, 1971; Schumm and Khan, 1972; Ikeda, 1973,1975; Ashmore, 1982,1991) and with theoretical models (e.g. Engelund and Skovgaard, 1973; Parker, 1976; Fredsoe, 1978; Hayashi and Ozaki, 1980; Blondeaux and Seminara, 1985; Fukuoka, 1989). It is generally accepted that the channel pattern is controlled by the supply of water and sediment and, in short term, by valley slope. Some have also invoked bank erodibility, specially as influenced by vegetation (Bridge, 1993). However, channel pattern also varies with bed material size, such that braiding occurs at lower slope and/or discharge as grain size decreases (Henderson, 1961,1966; Osterkamp, 1978; Carson, 1984; Ferguson, 1984,1987; Ferguson and Ashworth, 1991). The theoretical stability analyses of Parker (1976) and Hayashi and Ozaki (1980) predict that channel pattern types are controlled by width, depth and Froude number (F_r) (Bridge, 1993). The theoretical analyses of Engelund and Skovgaard (1973), Fredose (1978) and Fukuoka (1989) all indicate that the major control on braiding is B/h (being >50 for braiding to occur), with θ or (θ/θ_c) having a minor effect. θ is dimensionless bed shear stress, and θ_c is the value of θ at the threshold of bed load movement (Bridge,1993).

The chief explanations of braiding cited in the literature are erodible banks, rapid and large discharge variations, high regional slope, and abundant sediment load. Bank erodibility has been cited by various workers, notably Fisk (1944), Friedkin (1945), Mackin (1956), and Brice (1964). They argue that low bank cohesion leads to very wide channels in which shoaling occurs on central bars and ultimately leads to the development of multiple channels.

Doeglas (1951) considered large and sudden variations in runoff to be the chief factor involved in the formation of braids. But, Leopold and Wolman (1957) demonstrated by laboratory simulation that braids can in fact form without discharge fluctuation. Miall (1977) concluded that fluctuations in flow stage or discharge are a prerequisite for river braiding. According to Lane (1957) steep slope or a change in slope is an important factor in initiating braiding. Stebbings (1964) suggested that under conditions of heavy bed load transport, braiding may result from local overloading.

However, Ashmore (1982) reproduced the forms and processes of natural gravel braided rivers in constant discharge, constant slope flume experiments with equilibrium maintained using adjustable sediment feed. This led him to conclude that the mechanisms of bar initiation proposed by Doeglas (1951) and Miall (1977), which rely on a variable or falling discharge, are not uniquely responsible for braiding.

Further work has shown that bars may disappear at high flow stages, the implication being that some braided systems act as single channels at bankful stage and only adopt the characteristic braided pattern on the falling stage (Bluck 1979, Smith 1974, Carson 1984). However, Bristow and Best (1993) observed that the majority of the river systems, including the Brahmaputra River maintains their bars at both high

and low flow stages (Coleman 1969, Smith 1970, Cant and Walker 1978, Church and Jones 1982, Bridge et al. 1986, Bristow 1987).

2.2.2 Bars and Islands - Distinction

The problem of how best to differentiate between bars and islands within braided and anastomosed channel patterns has yet to be fully addressed. Brice (1964) defined bars as transient features that are submerged at bankfull stage and are unvegetated, whereas islands are stabilized features that are vegetated and are not submerged at bankfull stage. According to Williams and Rust (1969) islands are the most permanent features on the valley floor. They are the areas of highest elevation. The islands are characterized by a dense vegetational cover, which masks the original topographic roughness. Depending on the history of erosion and deposition, the sediment available to the river, and the climate, freshly emergent unvegetated bars may become progressively vegetated as they accrete vertically and laterally, thus it is difficult to assess when a bar becomes an island (Brice, 1964; Bridge et al., 1986). Bridge (1993) stated that the difficulty with the definition of bars and islands put forward by Brice (1964) is that the degree of vegetation that exists on a mid-channel feature is dependent on the length of time that feature remains emergent above the flow stage, the type of vegetation that is available for colonization, the nature of available sediment and the climate. Bridge (1993) further suggested that in order to overcome the subjective nature of terms such as 'transient', 'stable' and 'unstable', they should be replaced by quantitative measures of bar persistence, rates of deposition, migration and erosion.

2.3 ZONES OF FLOW CONVERGENCE AND DIVERGENCE

The essential features of flow in braided rivers are curved channel segments joined by zones of flow convergence (confluence) or divergence (diffluence) (Bridge, 1993). Flow around one side of a braid bar can be considered to be dynamically similar to flow in an undivided sinuous channel (Bridge, 1985; Bridge & Gabel, 1992) and flow in river confluences can be considered to be dynamically similar to braided channel convergence zone (Best, 1986). The link between flow convergence and the downstream division of flow has been neglected, despite the fact that this transition is the area, which may be of fundamental importance to the development of braid bars (Ashmore, 1991; Ashworth et al., 1992). The flow dynamics and morphology of regions of channel convergence have been studied by many researchers including Moseley (1976, 1982), Best (1988), Best and Roy (1991) and Roy and Bergeron (1990). However, the connection between flow convergence and the subsequent downstream divergence of flow has often been disregarded (Bristow and Best, 1993), Ashworth (1996) being a recent exception. Ashmore (1991), Ashworth et al. (1992) and Bristow and Best (1993) have all commented that the region of flow divergence is the area that may well be fundamental to the development of braid bars.

The flow dynamics and morphology of channel confluences have received considerable attention recently in geomorphology, sedimentology and hydraulic literature (Moseley, 1976; Ashmore and Parker, 1983; Best, 1988; Roy and Bergeron, 1990). Where channels converge in a braided system, rapid changes occur in the velocity and sediment distributions that result in rapid shifting of the channel geometry (Richards, 1980). Best (1988) found that increases in the confluence angle or discharge ratio resulted in greater confluence scour, deflection of sediment around the increased zone of turbulence and flow separation at the confluence centre.

The subject of the down stream flow divergence in braided rivers has received little attention despite the fact that this region may well be fundamental to understanding of bar genesis and evolution (Leopold and Wolman, 1957; Ashmore, 1991). In general, flow divergence is associated with flow deceleration and sediment deposition and, once deposition has been initiated, the sediment accumulation is likely to promote further flow division, deposition and bar formation. Divergent flow may also impinge on the bank at an increased angle leading to bank erosion, channel widening and local increase in available sediment, all of which are likely to lead to the development of a new braid bar (Carson, 1984; Thorne et al., 1993). Bristow and Best (1993) commented that there was clear need for both an understanding of the fluid dynamics of the diffluence zone and how this may influence braid bar initiation and internal structure. Ashworth (1996) presented a new model for explaining the long-term development of the confluence-difluence unit.

2.3.1 Division of Flow in Open Channels

The problem in division of flow is to find out the discharge distribution when a branch takes off from a parent channel, the conditions in the main channel upstream of the branch and physical features of the main and branch channels being known. The discharge distribution is affected by various factors like angle of off take, relative bed widths, shapes, slopes of the channels and conditions of flow in the channels.

2.3.1.1 Analysis based on energy principle

Pattabhiramiah and Rajaratnam (1960) attempted to find out analytical solution to the problem of division of flow in rectangular channels. The assumptions were: -

(i) The specific energy remains constant in the parent channel along the inlet to the branch; and

(ii) The branch channel inlet behaves as a weir of zero height.

Later, Sridharan and Rao (1966) concluded that the assumption of constant specific energy would give better results for sub-critical flow than for super-critical flow. They also stated that when the flow in the branch channel is sub-critical, the concept of side weir might not be applicable.

2.3.1.2 Constant velocity concept

Based on his experimental observations, Rajaratnam (1962) assumed that for super-critical flow in both the main and branch channels, the velocity is constant in the main channel along the branch inlet. He found that this assumption gave better result than the approach based on constant specific energy.

However, the above approach will not hold good for sub-critical flow in the main channel since the velocity will be falling along the inlet to the branch.

2.3.1.3 Division of stream around island

When a stream is divided into two channels by a long island, the discharge distribution between the two channels could be found out by making backwater computations (Chow, 1959). In this case, the two channels meet on the down-stream side of the island.

2.4 SECONDARY CURRENTS AROUND BRAID BARS OR ISLANDS

Secondary currents were originally defined by Prandtl (1952) as currents, which occur in the plane normal to the axis of the primary flow, they originate from interactions between the primary flow and gross channel features. Einstein and Li (1958) have defined secondary current as the flow, which is observed to possess a rotation or circulation around an axis parallel to the main flow, transforming into a helical or multi-helical flow. Two types of secondary currents have long been recognized; skew induced and stress induced secondary currents.

There have been few field and laboratory investigations of flow structures in braided rivers and as a consequence their link to braided morphology is little understood. Unlike meandering single thread rivers in which observations of key flow processes can be undertaken over a range of flow stages, in braided rivers most channel changes are associated with changes in bed morphology which occur at high discharges when observation is very difficult (Smith, 1974; Rust, 1978; Ashmore, 1982). As a result of the difficulty of studying flow structures in a braided environment, research to date has relied heavily on laboratory investigations. In addition, any mention of secondary currents in braided systems has been restricted to areas of channel confluence, and the effect of secondary currents in bifurcations and around braid bars has been largely neglected.

Moseley (1976) reported the presence of helical flow at the channel confluences in a general flume experiment of confluence behaviour. Using dye injection to visualize flow patterns, Moseley observed that the pattern of secondary flow at channel confluences consisted of a pair of helical cells, converging in the channel centre over the point of maximum scour and diverging at the bed. Moseley further stated that the helical flow structure resulted in most of the sediment transport in the confluence occurring at the channel fringes away from the area of maximum scour. There was also evidence found for smaller cells of reverse rotation further downstream from the channel confluence, resulting in elevated portion of the bed flanking the channel centerline. Moseley observed that this secondary flow pattern resulted in high rates of sediment transport restricted to the zones between opposing cells.

In another laboratory investigation, Ashmore (1982) successfully reproduced gravel-bed braided stream morphology in a small-scale constant discharge and slope

flume experiment. Again using dye injection as a visualization tool, Ashmore reported similar patterns of secondary flow associated with channel confluences and scour to those observed by Mosley (1976). Ashmore found that maximum scour at the channel confluence occurred in the zone of attachment of the helical cells and deposition occurred in the zone of separation of the cells.

The issue of secondary flows around braid bars has received little attention, with few field investigations undertaken. Ashworth et al. (1992) in a descriptive model for bed load transport and sorting around a braid bar proposed a secondary flow structure similar to that found in meandering channels. They suggested that the actual pattern of secondary flow in the two-anabranch channels around a braid bar would mirror the pattern in two 'back-to-back' meanders. This system of flow structure in anabranches around braid bars taken together with the observed patterns of secondary flow in channel confluences (Moseley, 1976; Ashmore, 1982; Ashmore et al., 1992) would lead to the following impact of secondary flow on the morphology of braid bars:

(a) Downstream of a channel confluence a double helical flow is set up with flow convergence at the surface and divergence at the bed. Bedload transport is concentrated in a narrow zone close to the channel centre.

(b) As the channel widens bar aggradation would be initiated, the double helix flow pattern would drive the finer sediment towards the outer banks and the down the anabranch channels, due to the relative weakness of the secondary flow compared to the primary flow, the coarser sediment is not affected in the same way and is therefore often deposited on the bar head.

(c) A cross over of the secondary flow pattern would then occur in the anabranch channels, from the double helix pattern at the bifurcation to single helical cells

rotating in the opposite direction similar to those reported in meandering channels.

(d) This pattern would now resemble two back-to-back meanders, with eroding outer banks, deep thalwegs and a pronounced point bar. Fine sediment would then be swept inwards by the single helical flow cell, collecting on the bar tail.

2.5 SCOUR AROUND ISLAND

Scouring is a natural phenomenon caused by the flow of water in rivers and streams. It is most pronounced in alluvial materials (Breusers and Raudkivi, 1991). Although, in literature, nothing has been found regarding scour around island it has been observed that there is some similarity between scour around island and scour around man made structures like spur, abutment, bridge piers etc. In the following sections, scour around structures has been briefly reviewed. Later, the parameters, which influence scour, are combined while modelling scour around island.

Scouring occurs naturally as part of the morphologic changes of rivers and as the result of man-made structures. Despite much study, the principles of analysis are not well established, and the results of various investigations often show differing trends (Breusers and Raudkivi, 1991).

2.5.1 Types of Scour

The scour, which may occur at a structure, can be divided into the following three categories (Breusers and Raudkivi, 1991):

A. *General scour*: which occurs in a river or stream as the result of natural processes irrespective of existence of a structure.

B. *Constriction scour*: which occurs if a structure causes the narrowing of a

watercourse or the rechanneling of berm or flood plain flow.

C. *Local scour*: which results directly from the impact of the structure on the flow. This scour, which is a function of the type of structure, is superimposed on the general and constricted scour.

2.5.2 Scour around Spur Dikes

Spur dikes are built out from the bank of a river to deflect the main river current away from an erodible bank. Dikes, in general, constrict the flow in a river and increase both the local velocities and the mean velocity in the main stream.

According to Liu and Skinner (1960), the scour hole increases indefinitely in the absence of sediment supply to the scour hole from the upstream. Garde et al. (1961) found that for all practical purposes, the maximum scour depth was obtained within 3 to 5 hours. This limiting scour depth is termed as the maximum scour depth. However, Melville and Chiew (1999) consider this maximum scour depth fully develops after a duration in the order of days.

In almost all cases, the investigators found that maximum scour depth occurs at the nose of the spur. The scour hole was conical in shape on upstream side and elongated and shallower on the downstream side (Garde et al., 1961).

Inglis (1949) analysed field data on the maximum scour depth observed near spur dikes and guide banks in India and Pakistan. He compared the total scour depth, $h + d_s$, with the three-dimensional Lacey regime depth, D_{3r}, which can be obtained from the equation

$$D_{3r} = 0.47\left(\frac{Q}{f}\right)^{1/3} \tag{2.1}$$

Where, h = uniform flow depth, d_s = scour relative to river bed, Q = total discharge, f = Lacey's silt factor = $1.76\sqrt{d_{50}}$, d_{50} = median diameter of bed material in mm.

The ratio $(h + d_s)/ D_{3r}$ ranged from 1.6 to 1.9, and Inglis recommended the use of the following values:

Scour at spur dikes angled upstream ($\alpha > 90°$) with	
steeply sloping noses (1.5V: 1H)	3.8
Scour at similar dikes but with long sloping noses	2.25
Scour at guide bank noses of large radius	2.75

The most readily useful of the available studies are those of Ahmed (1953), which provided information, particularly on the effect of the angle α on the depth of scour, and of Liu et al. (1961) whose results cover the widest range of pertinent variables. Most of the available results are for spur dikes in the form of a vertical wall. Various other studies have added marginally to the limited information on this subject: Laursen and Toch (1953, 1956), Laursen (1958, 1963), Richardson et al. (1975), Nwachukwa and Rajaratnam (1980) etc.

Ahmed (1953) investigated the problem of scour with dimensional analysis approach. He conducted experiments with 0.354 mm and 0.695 mm sediment sizes to study the effect of discharge intensity, sediment size, flow concentration and the angle of spur dike on the scour depth and scour pattern around spur dikes. His limited study led him to get the expression as:

$$h + d_s = K q_1^{(2/3)} \tag{2.2}$$

Where, h = depth of flow, d_s = depth of scour below bed level, q_1 = discharge intensity at the spur constriction, K = constant depending upon angle of inclination of the spur and position / location of the spur dike on the curved bank.

Garde et al. (1961) conducted experiments on scour with sediment size of 0.29mm, 0.45mm, 1.00mm and 2.25mm and opening ratios of 0.9, 0.835, 0.667 and 0.530 to study the effect of sediment characteristics on scour. According to them, in almost all the cases the maximum scour depth occurred at the nose of spur dike. The spur hole upstream of the spur dike was conical in shape, whereas downstream of the spur dike it was elongated and had a shallower depth.

Laursen and Toch (1953, 1956) and Laursen (1963) observed that the equlibrium depth of scour mainly depends on the flow depth for a given size of flow obstruction, e.g., bridge pier or abutment and that the flow velocity does not have any significant effect on scour depth.

In addition to the above studies, significant work on scour has been done by Melville and co-workers (1999). They used t_e as the time at which the scour hole develops to a depth (the equilibrium depth, d_{se}) at which the rate of increase of scour does not exceed 5% of the pier diameter in the succeeding 24 hour period.

2.5.3 Scour around Abutments

The scour at abutments is similar in character to that around spur dikes. Most of the limited amount of information about abutments comes from studies that have been performed at the University of Auckland (Wong 1982, Tey 1984, Kwan 1984). Melville and Raudkivi (1984) presented a summary of these.

Kwan (1984) investigated the similarity between scour at a pier and at an abutment by comparing measured scour depths at a cylindrical pier and at a semi-circular abutment of the same diameter.

Most experimental data were obtained for $u_* / u_{*c} = 0.9$ to 0.95 and $d_{50} = 0.8$ mm (without general bed load). They showed that both the slope of the abutment and the ratio of water depth to abutment length are important.

Kandasamy (1989) indicates that the live-bed scour depth at a wing-wall type abutment varies with u_* / u_{*c}, where u_{*c} is the limiting critical shear velocity for clear water scour conditions. At $u_* / u_{*c} = 1$, the scour depth has a maximum value. The scour depth decreases first when the $u_* / u_{*c} = 1$ value is exceeded and then increases again, analogous to the behaviour of scour at bridge piers.

2.5.4 Scour around Bridge Piers

Analysis of scour at bridge piers has been carried out by various investigators. Shen, et al. (1966), Baker (1980), Kothyari et al. (1992a, 1992b), Muzzammil and Gangadharaiah (1995) consider the horseshoe vortex induced by secondary flow at the pier base to be the main cause of scour. On the other hand, Hjorth (1975), Melville (1975), Ettema (1980) and Johnson and Ayyub (1992) consider that scour is caused mainly by downflow at the nose of the pier. A combination of analytical and experimental work has, however, revealed (Kumar et al., 1995) that downflow may not be the only agent responsible for scour; the horseshoe vortex also contributes significantly to the scour.

Shen et al. (1966) contend that the strength of the horseshoe vortex system is a function of pier Reynolds number Ub/ν, where b is the pier width. Based on the available data for bridge piers, they proposed the following enveloping equation.

$$d_{se} = 2.23 \times 10^{-4} \left(\frac{Ub}{\nu} \right)^{0.619} \tag{2.3}$$

Where, d_{se} = equilibrium scour depth below original bed in m.

By analysis of a large volume of laboratory data Jain (1981) proposed the following enveloping equation for the maximum depth of scour in clear water-flow.

$$\frac{d_{se}}{b} = 1.84 \left(\frac{h}{b} \right)^{0.3} (F_{rc})^{0.25} \tag{2.4}$$

Where, F_{rc} = Froude number of the flow corresponding to the critical velocity for incipient motion of the given sediment and the actual depth of flow.

Melville and Sutherland (1988) analysed a large volume of laboratory data and proposed an enveloping equation for scour in which several coefficients have been introduced to take care of pier shape, pier alignment, sediment non-uniformity etc.

Kothyari et al. (1992a, 1992b) have given a semi-analytical approach for calculation of temporal variation of scour depth as well as the equilibrium scour depth around circular bridge piers. Their method is applicable to both clear-water and live-bed scour and takes into account flow unsteadiness, sediment non-uniformity and stratification of bed.

Some other investigators who have contributed to the scour around piers are Melville and Chiew (1999), Oliveto and Hager (2002), Mia and Nago (2003) etc.

2.6 PROTECTION OF ISLAND

Erosion of island is a major problem in resource management. The river-stabilization structures designed to protect the river banks and prevent lateral migration of alluvial channels through bank erosion may be adopted for protection of island.

The protection works can be classified according to two different approaches (Julien, 2002):

(i) Direct protection works, which include those constructed directly on the banks in order to strengthen the banks, e.g., riprap revetment, vegetation, windrows and trenches, sacks and blocks, gabions and mattresses etc.

(ii) Indirect protection works include those, which are not constructed directly on the banks, but in front of them and thereby reducing hydrodynamic forces against stream banks, e.g., spurs, vanes etc.

In the following section, the usefulness of submerged vane as a bank protection device is discussed briefly.

2.6.1 Submerged Vanes

Use of revetment or spurs for bank protection can sometimes be inadequate and expensive. A relatively less costly and environmentally acceptable technique involves installation of submerged vanes on the streambed to modify the flow in the vicinity of the outer bank. The submerged vanes function by generating secondary circulation in the flow, which alters the magnitude, and direction of bed shear stresses and causes a change in the distributions of velocity, depth and sediment transport area affected by vanes. They are constructed on river or streambed and set with an angle of attack to the direction of flow to create secondary current.

The first known attempts to develop a theoretical design basis for submerged vanes were made by Odgaard and Kennedy (1983), and Odgaard and Spoljaric (1986). They proposed through the theoretical and physical model, that short vertical submerged vanes, installed at incidence to the channel axis in the outer half of a river-bend significantly reduce the secondary currents and the attendant undermining and high velocity attack of the outer bank.

Based on field data, Odgaard and Mosconi (1987) concluded that submerged vane technique is a feasible and realistic alternative to the traditional techniques, e.g., rock riprap and spur dikes. They proposed that the optimum angle of attack is generally about 20°.

Odgaard and Wang (1991a, 1991b) performed the laboratory test using vane angle 15° for the curved channel and 20° for straight channel.

Marelius and Sinha (1998) conducted laboratory experiments and found that the effect of vanes, i.e. strength of secondary flow in terms of moment of momentum induced by submerged vanes is maximum at angle of attack very close to 40°. The graphical plot provided by Marelius and Sinha (1998) shows that there is significant variation of strength of vortex created by submerged vanes between the angle of attack 20° and 40°.

Johnson et al. (2001) performed laboratory experiments to evaluate the effectiveness of vanes for preventing scour at single-span bridges with vertical wall abutments. They concluded that the vanes do not armour against scour or significantly reduce scour overall; rather, they use the scouring to occur towards the centre of channel, away from the abutment.

2.7 CONCLUDING REMARKS

In this chapter, various studies related to formation of braid bars or islands as well as mechanisms responsible for their occurrences have been reviewed. However, from the literature review, it can be observed that there is lack of extensive study involving flow hydraulics around island. In this context, one can feel the need to study the growth and decay of secondary currents around island in a quantitative manner.

Further, from the literature review, it can be discerned that the issue of scour around island has not been addressed at all. The shape of island may be an important factor in influencing scour around island. Therefore, investigation in this direction would not only help in understanding the scour phenomenon around island but also help in evolving some device for reducing scour around island and thereby providing stability to the island.

EXPERIMENTAL PROGRAMME

3.1 INTRODUCTION

Extensive experimental work for the present study was planned and carried out in the River Engineering Laboratory of WRD&M Deptt., Indian Institute of Technology Roorkee, Roorkee, India. The experimental programme was organised in four phases with the objectives of finding the variation of flow distribution around the island, the scour pattern around the island, the variation of strength of secondary current along the flow direction in the study domain and suggesting some effective measure for protecting island based on the above findings. All the experiments were performed in a 50 cm wide rigid bed flume of 11 m length using 5(five) rigid model islands of elliptical shape(in plan) and one model island of circular shape(in plan).

Details of the equipments used and the procedure adopted for carrying out the experiments are presented in this chapter.

3.2 LABORATORY FLUME AND OTHER ACCESSORIES

3.2.1 Laboratory Flume Used

Experiments were performed in an eleven metre long tilting flume, made of mild steel with side walls made of transparent perspex sheet. The flume has an in-built up-stream tank of 40 cm× 90 cm ×115 cm dimensions. The depth of flume is 50 cm and the width is 50 cm. Diagrammatic scheme of the experimental set-up is given in Fig. 3.1. The bed of the flume is supported on angle iron sections the lower ends of which are connected to a shaft, placed lengthwise parallel to the central portion of the flume

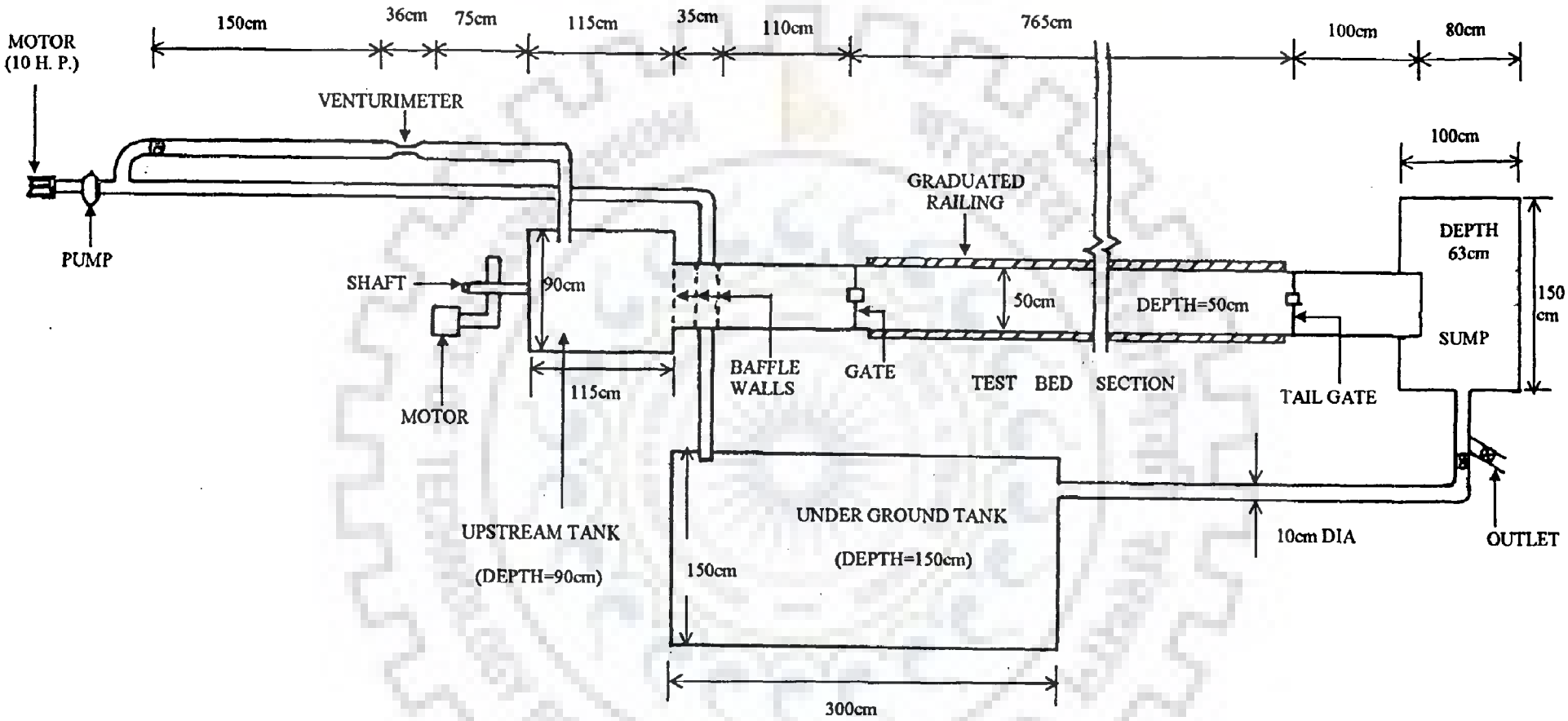

Fig. 3.1 Plan of tilting flume and its components used in experiments

below it. The shaft is movable horizontally backwards and forwards with the help of a gearbox and electric motor such that if the shaft moves towards the direction of flow the front portion of the flume moves upwards and the lower portion moves downwards and vice versa. This is the mechanism of changing slope of the flume. Two railings are mounted on the top edges of the side walls of the flume over which all the required equipments for measurement of velocity, depth, etc., can be placed. A trolley, which can be moved forward and backward, is placed over the railings. The trolley has the facility to fit the acoustic doppler velocimeter (ADV) on it. Scales are installed along the length of the flume and on the trolley and these are used to establish a co-ordinate system and channel morphology is measured in relation to it.

The water flowing in the flume falls into a sump which is connected to an underground tank of 1.5 m×1.5 m×3.0 m dimensions. From the underground tank water is lifted with the help of a centrifugal pump of 10 HP capacity. A 10 cm diameter pipe carries water from the underground tank to the up stream tank. The discharge is regulated with the help of a gate valve placed after the pump. A venturimeter is placed at a distance of 150 cm from the gate valve and 80 cm before the bend of pipe leading to the top of up stream tank. The venturimeter is attached to the mercury manometer. A movable tail gate of size 50 cm×60 cm has been provided at the end of the flume by which the depth of flow in the flume is controlled.

3.2.2 Sediment Used

Experiments were performed with a poorly sorted sand having d_{50} around 0.225 mm (geometric standard deviation of 1.36). The sieve analysis and the cummulative frequency curve of the above sand are shown in Table 3.1 and Fig. 3.2, respectively.

Table 3.1 : Sieve analysis of the sediment material of d_{50} = 0.225 mm

Size of sieves in mm	Weight retained on sieves in gm	% weight retained	Cumulative % retained	% finer
0.600	0.853	0.0853	0.0853	99.9147
0.425	22.125	2.2125	2.2978	97.7022
0.400	3.861	0.3861	2.6839	97.3161
0.300	160.881	16.0881	18.772	81.228
0.225	312.045	31.2045	49.9765	50.0235
0.150	419.955	41.9955	91.972	8.028
0.075	52.862	5.2862	97.2582	2.7418
0.063	13.017	1.3017	98.5599	1.4401

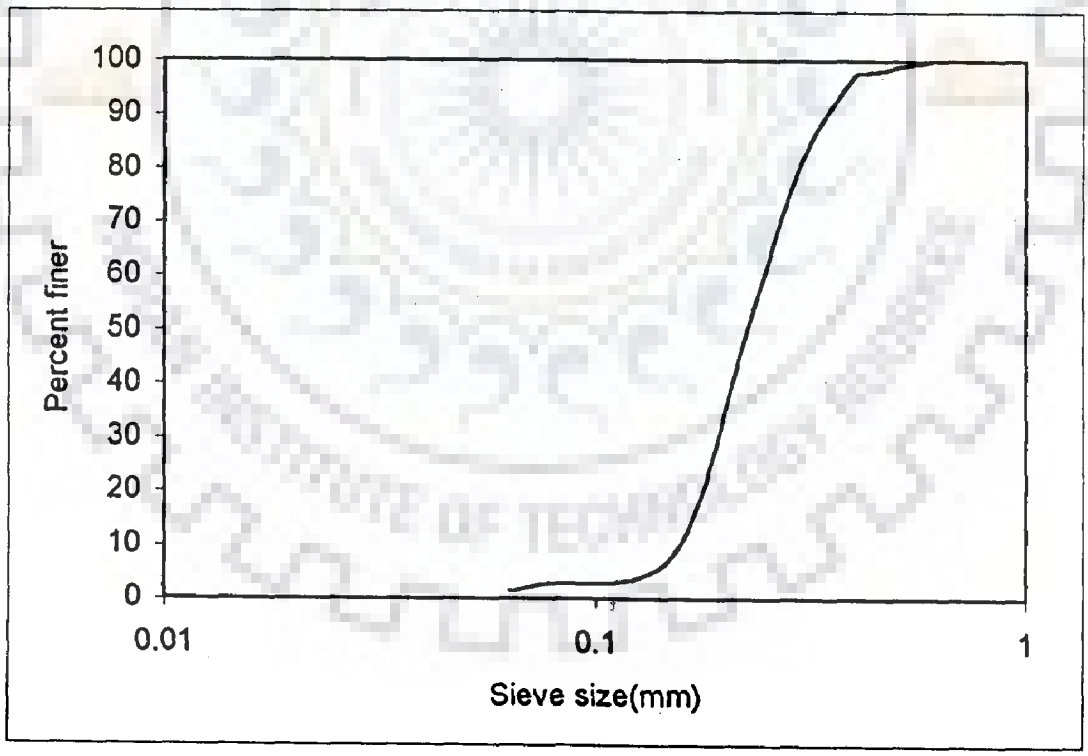

Fig. 3.2 Cumulative frequency curve for sand of d_{50} =0.225 mm

3.2.3 Other Equipments

The depth of flow along the length of flume and the scour pattern around the islands were measured with the help of a pointer gauge, which could be moved along the rails fitted at the top of the flume. The three-dimensional (3D) velocity components were measured by means of an acoustic doppler velocimeter (ADV). The velocimeter was capable of measuring all the three components of velocity with an accuracy of 0.25% of the velocity magnitude or 0.0025 m/s (whichever was greater).

The sampling rate used in the experiment was 20 to 25 Hz. A minimum of 800 values was taken at each measured point and the mean value of these measurements was taken as representative velocity. The technique employed in ADV is superior to the other conventional methods, since the actual sampling volume is located at a lower depth (about 5cm below the probe, in the present case) than the probe, and hence, is less disturbed.

3.3 PHASE ONE EXPERIMENTS

In the first phase of the experimental programme, five model islands of elliptical shape (in plan) and one model island of circular shape (in plan) were used. All the islands were made of G. I. sheet and the sides were kept vertical. All the islands have different minor axis and major axis ratios varying from 0.15 to 1.0 (1.0 for the circular island) as shown in Fig.3.3(a) to Fig.3.3(f). The first phase of experimental programme was completed in two stages. In the first stage, the experimental runs were carried out under rigid bed flow condition. Each model island was fixed on the rigid bed of the flume with its longitudinal axis coinciding the centre line of the flume (i.e., eccentricity,e=0%) and runs were carried out for different depth of flow, different

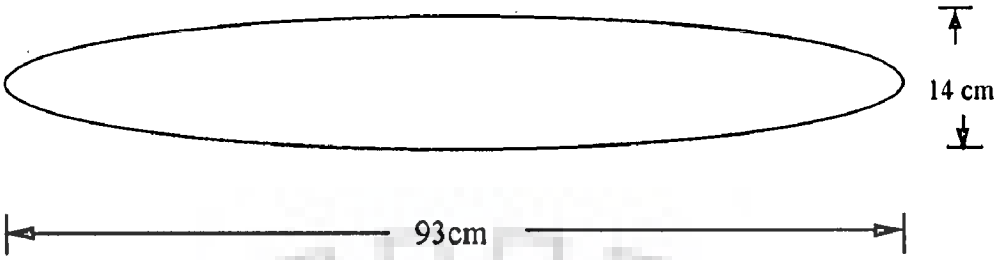

Fig. 3.3(a) Plan of elliptical island I_1 (a=93cm,b=14cm,b/a=0.15)

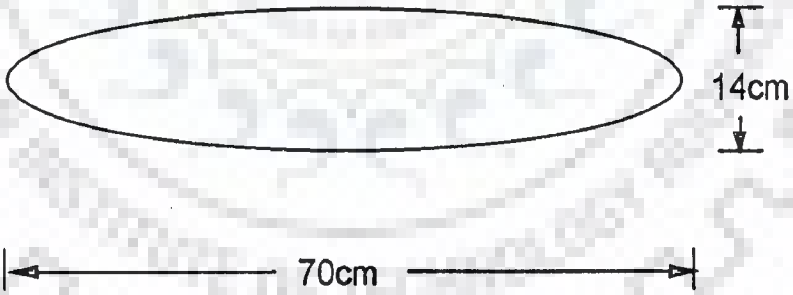

Fig. 3.3(b) Plan of elliptical island I_2 (a=70cm,b=14cm,b/a=0.2)

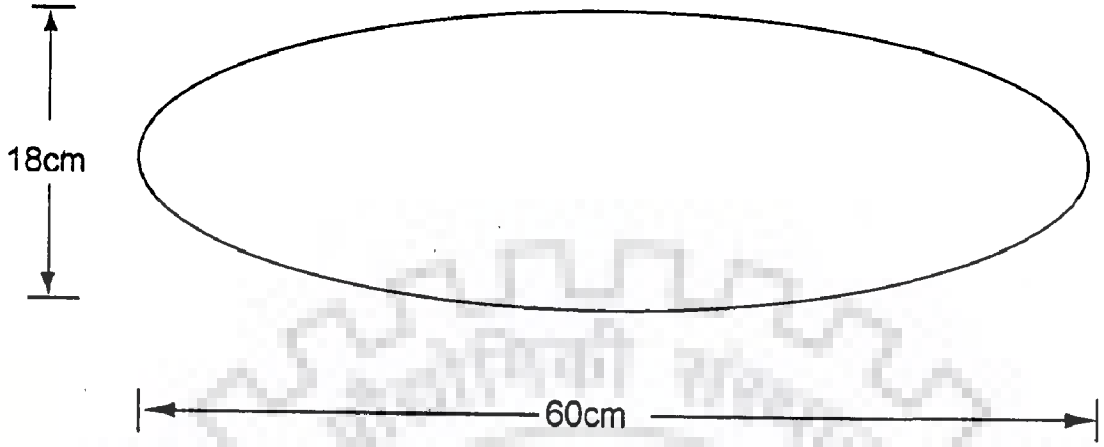

Fig. 3.3(c) Plan of elliptical island I_3 (a=60cm,b=18cm,b/a=0.3)

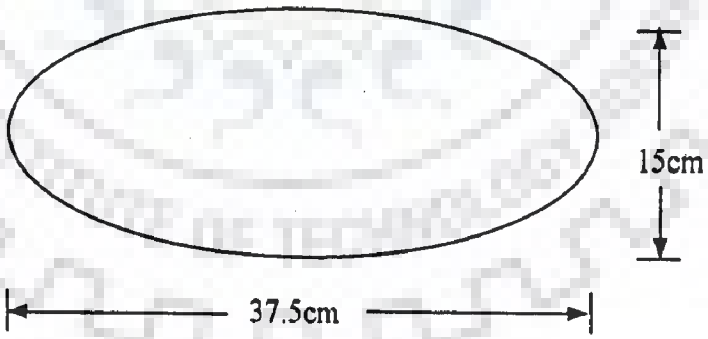

Fig. 3.3(d) Plan of elliptical island I_4 (a=37.5cm,b=15cm,b/a=0.4)

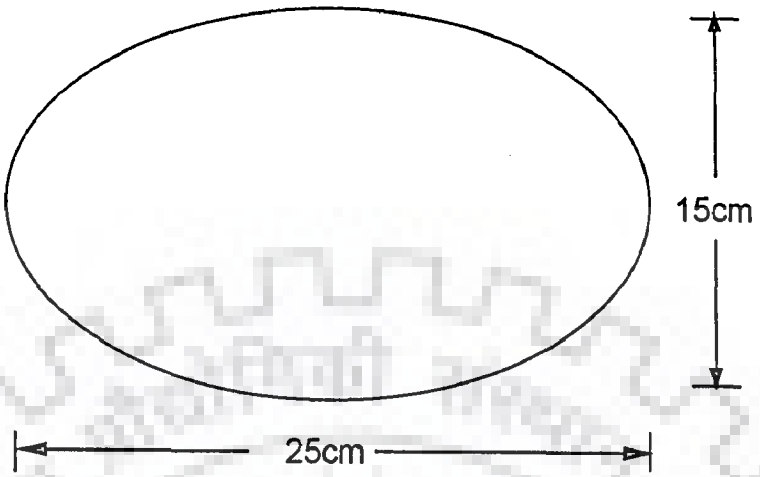

Fig. 3.3(e) Plan of elliptical island I_5 (a=25cm,b=15cm,b/a=0.6)

Fig. 3.3(f) Plan of the circular island I_6 (d=15cm)

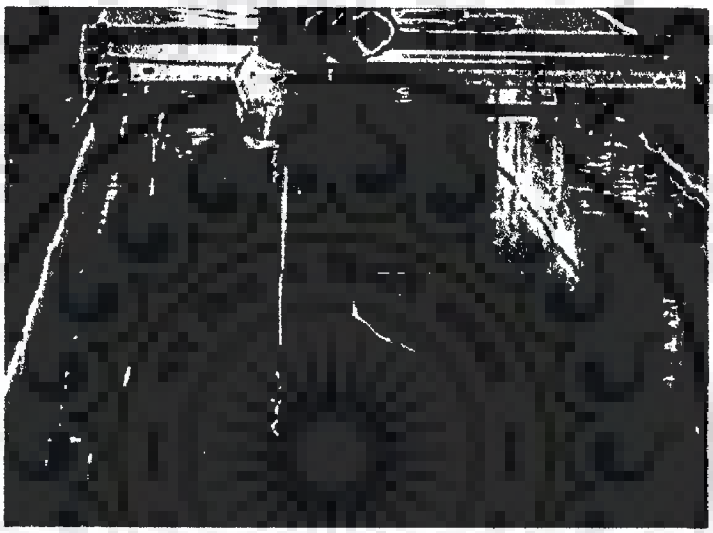

Plate 3.1 Showing stage one of phase one experiment in running condition

discharges and different Froude numbers. Few runs were also carried out by placing the islands 5 cm away from the centre line of the flume (i.e., eccentricity, e=20%) with the longitudinal axis of the island parallel to the centre line of the flume. Similarly, few runs were carried out by placing the islands 10 cm away from the centre line of the flume (i.e., eccentricity, e=40%). Discharge in the flume varied from 0.0127 m^3/s to 0.0196 m^3/s. The depth of flow in the flume was controlled by the tail gate and it was ranging from h=15 cm to h=23 cm. The Froude number was kept between F_r=0.105 and F_r=0.16. For each run, the entire length around the island was divided into a number of cross-sections preferably 10 cm away from each other and at each cross-section average velocity was determined on both sides of the island (i.e., in the right channel as well as in the left channel) using ADV. Experimental details relating to stage one have been summarised in Table 3.2 and related experimental data have been presented in Appendix A.

In the second stage of phase one experiment, experimental runs were carried out under mobile bed flow condition. For this purpose, a sediment bed layer of 15 cm depth was placed over the flume bed. The height of the model islands used in the first stage was extended by 15 cm and the extended portion was embedded below the sand bed layer. 15 runs were carried out by placing the islands with the longitudinal axis coinciding the centre line of the flume (i.e., eccentricity, e=0%) and 9 runs were carried out by placing the islands 5 cm away from the centre line of the flume (i.e., eccentricity, e=20%). For each run the average velocities were measured in the right channel as well as in the left channel around the island using ADV. Experimental details of stage two have been given in Table 3.3 and related experimental data have been presented in Appendix B.

Table 3.2. Stage one of phase one experiments

Experi-mental run	Q (m^3 /sec)	Flow depth,h (cm)	Froude number	Island shape	Island position
A1	0.0127	15.0	0.14	Elliptical island I_1 (a=93cm,b=14cm, b/a=0.15)	Longitudinal axis of island coinciding the centre line of the flume.
A2	0.01634	18.0	0.14		
A3	0.0146	15.0	0.16		
A4	0.0182	23.0	0.105	Elliptical island I_2 (a=70cm,b=14cm, b/a=0.2)	Longitudinal axis of island coinciding the centre line of the flume.
A5	0.0167	20.0	0.12		
A6	0.0146	17.0	0.13		
A7	0.0127	15.0	0.14		
A8	0.0146	15.0	0.16		
A9	0.0182	23.0	0.105	Elliptical island I_2 (a=70cm,b=14cm, b/a=0.2)	Longitudinal axis of island parallel to & 5cm away from the centre line of the flume.
A10	0.0167	20.0	0.12		
A11	0.0146	17.0	0.13		
A12	0.0182	23.0	0.105	Elliptical island I_2 (a=70cm,b=14cm, b/a=0.2)	Longitudinal axis of island parallel to & 10cm away from the centre line of the flume.
A13	0.01634	20.0	0.117		
A14	0.0146	17.0	0.13		
A15	0.0127	15.0	0.14	Elliptical island I_3 (a=60cm,b=18cm, b/a=0.3)	Longitudinal axis of island coinciding the centre line of the flume.
A16	0.01634	18.0	0.14		
A17	0.0146	15.0	0.16		
A18	0.01634	15.0	0.18		
A19	0.0179	17.0	0.16	Elliptical island I_3 (a=60cm,b=18cm, b/a=0.3)	Longitudinal axis of island parallel to & 5cm away from the centre line of the flume.
A20	0.01634	15.0	0.18		
A21	0.0196	23.0	0.11	Elliptical island I_4 (a=37.5cm,b=15cm, b/a=0.4)	Longitudinal axis of island coinciding the centre line of the flume.
A22	0.0182	20.0	0.13		
A23	0.0127	15.0	0.14		
A24	0.0159	17.0	0.145		
A25	0.0146	15.0	0.16		
A26	0.0196	23.0	0.11	Elliptical island I_4 (a=37.5cm,b=15cm, b/a=0.4)	Longitudinal axis of island parallel to & 5cm away from the centre line of the flume.
A27	0.0167	20.0	0.12		
A28	0.0146	17.0	0.13		
A29	0.0182	23.0	0.105	Elliptical island I_4 (a=37.5cm,b=15cm, b/a=0.4)	Longitudinal axis of island parallel to & 10cm away from the centre line of the flume.
A30	0.01634	20.0	0.117		
A31	0.0146	17.0	0.13		
A32	0.0146	17.0	0.13	Elliptical island I_5 (a=25cm,b=15cm, b/a=0.6)	Longitudinal axis of island coinciding the centre line of the flume.
A33	0.0127	15.0	0.14		
A34	0.0146	15.0	0.16		
A35	0.0182	23.0	0.105	Elliptical island I_5 (a=25cm,b=15cm, b/a=0.6)	Longitudinal axis of island parallel to & 10cm away from the centre line of the flume.
A36	0.01634	20.0	0.117		
A37	0.0146	17.0	0.13		
A38	0.0146	17.0	0.13	Circular I_6 island (d=15cm)	Longitudinal axis of island coinciding the centre line of
A39	0.0127	15.0	0.14		
A40	0.0146	15.0	0.16		
A41	0.0127	15.0	0.14	Circular I_6 island (d=15cm)	Longitudinal axis of island parallel to & 5cm away from the centre line of the flume.
A42	0.0146	15.0	0.16		
A43	0.0182	23.0	0.105	Circular I_6 island (d=15cm)	Longitudinal axis of island parallel to & 10cm away from the centre line of the flume.
A44	0.01634	20.0	0.117		
A45	0.0146	17.0	0.13		

Table 3.3. Stage two of phase one experiments

Experi-mental run	Q (m^3/sec)	Flow depth, h (cm)	Froude number	Island shape	Island position
B1	0.0146	15.0	0.16	Elliptical island I_1 (a=93cm,b=14cm, b/a=0.15)	Longitudinal axis of island coinciding the centre line of the flume.
B2	0.0173	15.0	0.19		
B3	0.0182	15.0	0.20		
B4	0.0146	15.0	0.16	Elliptical island I_2 (a=70cm,b=14cm, b/a=0.2)	Longitudinal axis of island coinciding the centre line of the flume.
B5	0.0173	15.0	0.19		
B6	0.0182	15.0	0.20		
B7	0.0146	15.0	0.16	Elliptical island I_2 (a=70cm,b=14cm, b/a=0.2)	Longitudinal axis of island parallel to & 5cm away from the centre line of the flume.
B8	0.0173	15.0	0.19		
B9	0.0146	15.0	0.16	Elliptical island I_3 (a=60cm,b=18cm, b/a=0.3)	Longitudinal axis of island coinciding the centre line of the flume.
B10	0.0173	15.0	0.19		
B11	0.0146	15.0	0.16	Elliptical island I_3 (a=60cm,b=18cm, b/a=0.3)	Longitudinal axis of island parallel to & 5cm away from the centre line of the flume.
B12	0.0193	18.0	0.16		
B13	0.0173	15.0	0.19		
B14	0.0193	18.0	0.16	Elliptical island I_4 (a=37.5cm,b=15cm, b/a=0.4)	Longitudinal axis of island coinciding the centre line of the flume.
B15	0.0173	15.0	0.19		
B16	0.0146	15.0	0.16	Elliptical island I_4 (a=37.5cm,b=15cm, b/a=0.4)	Longitudinal axis of island parallel to & 5cm away from the centre line of the flume.
B17	0.0193	18.0	0.16		
B18	0.0173	15.0	0.19		
B19	0.0146	15.0	0.16	Elliptical island I_5 (a=25cm,b=15cm, b/a=0.6)	Longitudinal axis of island coinciding the centre line of the flume.
B20	0.0173	15.0	0.19		
B21	0.0193	18.0	0.16	Elliptical island I_5 (a=25cm,b=15cm, b/a=0.6)	Longitudinal axis of island parallel to & 5cm away from the centre line of the flume.
B22	0.0139	15.0	0.15	Circular I_6 island (d=15cm)	Longitudinal axis of island coinciding the centre line of the flume.
B23	0.0157	15.0	0.17		
B24	0.0173	15.0	0.19		

3.4 PHASE TWO EXPERIMENTS

The second phase of the experimental programme was conducted with the purpose of finding the scour pattern around the islands. For this a sediment bed layer of 15 cm depth was placed over the flume bed.

Experiments were carried out in the following steps.

(i) First the flume was adjusted to required slope.

(ii) Before placement of the island, the sediment bed of the flume was levelled.

(iii) Then the island was fully embedded below the sediment bed layer with its longitudinal axis coinciding the centre line of the flume.

(iv) After placement of the island, the sediment bed of the flume was again levelled around the island.

(v) At the begining of each run, flow was introduced in the flume very slowly by closing the tail gate so that no scour occurs around the island.

(vi) Uniform flow without sediment motion corresponding to a selected discharge was established with the help of tail gate.

(vii) Runs were carried out until such time as the scour bed around the island did not change by 1 mm over a period of 4 hours. The corresponding scour depth was taken as equilibrium scour depth.

(viii) After the experiment was over, the scour pattern was measured with the help of a pointer gauge.

Experimental details relating to phase two have been summarised in Table 3.4 and related experimental data have been presented in Appendix-C.

Plate 3.2 Showing phase two experiment in running condition

Table 3.4. Phase two experiments

Experimental run	Q (m^3/sec)	Flow depth, h (cm)	Froude number	Island shape
C1	0.0146	15.0	0.16	Elliptical island I_1 (a=93cm,b=14cm, b/a=0.15)
C2	0.0173	15.0	0.19	
C3	0.0182	15.0	0.20	
C4	0.0146	15.0	0.16	Elliptical island I_2 (a=70cm,b=14cm, b/a=0.2)
C5	0.0173	15.0	0.19	
C6	0.0182	15.0	0.20	
C7	0.0146	15.0	0.16	Elliptical island I_3 (a=60cm,b=18cm, b/a=0.3)
C8	0.0173	15.0	0.19	
C9	0.0146	15.0	0.16	Elliptical island I_4 (a=37.5cm,b=15cm, b/a=0.4)
C10	0.0173	15.0	0.19	
C11	0.0182	14.0	0.20	
C12	0.0146	15.0	0.16	Elliptical island I_5 (a=25cm,b=15cm, b/a=0.6)
C13	0.0173	15.0	0.19	
C14	0.0182	15.0	0.20	
C15	0.0146	15.0	0.16	Circular I_6 island (d=15cm)
C16	0.0173	15.0	0.19	

3.5 PHASE THREE EXPERIMENTS

In the third phase of the experimental programme, experiments were conducted in order to find the variation of strength of secondary current along the flow direction in the study region, i.e., around the island. Seventeen experimental runs were carried out using the six rigid model islands mentioned earlier under rigid bed flow conditions for three Froude numbers i.e., F_r=0.14, F_r=0.16 and F_r=0.19. For each run the island was placed with its longitudinal axis coinciding the centre line of the flume. To collect the experimental data, the flow region around the island was divided into a number of cross-sections and 10 cm×3 cm grids were taken at each cross-section. All the three velocity components were measured at each grid point using the ADV. Table 3.5 describes the summary of phase three experiments. Experimental data relating to this phase have been presented in Appendix-D.

Table 3.5 Phase three experiments

Experimental run	Q (m^3/sec)	Flow depth, h (cm)	Froude number	Island shape
D1	0.0127	15.0	0.14	Elliptical island I_1 (a=93cm,b=14cm, b/a=0.15)
D2	0.0146	15.0	0.16	
D3	0.0173	15.0	0.19	
D4	0.0127	15.0	0.14	Elliptical island I_2 (a=70cm,b=14cm, b/a=0.2)
D5	0.0146	15.0	0.16	
D6	0.0173	15.0	0.19	
D7	0.0127	15.0	0.14	Elliptical island I_3 (a=60cm,b=18cm, b/a=0.3)
D8	0.0146	15.0	0.16	
D9	0.0173	15.0	0.19	
D10	0.0127	15.0	0.14	Elliptical island I_4 (a=37.5cm,b=15cm, b/a=0.4)
D11	0.0146	15.0	0.16	
D12	0.0173	14.0	0.19	
D13	0.0127	15.0	0.14	Elliptical island I_5 (a=25cm,b=15cm, b/a=0.6)
D14	0.0146	15.0	0.16	
D15	0.0173	15.0	0.19	
D16	0.0127	15.0	0.14	Circular I_6 island (d=15cm)
D17	0.0146	15.0	0.16	

3.6 PHASE FOUR EXPERIMENTS

In the fourth phase of the experimental programme, experiments were carried out with the purpose of reducing scour around circular island and thereby, protecting the island. Other islands (elliptical islands) were not included in the study as the scour was maximum around the circular island. Four V-shaped deflectors, having length of each limb=0.2 d=3.0 cm were used at 11.25 cm (0.75 d), 15 cm (1.0 d), 22.5 cm (1.5 d) and 30 cm (2.0 d) upstream of the centre of the circular island and four V-shaped deflectors of length of each limb=0.3 d=4.5 cm were used at 15 cm (1.0 d), 18.75 cm (1.25 d), 22.5 cm (1.5 d) and 30 cm (2.0 d) upstream of the centre of the island. For each location, the included angle of the V-shaped deflector was so adjusted that the two limbs of the deflector were tangential to the periphery of the island. Fig. 3.4(a) to Fig. 3.4(e) shows the location of V-shaped deflectors with respect to the circular island along with their included angles. The V-shaped deflectors were made of plastic sheet and their heights were such that they were not submerged in water. To conduct the experiments the flume was filled with sediment bed layer of 15 cm depth and the circular island as well as the deflector were embedded below the sediment bed layer and both were placed along the centre line of the flume.

Experimental details of phase four have been summarized in Table 3.6 and related experimental data have been presented in Appendix-E.

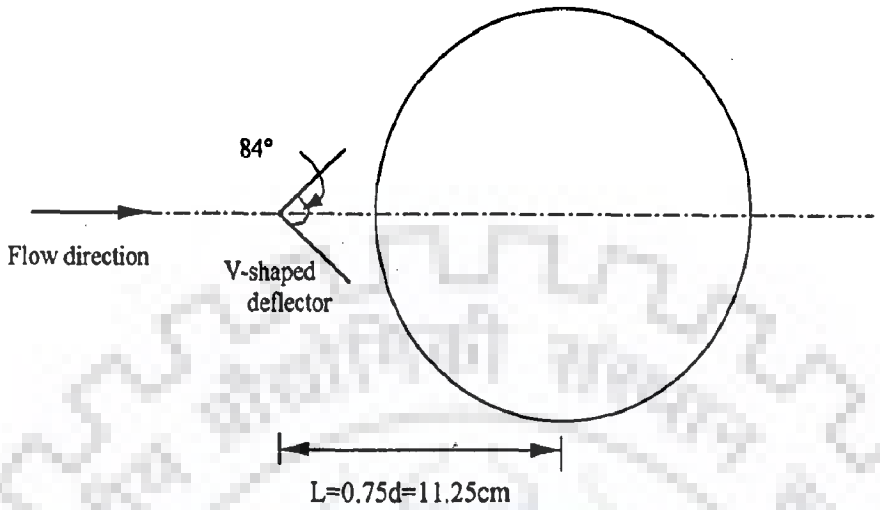

Fig. 3.4(a) Plan showing the V-shaped deflector located 11.25 cm upstream of the centre of the island

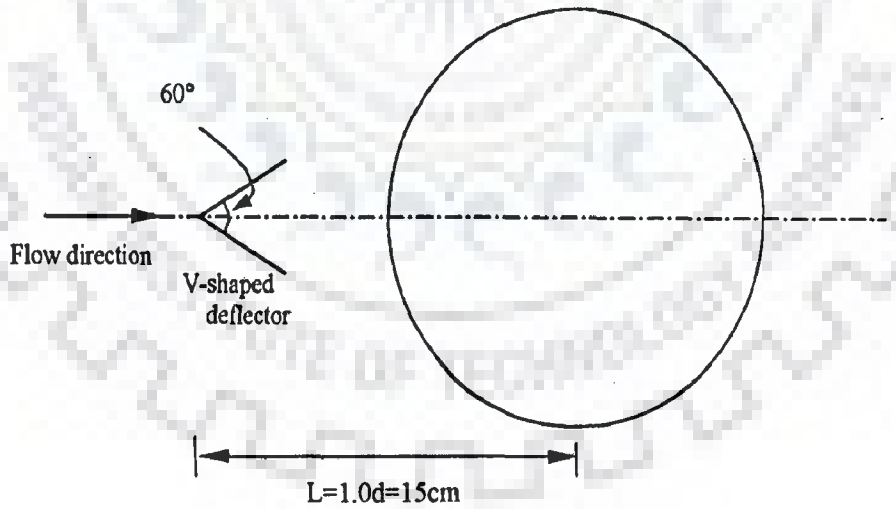

Fig. 3.4(b) Plan showing the V-shaped deflector located 15 cm upstream of the centre of the island

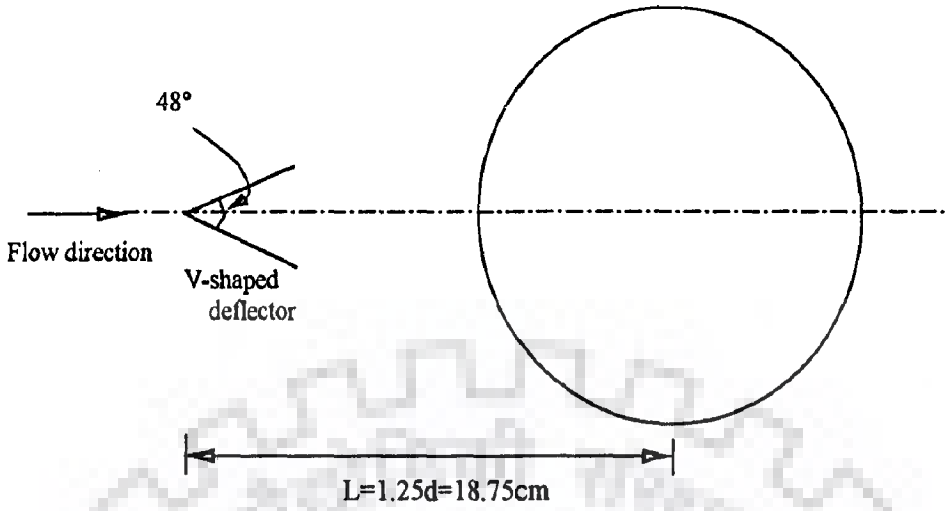

Fig. 3.4(c) Plan showing the V-shaped deflector located 18.75 cm upstream of the centre of the island

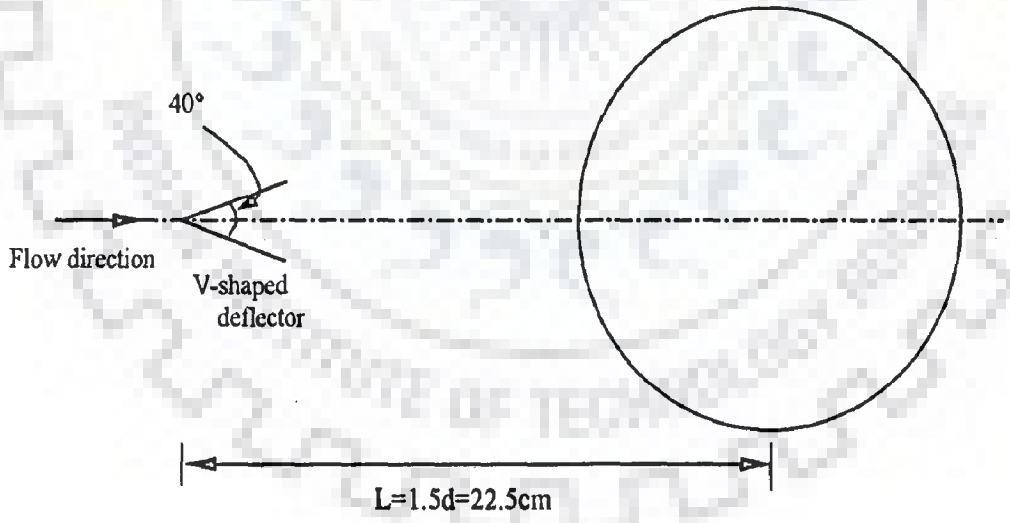

Fig. 3.4(d) Plan showing the V-shaped deflector located 22.5 cm upstream of the centre of the island

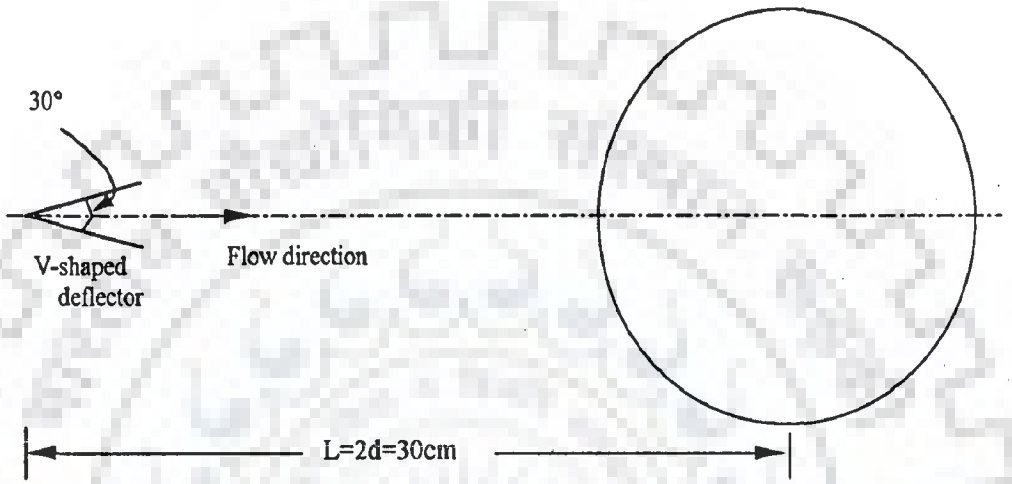

Fig. 3.4(e) Plan showing the V-shaped deflector located 30 cm upstream of the centre of the island

Table 3.6 Phase four experiments

Experim-ental run	Q (m^3/sec)	Flow depth, h (cm)	Froude number	Distance of V-shaped deflector, L (cm)	Length of each limb of V-shaped deflector, l (cm)	Included angle, θ
E1	0.0146	15.0	0.16	0.75d=11.25	0.2d=3.0	84°
E2	0.0146	15.0	0.16	1.0d=15.00	0.2d=3.0	60°
E3	0.0146	15.0	0.16	1.5d=22.50	0.2d=3.0	40°
E4	0.0146	15.0	0.16	2.0d=30.00	0.2d=3.0	30°
E5	0.0173	15.0	0.19	0.75d=11.25	0.2d=3.0	84°
E6	0.0173	15.0	0.19	1.0d=15.00	0.2d=3.0	60°
E7	0.0173	15.0	0.19	1.5d=22.50	0.2d=3.0	40°
E8	0.0173	15.0	0.19	2.0d=30.00	0.2d=3.0	30°
E9	0.0146	15.0	0.16	1.0d=15.00	0.3d=4.5	60°
E10	0.0146	15.0	0.16	1.25d=18.75	0.3d=4.5	48°
E11	0.0146	15.0	0.16	1.5d=22.50	0.3d=4.5	40°
E12	0.0146	15.0	0.16	2.0d=30.00	0.3d=4.5	30°
E13	0.0173	15.0	0.19	1.0d=15.00	0.3d=4.5	60°
E14	0.0173	15.0	0.19	1.25d=18.75	0.3d=4.5	48°
E15	0.0173	15.0	0.19	1.5d=22.50	0.3d=4.5	40°
E16	0.0173	15.0	0.19	2.0d=30.00	0.3d=4.5	30°

FLOW DIVISION AROUND ISLAND

4.1 GENERAL

When an island divides flow in a stream, it is important to find out the division of flow between the two channels. In fact, if the channel cross-sections and eccentricity of island are known, the problem can be reduced to the determination of the discharge in each of the two channels. The present chapter is devoted exclusively to development of a simple approach for finding distribution or division of flow around an island. Rigid as well as mobile bed situations are covered and the investigated flow is in sub-critical regime.

4.2 DEVELOPING AN EQUATION FOR DIVISION OF FLOW

Attempt was made to develop a simple relation for division of flow between the two channels using Manning's equation. Referring to the Fig. 4.1, one can write

$$Q = Q_1 + Q_2 \tag{4.1}$$

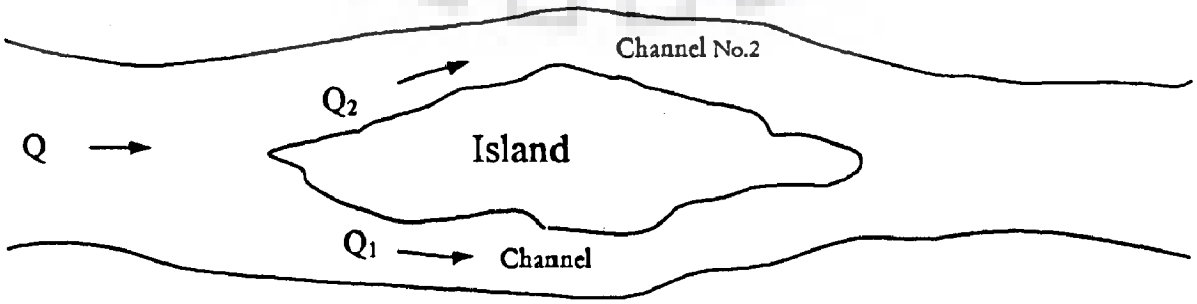

Fig. 4.1 Flow around an island

Applying Manning's equation, Q_1 and Q_2 can be expressed as

$$Q_1 = \frac{1}{n} A_1 R_1^{(2/3)} S_{f_1}^{(1/2)} \tag{4.2}$$

$$Q_2 = \frac{1}{n} A_2 R_2^{(2/3)} S_{f_2}^{(1/2)} \tag{4.3}$$

In equations (4.2) and (4.3), n=Manning's roughness coefficient, A_1= average cross-sectional area of right channel around island, A_2= average cross-sectional area of left channel around island, S_{f_1} = slope of energy gradient for the right channel around island, S_{f_2} = slope of energy gradient for the left channel around island.

From equations (4.1), (4.2) and (4.3)

$$\frac{Q - Q_1}{Q_1} = \left(\frac{A_2}{A_1}\right)\left(\frac{R_2}{R_1}\right)^{(2/3)}\left(\frac{S_{f_2}}{S_{f_1}}\right)^{(1/2)} \tag{4.4}$$

Assuming, $S_{f_1} = S_{f_2}$, equation (4.4) can be written as

$$\frac{Q}{Q_1} = 1 + \left(\frac{A_2}{A_1}\right)\left(\frac{R_2}{R_1}\right)^{(2/3)} \tag{4.5}$$

If the total discharge (Q) in the stream, average cross-sectional areas (A_1 & A_2) of the two channels and the average hydraulic radii (R_1 & R_2) of the two channels are known, Q_1 and Q_2 can be computed from equations (4.5) and (4.1).

4.3 DEVIATION OF COMPUTED DISCHARGE VALUES FROM EXPERIMENTAL DATA

In the present work, 45 runs were carried out in an 11m long and 50 cm wide channel under rigid bed flow conditions to see whether the computed values of Q_1 and Q_2 agree with the experimental values. For this purpose 6 (six) rigid model islands

having b/a ratios of 0.15, 0.2, 0.3, 0.4, 0.6 and 1.0 were used. Experiments were conducted by placing the islands at 3 different eccentricities. 23 runs were carried out by placing the islands with the longitudinal axis of islands coinciding the centre line of channel (i.e., eccentricity, e = 0%). 10 runs were carried out by placing the islands 5 cm away from the centre line of the channel (i.e., eccentricity, e = 20%) and 12 runs were carried out by placing the islands 10 cm away from the centre line of the channel (i.e., eccentricity, e = 40%) (Table 4.1).

Table 4.1 Number of runs corresponding to different eccentricities and b/a ratio

	Number of runs for		
	e = 0%	e = 20%	e = 40%
b/a=0.15	3 runs		
b/a=0.2	5 runs	3 runs	3 runs
b/a=0.3	4 runs	2 runs	
b/a=0.4	5 runs	3 runs	3 runs
b/a=0.6	3 runs		3 runs
b/a=1.0	3 runs	2 runs	3 runs

Details of the experimental data and the deviation of the computed discharge values of Q_1 and Q_2 [based on equations (4.1) and (4.5)] from the corresponding experimental values are shown in Table 4.2.

Table 4.2 Percentage deviation of computed flow division from experimental values

e (%)	b/a	Run	Q (m^3/s)	Q_1 from eq. (4.5) (m^3/s)	$Q_2=Q-Q_1$ (m^3/s)	Experimental value of Q_1 (m^3/s)	Experimental value of Q_2 (m^3/s)	Deviation of Q_1 (%)	Deviation of Q_2 (%)
0	0.15	A1	0.0127	0.00635	0.00635	0.006199	0.006291	2.38	0.93
		A2	0.01634	0.00817	0.00817	0.008741	0.008913	-6.99	-9.09
		A3	0.0146	0.0073	0.0073	0.007281	0.007377	0.26	-1.05
	0.2	A4	0.0182	0.00910	0.00910	0.008764	0.008216	3.69	9.71
		A5	0.0167	0.00835	0.00835	0.008180	0.008397	2.04	-0.56
		A6	0.0146	0.0073	0.0073	0.0074	0.007406	-1.37	-1.45
		A7	0.0127	0.00635	0.00635	0.005959	0.006261	6.16	1.40
		A8	0.0146	0.0073	0.0073	0.006524	0.006723	10.63	7.90
	0.3	A15	0.0127	0.00635	0.00635	0.006208	0.006290	2.24	0.94
		A16	0.01634	0.00817	0.00817	0.008212	0.007722	-0.51	5.48
		A17	0.0146	0.0073	0.0073	0.007094	0.007022	2.82	3.81
		A18	0.01634	0.00817	0.00817	0.008242	0.008168	-0.88	0.02
	0.4	A21	0.0196	0.0098	0.0098	0.010103	0.00998	-3.09	-1.84
		A22	0.0182	0.00910	0.00910	0.008850	0.008987	2.75	1.24
		A23	0.0127	0.00635	0.00635	0.006373	0.006123	-0.36	3.57
		A24	0.0159	0.00795	0.00795	0.007837	0.007893	1.42	0.72
		A25	0.0146	0.0073	0.0073	0.007570	0.006877	-3.70	5.79
	0.60	A32	0.0146	0.0073	0.0073	0.00706	0.00741	3.29	-1.51
		A33	0.0127	0.00635	0.00635	0.006397	0.006107	-0.74	3.83
		A34	0.0146	0.0073	0.0073	0.006917	0.007483	5.25	-2.51
	1.0	A38	0.0146	0.0073	0.0073	0.007470	0.007070	-2.33	3.15
		A39	0.0127	0.00635	0.00635	0.006108	0.005988	3.81	5.70
		A40	0.0146	0.0073	0.0073	0.007277	0.007179	0.31	1.66
20	0.2	A9	0.0182	0.012372	0.005828	0.011364	0.006930	8.15	-18.91
		A10	0.0167	0.011316	0.005384	0.010087	0.006260	10.86	-16.27
		A11	0.0146	0.009854	0.004746	0.009053	0.005543	8.13	-16.79
	0.3	A19	0.0179	0.012307	0.005593	0.011486	0.006788	6.67	21.37
		A20	0.01634	0.011198	0.005142	0.010396	0.005674	7.16	-10.35
	0.4	A26	0.0196	0.012940	0.006113	0.012160	0.006710	6.08	-9.77
		A27	0.0167	0.011303	0.005397	0.011187	0.006097	1.03	-12.97
		A28	0.0146	0.009846	0.004754	0.009763	0.005347	0.84	-12.47
	1.0	A41	0.0127	0.008564	0.004136	0.008112	0.004855	5.28	-17.38
		A42	0.0146	0.009845	0.004755	0.009208	0.005541	6.47	-16.53
40	0.2	A12	0.0182	0.01522	0.00297	0.013123	0.004377	13.83	-47.32
		A13	0.01634	0.01362	0.00271	0.011968	0.003954	12.17	-45.74
		A14	0.0146	0.012125	0.002475	0.010818	0.003683	10.78	-48.81
	0.4	A29	0.0182	0.01521	0.00298	0.013673	0.004225	10.13	-41.49
		A30	0.01634	0.01361	0.00272	0.012265	0.003829	9.90	-40.41
		A31	0.0146	0.012113	0.002487	0.010998	0.003516	9.20	-41.37
	0.6	A35	0.0182	0.01521	0.00298	0.014383	0.004676	5.46	-56.4
		A36	0.01634	0.01361	0.00272	0.012507	0.004103	8.12	-50.46
		A37	0.0146	0.012113	0.002487	0.010537	0.003529	13.01	-41.90
	1.0	A43	0.0182	0.01527	0.00292	0.013592	0.004121	11.01	-40.79
		A44	0.01634	0.01366	0.00267	0.012903	0.003746	5.59	-40.14
		A45	0.0146	0.012161	0.002439	0.010991	0.003324	9.62	-36.28

4.4 NEW RELATIONSHIP FOR DIVISION OF FLOW

It can be seen from Table 4.2 that as the eccentricity of island increases from 0% to 40%, the deviation of discharge values in the two channels computed by using equation (4.5) from the corresponding experimental values also increases. Although in case of eccentricity of 0%, the deviation was not significant but for eccentricity of 40% the deviation was found to be very high. In the present study attempt was made to have a new relationship for division of flow as shown below by simply introducing a correction factor α in equation (4.5), i.e.,

$$\frac{Q}{Q_1} = 1 + \alpha \left(\frac{A_2}{A_1} \right) \left(\frac{R_2}{R_1} \right)^{(2/3)} \tag{4.6}$$

The values of α for some arbitrarily selected runs covering the whole range of b/a ratios and eccentricities were calculated so that the computed values of discharge in the two channels agree with the experimental values. The values of α for the above runs along with the average values are listed in Table 4.3.

It can be seen from Table 4.3 that for eccentricity of 0% the value of α varies from 0.94 to 1.08, for eccentricity of 20% α varies from 1.14 to 1.30 and for eccentricity of 40%, α varies from 1.48 to 1.71. Fig. 4.2 shows the variation of average values of α against b/a ratios for different eccentricities.

Table 4.3 Correction factor, α

b/a	Values of α for			Average Values of α for		
	e=0%	e=20%	e=40%	e=0%	e=20%	e=40%
0.15	1.01484(RunA1)			1.0140		
	1.01318(RunA3)					
0.2	0.93747(RunA4)	1.30437(RunA10)	1.70967(RunA12)	0.9883	1.2878	1.6846
	1.02653(RunA5)	1.27127(RunA11)	1.65945(RunA13)			
	1.00081(RunA6)					
0.3	1.0132(RunA15)	1.30041(RunA19)		1.0015	1.3004	
	0.98985(RunA17))					
0.4	0.98327(RunA21)	1.16871(RunA26)	1.57441(RunA29)	0.9865	1.1564	1.5664
	1.01547(RunA22)	1.14411(RunA27)	1.55842(RunA30)			
	0.96077(RunA23)					
0.6	1.04958(RunA32)		1.65644(RunA35)	1.0287		1.6470
	0.95467(RunA33)		1.63764(RunA36)			
	1.08183(RunA34)					
1.0	0.94645(RunA38)	1.23925(RunA41)	1.58205(RunA43)	0.971	1.2426	1.5332
	0.98035(RunA39)	1.24591(RunA42)	1.4844(RunA44)			
	0.98635(RunA40)					

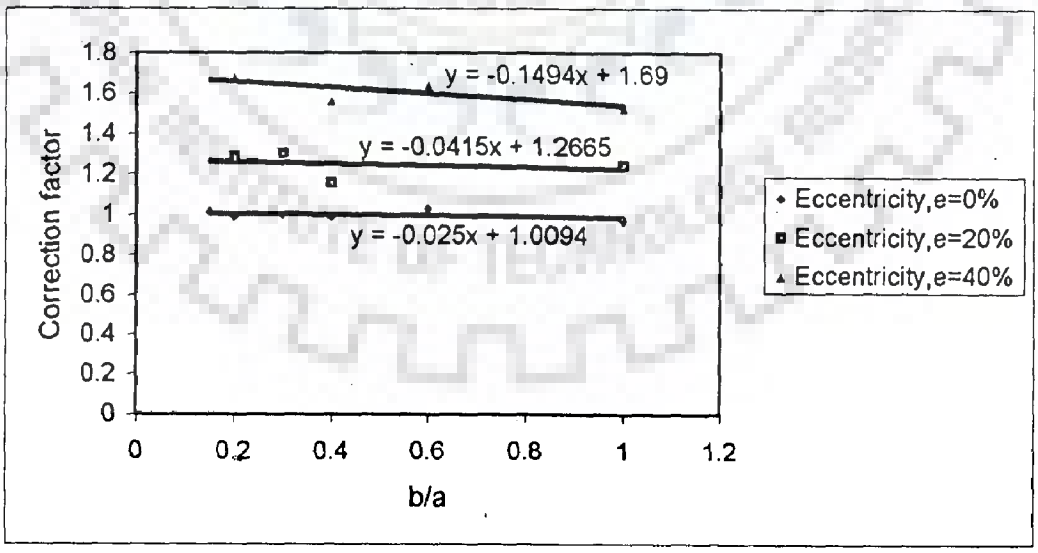

Fig. 4.2 Variation of correction factor with b/a ratio

4.5 RELATIONSHIPS FOR CORRECTION FACTOR, α

From Fig.4.2, it can be seen that the variation of correction factor α with b/a ratio follows some definite trend. Assuming linear trend of variation, the relationships between correction factor α and b/a ratio were obtained as follows:

$$\text{For } e=0\%,\ \alpha = -0.025\,(b/a) + 1.0094 \tag{4.7a}$$

$$\text{For } e=20\%,\ \alpha = -0.0415\,(b/a) + 1.2665 \tag{4.7b}$$

$$\text{For } e=40\%,\ \alpha = -0.1494\,(b/a) + 1.69 \tag{4.7c}$$

Fig. 4.2 can be used to determine the correction factor α for any value of eccentricity between 0% to 40% and any value of b/a ratio from 0.15 to 1.0.

4.6 APPLICABILITY TO RIGID BED CONDITIONS

It is clear from Fig. 4.2 that at eccentricity of 0%, the value of α remains close to one irrespective of the b/a ratio. In other words, the equation (4.6) may be assumed to reduce to equation (4.5). As eccentricity increases the value of α also increases. Thus, at higher eccentricity the deviation of computed discharge values by equation (4.5) from the observed discharge values should be more than the deviation of computed discharge values by equation (4.6) from observed values. In the present study, it was tried to compare the deviation of computed discharge values obtained through equation (4.5) and equation (4.6) from observed discharge values using the runs under rigid bed flow condition which were not included in the calibration of correction factor α. Fig. 4.3(a) to Fig. 4.3(n) shows the results of the above study.

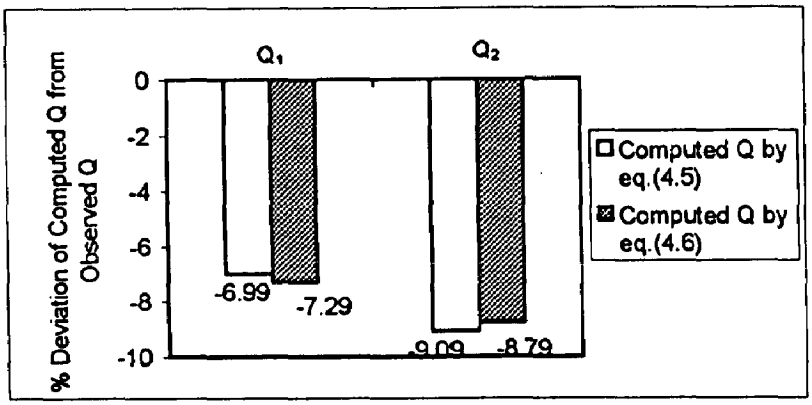

Fig. 4.3(a) Deviation of computed discharge from observed discharge for RunA2 (b/a=0.15, e=0%)

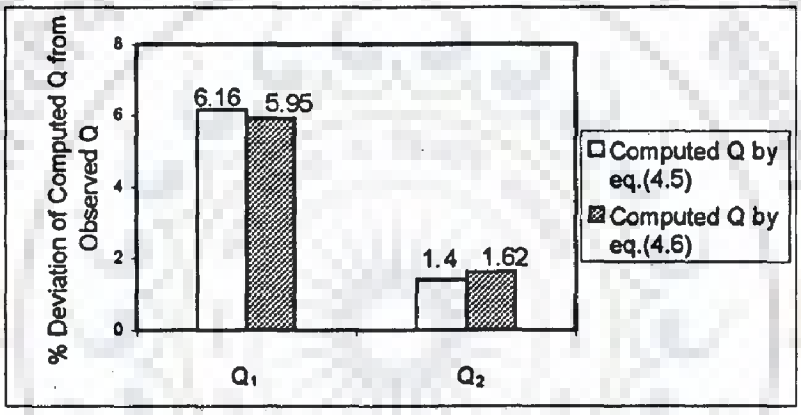

Fig. 4.3(b) Deviation of computed discharge from observed discharge for RunA7 (b/a=0.2, e=0%)

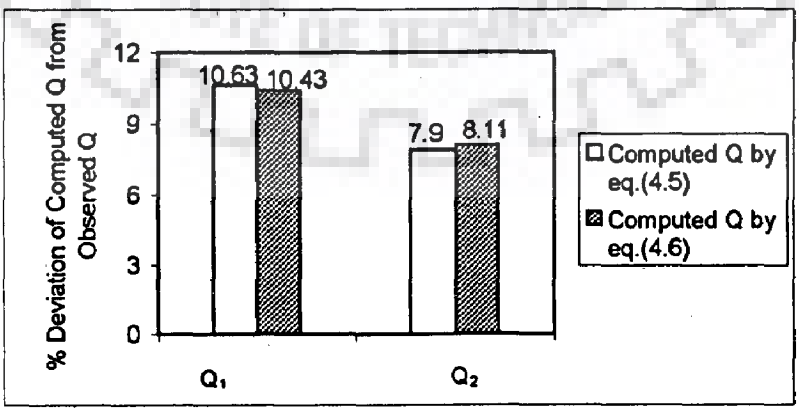

Fig. 4.3(c) Deviation of computed discharge from observed discharge for RunA8 (b/a=0.2, e=0%)

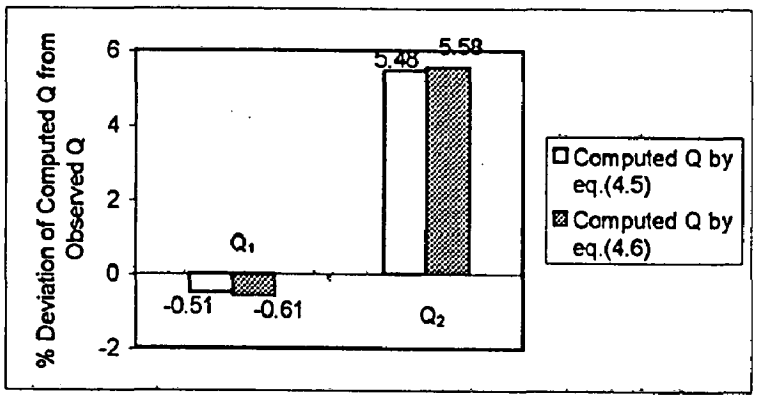

Fig. 4.3(d) Deviation of computed discharge from observed discharge for RunA16 (b/a=0.3, e=0%)

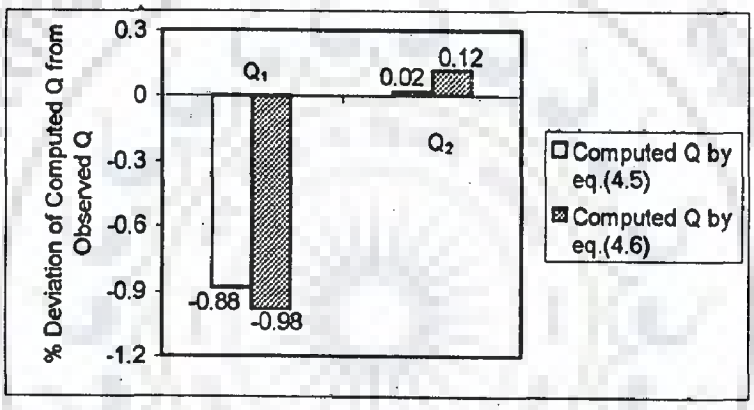

Fig. 4.3(e) Deviation of computed discharge from observed discharge for RunA18 (b/a=0.3, e=0%)

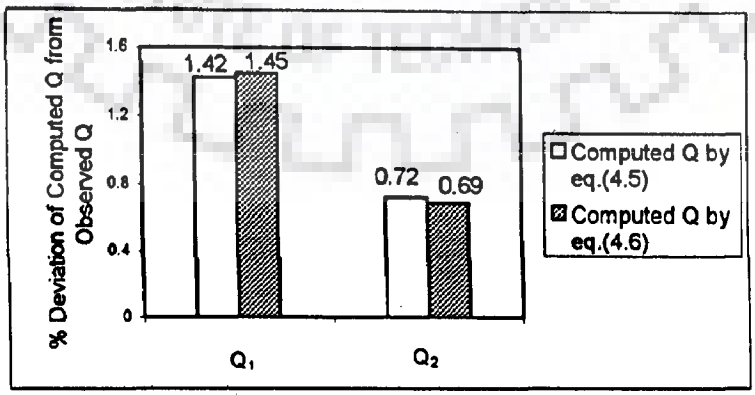

Fig. 4.3(f) Deviation of computed discharge from observed discharge for RunA24 (b/a=0.4, e=0%)

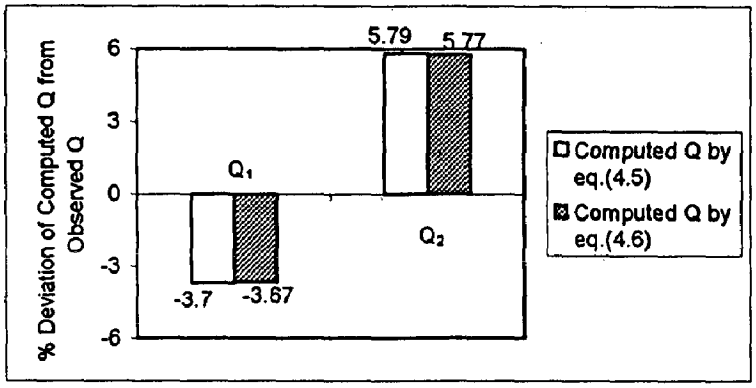

Fig. 4.3(g) Deviation of computed discharge from observed discharge for RunA25 (b/a=0.4, e=0%)

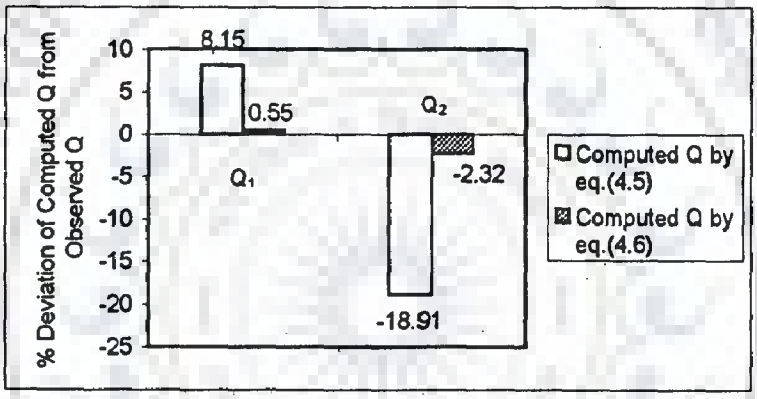

Fig. 4.3(h) Deviation of computed discharge from observed discharge for RunA9 (b/a=0.2, e=20%)

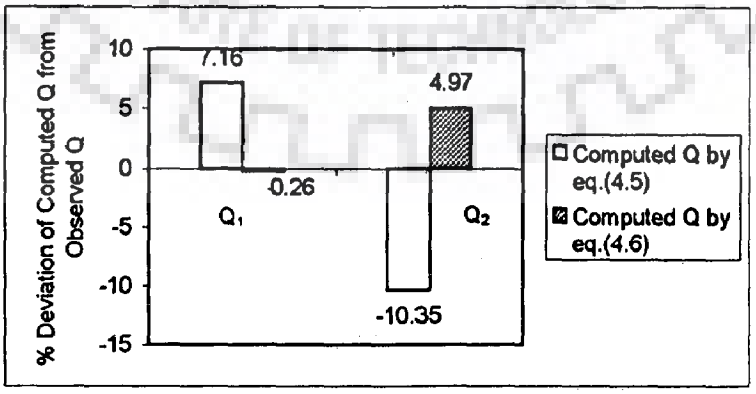

Fig. 4.3(i) Deviation of computed discharge from observed discharge for RunA20 (b/a=0.3, e=20%)

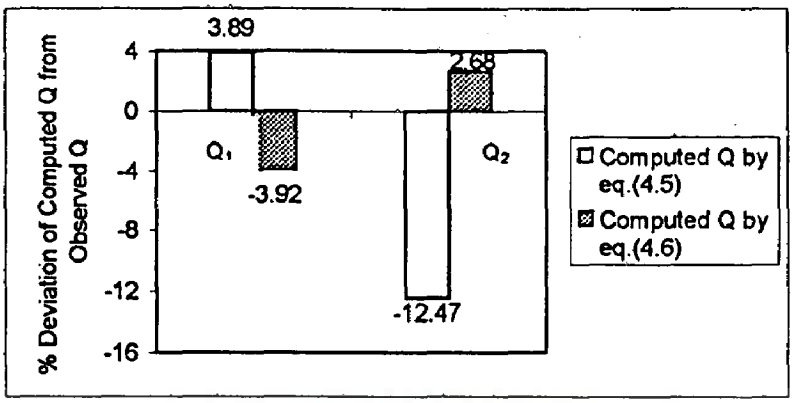

Fig. 4.3(j) Deviation of computed discharge from observed discharge for RunA28 (b/a=0.4, e=20%)

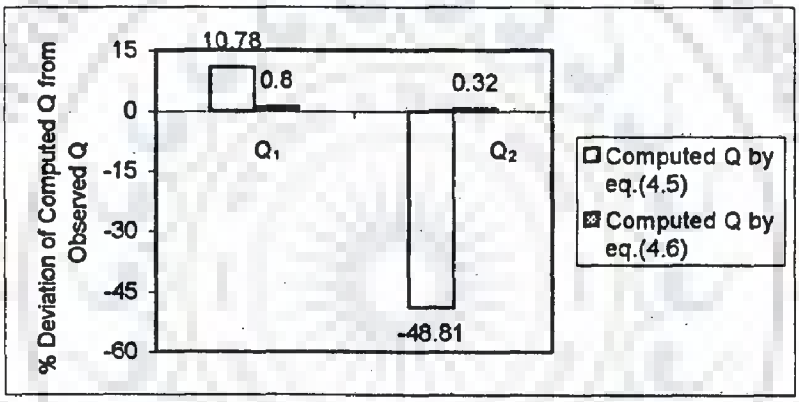

Fig. 4.3(k) Deviation of computed discharge from observed discharge for RunA14 (b/a=0.2, e=40%)

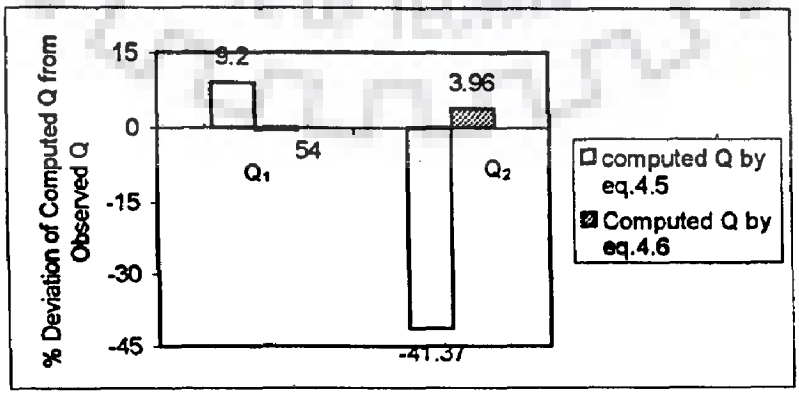

Fig. 4.3(l) Deviation of computed discharge from observed discharge for RunA31 (b/a=0.4, e=40%)

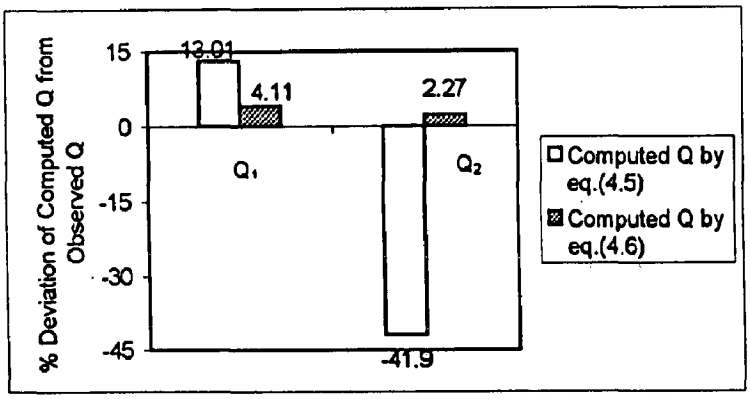

Fig. 4.3(m) Deviation of computed discharge from observed discharge for RunA37 (b/a=0.6, e=40%)

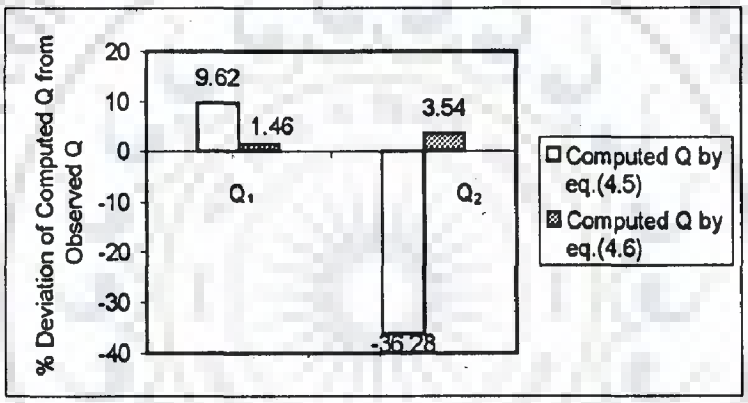

Fig. 4.3(n) Deviation of computed discharge from observed discharge for RunA45 (b/a=1.0, e=40%)

It can be seen from Fig. 4.3(a) to Fig. 4.3(g) that for eccentricity of 0%, the flow divisions around island computed by using equation (4.5) (i.e., without correction factor) and equation (4.6) (i.e., with correction factor) give almost equal values. Also, in this case the deviation of computed discharge from observed discharge is within ±10%. But, in case of eccentricity of 20% [Fig. 4.3(h) to Fig. 4.3(j)], the deviation of computed discharge values from observed values obtained by equation (4.5) is much higher than that obtained by equation (4.6). In this case, the deviation of computed

discharge from observed discharge obtained by equation (4.6) is within ±5%. As the eccentricity of island increases to 40% [Fig. 4.3(k) to Fig. 4.3(n)], the deviation of computed discharge values without correction factor was found to be much higher than the deviation obtained with the correction factor.

4.7 APPLICABILITY TO MOBILE BED CONDITIONS

As equation (4.6) is independent of Manning's roughness coefficient (n), it is expected to work well in case of mobile bed condition. To verify this, experiments with mobile bed were performed at e=0% and e=20%. The results of the experiments are shown through Fig. 4.4(a) to Fig. 4.4(x). Similar to rigid bed condition, for eccentricity of 0%, the flow divisions around island computed by using equation (4.5) (i.e., without correction factor) and equation (4.6) (i.e., with correction factor) give almost equal values [Fig. 4.4 (a) to Fig. 4.4(o)]. But, at eccentricity of 20% [Fig. 4.4(p) to Fig. 4.4(x)], for most of the runs, the deviation of computed discharge values from observed values obtained by equation (4.5) is much higher than that obtained by equation (4.6).

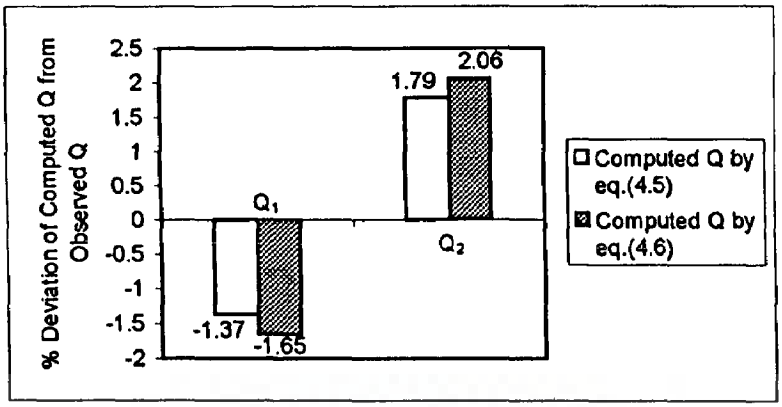

Fig. 4.4(a) Deviation of computed discharge from observed discharge for RunB1 (b/a=0.15, e=0%)

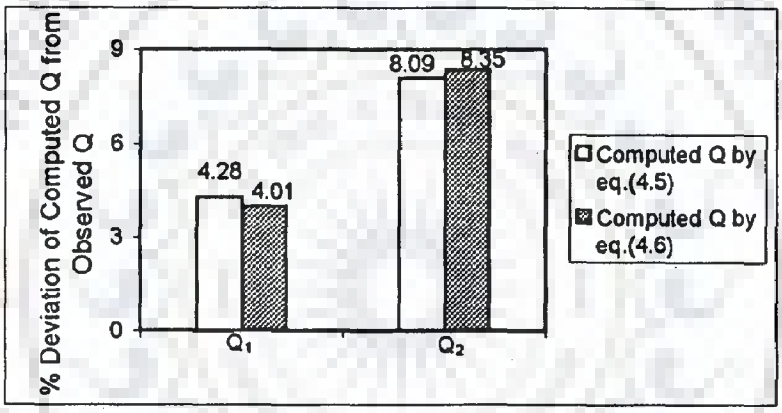

Fig. 4.4(b) Deviation of computed discharge from observed discharge for RunB2 (b/a=0.15, e=0%)

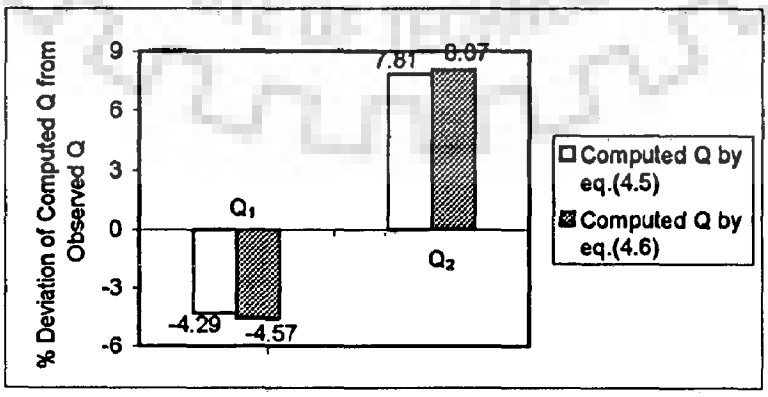

Fig. 4.4(c) Deviation of computed discharge from observed discharge for RunB3 (b/a=0.15, e=0%)

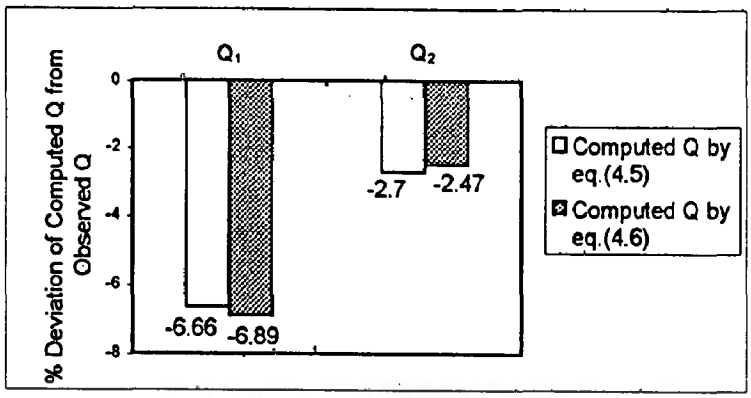

Fig. 4.4(d) Deviation of computed discharge from observed discharge for RunB4 (b/a=0.2, e=0%)

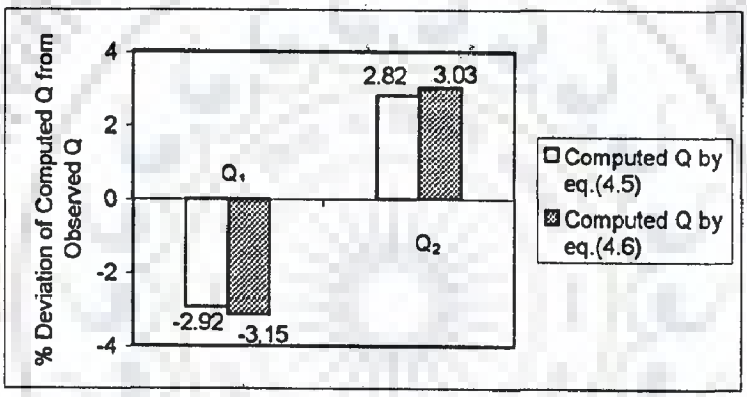

Fig. 4.4(e) Deviation of computed discharge from observed discharge for RunB5 (b/a=0.2, e=0%)

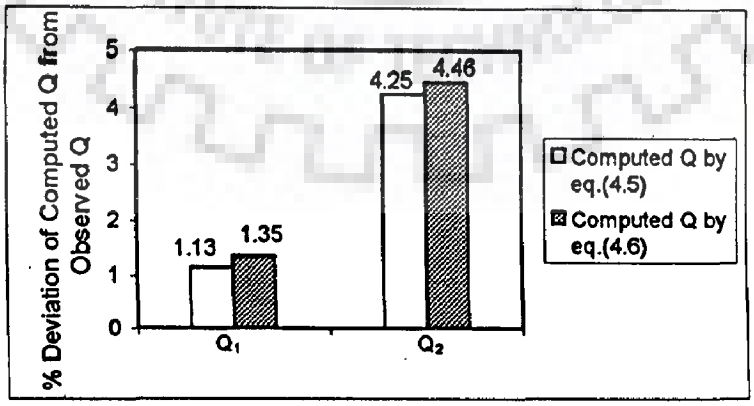

Fig. 4.4(f) Deviation of computed discharge from observed discharge for RunB6 (b/a=0.2, e=0%)

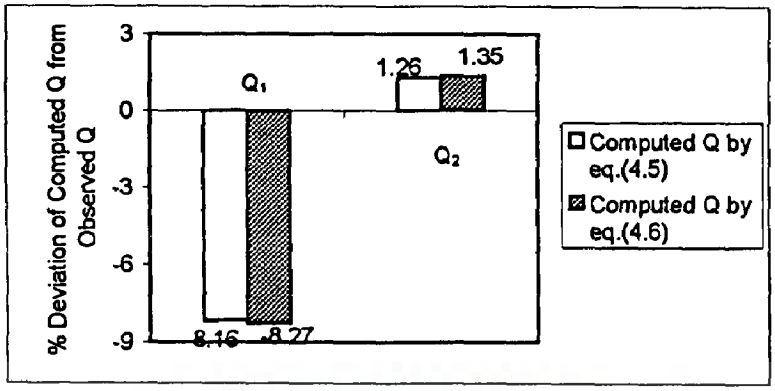

Fig. 4.4(g) Deviation of computed discharge from observed discharge for RunB9 (b/a=0.3, e=0%)

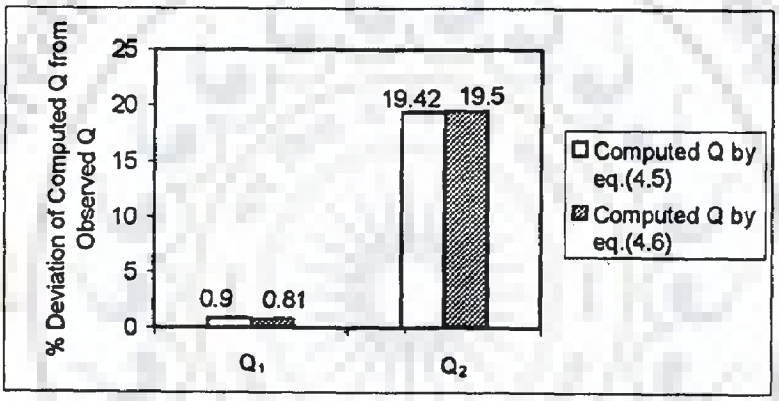

Fig. 4.4(h) Deviation of computed discharge from observed discharge for RunB10 (b/a=0.3, e=0%)

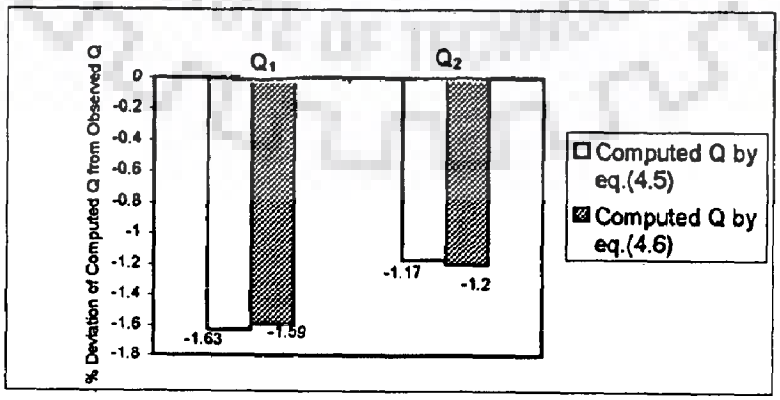

Fig. 4.4(i) Deviation of computed discharge from observed discharge for RunB14 (b/a=0.4, e=0%)

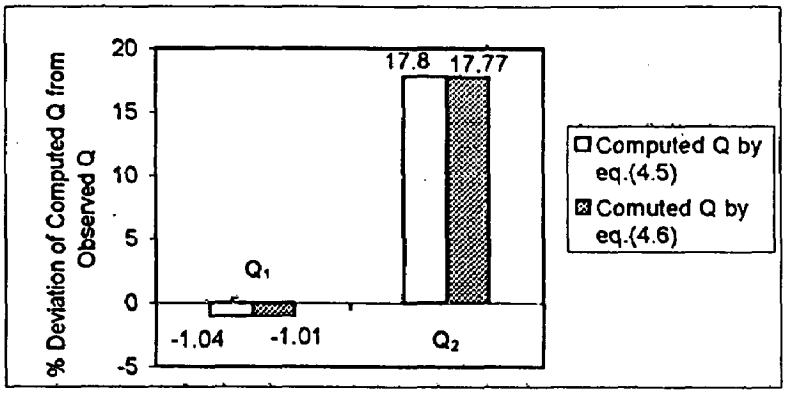

Fig. 4.4(j) Deviation of computed discharge from observed discharge for RunB15 (b/a=0.4, e=0%)

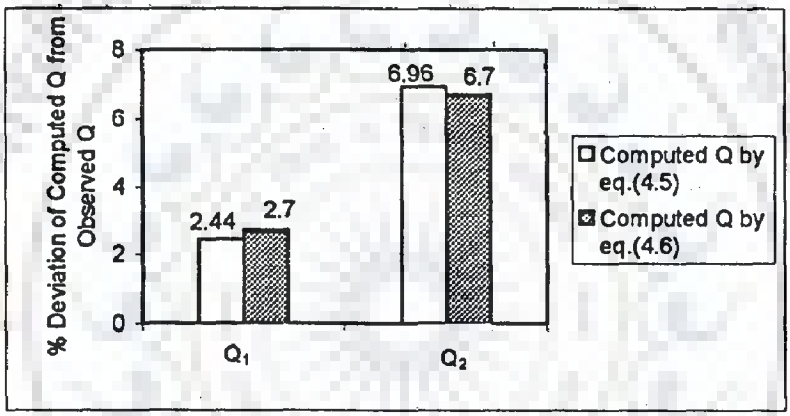

Fig. 4.4(k) Deviation of computed discharge from observed discharge for RunB19 (b/a=0.6, e=0%)

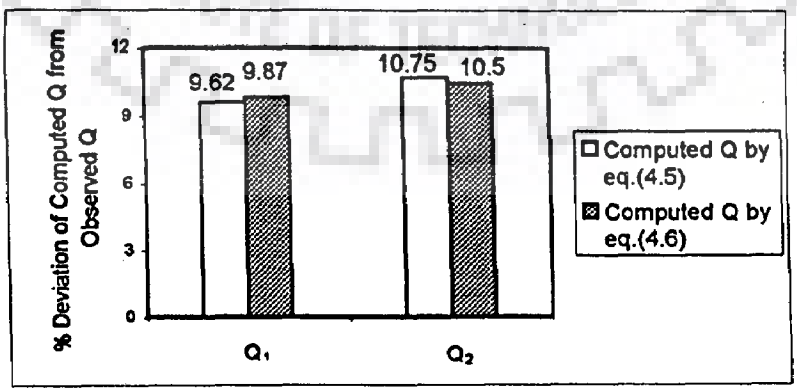

Fig. 4.4(l) Deviation of computed discharge from observed discharge for RunB20 (b/a=0.6, e=0%)

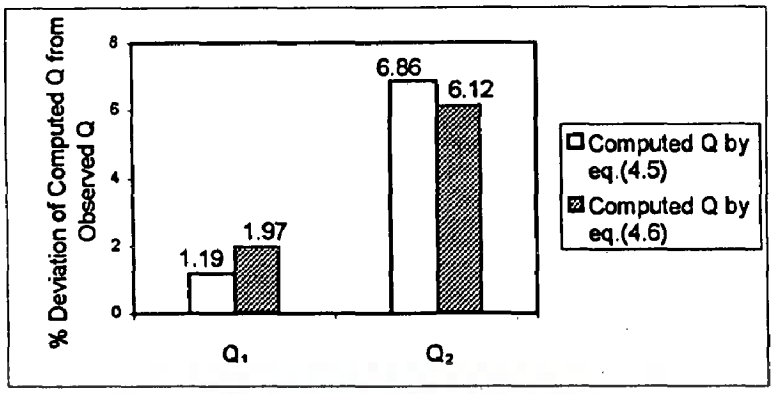

Fig. 4.4(m) Deviation of computed discharge from observed discharge for RunB22 (b/a=1.0, e=0%)

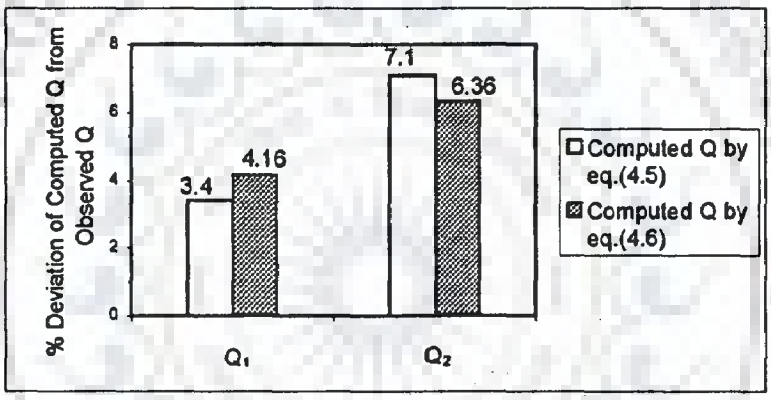

Fig. 4.4(n) Deviation of computed discharge from observed discharge for RunB23 (b/a=1.0, e=0%)

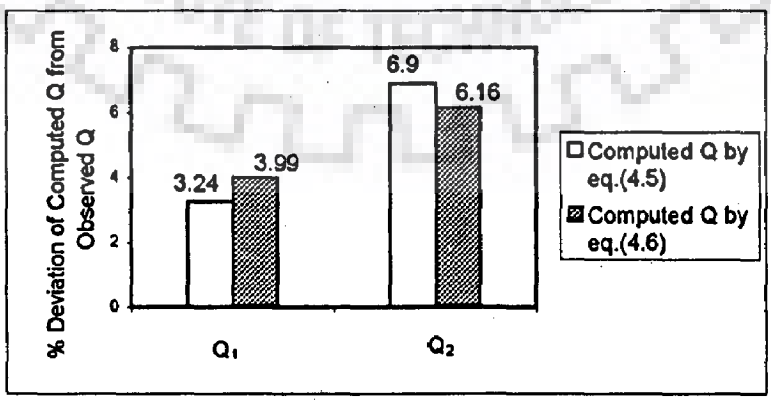

Fig. 4.4(o) Deviation of computed discharge from observed discharge for RunB24 (b/a=1.0, e=0%)

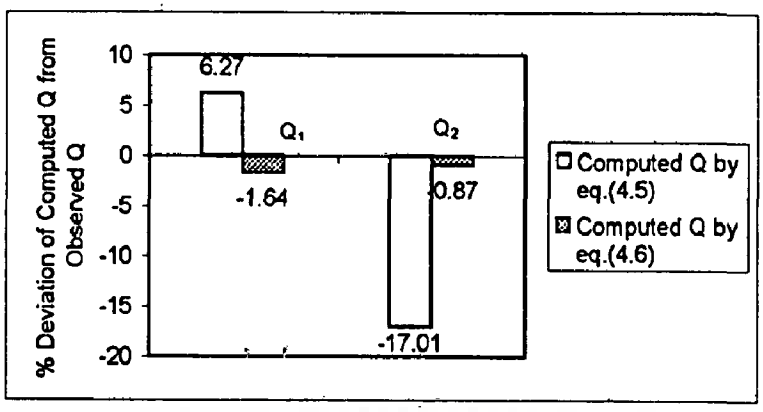

Fig. 4.4(p) Deviation of computed discharge from observed discharge for RunB7 (b/a=0.2, e=20%)

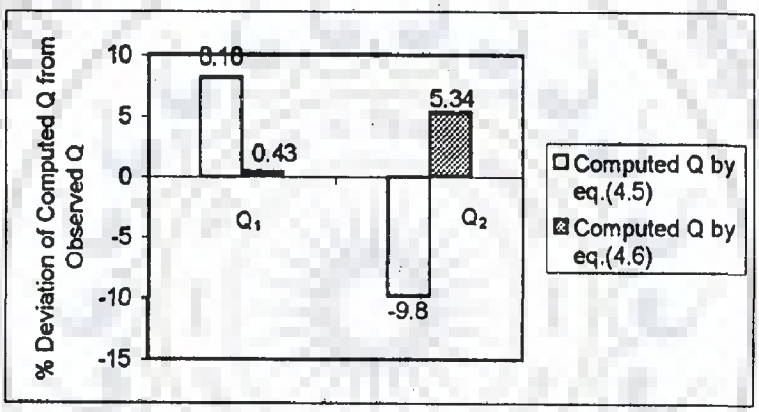

Fig. 4.4(q) Deviation of computed discharge from observed discharge for RunB8 (b/a=0.2, e=20%)

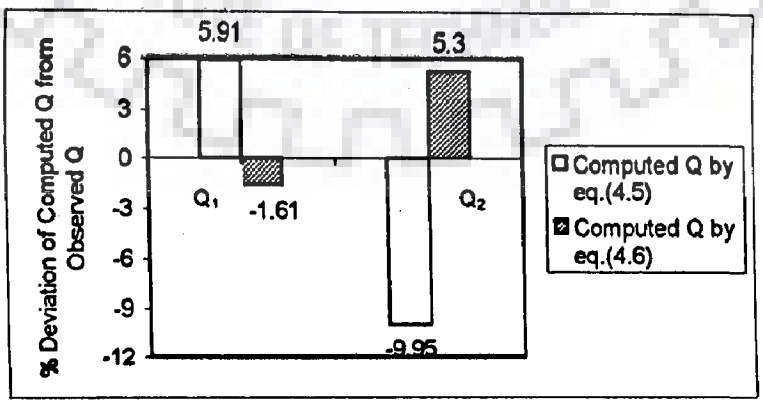

Fig. 4.4(r) Deviation of computed discharge from observed discharge for RunB11 (b/a=0.3, e=20%)

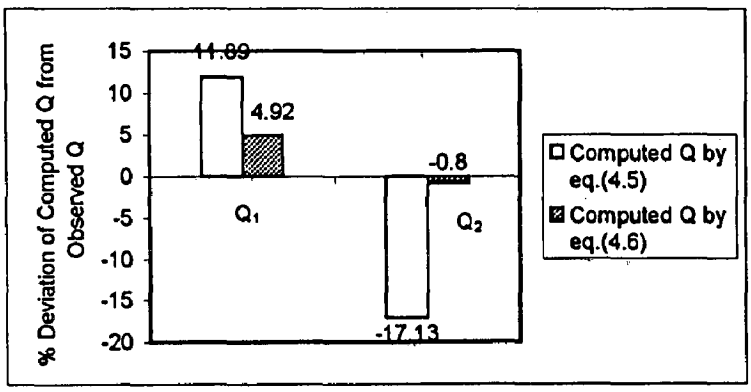

Fig. 4.4(s) Deviation of computed discharge from observed discharge for RunB12 (b/a=0.3, e=20%)

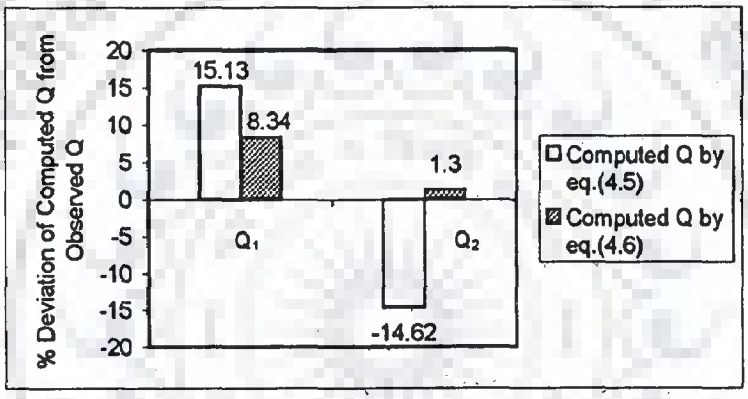

Fig. 4.4(t) Deviation of computed discharge from observed discharge for RunB13 (b/a=0.3, e=20%)

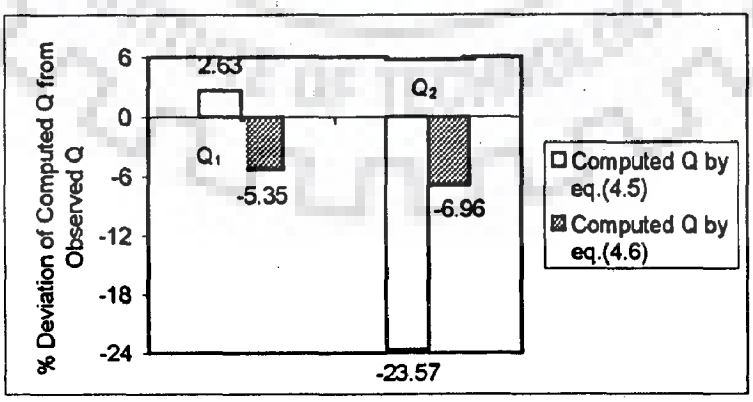

Fig. 4.4(u) Deviation of computed discharge from observed discharge for RunB16 (b/a=0.4, e=20%)

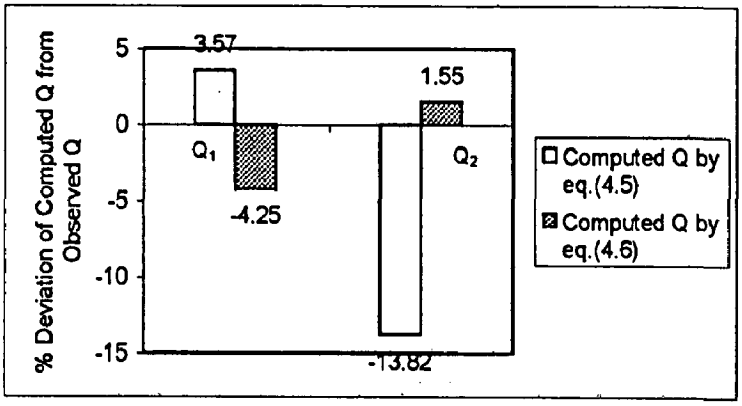

Fig. 4.4(v) Deviation of computed discharge from observed discharge for RunB17 (b/a=0.4, e=20%)

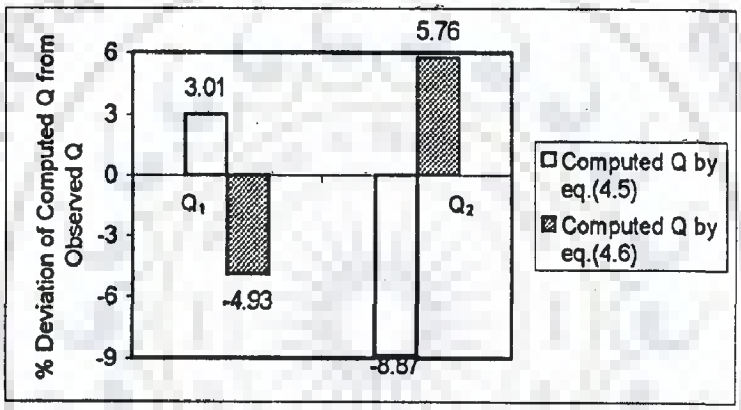

Fig. 4.4(w) Deviation of computed discharge from observed discharge for RunB18 (b/a=0.4, e=20%)

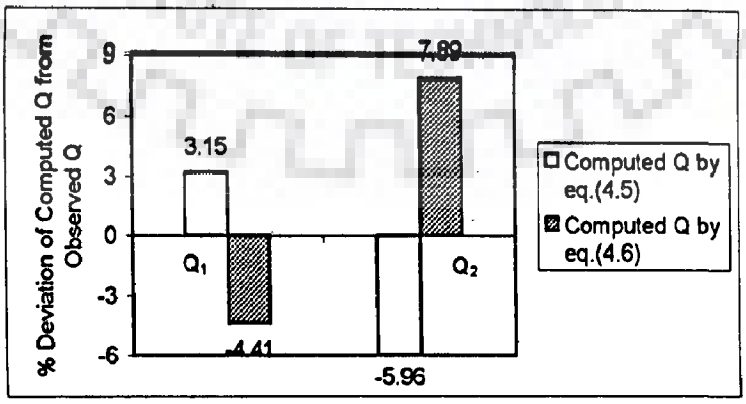

Fig. 4.4(x) Deviation of computed discharge from observed discharge for RunB21 (b/a=0.6, e=20%)

4.8 SUMMARY

In this chapter, based on the experimental data, a relationship has been proposed for division of flow around an island. The applicability of the proposed relationship has been tested for both rigid and mobile bed flow conditions and it has been found that for both the flow conditions the relationship gives good result. Thus, considering the fact that there is no readily available function or relation for determining division of flow around an island, if the average width and the flow depth in the two channels developed due to the presence of the island are known, the discharge values in the two channels can be determined easily using the proposed relationship.

SCOUR PATTERN AROUND ISLAND

5.1 INTRODUCTION

Considering the fact that the islands may have different width to length ratios, five elliptical model islands (rigid) having different width to length ratios (0.15, 0.2, 0.3, 0.4 and 0.6) and a circular model island (width to length ratio of one) were used in the second phase of experiments. The objective of these experiments was to find out the value of width to length ratio of island for which the scour around the island was maximum. For identical conditions of flow, the pattern of scour around the island in the difluence, confluence and transition zones was used to identify the width to length ratio of island corresponding to maximum scour at different Froude numbers.

5.2 SCOUR AROUND ISLANDS

To study this, a set of experiments has been conducted involving five elliptical model islands (rigid) namely I_1 (a=93cm, b=14cm, b/a=0.15), I_2 (a=70cm, b=14cm, b/a=0.2), I_3 (a=60cm, b=18cm, b/a=0.3), I_4 (a=37.5cm, b=15cm, b/a=0.4) and I_5 (a=25cm, b=15cm, b/a=0.6) and a circular model island I_6 (d=15cm). To show the extent of scour around the island, a series of plates are included in this chapter. It can be seen that the scour around the island in the leading edge i.e., in the difluence zone and in the transition zone is different for islands having different width to length ratios under similar flow conditions (Plate 5.1 to Plate 5.15). Experiments were performed at three Froude numbers, i.e., F_r=0.16, F_r=0.19 and F_r=0.2.

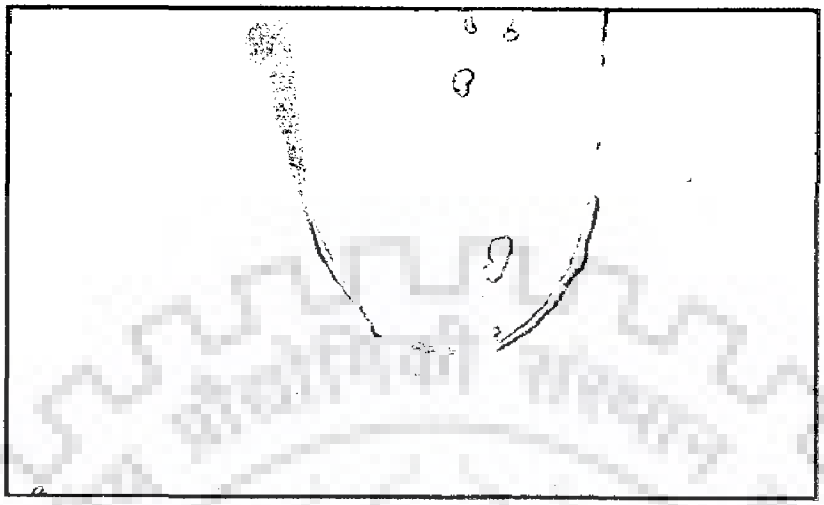

Plate 5.1 Scour around elliptical island I_1 (a=93cm,b=14cm,b/a=0.15) in the difluence and transition zones at Fr=0.16 and h=15cm (RunC1)

Plate 5.2 Scour around elliptical island I_1 (a=93cm,b=14cm,b/a=0.15) in the difluence and transition zones at Fr=0.2 and h=15cm (RunC3)

Plate 5.3 Scour around elliptical island I_2 (a=70cm,b=14cm,b/a=0.2) in the difluence and transition zones at Fr=0.16 and h=15cm (RunC4)

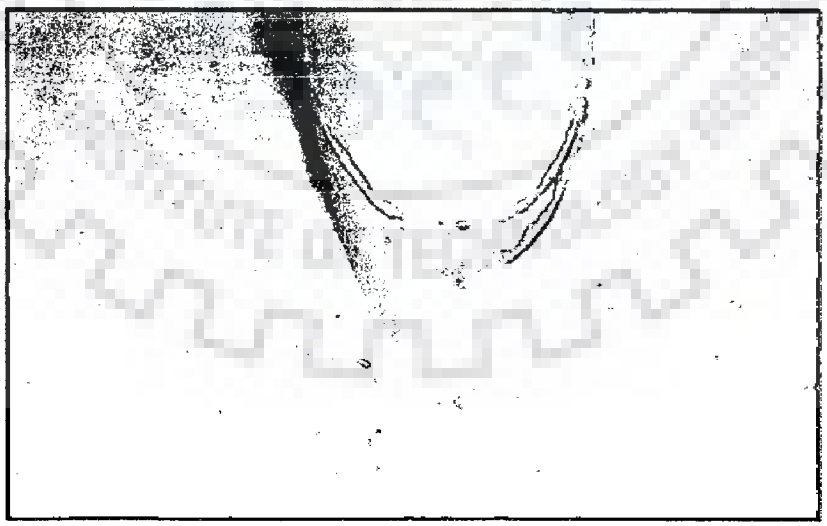

Plate 5.4 Scour around elliptical island I_2 (a=70cm,b=14cm,b/a=0.2) in the difluence and transition zones at Fr=0.19 and h=15cm (RunC5)

Plate 5.5 Scour around elliptical island I_2 (a=70cm,b=14cm,b/a=0.2) in the difluence and transition zones at Fr=0.2 and h=15cm (RunC6)

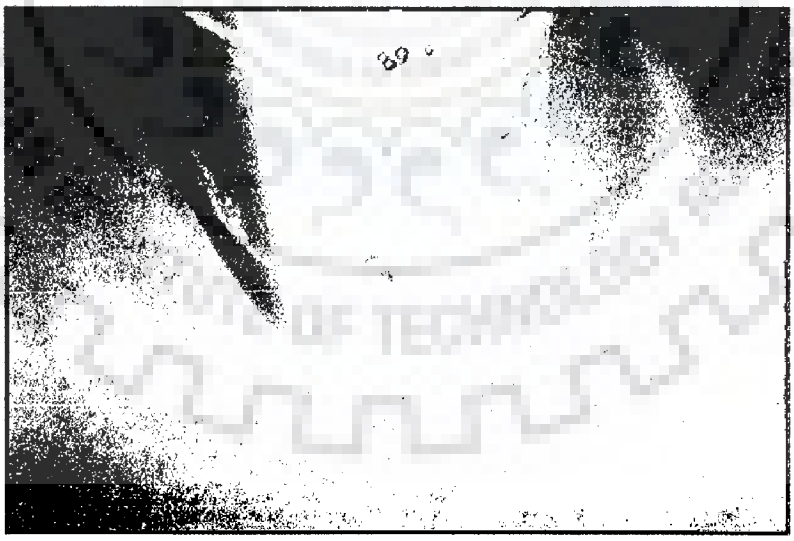

Plate 5.6 Scour around elliptical island I_3 (a=60cm,b=18cm,b/a=0.3) in the difluence and transition zones at Fr=0.16 and h=15cm (RunC7)

Plate 5.7 Scour around elliptical island I_3 (a=60cm,b=18cm,b/a=0.3) in the difluence and transition zones at Fr=0.19 and h=15cm (RunC8)

Plate 5.8 Scour around elliptical island I_4 (a=37.5cm,b=15cm,b/a=0.4) in the difluence and transition zones at Fr=0.16 and h=15cm (RunC9)

Plate 5.9 Scour around elliptical island I_4 (a=37.5cm,b=15cm,b/a=0.4) in the difluence and transition zones at Fr=0.19 and h=15cm (RunC10)

Plate 5.10 Scour around elliptical island I_4 (a=37.5cm,b=15cm,b/a=0.4) in the difluence and transition zones at Fr=0.2 and h=15cm (RunC11)

Plate 5.11 Scour around elliptical island I_5 (a=25cm,b=15cm,b/a=0.6) in the difluence and transition zones at Fr=0.16 and h=15cm (RunC12)

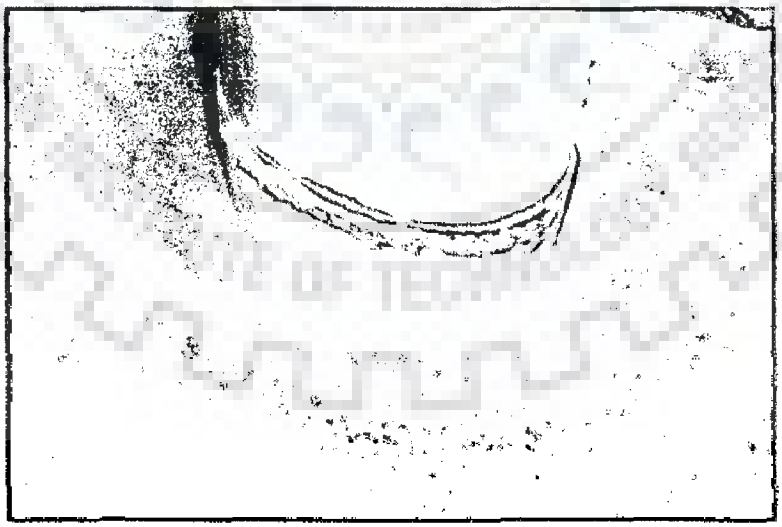

Plate 5.12 Scour around elliptical island I_5 (a=25cm,b=15cm,b/a=0.6) in the difluence and transition zones at Fr=0.19 and h=15cm (RunC13)

Plate 5.13 Scour around elliptical island I_5 (a=25cm,b=15cm,b/a=0.6) in the difluence and transition zones at Fr=0.2 and h=15cm (RunC14)

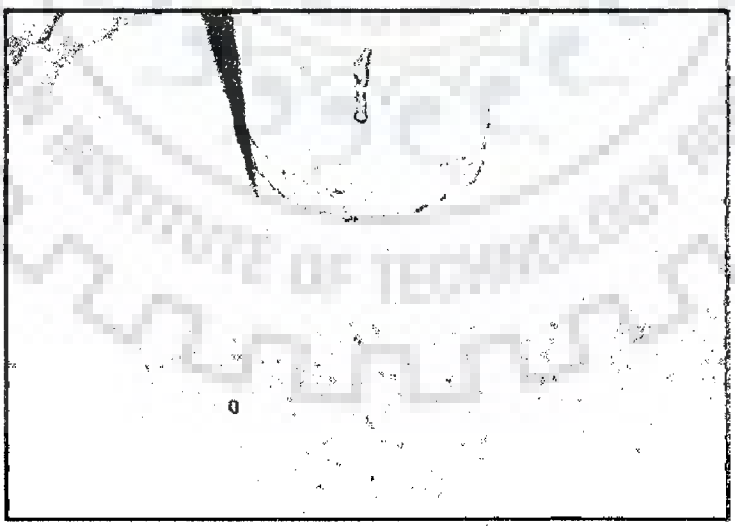

Plate 5.14 Scour around circular island I_6 (d=15cm) in the difluence and transition zones at Fr=0.16 and h=15cm (RunC15)

Plate 5.15 Scour around circular island I_6 (d=15cm) in the difluence and transition zones at Fr=0.19 and h=15cm (RunC16)

5.3 EXPERIMENTS AT FROUDE NUMBER F_r= 0.16

In case of elliptical island I_1, it was observed that initially scour started at the leading edge, i.e., in the difluence zone of island as well as near the middle of the transition zone and then the scour extended towards downstream. Referring to Fig. 5.1 and Fig. 5.2, scour was maximum near the middle of the transition zone. From Fig. 5.3 to Fig. 5.10, it is clear that the scour pattern around elliptical islands I_2, I_3, I_4 and I_5 was similar to that around island I_1, except that for islands I_4 and I_5, the maximum scour was observed near the leading edge of island. In all the cases, deposition was found to occur in the confluence zone starting from the end part of the transition zone. In case of the circular island I_6 (Fig.5.11 & Fig. 5.12), scour was found to increase gradually from the difluence zone, with maximum scour near the middle of transition zone and deposition started to occur in the confluence zone some distance downstream of the rear end of the island. Almost in all the cases, in the difluence zone scour increased towards the island and in the transition zone scour increased away from the island.

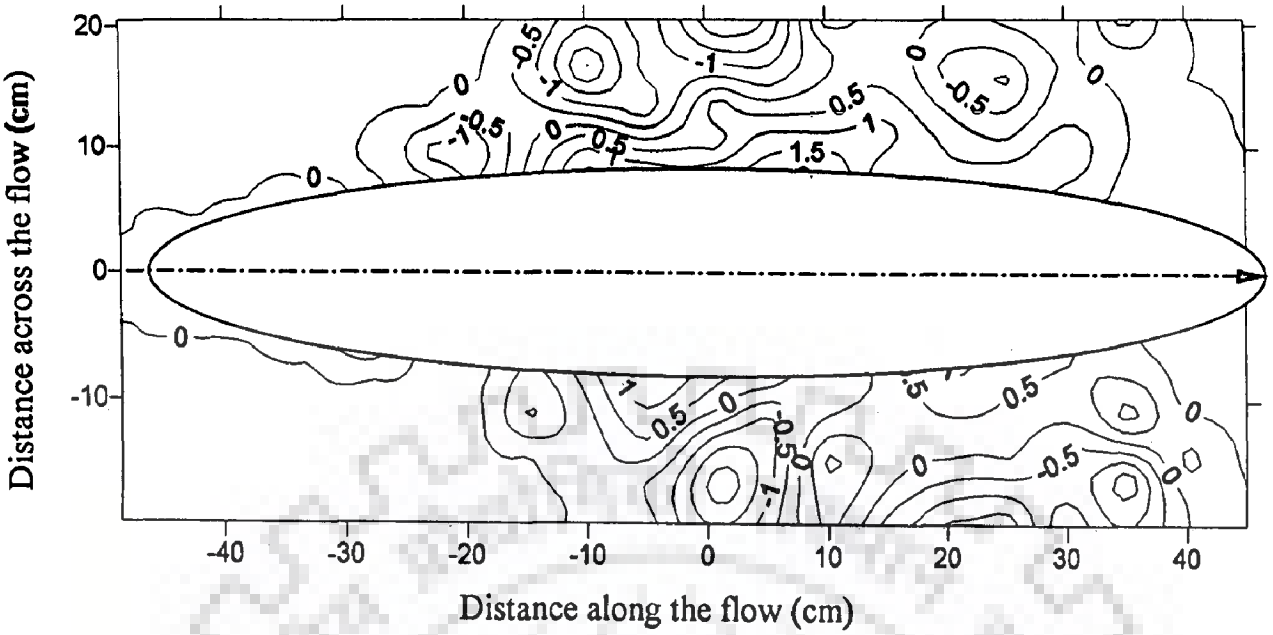

Fig. 5.1 Scour pattern around elliptical island I_1 (b/a=0.15) at F_r=0.16 & h=15cm (contour interval in cm) (RunC1)

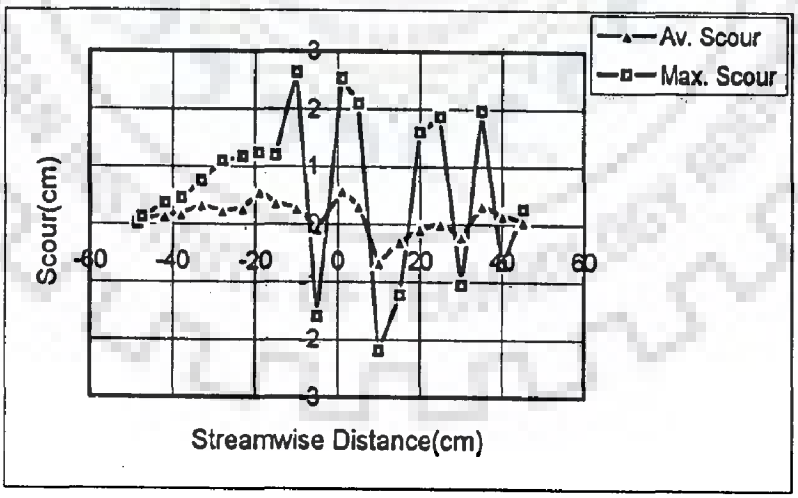

Fig. 5.2 Streamwise variation of scour around elliptical island I_1 (b/a=0.15) at F_r =0.16 & h=15cm (RunC1)

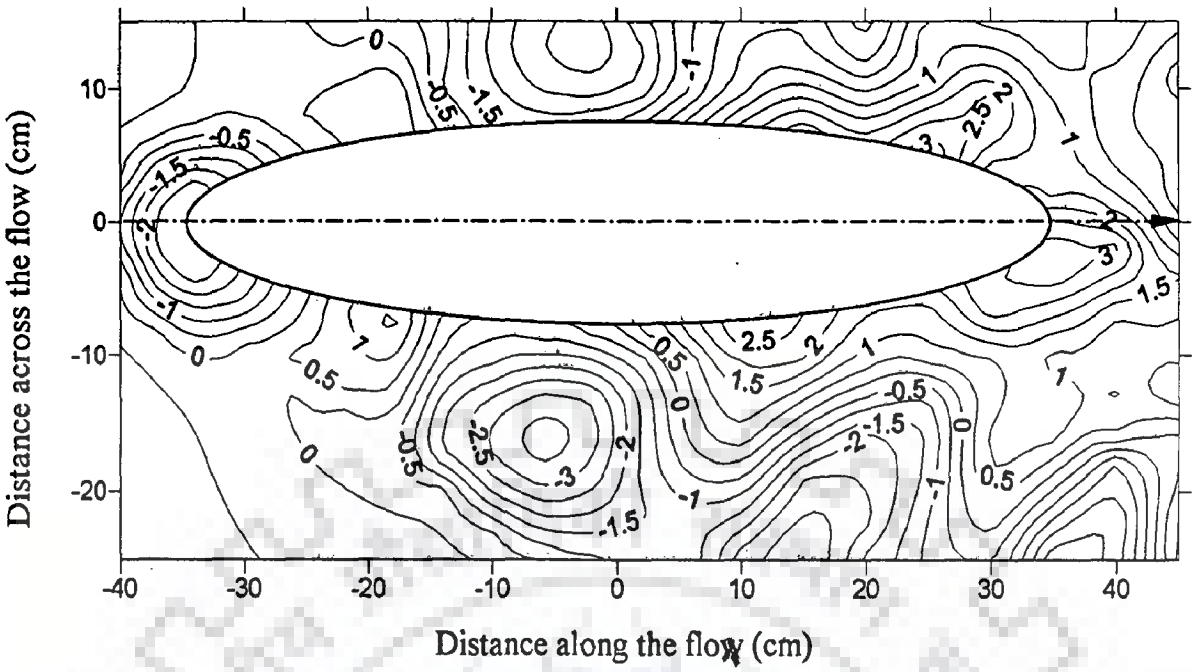

Fig. 5.3 Scour pattern around elliptical island I_2 (b/a=0.2) at F_r=0.16 & h=15cm (contour interval in cm) (RunC4)

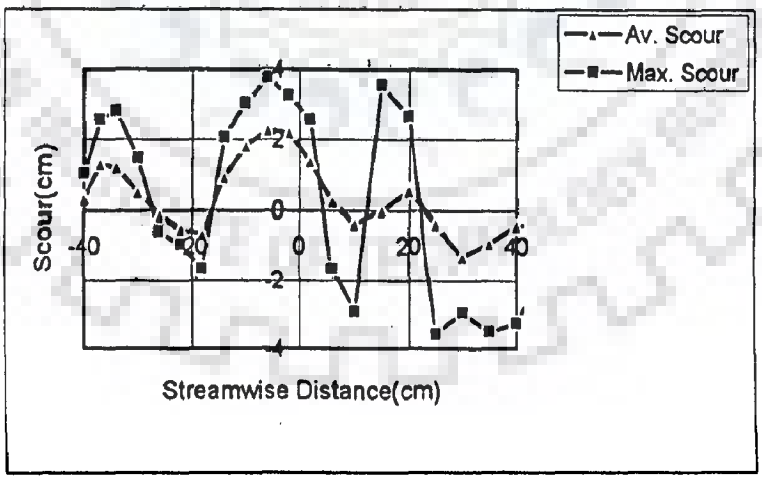

Fig. 5.4 Streamwise variation of scour around elliptical island I_2 (b/a=0.2) at F_r =0.16 & h=15cm (RunC4)

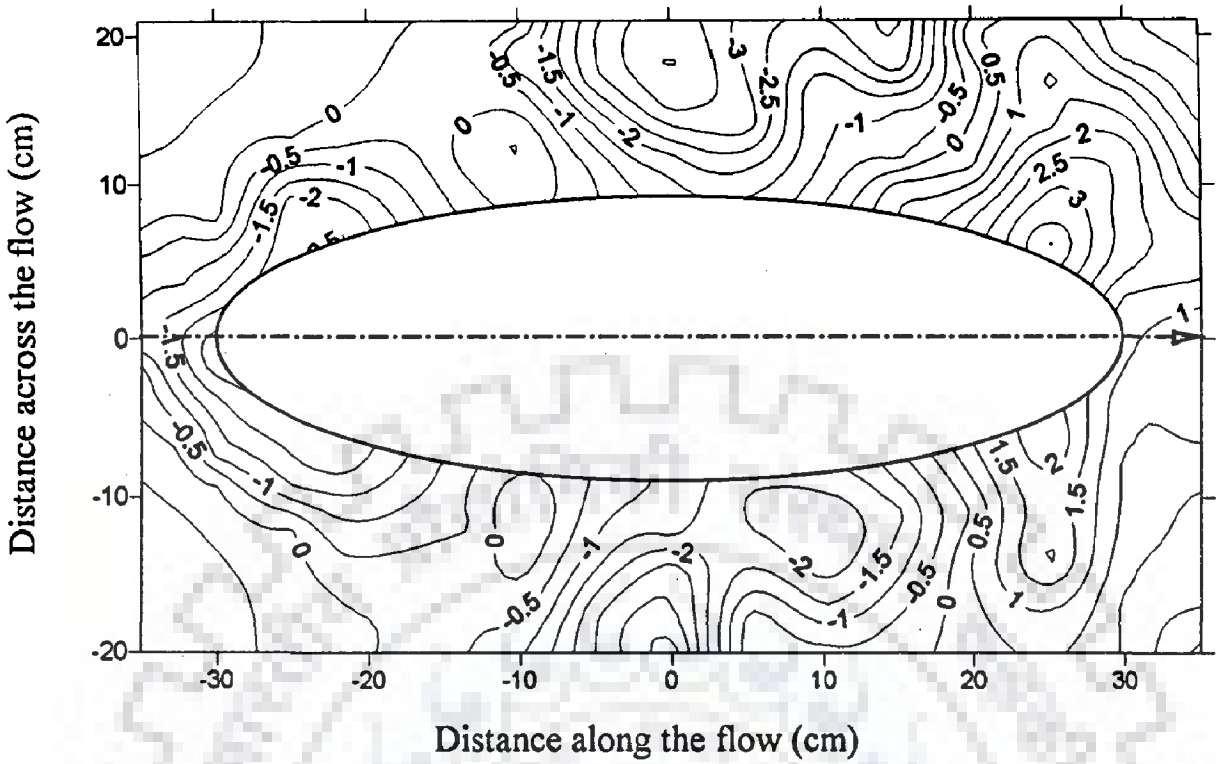

Fig. 5.5 Scour pattern around elliptical island I_3 (b/a=0.3) at F_r=0.16 & h=15cm (contour interval in cm) (RunC7)

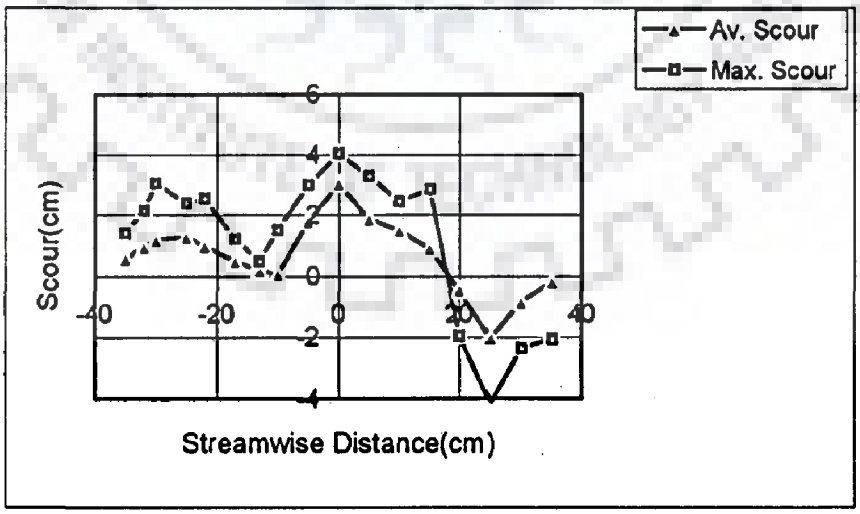

Fig. 5.6 Streamwise variation of scour around elliptical island I_3 (b/a=0.3) at F_r =0.16 & h=15cm (RunC7)

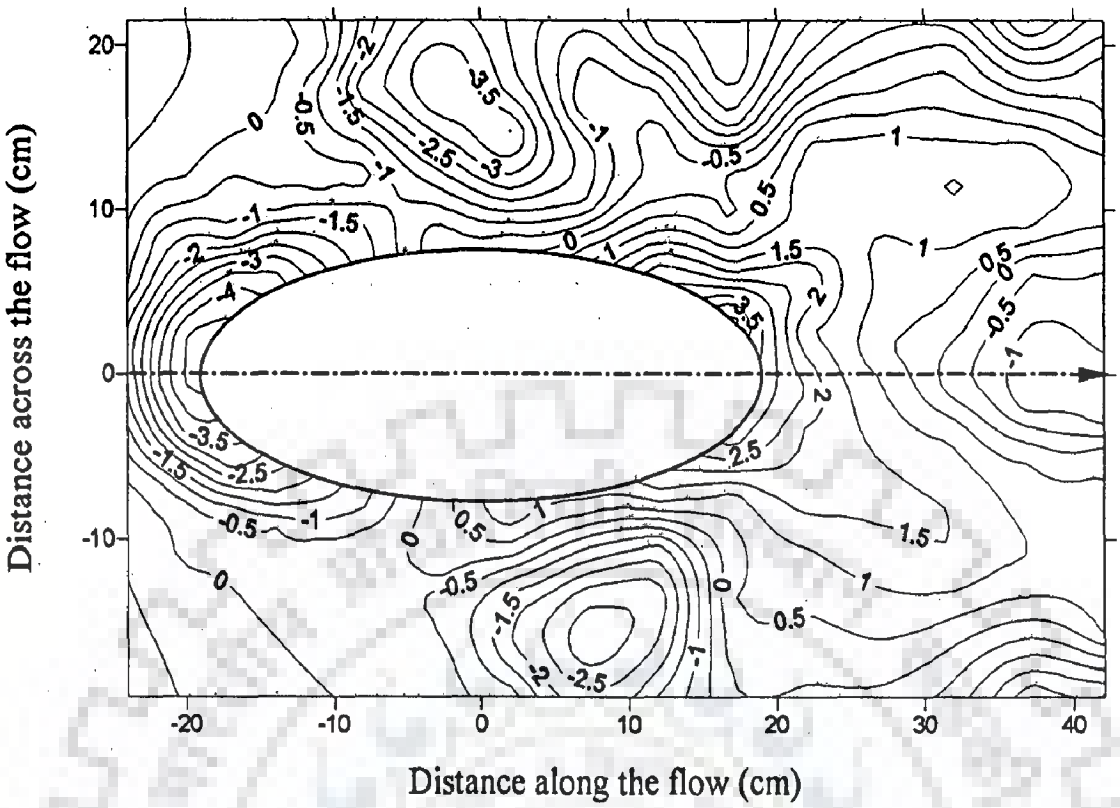

Fig. 5.7 Scour pattern around elliptical island I_4 (b/a=0.4) at F_r=0.16 & h=15cm (contour interval in cm) (RunC9)

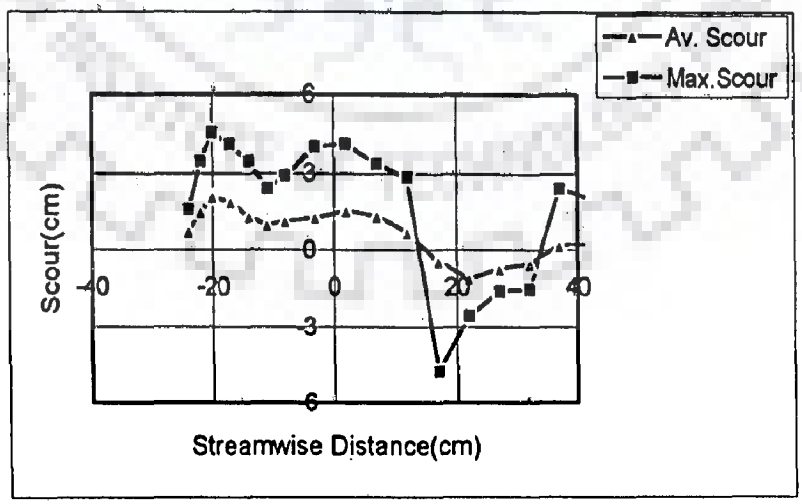

Fig. 5.8 Streamwise variation of scour around elliptical island I_4 (b/a=0.4) at F_r =0.16 & h=15cm (RunC9)

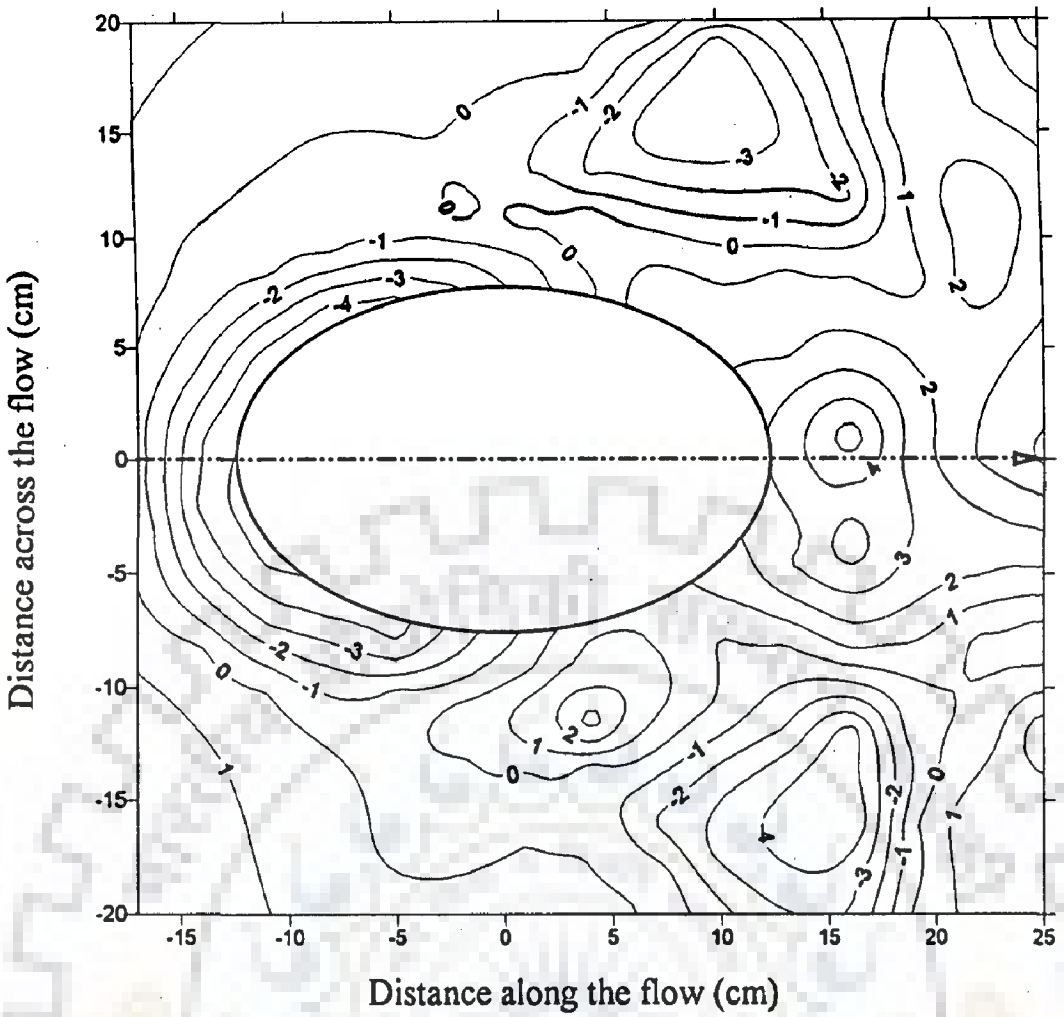

Fig. 5.9 Scour pattern around elliptical island I_5 (b/a=0.6) at F_r=0.16 & h=15cm (contour interval in cm) (RunC12)

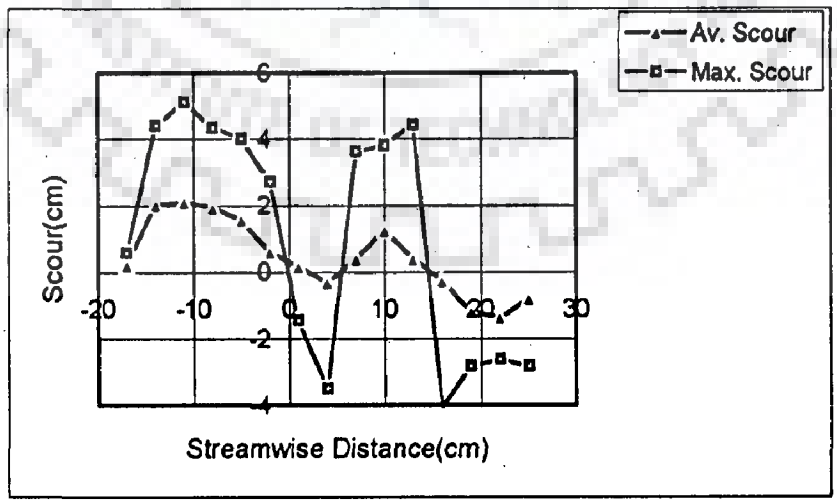

Fig. 5.10 Streamwise variation of scour around elliptical island I_5 (b/a=0.6) at F_r =0.16 & h=15cm (RunC12)

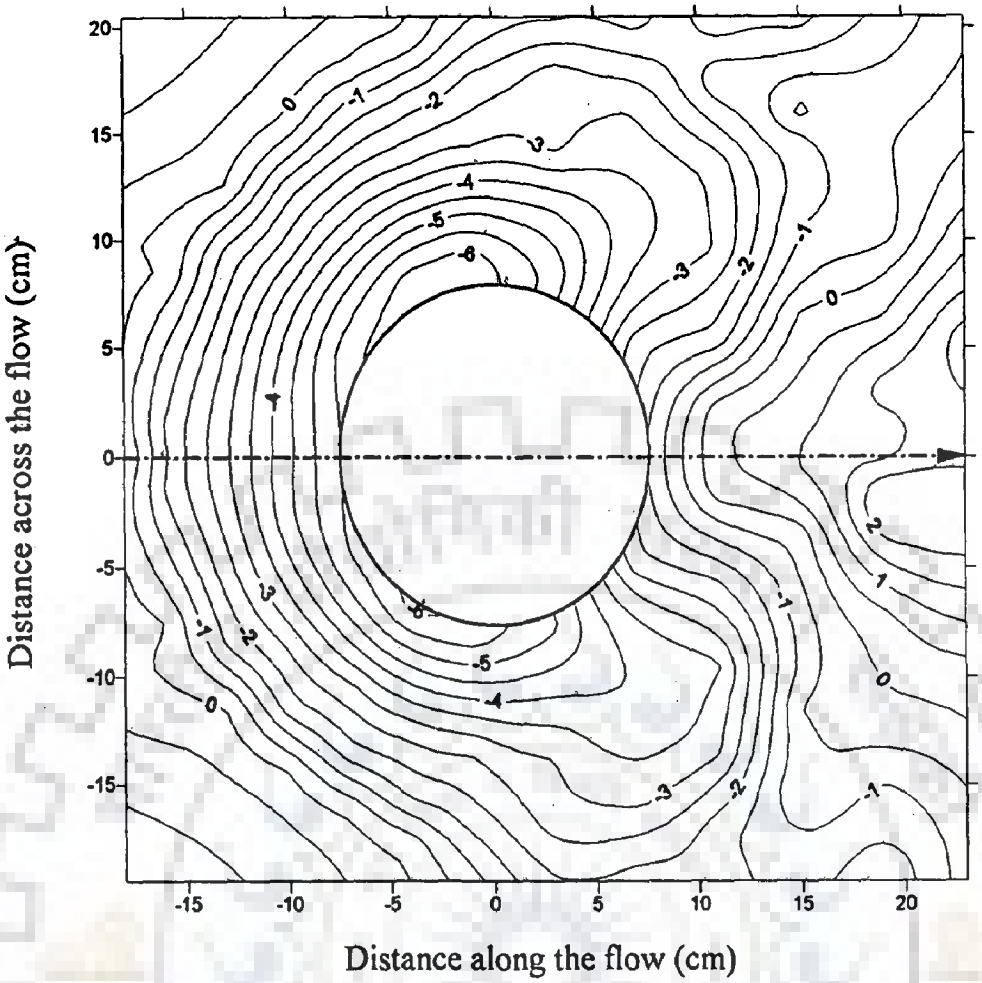

Fig. 5.11 Scour pattern around circular island I_6 (d=15cm) at F_r=0.16& h=15cm (contour interval in cm) (RunC15)

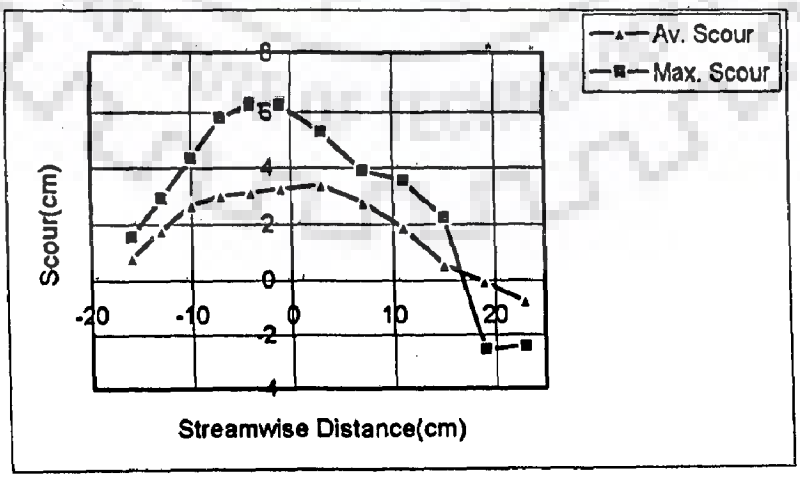

Fig. 5.12 Streamwise variation of scour around circular island I_6 (d=15cm) at F_r =0.16& h=15cm (RunC15)

5.4 EXPERIMENTS AT FROUDE NUMBER F_r= 0.19

It is seen from Fig. 5.13 to Fig. 5.18 that for islands I_1 and I_2, the scour was maximum near the leading edge of the island, i.e., in the difluence zone while in case of island I_3, scour was maximum near the middle of the transition zone. For islands I_1 and I_2, deposition started to occur from the end part of the transition zone and for island I_3, deposition started to occur from the beginning of the confluence zone. For island I_4 (Fig. 5.19 and Fig. 5.20), maximum scour was observed near the leading edge of the island and deposition was found to occur just from the beginning of the confluence zone. For island I_5 (Fig. 5.21 and Fig. 5.22), maximum scour occurred near the leading edge of the island, then scour gradually decreased and deposition started to occur from the end part of the transition zone. In case of island I_6 (Fig. 5.23 and Fig. 5.24), scour gradually increased from the difluence zone and was maximum near the middle of the transition zone. Then scour gradually decreased and deposition started to occur in the confluence zone far distance downstream of the island.

5.5 EXPERIMENTS AT FROUDE NUMBER F_r= 0.2

In case of islands I_1 and I_2 (Fig. 5.25 to Fig. 5.28), the maximum scour was observed near the leading edge of the island, i.e., in the difluence zone around the island and deposition started to occur from the end part of the transition zone. For islands I_4 and I_5 (Fig. 5.29 to Fig. 5.32), the maximum value of scour was observed near the leading edge of the island. Then scour gradually decreased and deposition started to occur from the end part of the transition zone.

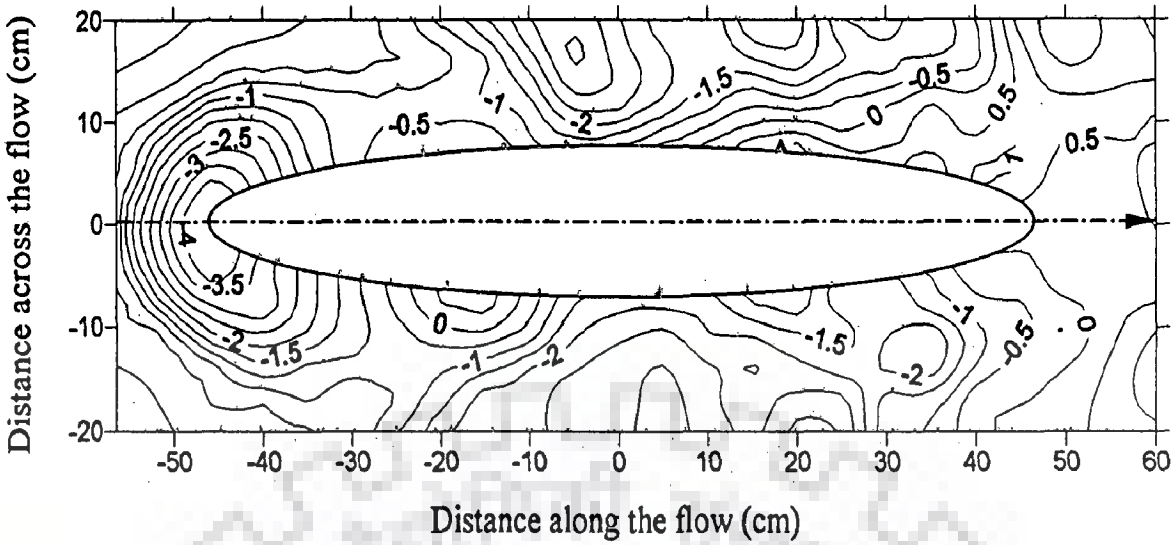

Fig. 5.13 Scour pattern around elliptical island I_1 (b/a=0.15) at F_r=0.19 & h=15cm (contour interval in cm) (RunC2)

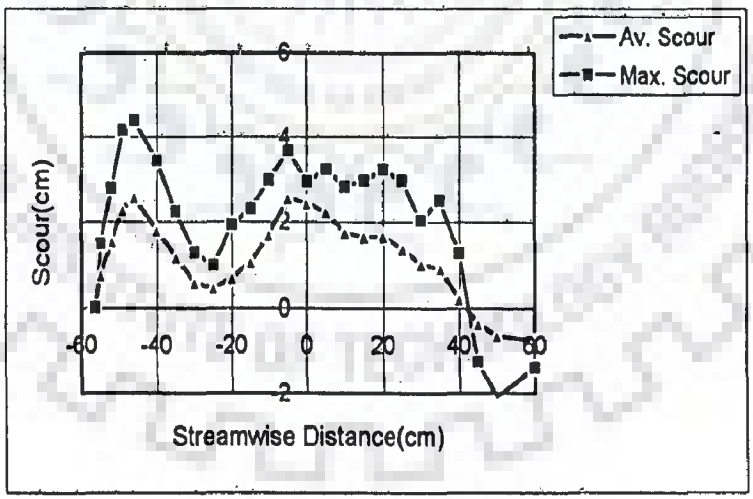

Fig. 5.14 Streamwise variation of scour around elliptical island I_1 (b/a=0.15) at F_r =0.19 & h=15cm (RunC2)

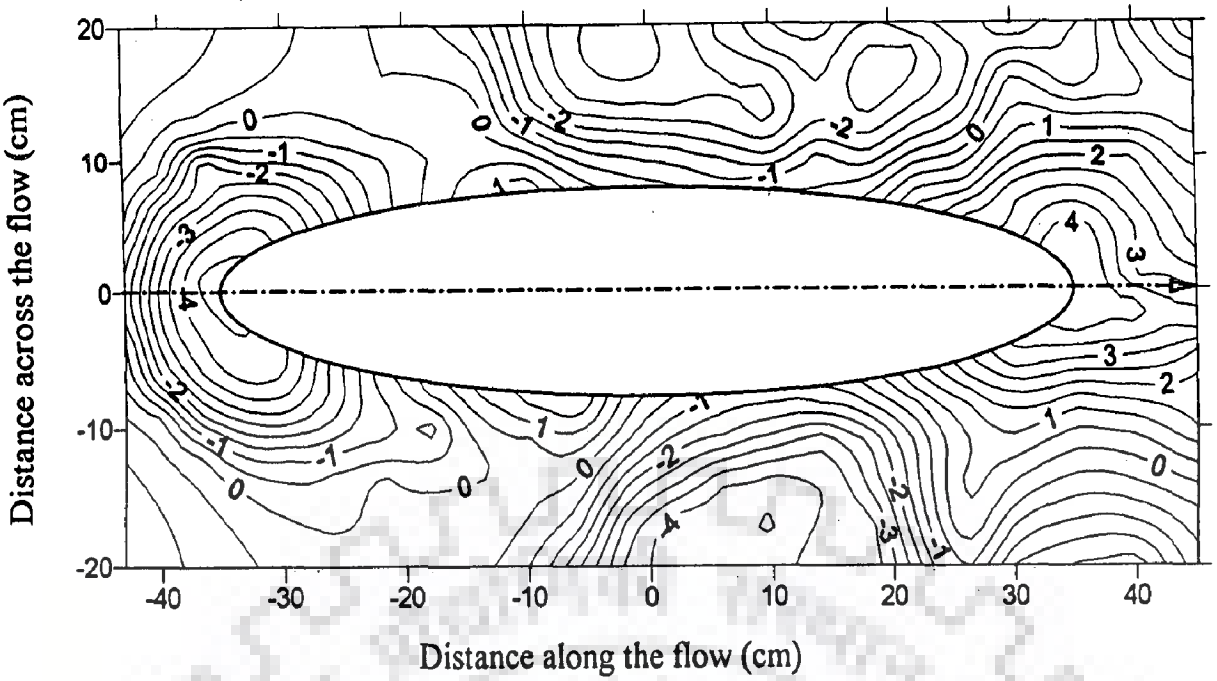

Fig. 5.15 Scour pattern around elliptical island I_2 (b/a=0.2) at F_r=0.19 & h=15cm (contour interval in cm) (RunC5)

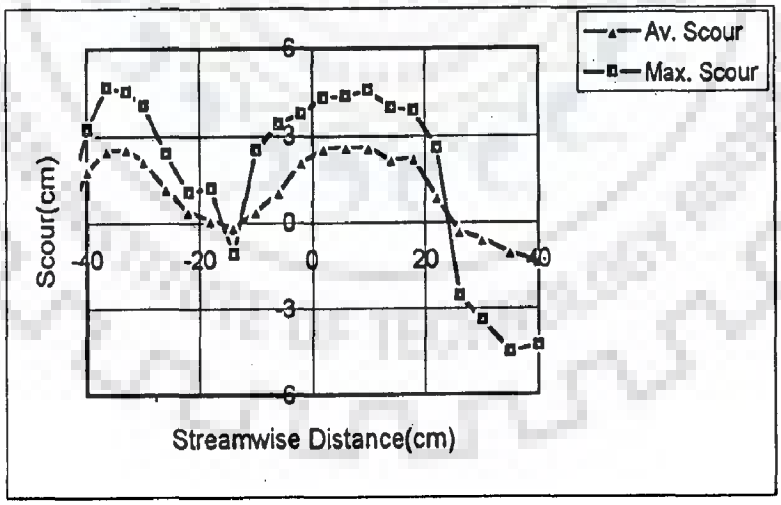

Fig. 5.16 Streamwise variation of scour around elliptical island I_2 (b/a=0.2) at F_r =0.19 & h=15cm (RunC5)

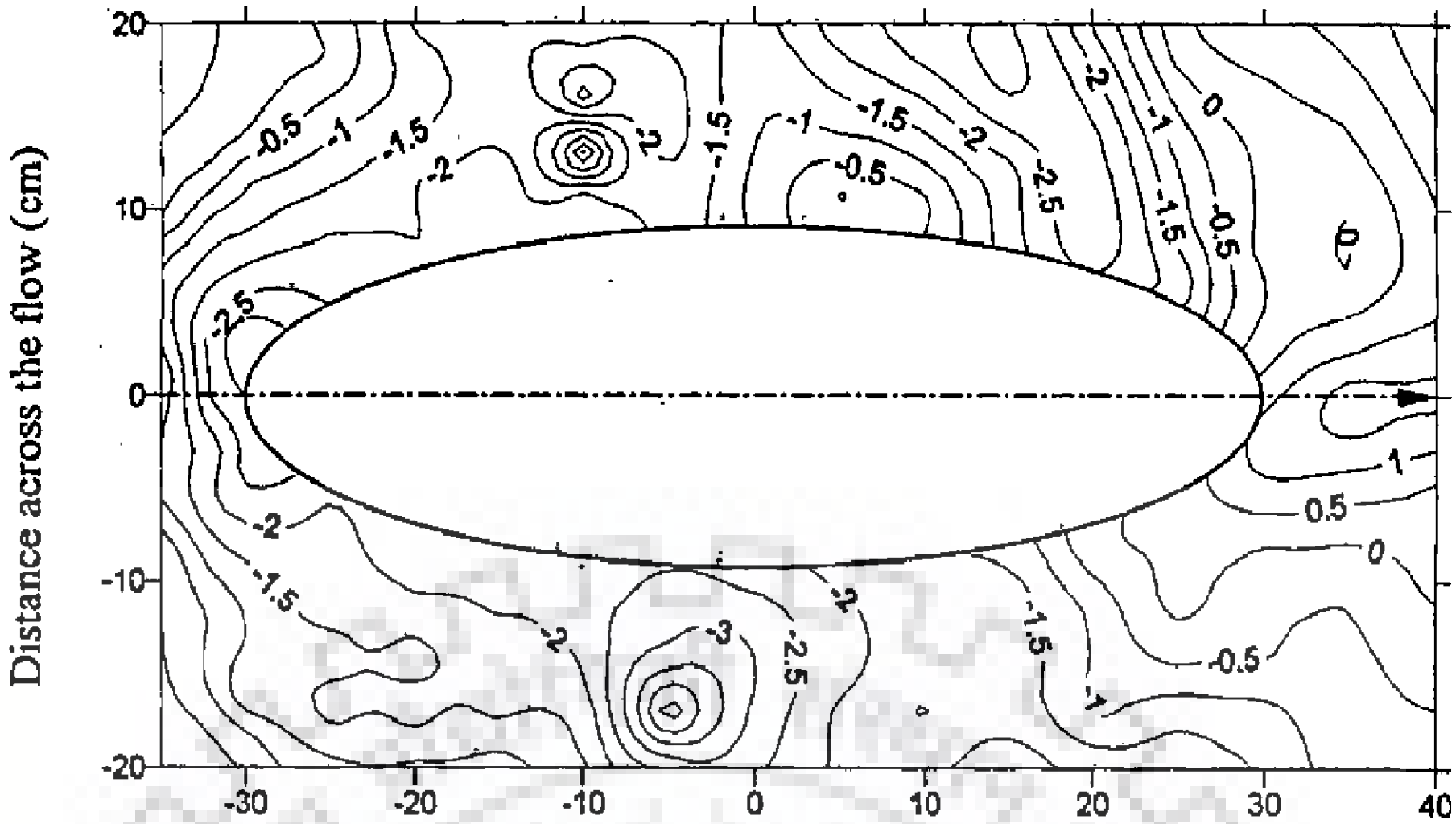

Fig. 5.17 Scour pattern around elliptical island I_3 (b/a=0.3) at F_r=0.19 & h=15cm (contour interval in cm) (RunC8)

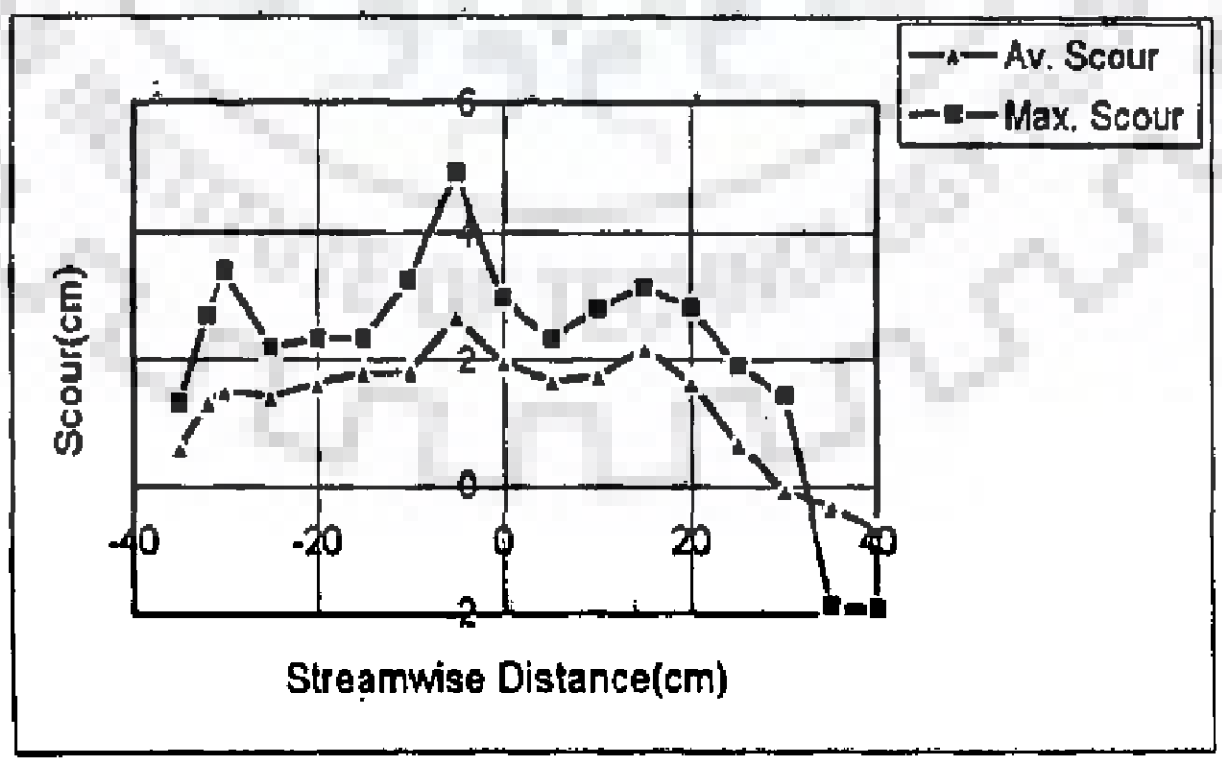

Fig. 5.18 Streamwise variation of scour around elliptical island I_3 (b/a=0.3) at F_r =0.19 & h=15cm (RunC8)

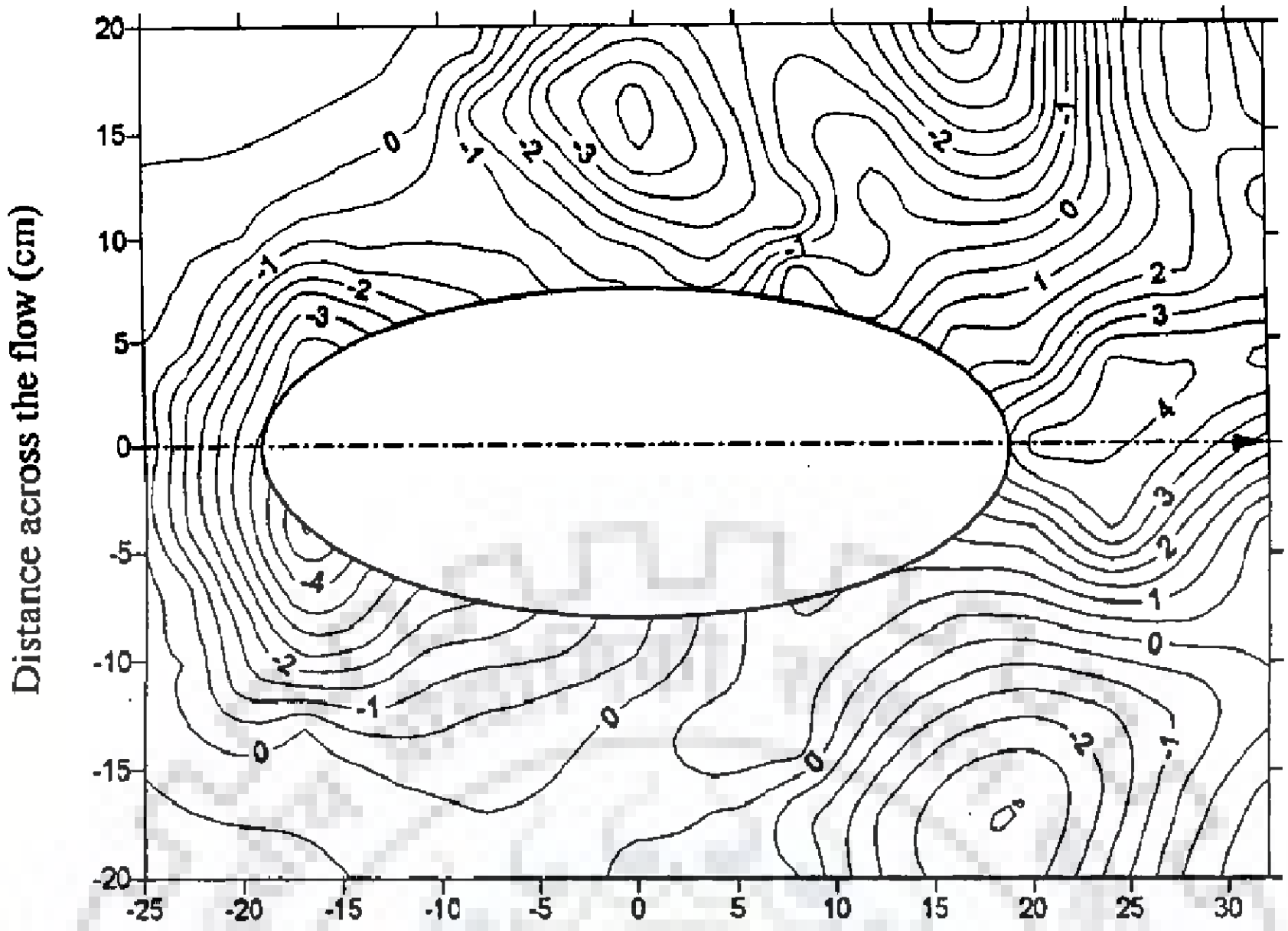

Fig. 5.19 Scour pattern around elliptical island I_4 (b/a=0.4) at F_r=0.19 & h=15cm (contour interval in cm) (RunC10)

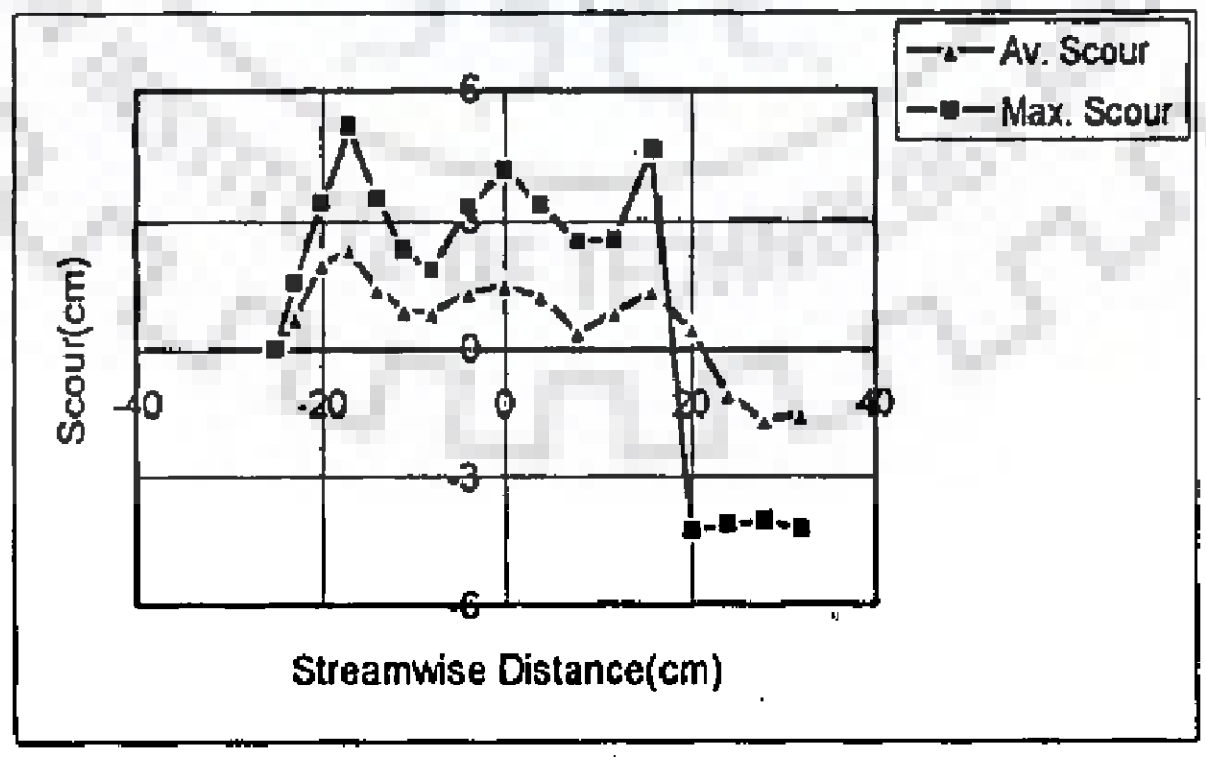

Fig. 5.20 Streamwise variation of scour around elliptical island I_4 (b/a=0.4) at F_r =0.19 & h=15cm (RunC10)

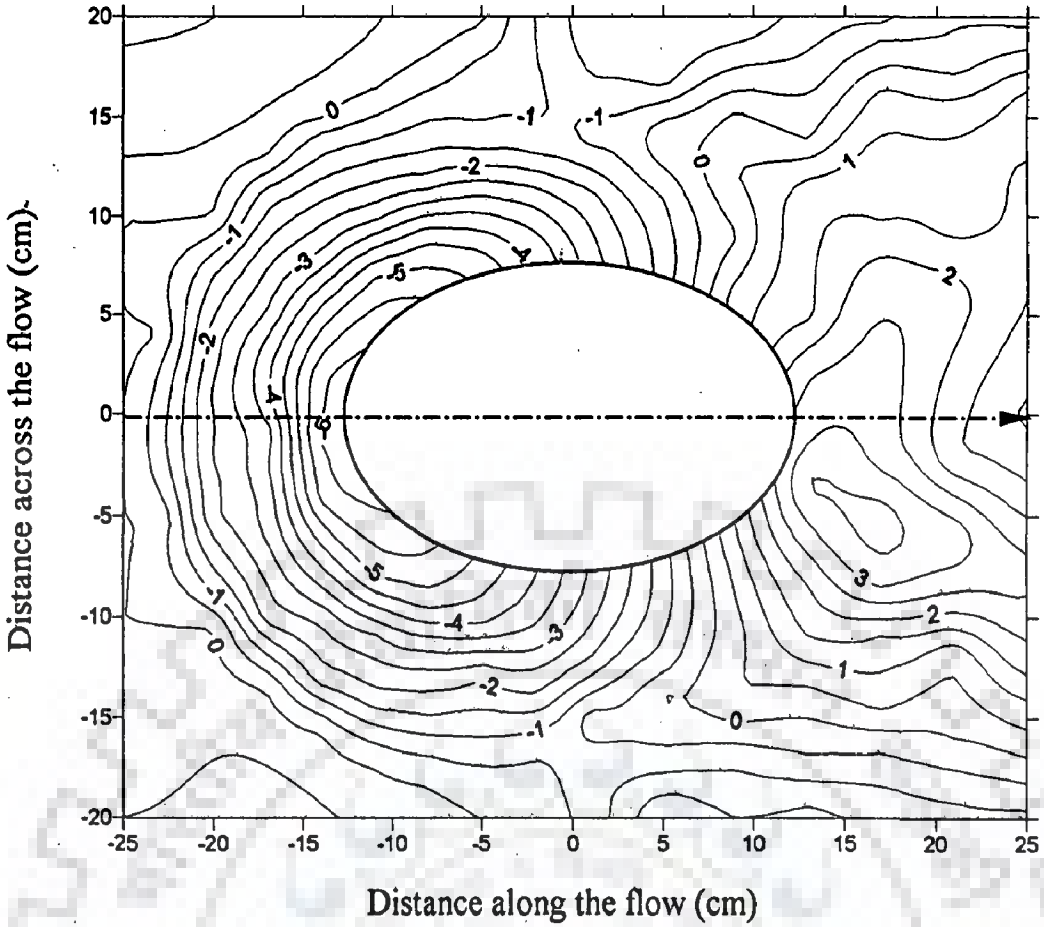

Fig. 5.21 Scour pattern around elliptical island I_5 (b/a=0.6) at F_r=0.19 & h=15cm (contour interval in cm) (RunC13)

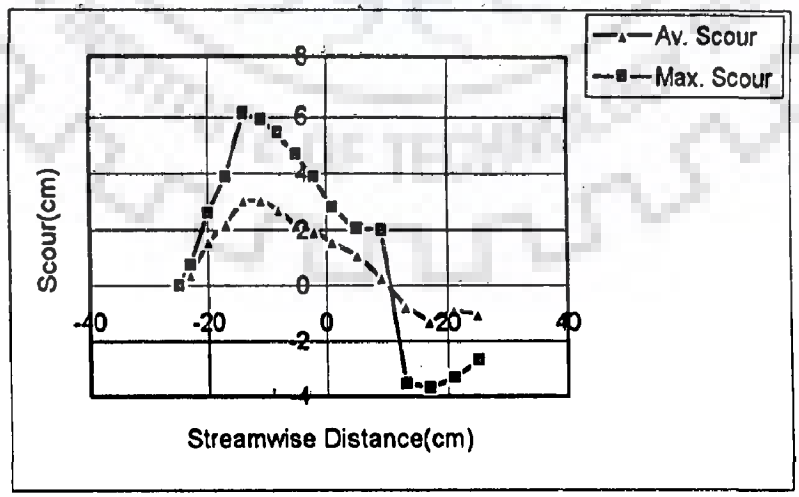

Fig. 5.22 Streamwise variation of scour around elliptical island I_5 (b/a=0.6) at F_r =0.19 & h=15cm (RunC13)

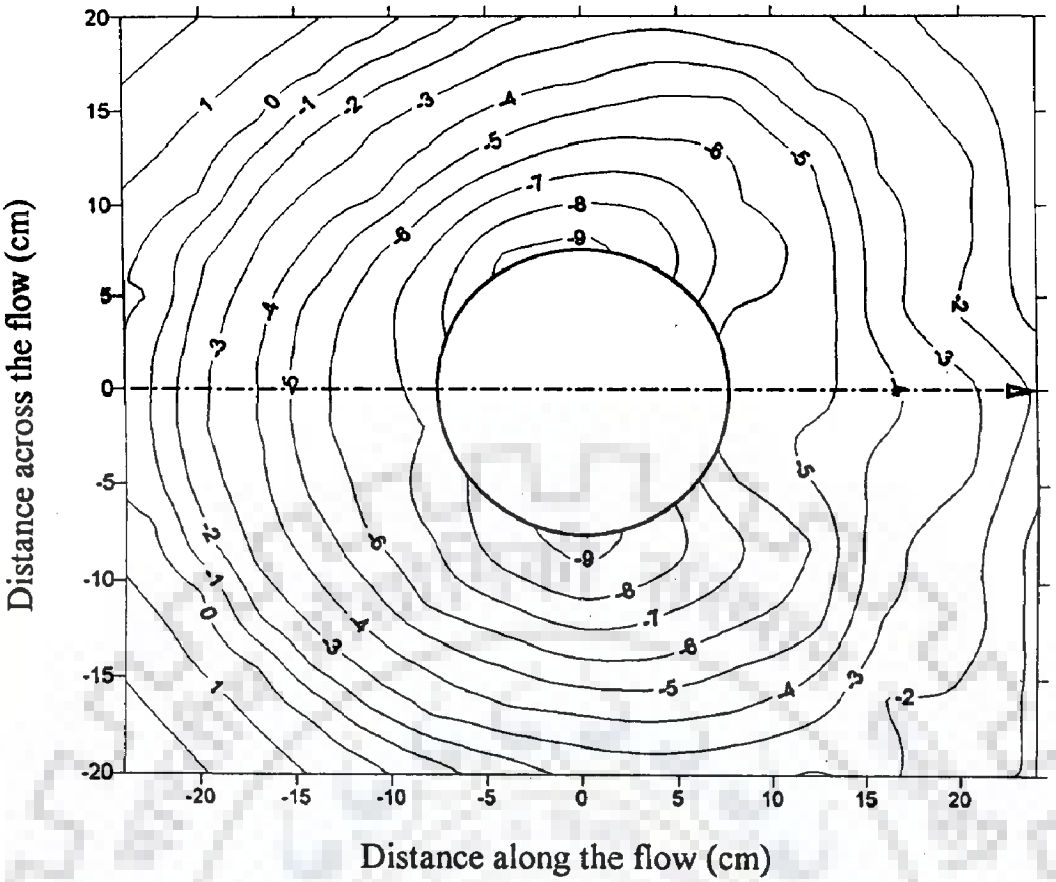

Fig. 5.23 Scour pattern around circular island I_6 (d=15cm) at F_r=0.19& h=15cm (contour interval in cm) (RunC16)

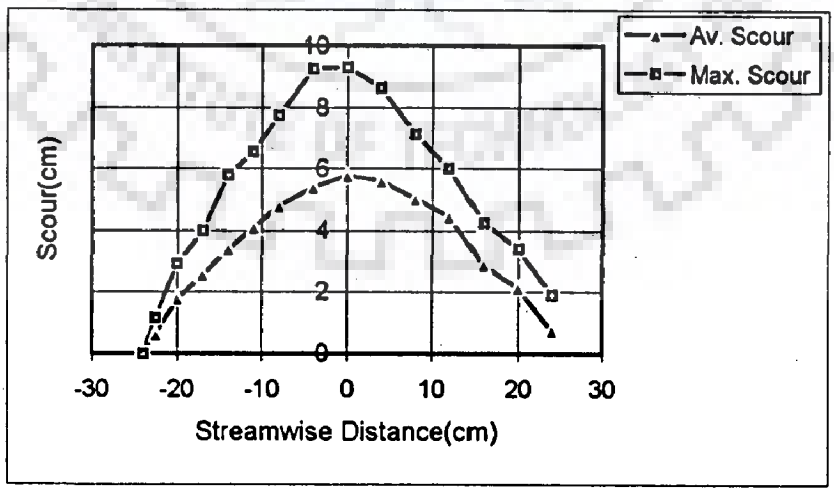

Fig. 5.24 Streamwise variation of scour around circular island I_6 (d=15cm) at F_r =0.19& h=15cm (RunC16)

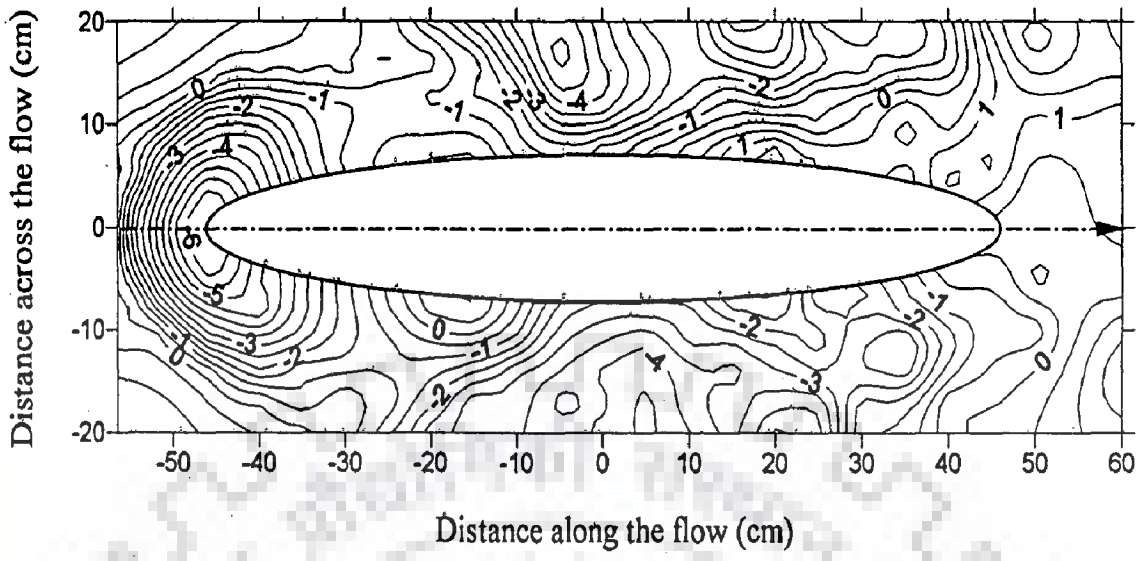

Fig. 5.25 Scour pattern around elliptical island I_1 (b/a=0.15) at F_r=0.20 & h=15cm (contour interval in cm) (RunC3)

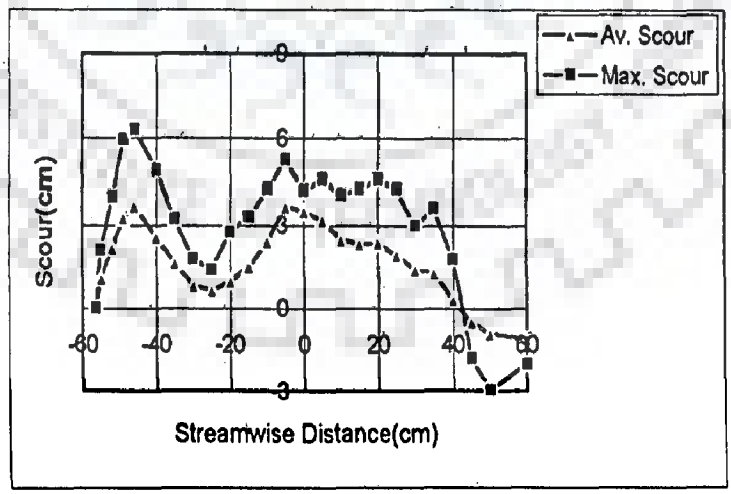

Fig. 5.26 Streamwise variation of scour around elliptical island I_1 (b/a=0.15) at F_r =0.2 & h=15cm (RunC3)

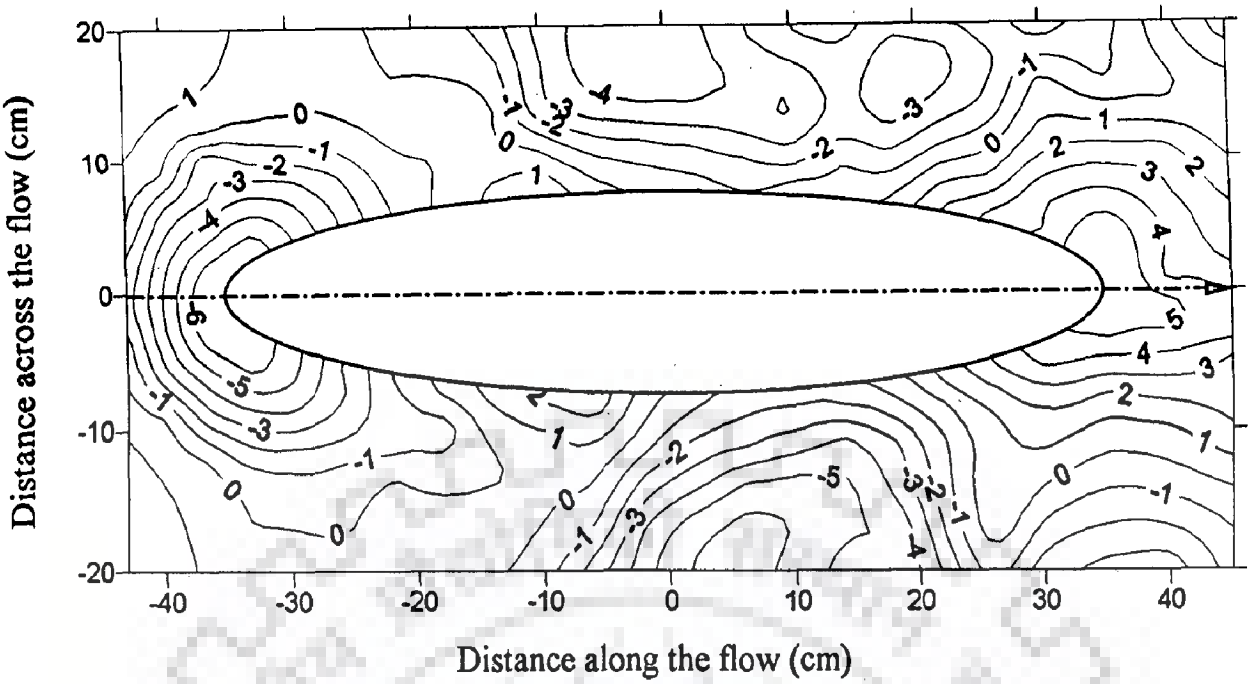

Fig. 5.27 Scour pattern around elliptical island I_2 (b/a=0.2) at F_r=0.2 & h=15cm (contour interval in cm) (RunC6)

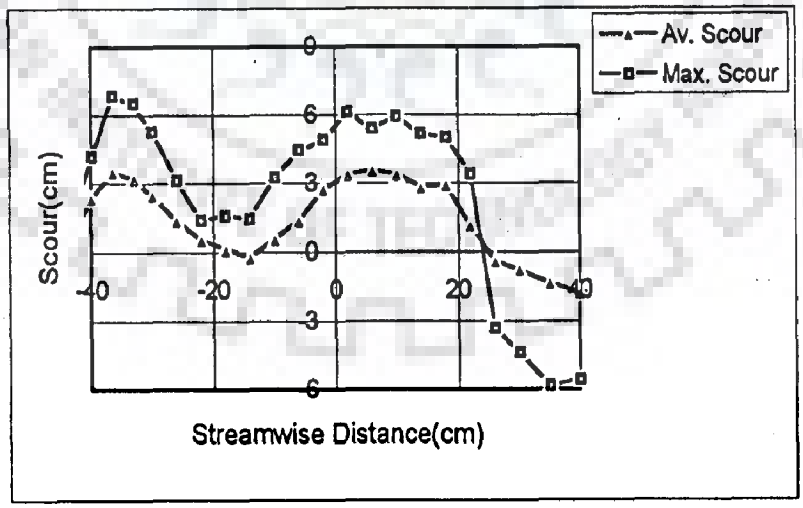

Fig. 5.28 Streamwise variation of scour around elliptical island I_2 (b/a=0.2) at F_r =0.2 & h=15cm (RunC6)

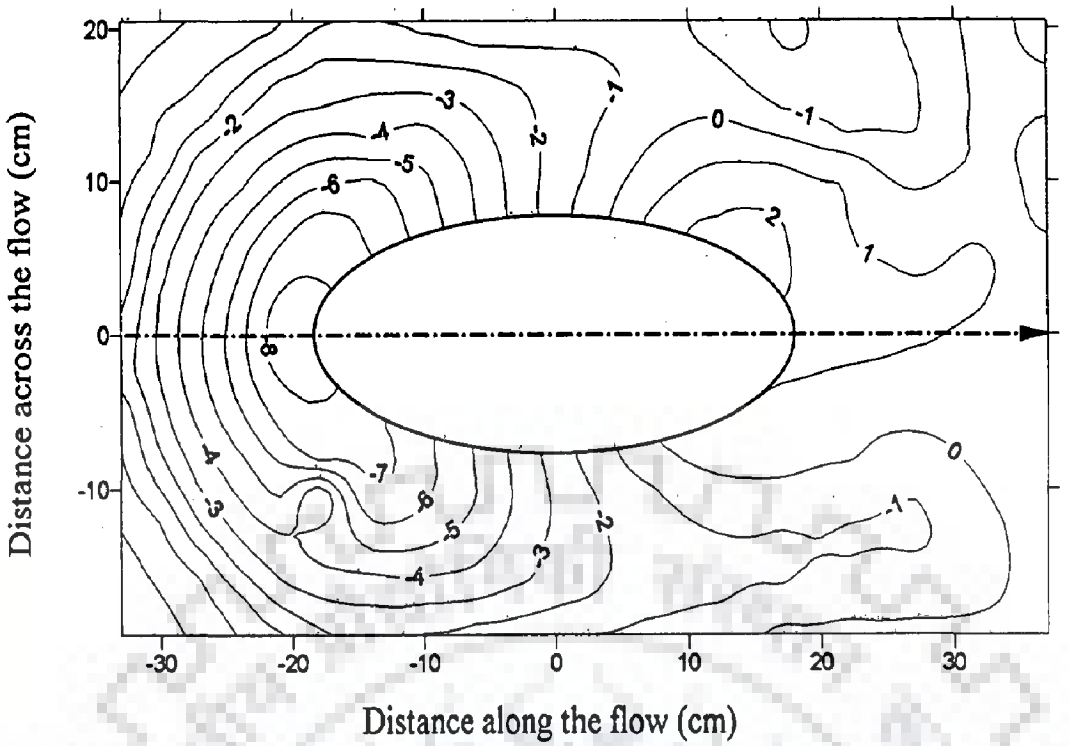

Fig. 5.29 Scour pattern around elliptical island I_4 (b/a=0.4) at F_r=0.20 & h=15cm (contour interval in cm) (RunC11)

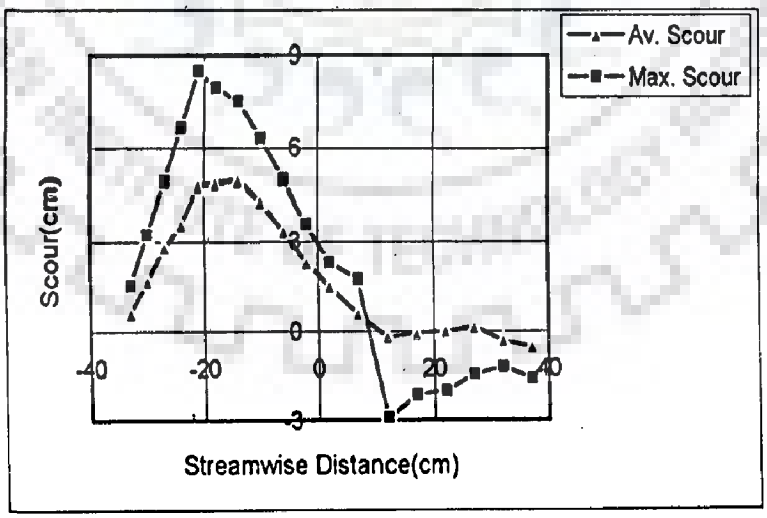

Fig. 5.30 Streamwise variation of scour around elliptical island I_4 (b/a=0.4) at F_r =0.20 & h=15cm (RunC11)

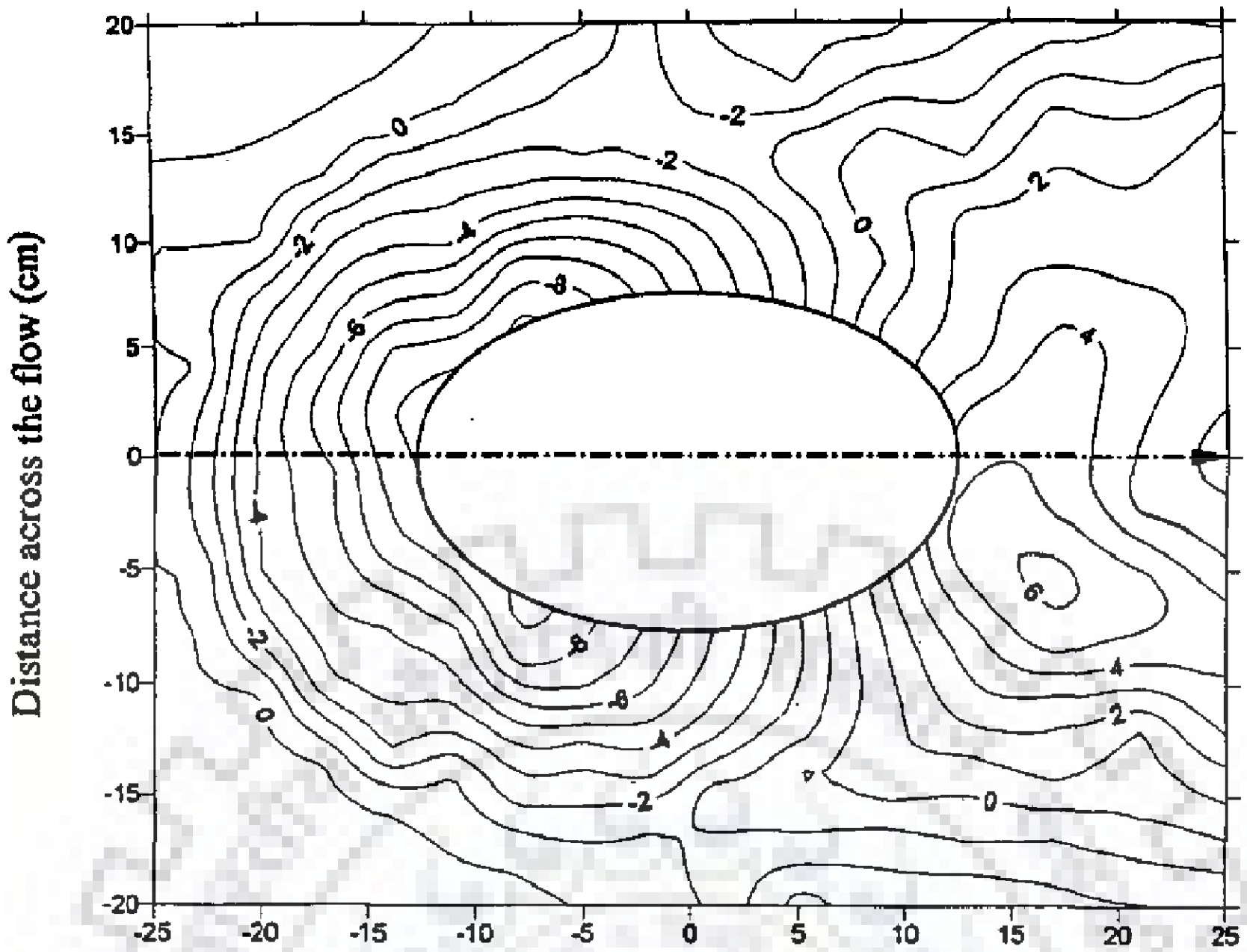

Fig. 5.31 Scour pattern around elliptical island I_5 (b/a=0.6) at F_r=0.2 & h=15cm (contour interval in cm) (RunC14)

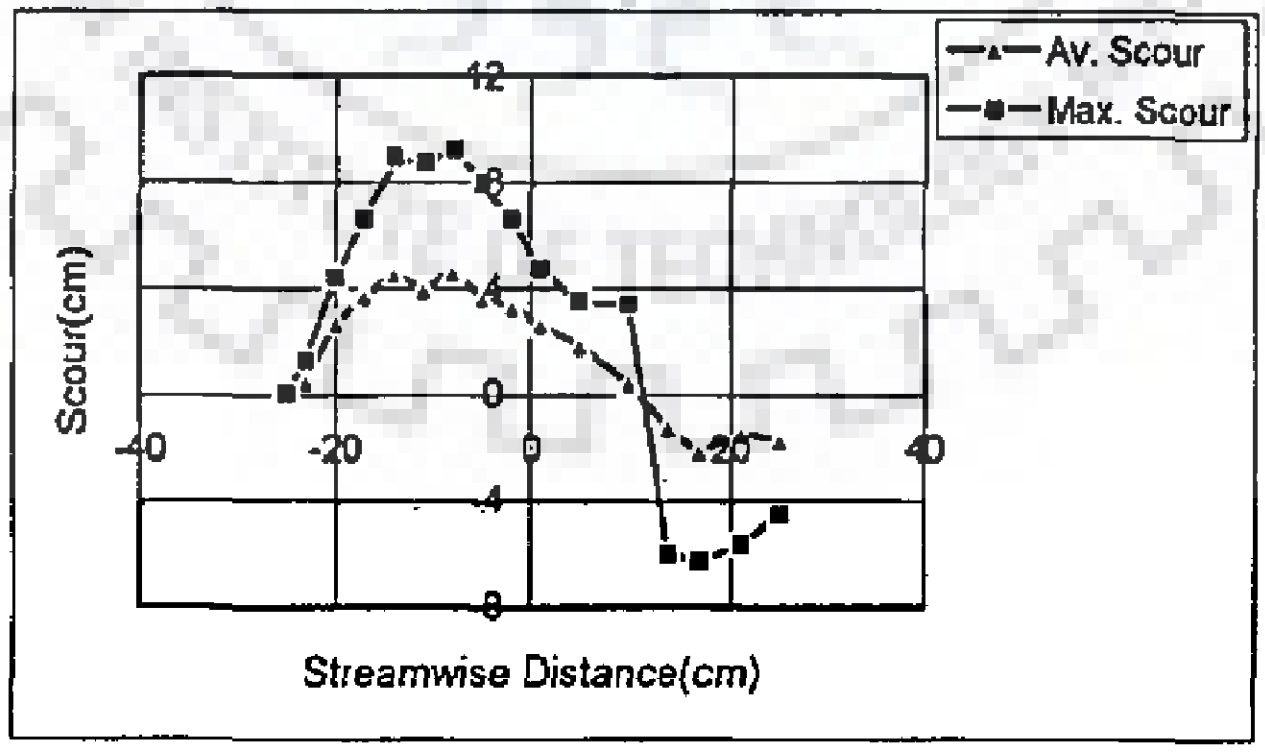

Fig. 5.32 Streamwise variation of scour around elliptical island I_5 (b/a=0.6) at F_r =0.2 & h=15cm (RunC14)

5.6 RESULTS

From the experimental data available attempt was made to find the trend of scour around island for three different Froude numbers. Assuming a linear trend of variation, it has been observed from Fig. 5.33 that the maximum scour around the island increases with the increase in b/a ratio of island. It was also tried to find the variation of average scour around island with b/a ratio of island. Table 5.2 and Fig. 5.34 show that average scour around island increases with increase in b/a ratio. From the above study, it can be concluded that under similar flow conditions, scour around island increases with the increase in width to length ratio of island.

Table 5.1 Variation of maximum scour (in cm) around island

b/a / F_r	0.15	0.2	0.3	0.4	0.6	1.0
0.16	2.64	3.75	4.05	4.56	5.13	6.25
0.19	4.41	4.67	4.92	5.15	6.10	9.30
0.2	6.3	6.82	–	8.50	9.26	–

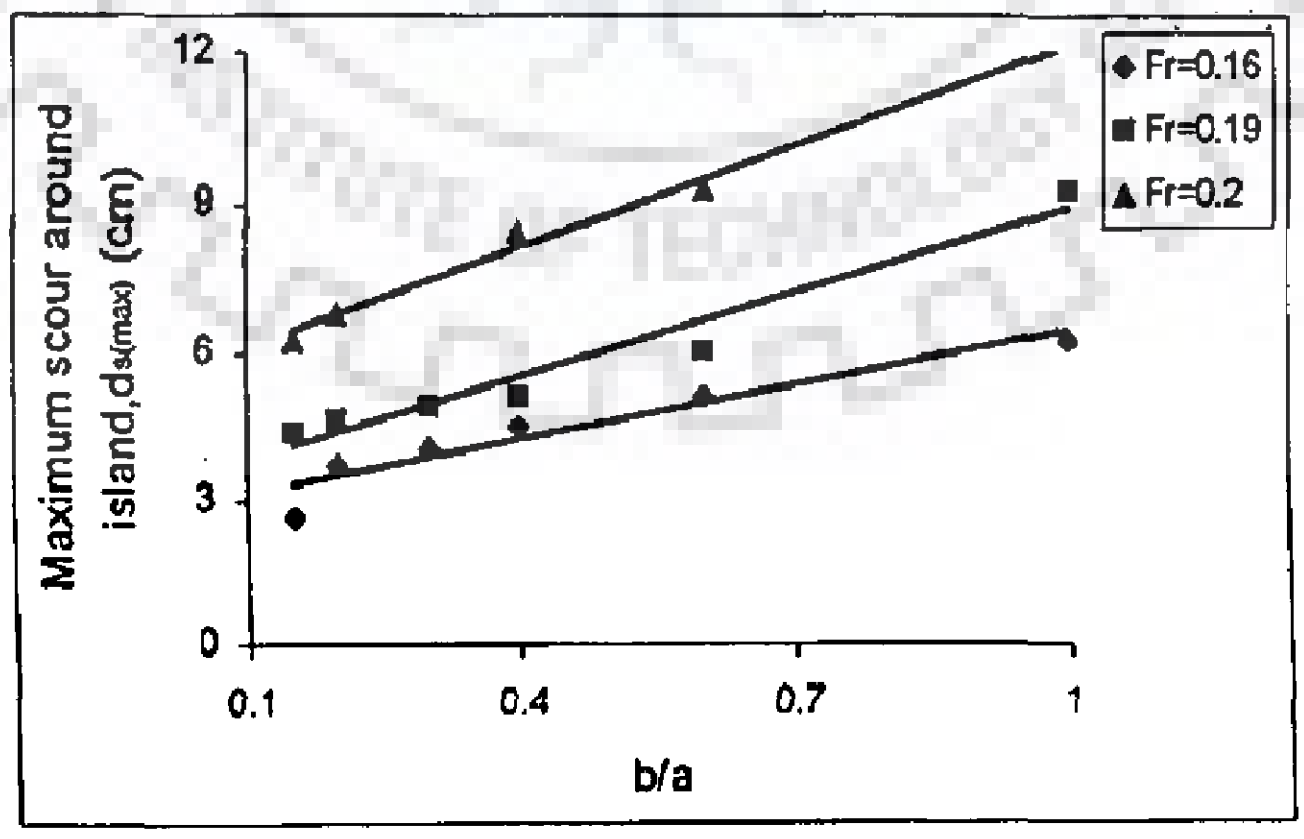

Fig. 5.33 Variation of maximum scour around island with b/a ratio

Table 5.2 Variation of average scour (in cm) around island

F_r \ b/a	0.15	0.2	0.3	0.4	0.6	1.0
0.16	0.289	0.757	1.146	1.302	0.86	2.342
0.19	1.423	1.574	1.605	1.221	1.916	3.731
0.2	2.033	2.056	–	3.104	3.046	–

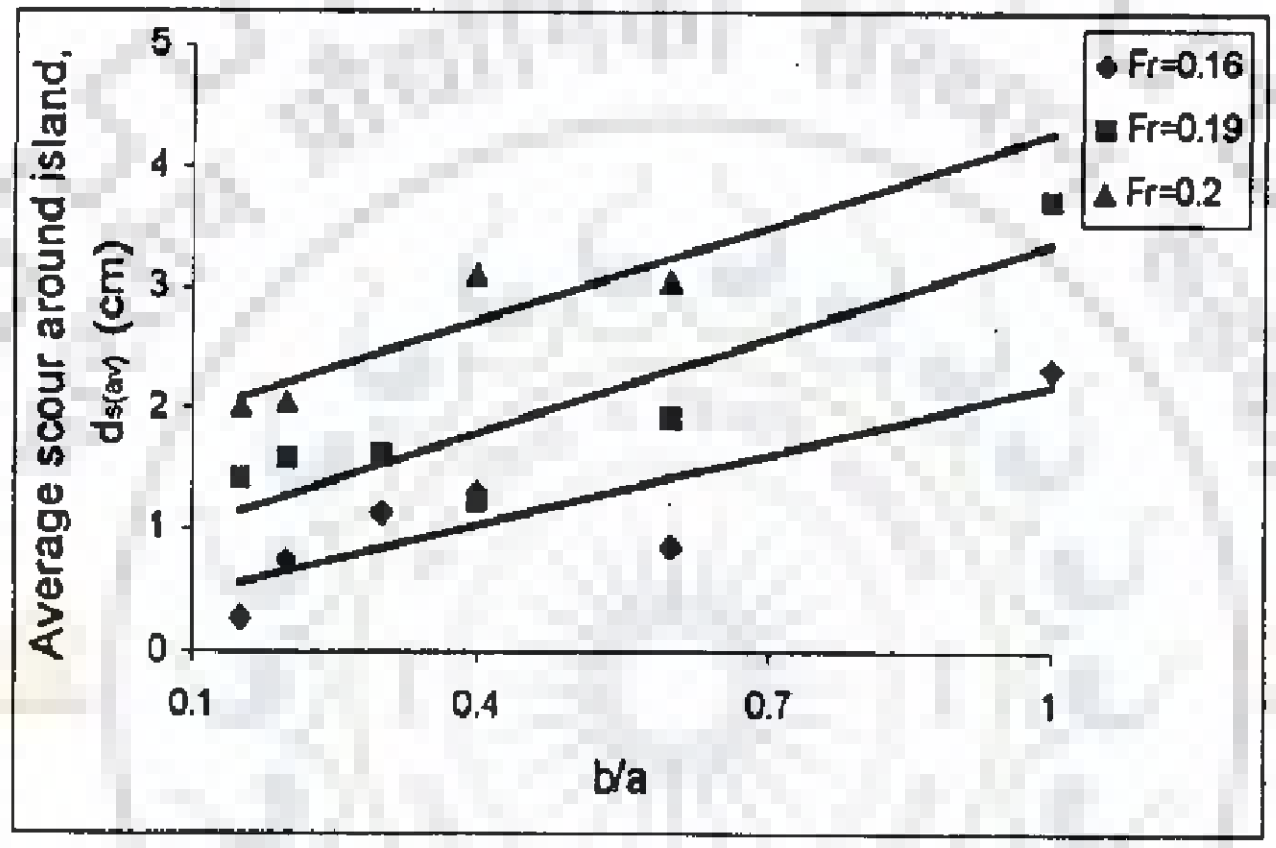

Fig. 5.34 Variation of average scour around island with b/a ratio

One can see from Fig. 5.33 and Fig. 5.34 that maximum scour and average scour are dimensional quantities, while b/a and Froude number are dimensionless quantities. Thus, it was considered desirable to express the maximum scour or the average scour in dimensionless form in order to maintain consistency. In Fig. 5.35, it has been attempted to show the variation of dimensionless maximum scour in terms of maximum scour, $d_{s(max)}$ / flow depth (h) with b/a ratio for different Froude numbers.

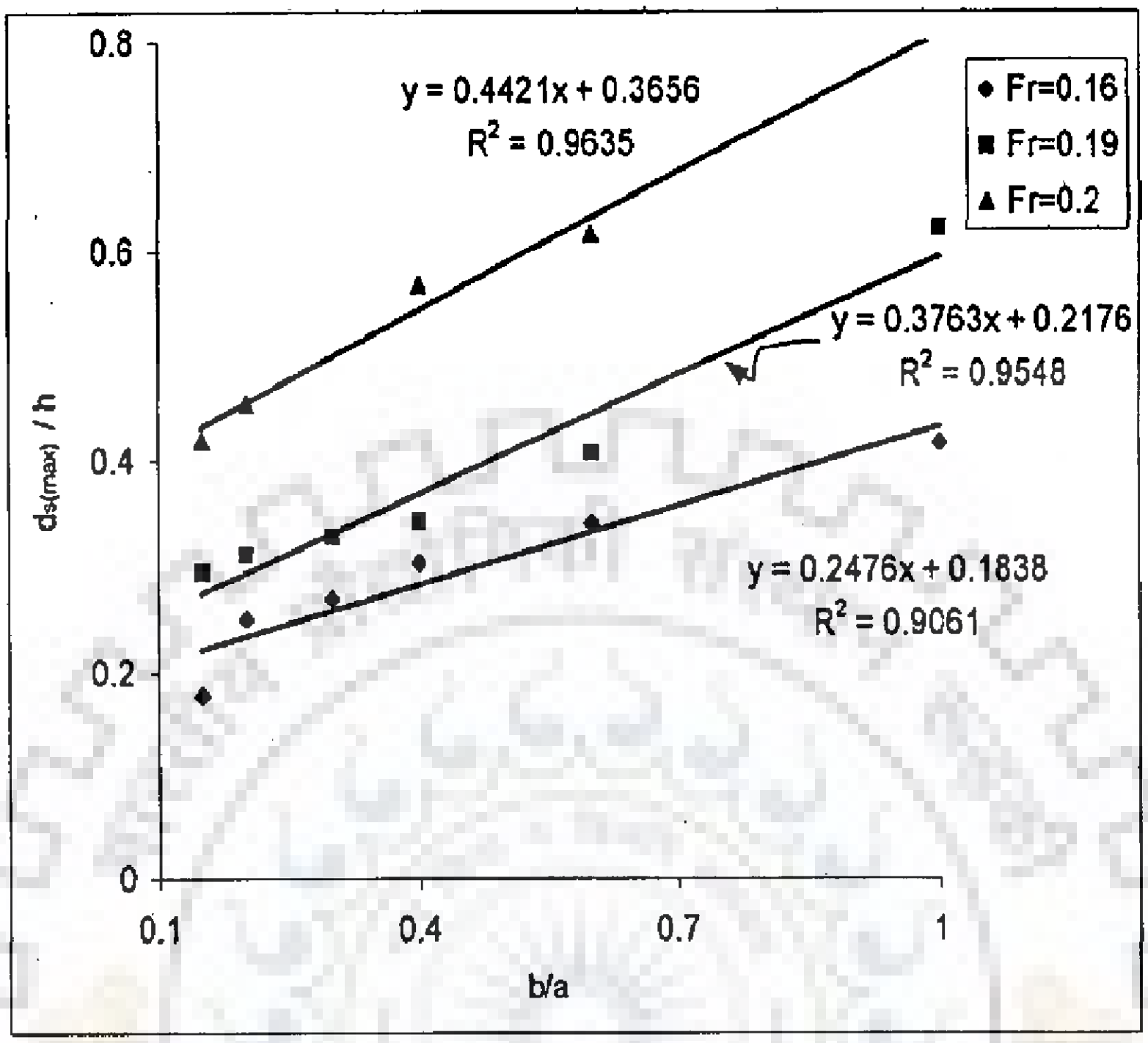

Fig. 5.35 Variation of dimensionless maximum scour around island with b/a ratio

From Fig. 5.35, it can still be observed that the role of Froude number and width to length ratio of island is evident on the scour depth. In the following section, the influence of energy expenditure along the island on the scour depth is explored.

5.7 VARIATION OF ENERGY GRADIENT ACROSS THE ISLAND AND ITS INFLUENCE ON SCOUR

In this section, it has been attempted to study the loss of energy across the island in the flow direction and its relationship with scour.

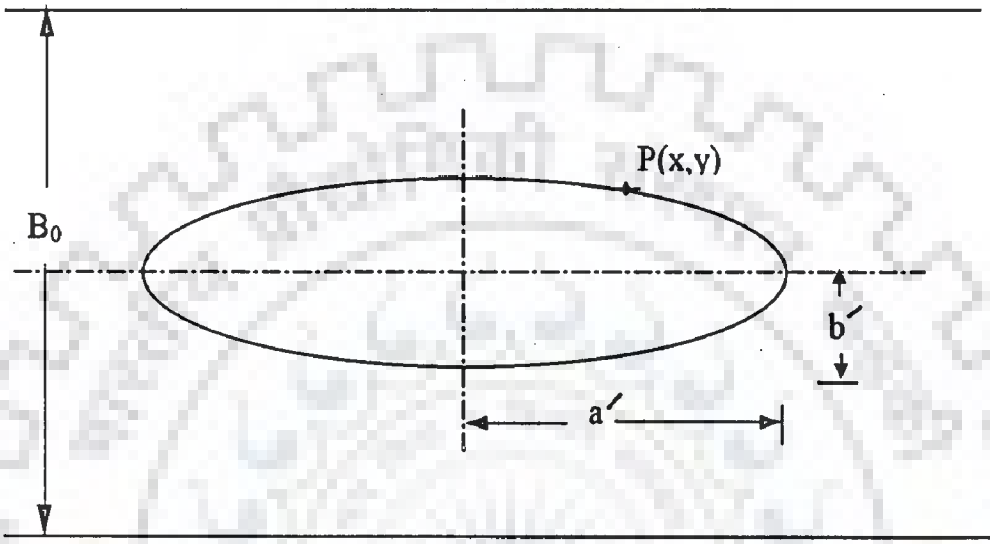

Fig. 5.36 Plan showing the elliptical profile of island

Elliptical profile of island is given by (Fig. 5.36),

$$\frac{x^2}{a'^2}+\frac{y^2}{b'^2}=1$$

$$\text{Or, } y=b'\sqrt{1-\frac{x^2}{a'^2}} \tag{5.1}$$

Total energy head at any section is

$$E=h+\frac{Q^2}{2gB^2h^2}$$

Assuming that h does not change with x, one can write

$$\frac{dE}{dx}=\frac{dh}{dx}+\frac{1}{2gh^2}\frac{d}{dx}\left(Q^2B^{-2}\right)$$

Or,
$$\frac{dE}{dx} = \frac{Q^2}{2gh^2}\left(-2B^{-3}\right)\frac{dB}{dx} + \frac{B^{-2}}{2gh^2}(2Q)\left(\frac{dQ}{dx}\right)$$

$$= -\frac{Q^2 B^{-3}}{gh^2}\left(\frac{dB}{dx}\right) \quad \left[\text{ as } \frac{dQ}{dx} \text{ is zero }\right] \tag{5.2}$$

Again, flow width at any section across the island is

$$B = B_0 - 2y$$

$$= B_0 - 2b'\sqrt{1-\frac{x^2}{a'^2}} \tag{5.3}$$

This leads to

$$\frac{dB}{dx} = -2b' \cdot \frac{1}{2}\left(1-\frac{x^2}{a'^2}\right)^{-1/2}\left(-\frac{2x}{a'^2}\right)$$

$$= 2b'\left(1-\frac{x^2}{a'^2}\right)^{-1/2}\left(\frac{x}{a'^2}\right) \tag{5.4}$$

From equation (5.2),

$$\frac{dE}{dx} = -\frac{2Q^2}{gh^2}\left[B_0 - 2b'\sqrt{1-\frac{x^2}{a'^2}}\right]^{-3} b'\left(1-\frac{x^2}{a'^2}\right)^{-1/2}\left(\frac{x}{a'^2}\right) \tag{5.5}$$

Based on equation (5.5), it has been tried to compute the energy gradient the island in the flow direction under different flow conditions, i.e., at different Froude numbers. The results of these computations are shown from Fig. 5.37 to Fig. 5.42.

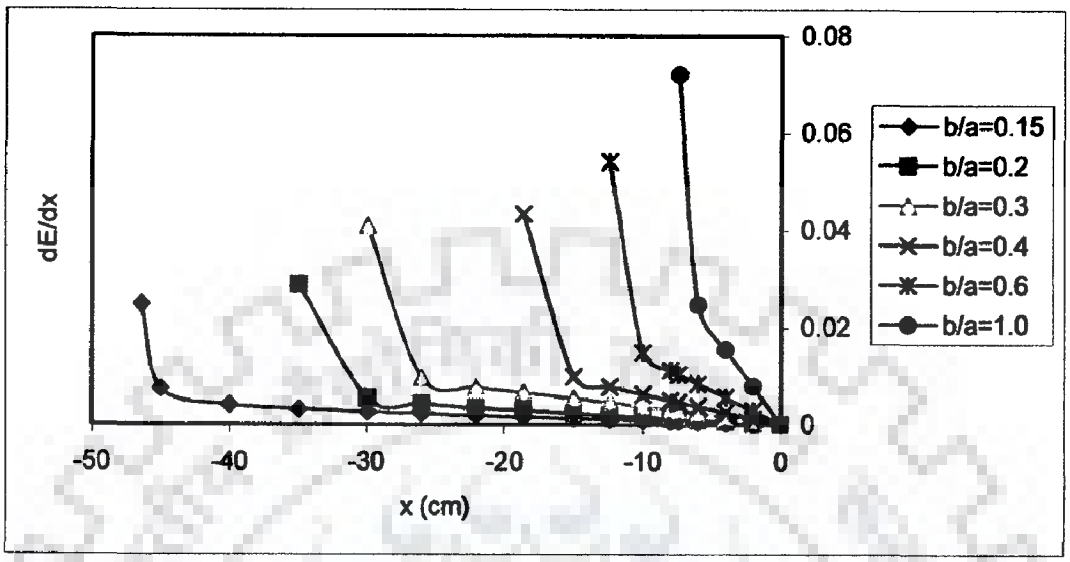

Fig. 5.37 Streamwise variation of dE/dx at F_r=0.105 & h=23cm

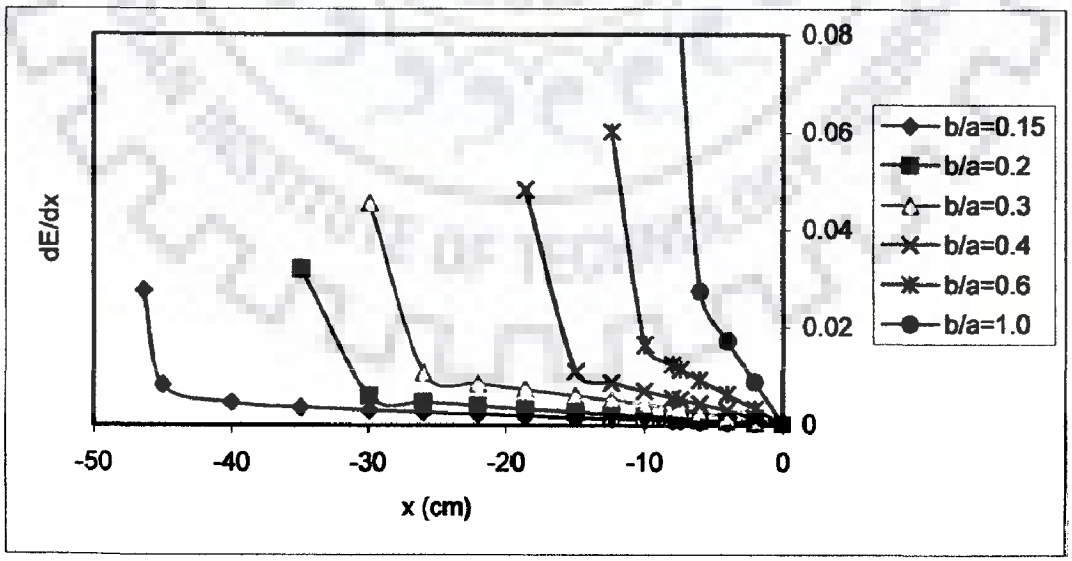

Fig. 5.38 Streamwise variation of dE/dx at F_r=0.12 & h=20cm

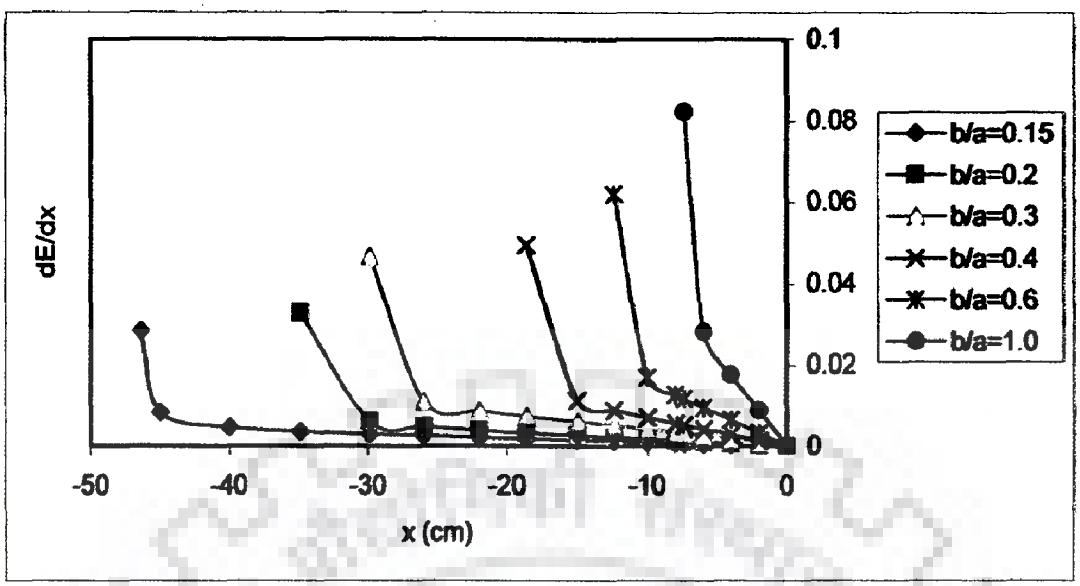

Fig. 5.39 Streamwise variation of dE/dx at F_r=0.14 & h=15cm

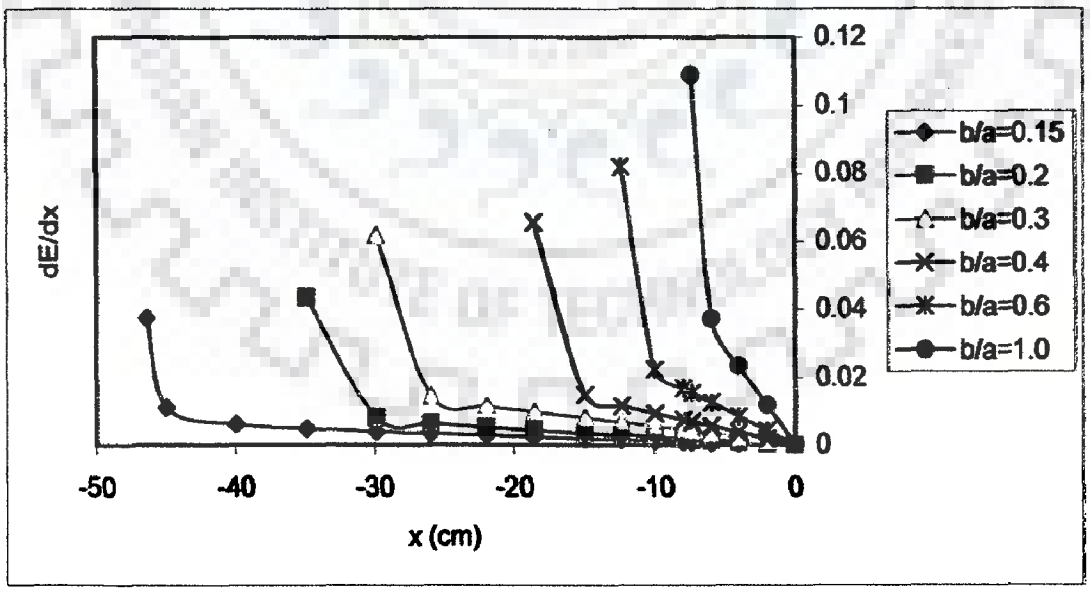

Fig. 5.40 Streamwise variation of dE/dx at F_r=0.16 & h=15cm

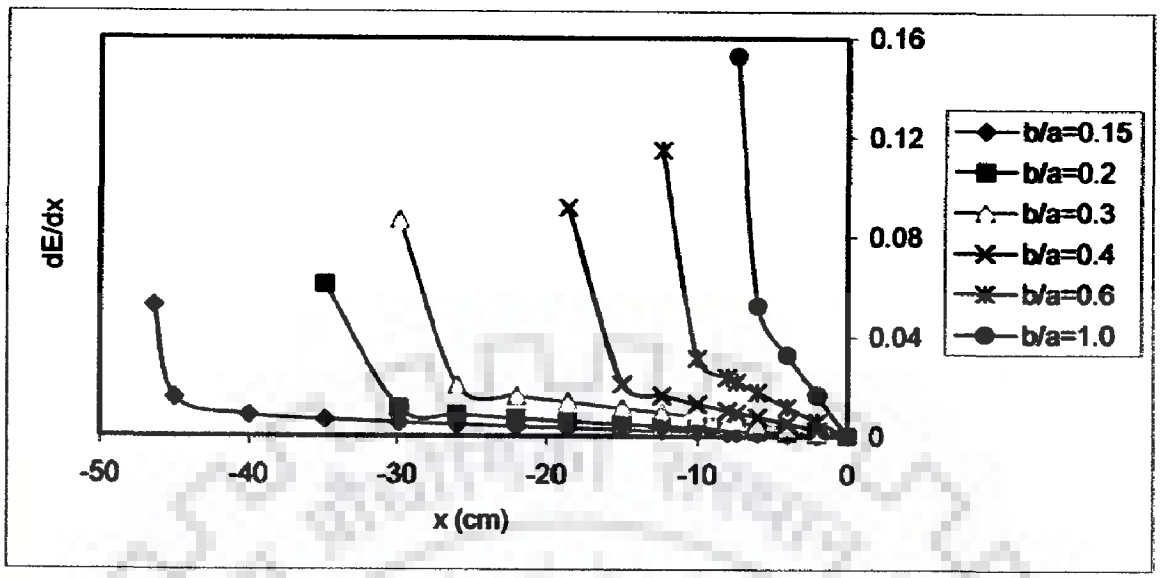

Fig. 5.41 Streamwise variation of dE/dx at F_r=0.19 & h=15cm

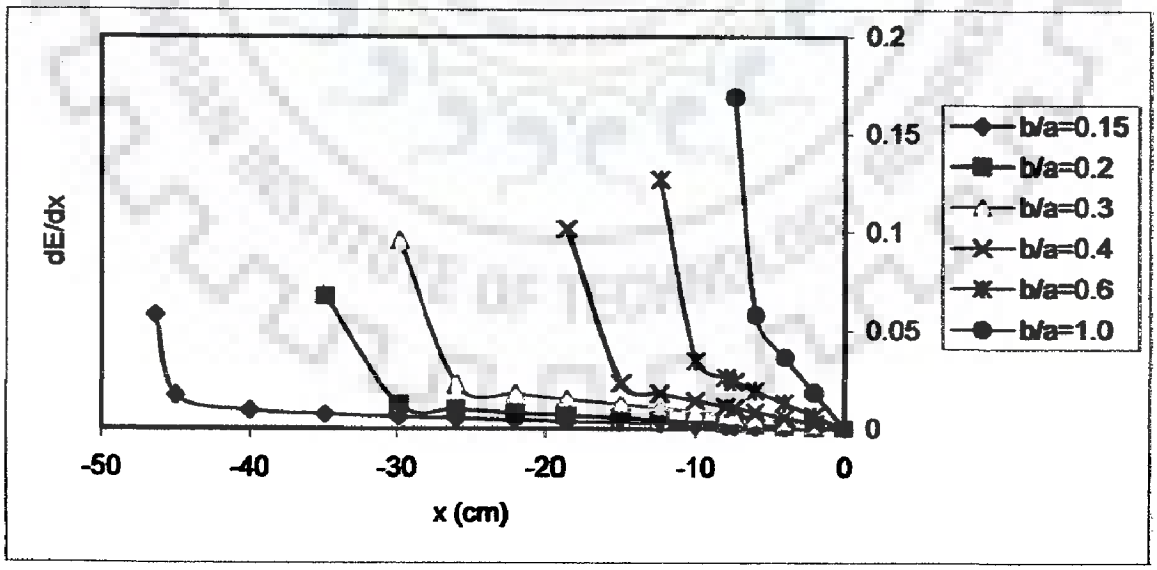

Fig. 5.42 Streamwise variation of dE/dx at F_r=0.2 & h=15cm

From Fig. 5.37 to Fig. 5.42, it can be observed that for each flow condition, as the width to length ratio of island increases, the energy gradient curve becomes steeper. To give more clarity to above finding, the total loss of energy across the island, ΔE has been computed as follows.

$$\Delta E = 2\int_{-x_{max}}^{0} \frac{dE}{dx}dx$$

$$= 2\int_{-x_{max}}^{0} \left(-\frac{2Q^2}{gh^2}\right)\left[B_0 - 2b'\sqrt{1-\frac{x^2}{a'^2}}\right]^{-3} b'\left(1-\frac{x^2}{a'^2}\right)^{-1/2}\left(\frac{x}{a'^2}\right)dx$$

$$= \int_{-x_{max}}^{0} A\left(B_0 - C\sqrt{1-\frac{x^2}{D}}\right)^{-3}\left(1-\frac{x^2}{D}\right)^{-1/2}\left(\frac{x}{D}\right)dx \qquad (5.6)$$

where, $A = -\frac{4b'Q^2}{gh^2}, C = 2b', D = a'^2$

Now, let $B_0 - C\sqrt{1-\frac{x^2}{D}} = z$

$$\therefore \left(1-\frac{x^2}{D}\right)^{-1/2}\left(\frac{x}{D}\right)dx = \frac{dz}{C} \qquad (5.7)$$

At $x = -x_{max}, z = B_0 - C\sqrt{1-\frac{x_{max}^2}{D}}$

and at $x = 0, z = B_0 - C$ (5.8)

Thus $\Delta E = \int_{B_0 - C\sqrt{1-\frac{x_{max}^2}{D}}}^{B_0 - C} A.z^{-3}.\frac{dz}{C}$

$$= -\frac{A}{2C}\left[\frac{1}{(B_0 - C)^2} - \frac{1}{\left(B_0 - C\sqrt{1 - \frac{x_{max}^{\ 2}}{D}}\right)^2}\right]$$

$$= \frac{4b'Q^2}{2.gh^2.2b'}\left[\frac{1}{(0.5 - 2b')^2} - \frac{1}{\left(0.5 - 2b'\sqrt{1 - \frac{x_{max}^{\ 2}}{a'^2}}\right)^2}\right]$$

$$\text{Or, } \Delta E = \frac{Q^2}{gh^2}\left[\frac{1}{(0.5 - 2b')^2} - \frac{1}{\left(0.5 - 2b'\sqrt{1 - \frac{x_{max}^{\ 2}}{a'^2}}\right)^2}\right] \qquad (5.9)$$

The total loss of energy across the islands having varying width to length ratio under different flow conditions has been computed using equation (5.9). Fig. 5.43 shows the plot of total loss of energy per unit length of island against width to length ratio of island. It can be seen from the figure that under similar flow condition, as the width to length ratio of island increases, the total expenditure of energy per unit length of island also increases. But already, it has been established that as the width to length ratio of island increases, the scour around island increases. Thus, it may be concluded that there is a definite correlation between the energy expenditure across the island and the scour around the island.

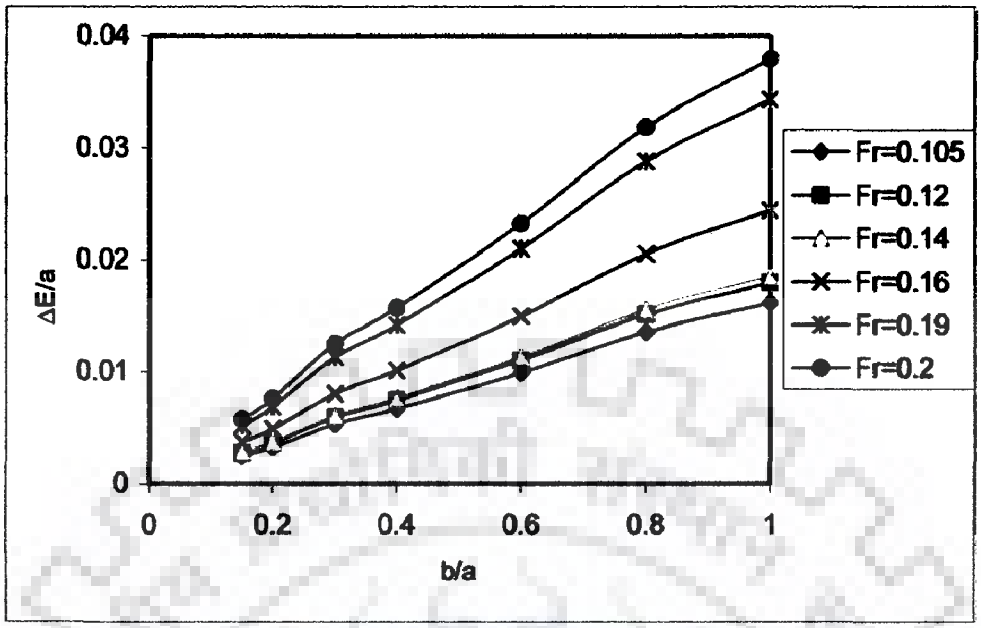

Fig. 5.43 Variation of total loss of energy across the island per unit length with width to length ratio of island

To explore the correlation between the energy expenditure across the island and the scour around island, using the experimental data (Table 5.1) the dimensionless maximum scour depth has been plotted against the total energy loss per unit length of island at three Froude numbers, i.e., F_r=0.16, F_r=0.19 and F_r=0.2. Assuming linear trend of variation, it can be seen that for all the three flow conditions, the scour around island increases with the increase in total energy expenditure per unit length of island [Fig. 5.44(a), Fig. 5.44(b) and Fig. 5.44(c)]. Variation of $d_{s(max)}/h$ vs. $\Delta E/a$, as shown in Fig. 5.44(a) to Fig. 5.44(c) also indicate the possibility of computing maximum scour depth around an island. Literature does not indicate the availability of scour estimation models for islands with varying b/a ratio. For this reason, no attempt is made to test the applicability of existing models.

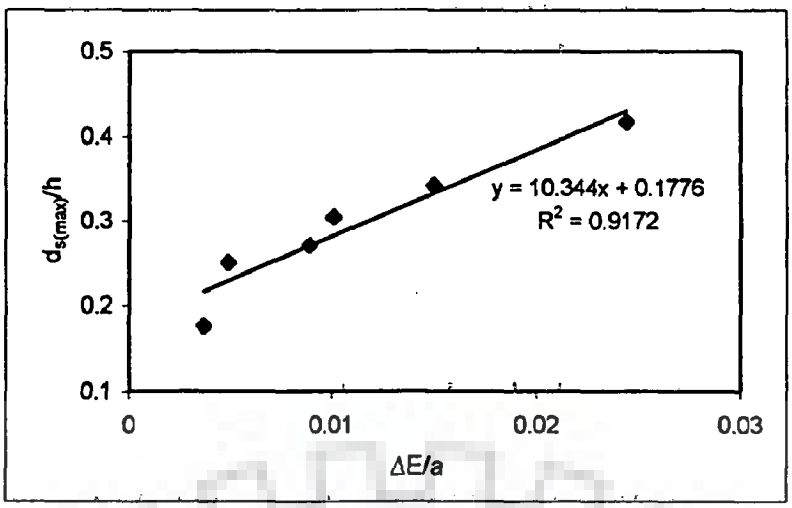

Fig. 5.44(a) Variation of dimensionless maximum scour depth with total energy loss per unit length of island at F_r=0.16

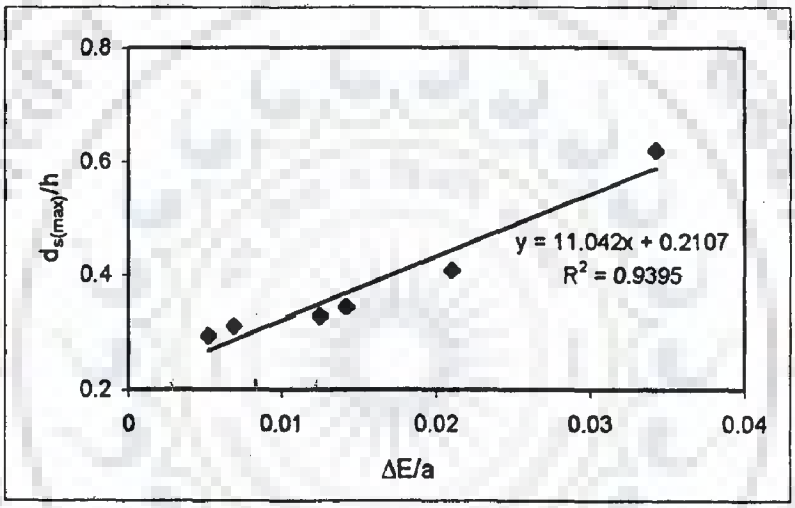

Fig. 5.44(b) Variation of dimensionless maximum scour depth with total energy loss per unit length of island at F_r=0.19

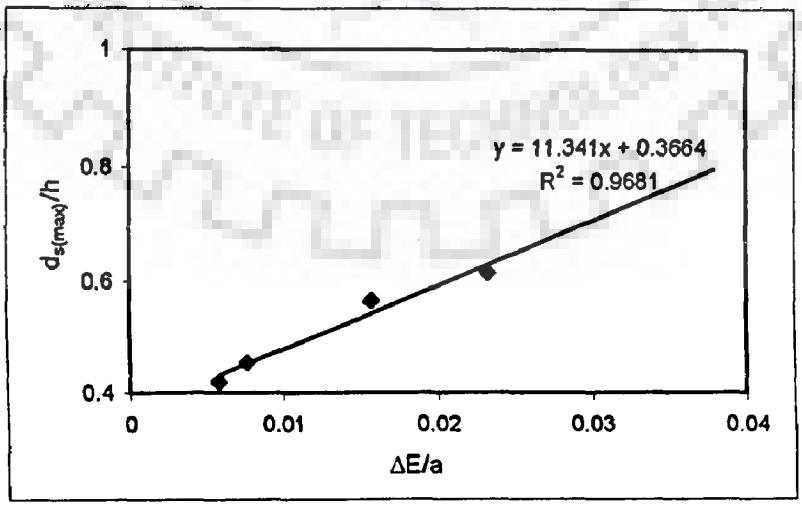

Fig. 5.44(c) Variation of dimensionless maximum scour depth with total energy loss per unit length of island at F_r=0.2

VARIATION OF STRENGTH OF SECONDARY CURRENT AROUND ISLAND

6.1 INTRODUCTION

Energy based approach has indicated that islands with lesser b/a values are safer under identical flow conditions. To further strengthen this finding and to investigate the growth and decay of secondary current around island, in the present work, the moment of momentum (MOM) was chosen as a representative quantity to define the strength of secondary current at a section. The moment of momentum is calculated by taking the tangential component of the momentum multiplied by the radial distance to a specific origin. One advantage of using moment of momentum as opposed to other quantities (e.g., the circulation or transverse components of velocities) is that it is proportional to the force exerted by the induced vortex on the river boundary and, therefore, provides a quantitative measure of the vortex strength (Marelius and Sinha, 1998).

4.2 ASSESSMENT OF STRENGTH OF SECONDARY CURRENT

To assess the variation of strength of secondary current around the island the study region covering the dfluence zone, confluence zone and the transition zone was divided into a number of cross-sections at 10 cm interval, as shown in Fig. 6.1.

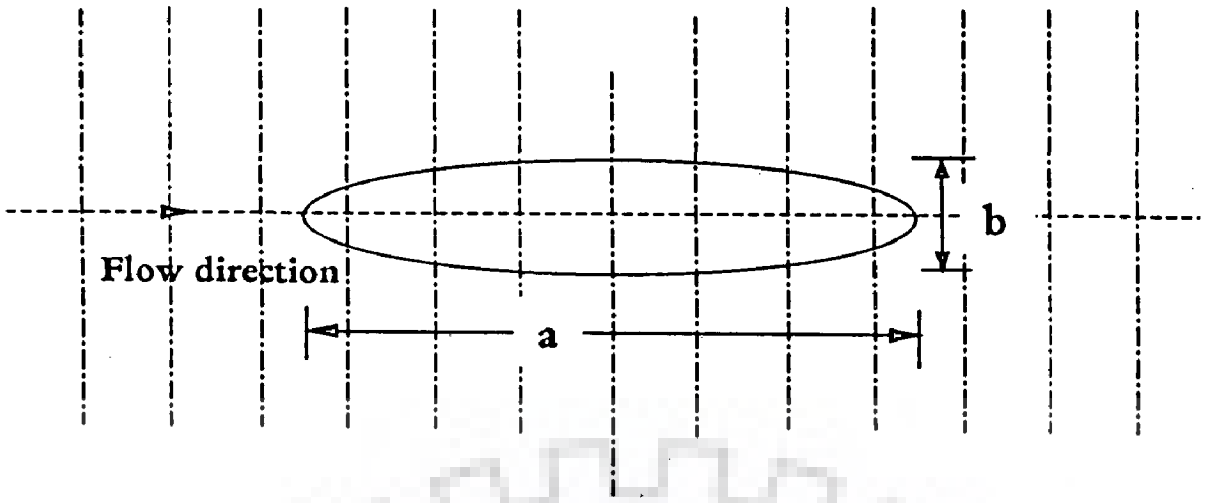

Fig. 6.1 Plan showing the different cross-sections around the island

Further, each cross-section was divided into 10cm × 3cm grids. At each grid point, all the three components of velocity were measured using ADV (Acoustic Doppler Velocimeter). Fig. 6.2 shows the layout of grids in flow area cross-section. Velocity near the wall of the flume was not considered for the calculation of strength of secondary current in order to neglect the wall effect on the generation of secondary flow due to presence of the island. Although, the exact centre of vortex due to the secondary flow was not known, it was observed that the height of centre of vortex was at 0.75h to 0.8h from the bed of the flume. The origin was taken at the centre of the island (in plan) at the initial bed level.

For a mass m concentrated at point A (Fig. 6.3), one can write the following expression for moment of momentum, MOM_A.

$$MOM_A = m\ (\vec{R} \times \vec{V}) \qquad (6.1)$$

In equation (6.1), $\vec{R}$ represents the location vector of point A with respect to centre of vortex C and is given as $\overrightarrow{CA}$.

The location vector of point A with respect to origin O is given as $\overrightarrow{OA}$,

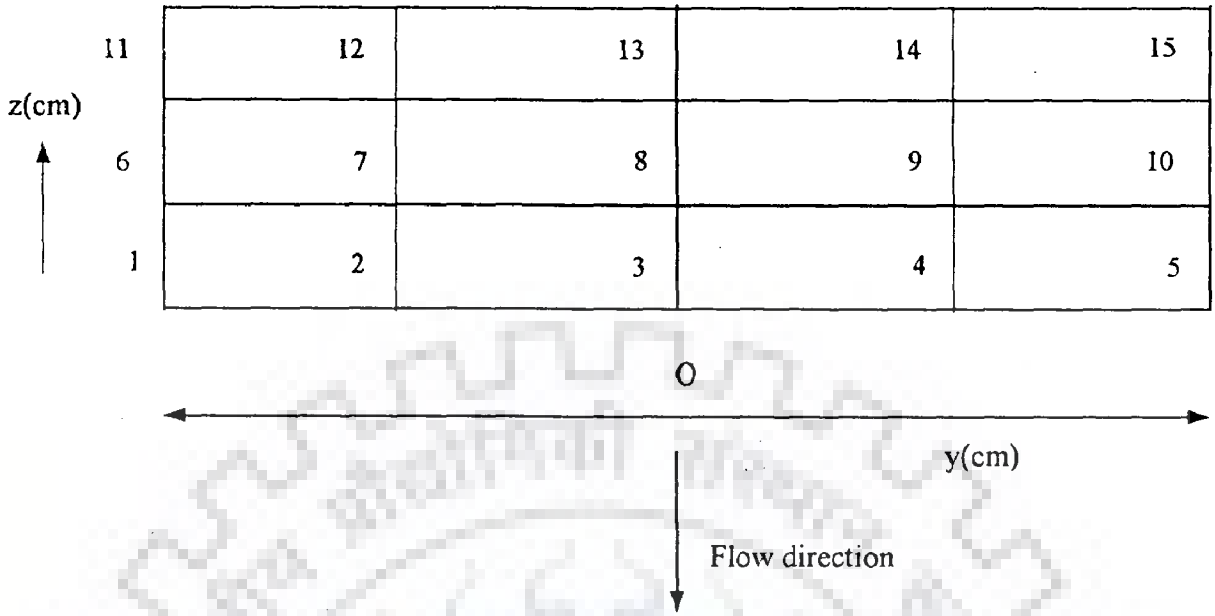

Fig. 6.2 Grid points for collection of data

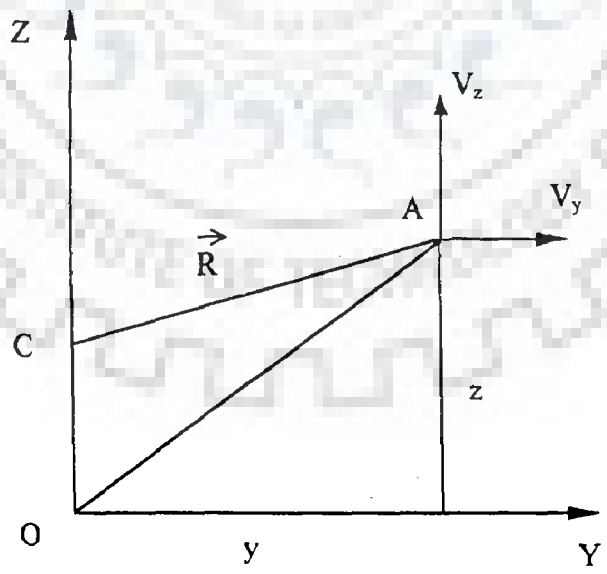

Fig. 6.3 Definition sketch for velocity vectors

where, $\vec{OA} = y\,\vec{j} + z\,\vec{k}$ (6.2)

In equation (6.2), y and z are coordinates of grid point A and $\vec{j}$ and $\vec{k}$ are unit vectors along Y and Z directions respectively.

Location vector of point A with respect to point C can be written as

$$\vec{R} = \vec{OA} - \vec{OC}$$

$$= y\,\vec{j} + z\,\vec{k} - OC\,\vec{k}$$

$$= y\,\vec{j} + (z - OC)\,\vec{k} \quad (6.3)$$

Thus, moment of momentum of mass m at point A with respect to centre of vortex C can be expressed as

$$MOM_A = m\,[\{y\,\vec{j} + (z - OC)\,\vec{k}\} \times (V_y\,\vec{j} + V_z\,\vec{k})]$$

$$= m\,[\,y\,V_z\,\vec{i} - (z - OC)\,V_y\,\vec{i}\,]$$

$$= m\,\vec{i}\,[\,y\,V_z + (OC - z)\,V_y\,] \quad (6.4)$$

In equation (6.4), $\vec{i}$ indicates the direction of MOM along the direction of flow of fluid (water), (myV_z) is MOM due to vertical velocity and [m (OC – z) V_y] is MOM due to transverse velocity.

Thus, total MOM at any section can be expressed as

$$\text{Total MOM} = \sum MOM_i \quad (6.5)$$

6.3 VARIATION OF STRENGTH OF SECONDARY CURRENT ALONG THE ISLAND

Variation of strength of secondary current around each model island has been experimentally investigated at Froude numbers of 0.14, 0.16 and 0.19 under rigid bed flow condition. The experimental programme has been explained in Chapter 3. The total MOM as computed by equation (6.5) at different sections for each run were plotted against streamwise distance considering the section passing through the centre of the island as origin (x=0cm). The MOM at each section was computed for two centres of vortex, i.e., at 0.75h and at 0.8h from the bed of the flume. Some of the plots are shown through Fig. 6.4(a) to Fig. 6.4(o).

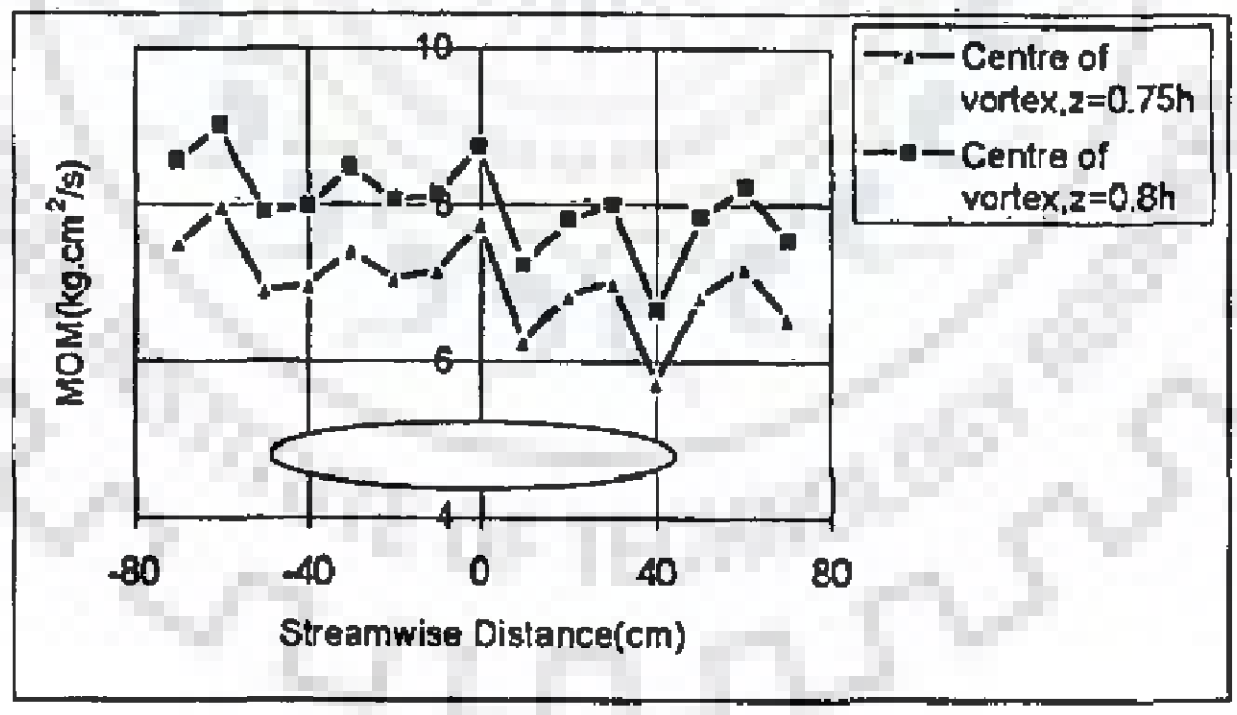

Fig. 6.4(a) Streamwise variation of MOM for elliptical island I_1 (a=93cm,b=14cm,b/a=0.15) at F_r=0.14 and h=15cm (RunD1)

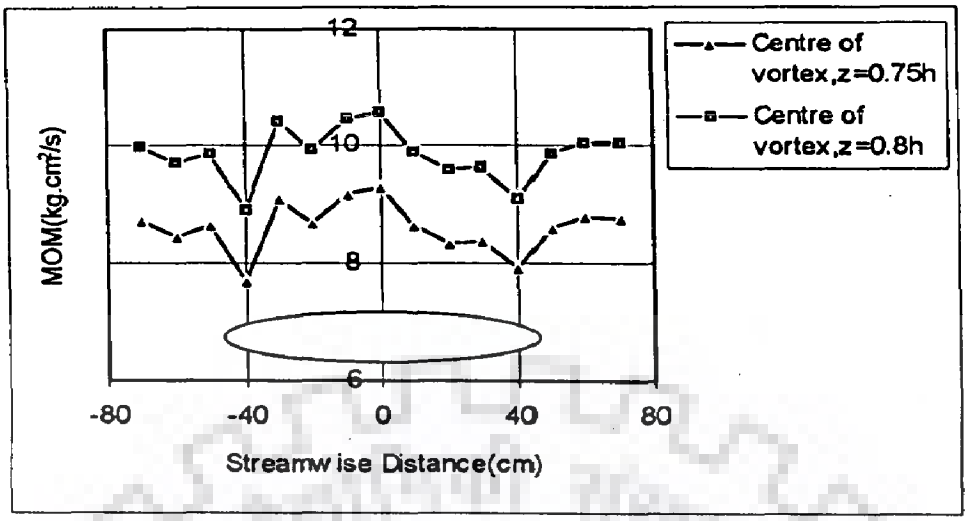

Fig. 6.4(b) Streamwise variation of MOM for elliptical island I_1 (a=93cm,b=14cm,b/a=0.15) at F_r=0.16 and h=15cm (RunD2)

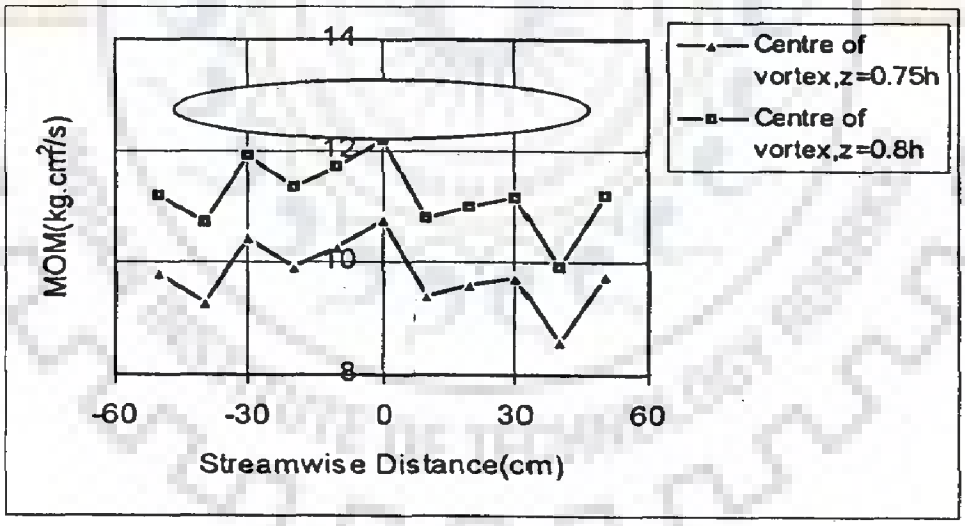

Fig. 6.4(c) Streamwise variation of MOM for elliptical island I_1 (a=93cm,b=14cm,b/a=0.15) at F_r=0.19 and h=15cm (RunD3)

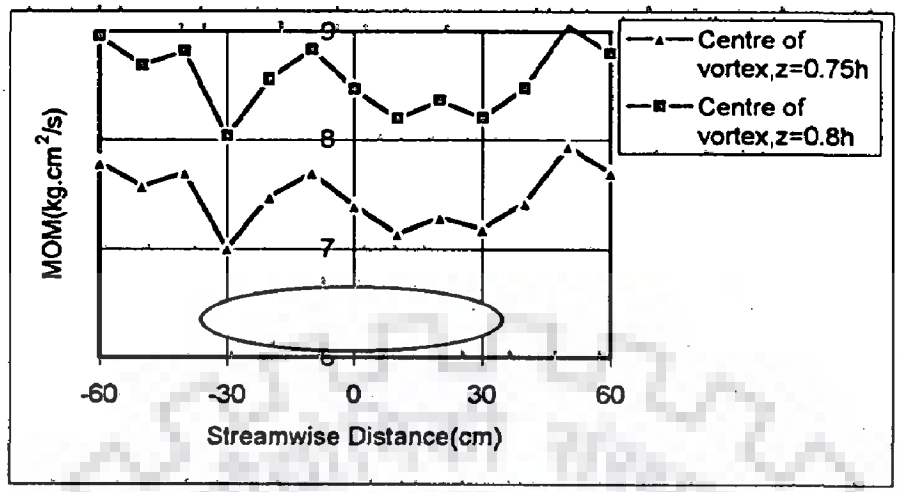

Fig. 6.4(d) Streamwise variation of MOM for elliptical island I_2 (a=70cm,b=14cm,b/a=0.2) at F_r=0.14 and h=15cm (RunD4)

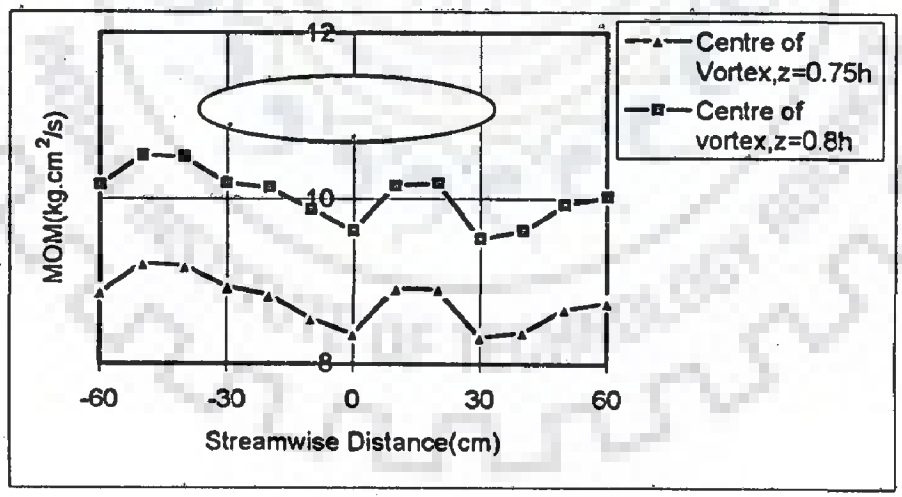

Fig. 6.4(e) Streamwise variation of MOM for elliptical island I_2 (a=70cm,b=14cm,b/a=0.2) at F_r=0.16 and h=15cm (RunD5)

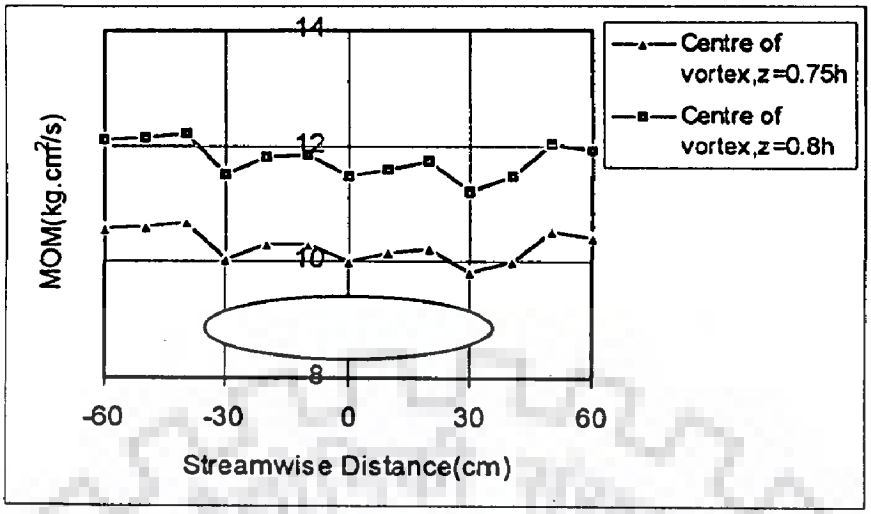

Fig. 6.4(f) Streamwise variation of MOM for elliptical island I_2 (a=70cm,b=14cm,b/a=0.2) at F_r=0.19 and h=15cm (RunD6)

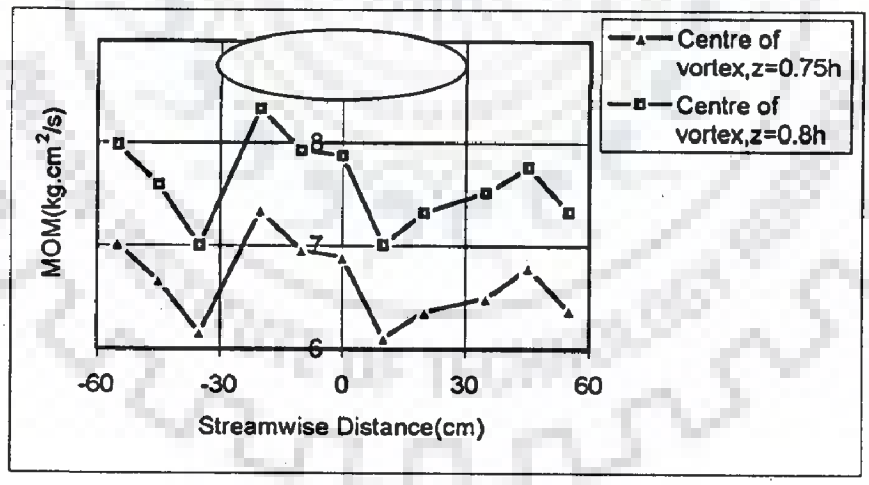

Fig. 6.4(g) Streamwise variation of MOM for elliptical island I_3 (a=60cm,b=18cm,b/a=0.3) at F_r=0.14 and h=15cm (RunD7)

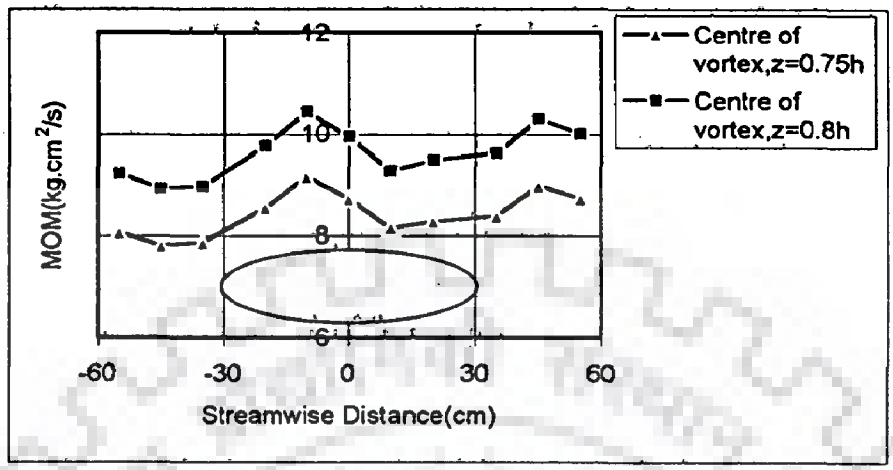

Fig. 6.4(h) Streamwise variation of MOM for elliptical island I_3 (a=60cm,b=18cm,b/a=0.3) at F_r=0.16 and h=15cm (RunD8)

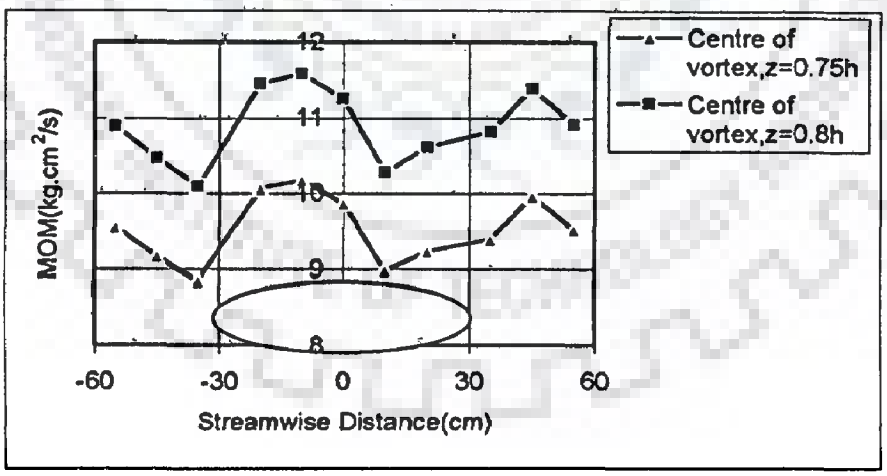

Fig. 6.4(i) Streamwise variation of MOM for elliptical island I_3 (a=60cm,b=18cm,b/a=0.3) at F_r=0.19 and h=15cm (RunD9)

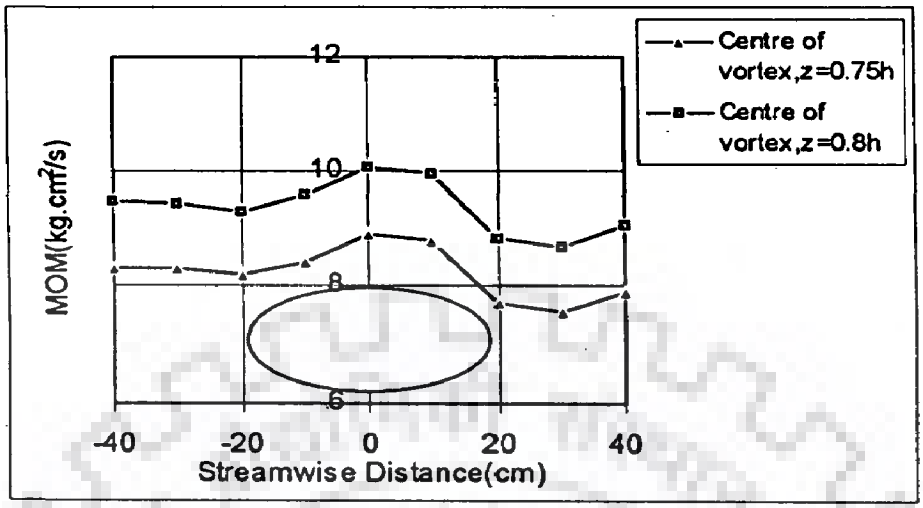

Fig. 6.4(j) Streamwise variation of MOM for elliptical island L_4 (a=37.5cm,b=15cm,b/a=0.4) at F_r=0.14 and h=15cm (RunD10)

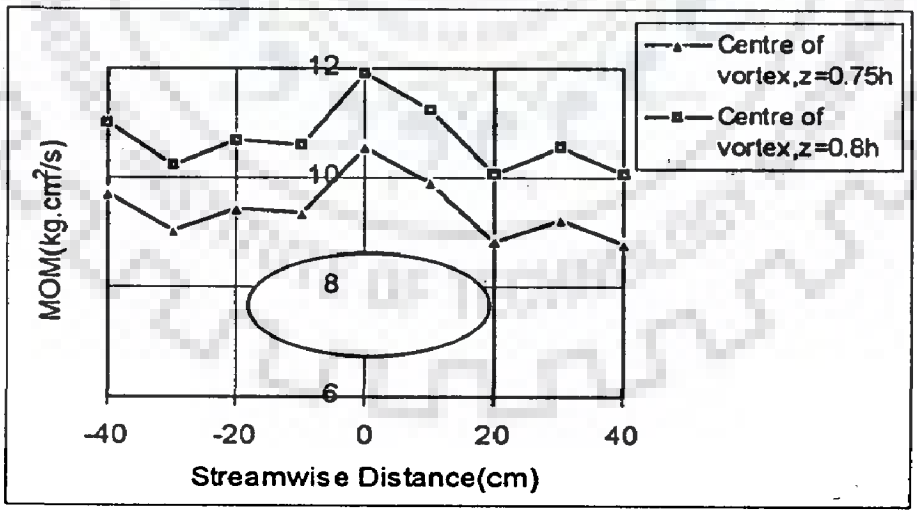

Fig. 6.4(k) Streamwise variation of MOM for elliptical island L_4 (a=37.5cm,b=15cm,b/a=0.4) at F_r=0.16 and h=15cm (RunD11)

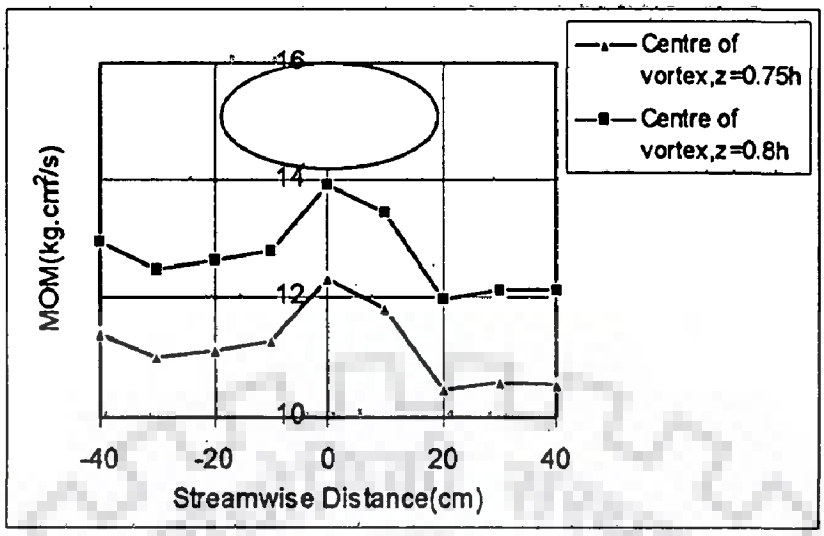

Fig. 6.4(l) Streamwise variation of MOM for elliptical island I_4 (a=37.5cm,b=15cm,b/a=0.4) at F_r=0.19 and h=15cm (RunD12)

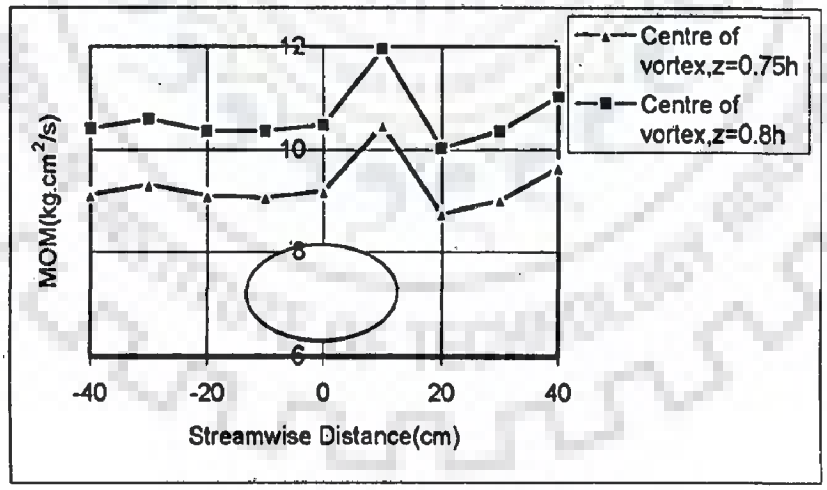

Fig. 6.4(m) Streamwise variation of MOM for elliptical island I_5 (a=25cm,b=15cm,b/a=0.6) at F_r=0.14 and h=15cm (RunD13)

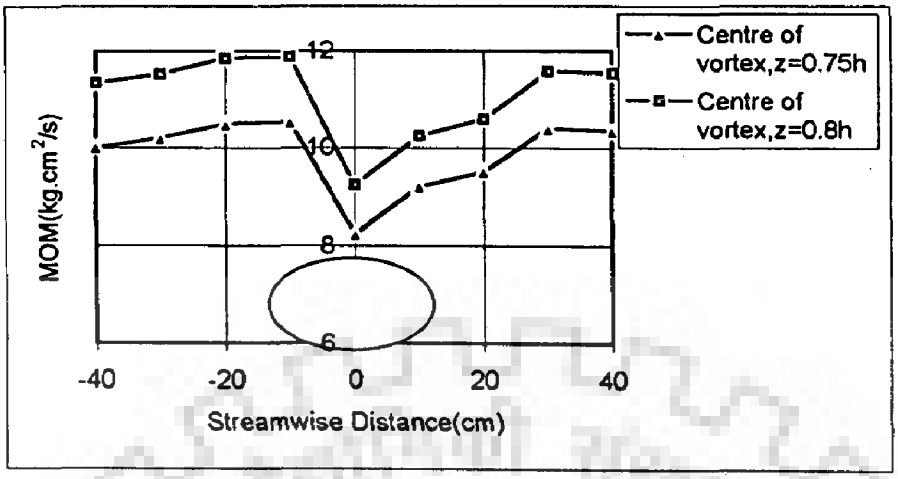

Fig. 6.4(n) Streamwise variation of MOM for elliptical island I_5 (a=25cm,b=15cm,b/a=0.6) at F_r=0.16 and h=15cm (RunD14)

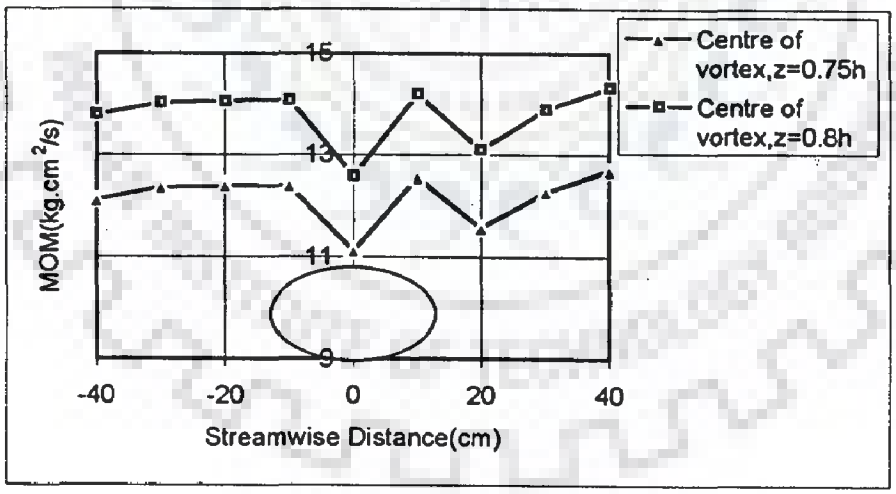

Fig. 6.4(o) Streamwise variation of MOM for elliptical island I_5 (a=25cm,b=15cm,b/a=0.6) at F_r=0.19 and h=15cm (RunD15)

It can be seen from Fig. 6.4(a) to Fig. 6.4(o) that the pattern of variation of MOM with distance for the two heights of centre of vortex for each run was similar. But the pattern of streamwise variation of MOM with respect to Froude number as well as with respect to width to length ratio of island was not consistent. This is due to the fact that while calculating the MOM in the transition zone, the area covered by the island was neglected. Therefore, it was decided that instead of using MOM, MOM per unit flow width (MOM/B) may be considered as a representative parameter to study the variation of strength of secondary current around the island [Fig. 6.5(a) to Fig. 6.5(o)]. To study this, plots were prepared corresponding to centre of vortex, z=0.75h only.

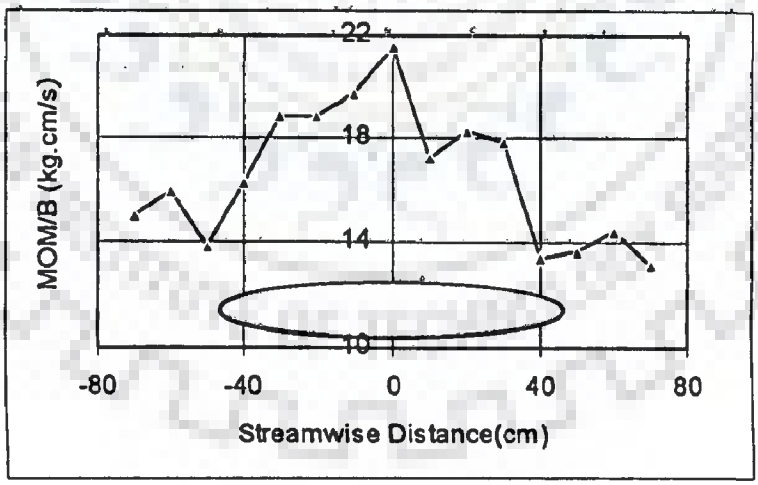

Fig. 6.5(a) Streamwise variation of MOM per unit flow width for elliptical island I_1 (a=93cm,b=14cm,b/a=0.15) at F_r=0.14 and h=15cm (RunD1)

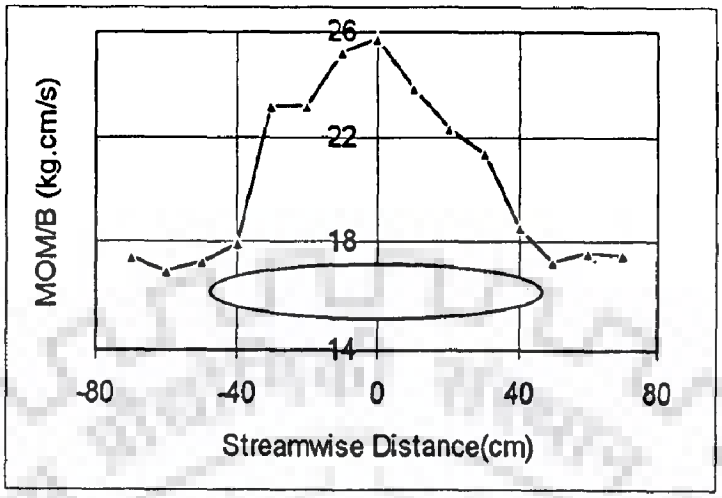

Fig. 6.5(b) Streamwise variation of MOM per unit flow width for elliptical island I_1 (a=93cm,b=14cm,b/a=0.15) at F_r=0.16 and h=15cm (RunD2)

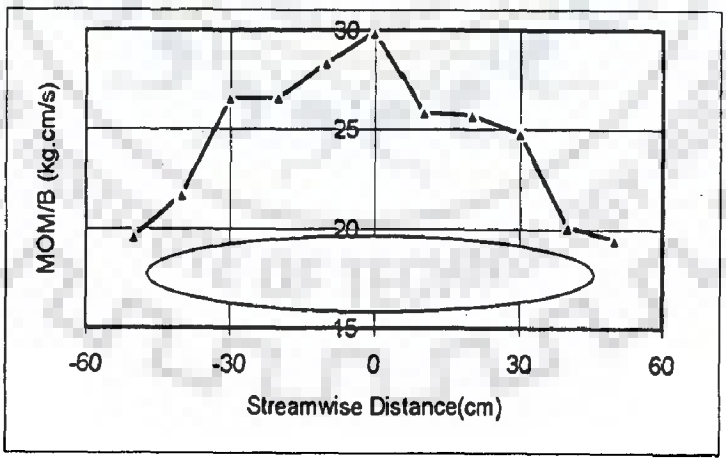

Fig. 6.5(c) Streamwise variation of MOM per unit flow width for elliptical island I_1 (a=93cm,b=14cm,b/a=0.15) at F_r=0.19 and h=15cm (RunD3)

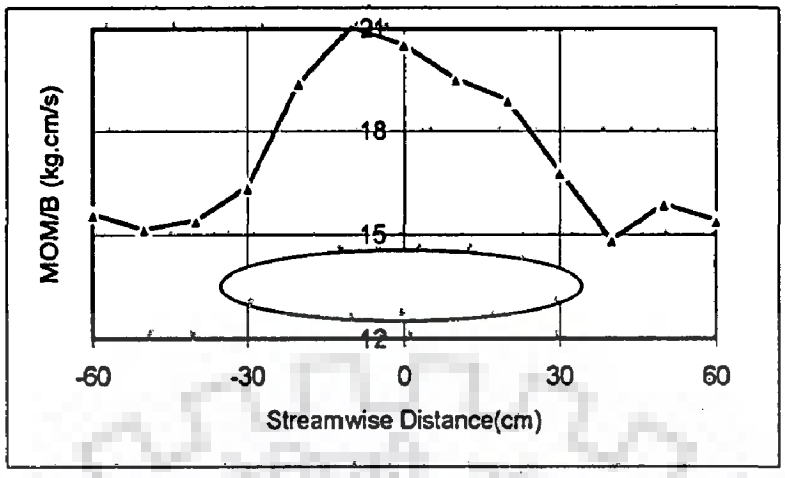

Fig. 6.5(d) Streamwise variation of MOM per unit flow width for elliptical island I_2 (a=70cm,b=14cm,b/a=0.2) at F_r=0.14 and h=15cm (RunD4)

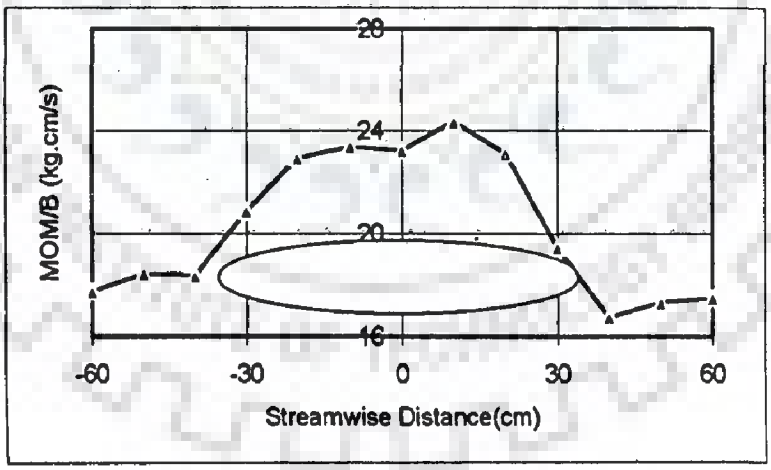

Fig. 6.5(e) Streamwise variation of MOM per unit flow width for elliptical island I_2 (a=70cm,b=14cm,b/a=0.2) at F_r=0.16 and h=15cm (RunD5)

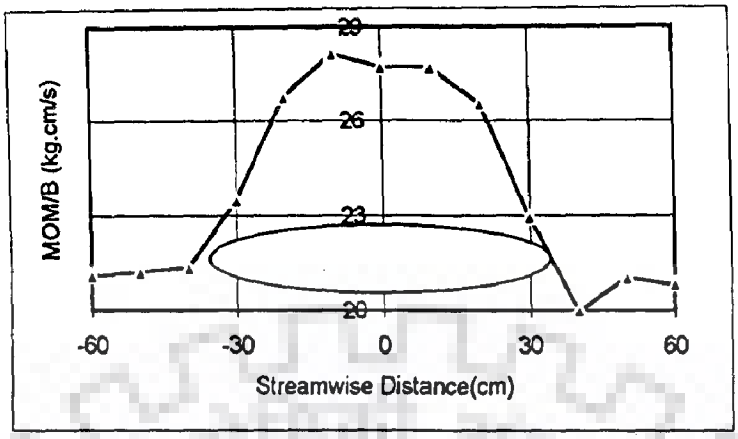

Fig. 6.5(f) Streamwise variation of MOM per unit flow width for elliptical island I_2 (a=70cm,b=14cm,b/a=0.2) at F_r=0.19 and h=15cm (RunD6)

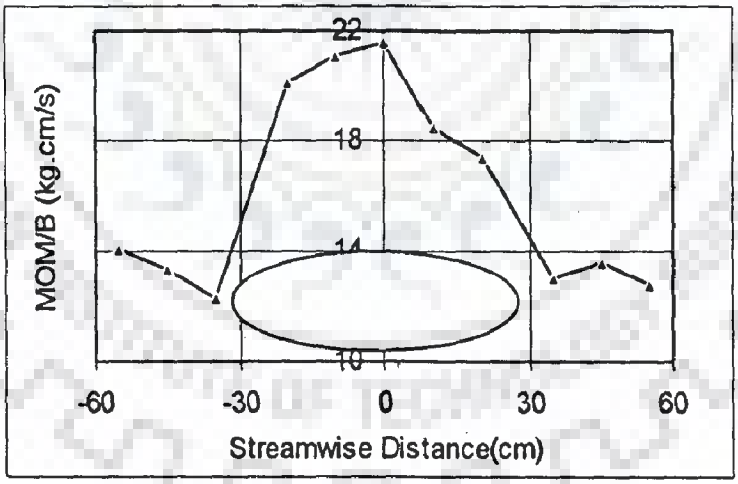

Fig. 6.5(g) Streamwise variation of MOM per unit flow width for elliptical island I_3 (a=60cm,b=18cm,b/a=0.3) at F_r=0.14 and h=15cm (RunD7)

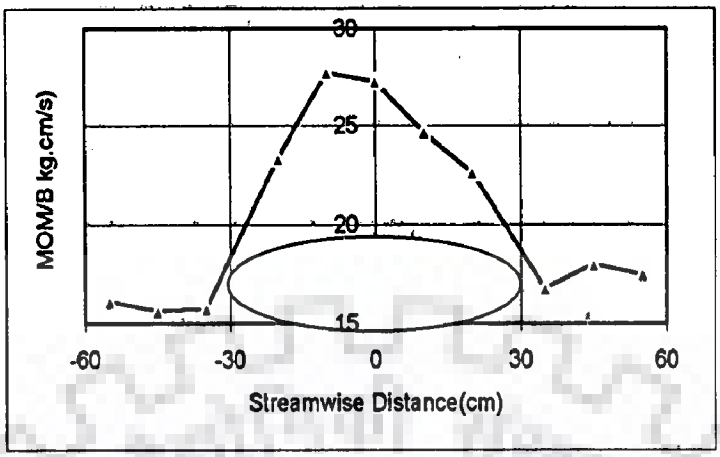

Fig. 6.5(h) Streamwise variation of MOM per unit flow width for elliptical island I_3 (a=60cm,b=18cm,b/a=0.3) at F_r=0.16 and h=15cm (RunD8)

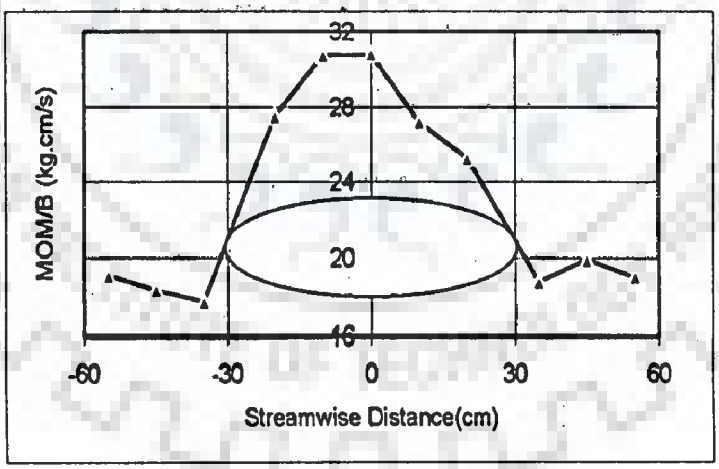

Fig. 6.5(i) Streamwise variation of MOM per unit flow width for elliptical island I_3 (a=60cm,b=18cm,b/a=0.3) at F_r=0.19 and h=15cm (RunD9)

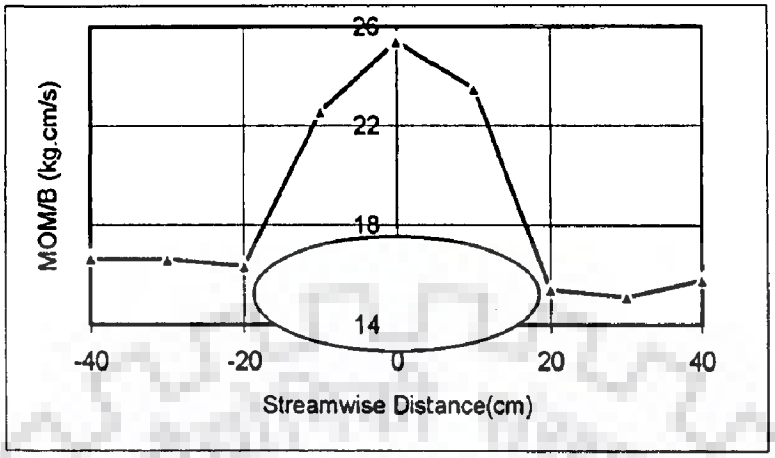

Fig. 6.5(j) Streamwise variation of MOM per unit flow width for elliptical island I_4 (a=37.5cm,b=15cm,b/a=0.4) at F_r=0.14 and h=15cm (RunD10)

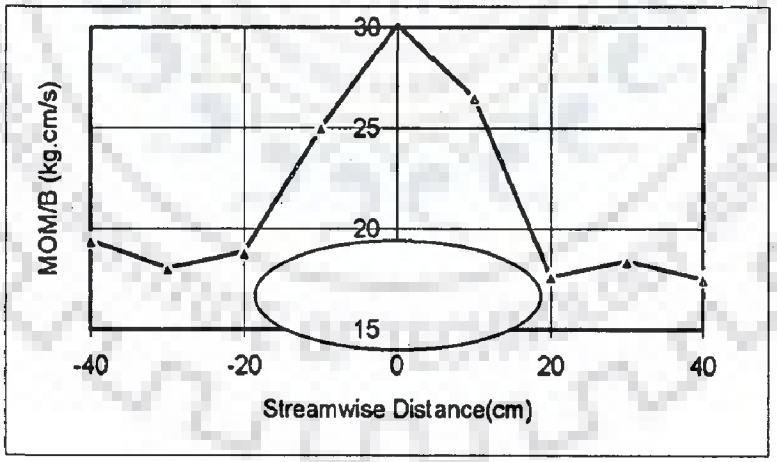

Fig. 6.5(k) Streamwise variation of MOM per unit flow width for elliptical island I_4 (a=37.5cm,b=15cm,b/a=0.4) at F_r=0.16 and h=15cm (RunD11)

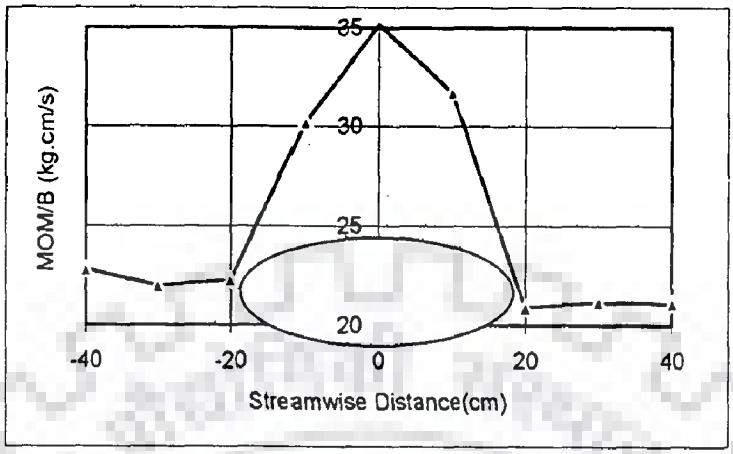

Fig. 6.5(l) Streamwise variation of MOM per unit flow width for elliptical island L_4 (a=37.5cm,b=15cm,b/a=0.4) at F_r=0.19 and h=15cm (RunD12)

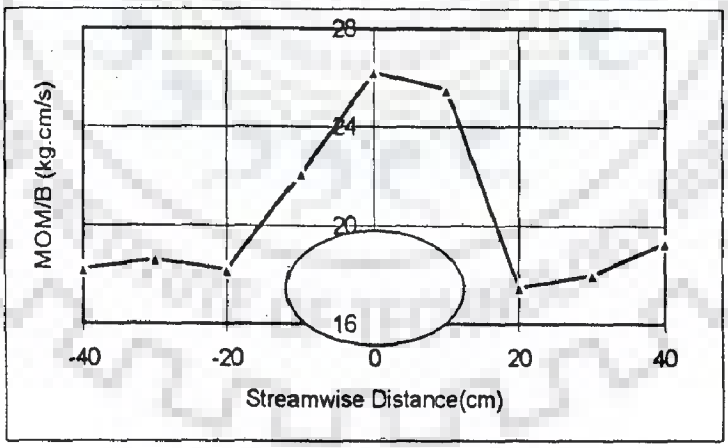

Fig. 6.5(m) Streamwise variation of MOM per unit flow width for elliptical island I_5 (a=25cm,b=15cm,b/a=0.6) at F_r=0.14 and h=15cm (RunD13)

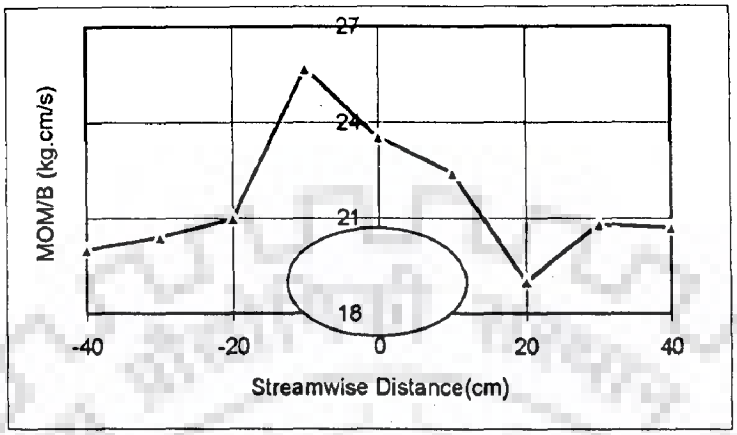

Fig. 6.5(n) Streamwise variation of MOM per unit flow width for elliptical island I_5 (a=25cm,b=15cm,b/a=0.6) at F_r=0.16 and h=15cm (RunD14)

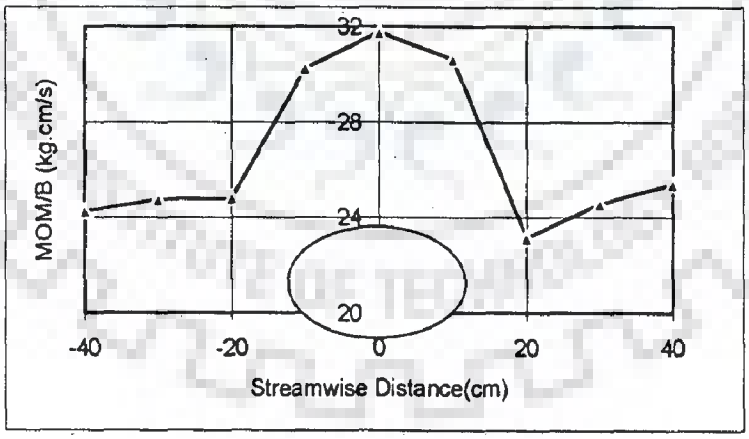

Fig. 6.5(o) Streamwise variation of MOM per unit flow width for elliptical island I_5 (a=25cm,b=15cm,b/a=0.6) at F_r=0.19 and h=15cm (RunD15)

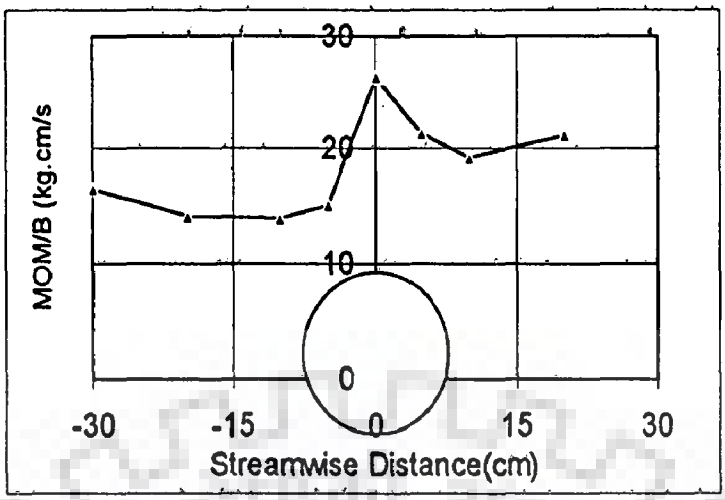

Fig. 6.5(p) Streamwise variation of MOM per unit flow width for circular island I_6 (d=15cm) at F_r=0.14 and h=15cm (RunD16)

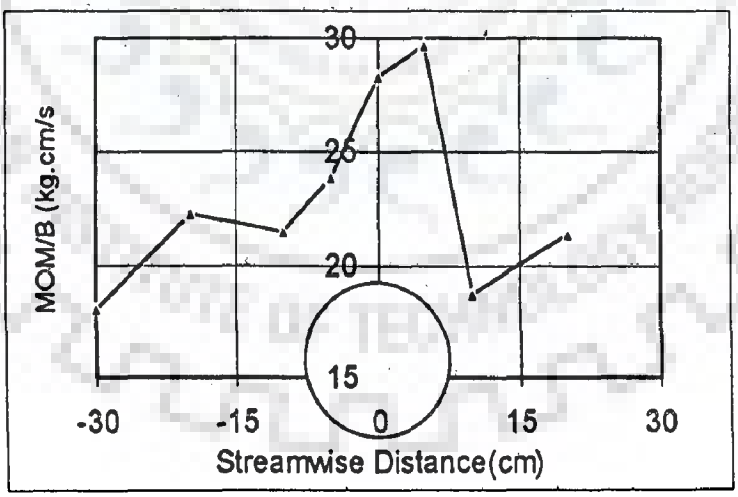

Fig. 6.5(q) Streamwise variation of MOM per unit flow width for circular island I_6 (d=15cm) at F_r=0.16 and h=15cm (RunD17)

6.4 RESULTS

One can see from Fig. 6.5(a) to 6.5(q) that MOM per unit flow width is maximum near the middle of the transition zone for almost all the runs. The purpose of this study was to investigate how the variation of MOM along the flow direction affects scour around island. Initially, it was tried to find the variation of area under MOM/B curve per unit length of island with width to length ratio (b/a) of island at three Froude numbers i.e., F_r=0.14, F_r=0.16 and F_r=0.19. The results can be seen from Fig. 6.6. The figure demonstrates that as the width to length ratio of island increases, the area under MOM/B per unit length of island also increases for a particular flow condition.

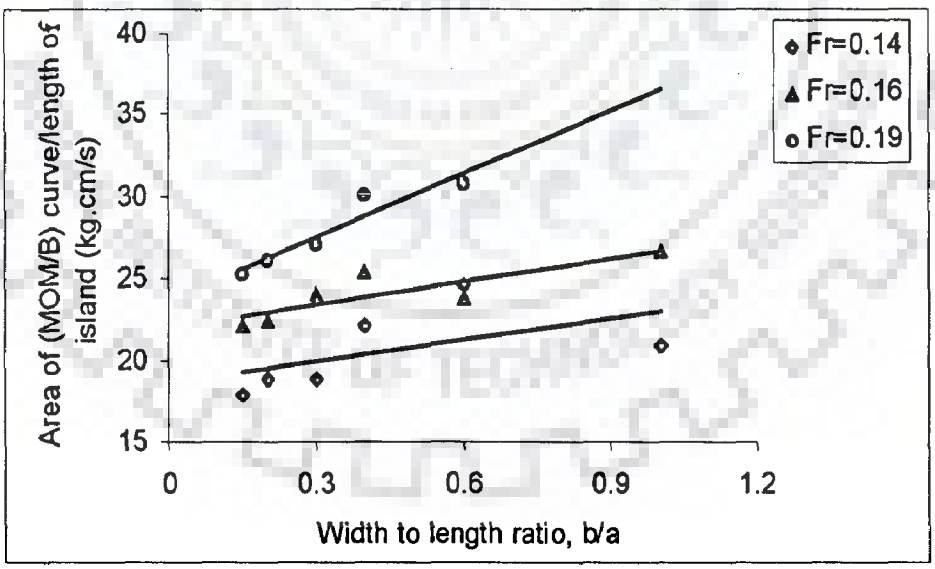

Fig. 6.6 Variation of area under MOM/B curve per unit length of island with width to length ratio of island

At the second instance, it was attempted to relate the variation of MOM with scour around island. The study was carried out for two flow conditions, i.e., for F_r=0.16 and F_r=0.19. From Fig. 6.7(a) and Fig. 6.7(b), it can be seen that for both the flow conditions, the scour around island increases with the increase in total MOM per unit length of island.

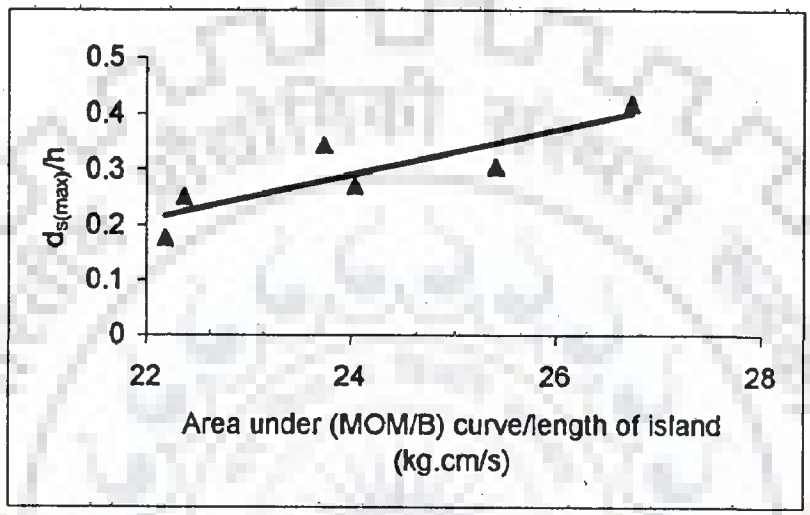

Fig. 6.7(a) Variation of dimensionless maximum scour with total MOM per unit length of island at F_r=0.16

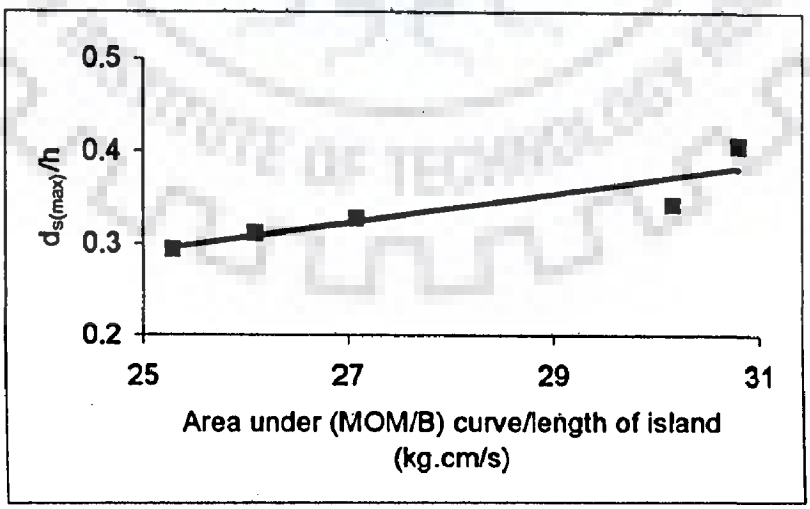

Fig. 6.7(b) Variation of dimensionless maximum scour with total MOM per unit length of island at F_r=0.19

6.5 SUMMARY

In this chapter, the growth and decay of secondary current around island has been presented for three conditions of Froude numbers. The strength of secondary current at any section has been expressed in terms of MOM per unit flow width. The influence of width to length ratio of island on the total MOM across the island has been explored. In addition, the correlation between the total MOM across the island per unit length with the scour around island has been investigated.

PROTECTION OF ISLAND

7.1 GENERAL

The methods used for river bank stabilization like riprap revetment, vegetation, windrows and trenches, sacks and blocks, gabions and mattresses, etc., may be adopted for protection of island. In the present work, instead of using the above conventional methods, attempt has been made to use the results of the study related to the scour pattern around islands, as explained in Chapter 5 for protection of island. One can see from Chapter 5 that as the width to length ratio of island decreases, the scour around the island also decreases. In the present study it was attempted to decrease the effective width to length ratio of island by placing V-shaped deflector upstream of the island and thereby reducing the scour around island. Only the circular model island (d=15 cm) was included in the present study as the scour around the circular island was found to be maximum under similar flow conditions.

7.2 EXPERIMENTS WITH V-SHAPED DEFLECTOR HAVING LENGTH OF EACH LIMB, l = 0.2d=3.0 cm

Table 3.6 lists as many as 16 experimental runs which differ in terms of Froude number, distance of V-shaped deflector upstream of the centre of the circular island, length of each limb of deflector and included angle of deflector. Froude number varies from 0.16 to 0.19, whereas the distance of V-shaped defector from the centre of the circular island varies from 0.75d to 2.0d (where d is the diameter of the circular island).

Similarly, length of each limb of deflector varies from 0.2d to 0.3d. The included angle of the V-shaped deflector also varies from 30° to 84°. For each location, the included angle of the deflector was so adjusted that if the two limbs of the deflector are extended, they become tangential to the periphery of the circular island.

As there was no idea regarding the size of deflector as well as the location of deflector, initially it was tried to use a smaller deflector having length of each limb, l=0.2 d=3.0 cm at a distance of 0.75 d=11.25 cm upstream of the centre of the circular island, the included angle (θ) of the deflector being 84° (Plate 7.1). The Froude number was kept at F_r=0.16. From Fig. 7.1 and Fig. 7.2, it can be seen that the maximum scour occurred near the middle of the circular island. But the maximum scour decreased from 6.25 cm (without deflector) to 4.98 cm (with deflector). Similarly, experimental runs were carried out at the same Froude number by placing the V-shaped deflectors having limbs of same length at 1.0 d=15.0 cm (Plate 7.2), 1.5 d=22.5 cm (Plate 7.3) and 2.0 d=30 cm (Plate 7.4) upstream of the centre of the island. It can be seen from Fig. 7.3 to Fig. 7.8 that for each location, the maximum scour decreased and the scour reduced to a minimum when the deflector was placed 15 cm (1.0 d) upstream of the centre of the island (Fig. 7.4). The above set of experimental runs was repeated at Froude number of 0.19 (Plate 7.5 to Plate 7.8 and Fig. 7.9 to Fig. 7.16) and again it was observed that the scour around the circular island reduced to a minimum when the deflector was placed 15 cm (1.0 d) upstream of the centre of the island (Fig. 7.12).

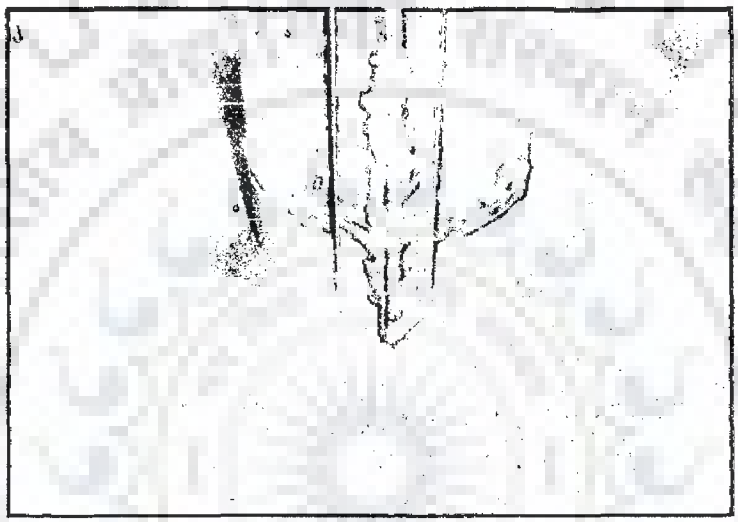

Plate 7.1 Scour around circular island (d=15 cm) at Fr=0.16 and h=15 cm with V-shaped deflector (limb length=3 cm) at 11.25 cm upstream of island (RunE1)

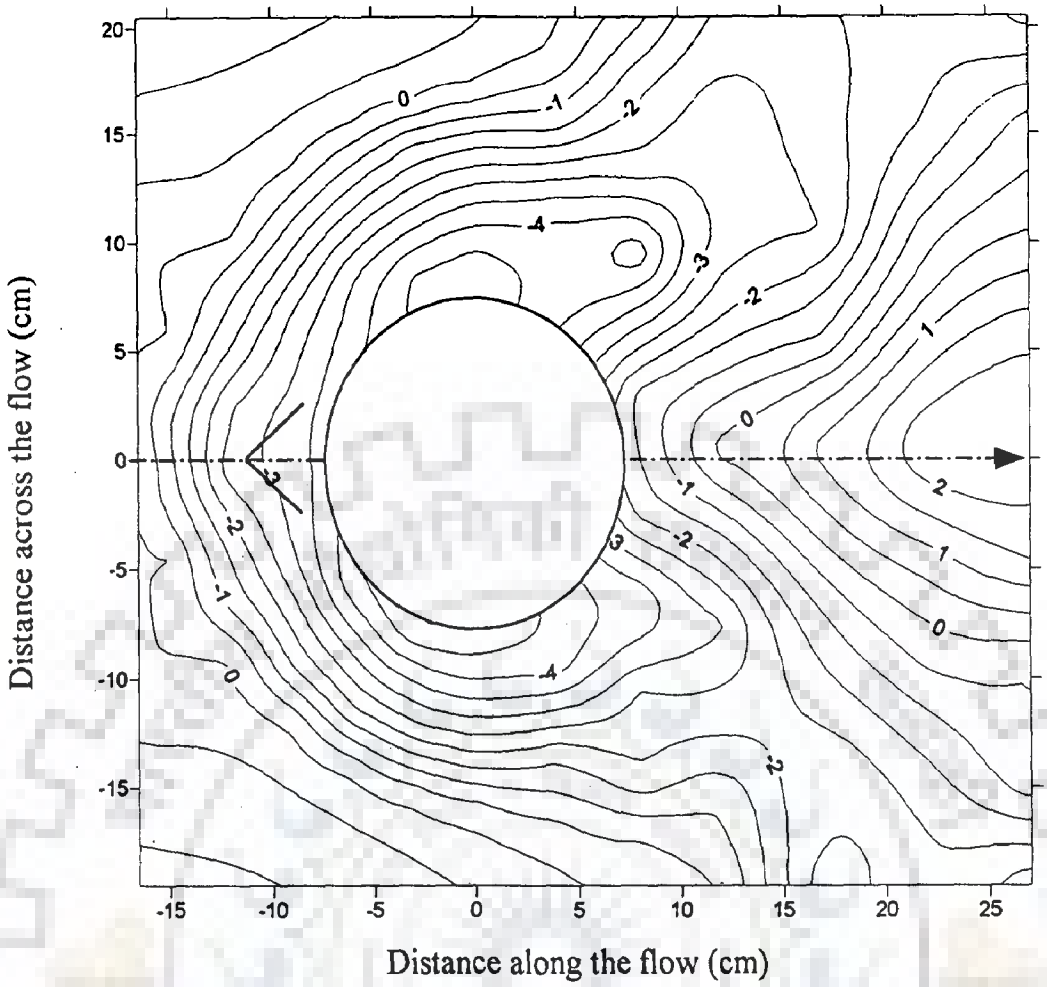

Fig. 7.1 Scour pattern around circular island (d=15 cm) at F_r=0.16 & h= 15cm with V-shaped deflector (limb length= 3cm) at 11.25 cm upstream of island (contour interval in cm) (RunE1)

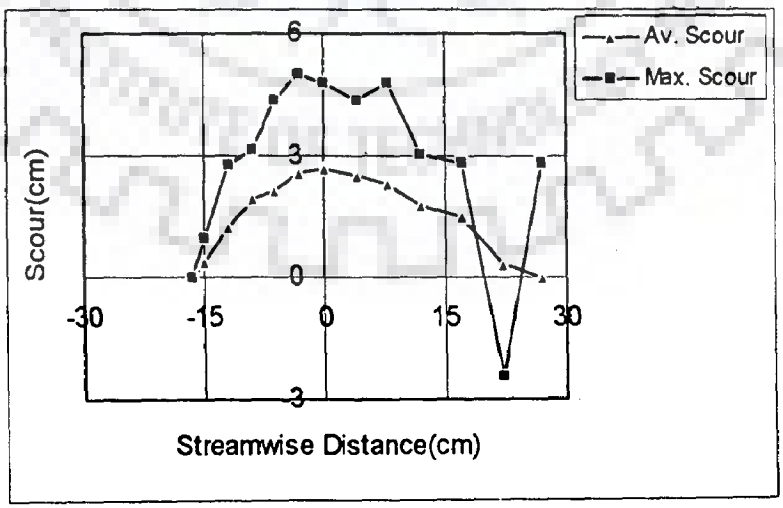

Fig. 7.2 Streamwise variation of scour around circular island (d=15 cm) at F_r =0.16 & h=15 cm with V-shaped deflector (limb length =3 cm) at 11.25cm upstream of island (RunE1)

Plate 7.2 Scour around circular island (d=15 cm) at Fr=0.16 and h=15 cm with V-shaped deflector (limb length = 3cm) at 15 cm upstream of island (RunE2)

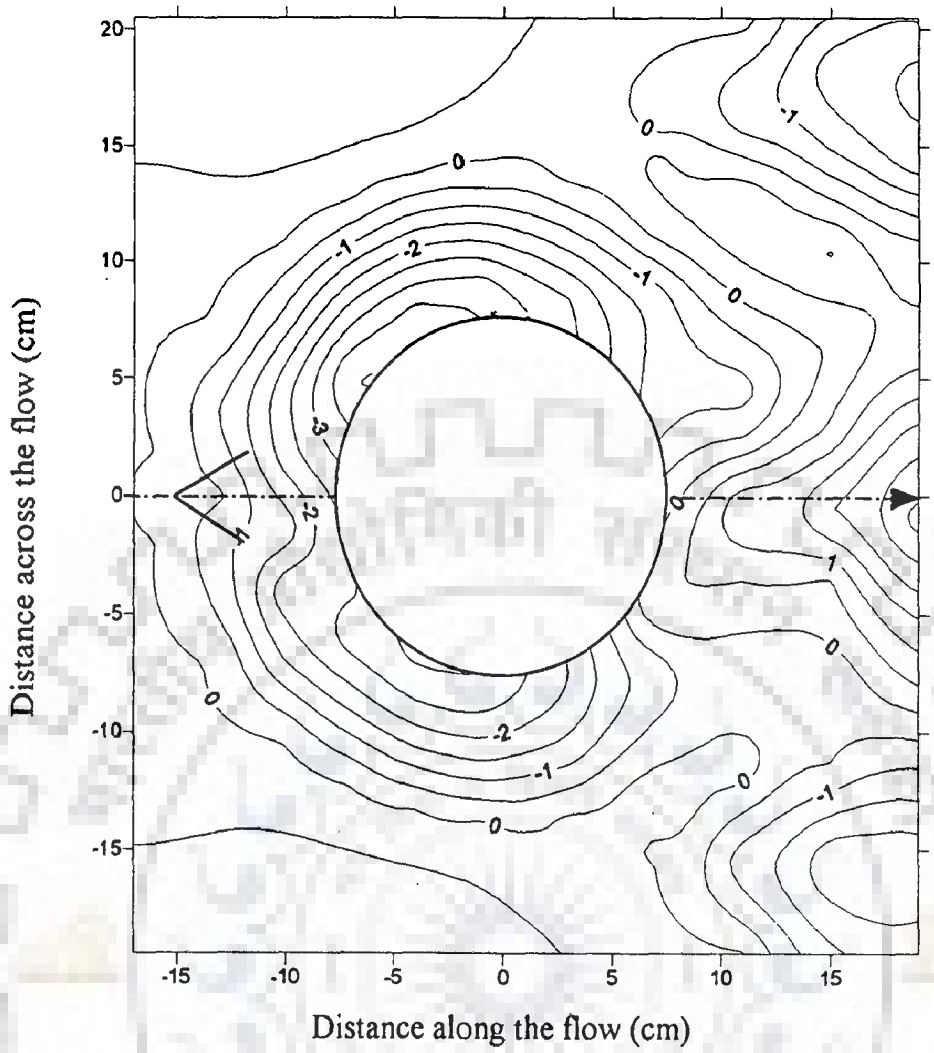

Fig. 7.3 Scour pattern around circular island (d=15 cm) at F_r=0.16 & h=15 cm with V-shaped deflector (limb length =3 cm) at 15 cm upstream of island (contour interval in cm) (RunE2)

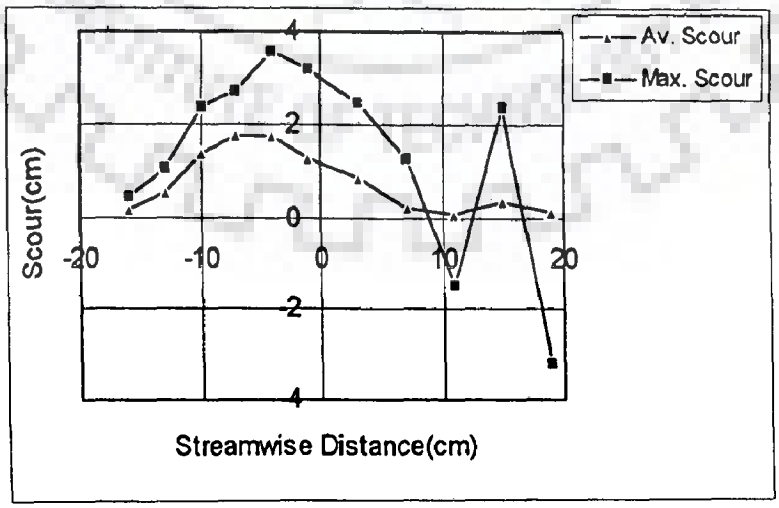

Fig. 7.4 Streamwise variation of scour around circular island (d=15 cm) at F_r =0.16 & h=15 cm with V-shaped deflector (limb length =3 cm) at 15 cm upstream of island (RunE2)

Plate 7.3 Scour around circular island (d=15 cm) at Fr=0.16 and h=15 cm with V-shaped deflector (limb length =3 cm) at 22.5 cm upstream of island (RunE3)

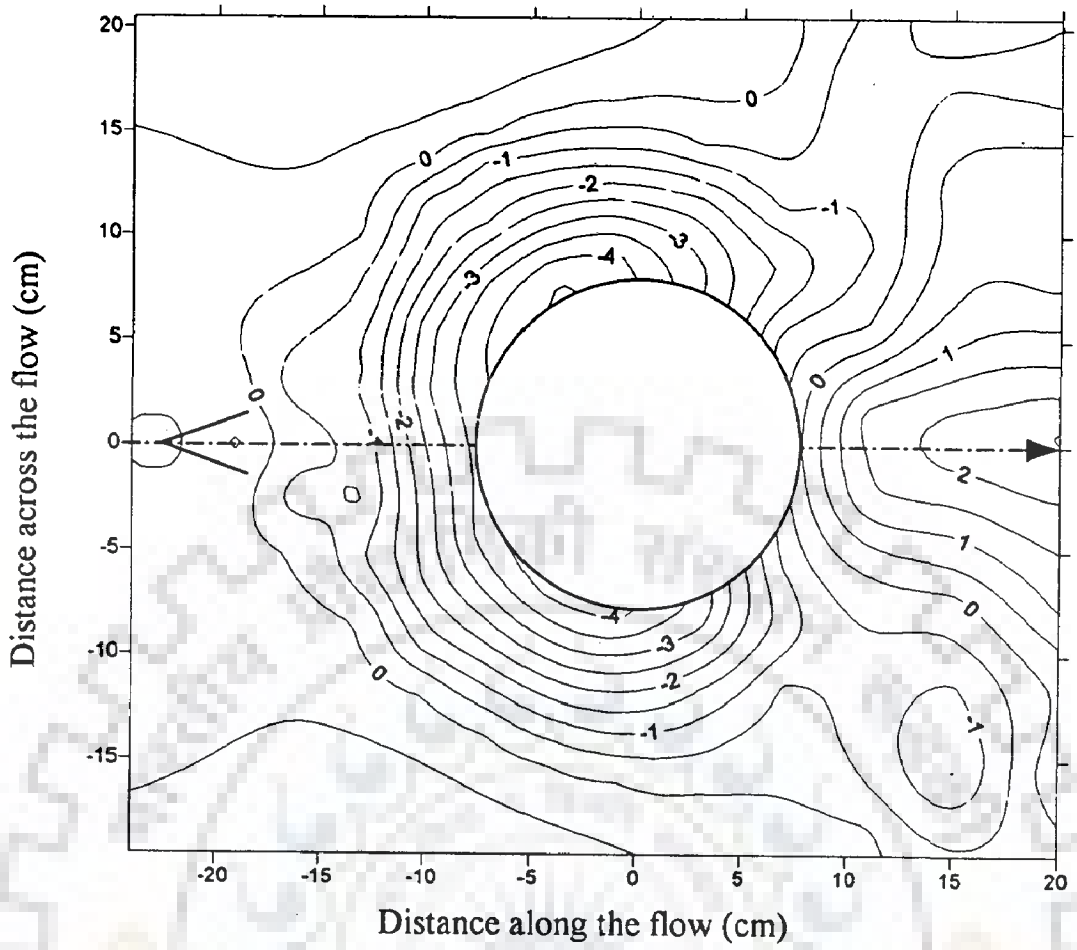

Fig. 7.5 Scour pattern around circular island (d=15 cm) at F_r=0.16 & h=15 cm with V-shaped deflector (limb length =3 cm) at 22.5 cm upstream of island (contour interval in cm) (RunE3)

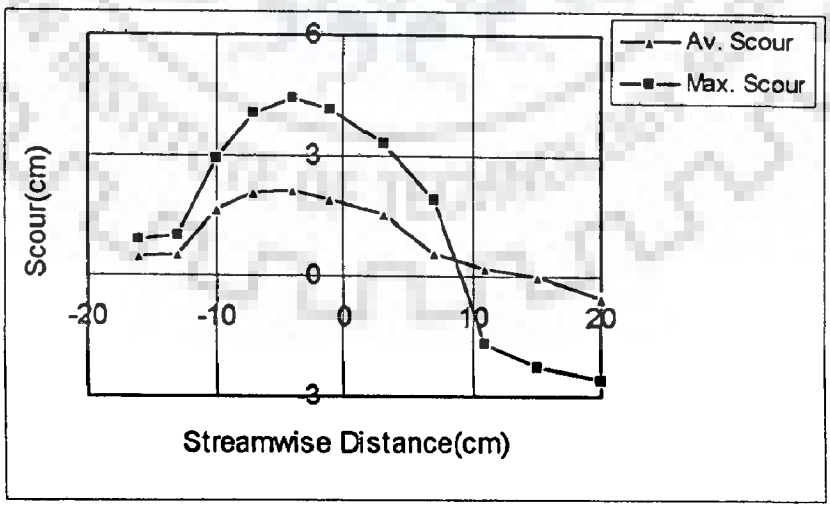

Fig. 7.6 Streamwise variation of scour around circular island (d=15 cm) at F_r =0.16 & h=15 cm with V-shaped deflector (limb length =3 cm) at 22.5 cm upstream of island (RunE3)

Plate 7.4 Scour around circular island (d=15 cm) at Fr=0.16 and h=15 cm with V-shaped deflector (limb length =3 cm) at 30 cm upstream of island (RunE4)

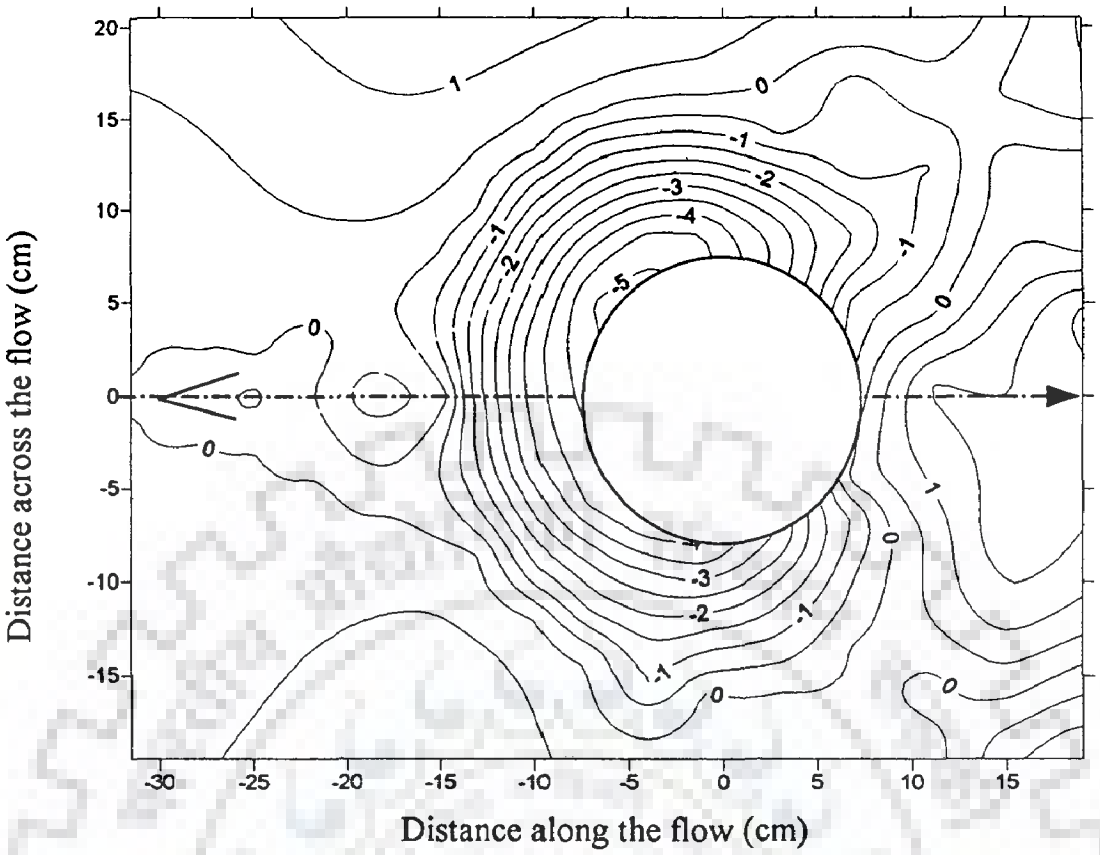

Fig. 7.7 Scour pattern around circular island (d=15 cm) at F_r=0.16 & h=15 cm with V-shaped deflector (limb length =3 cm) at 30 cm upstream of island (contour interval in cm) (RunE4)

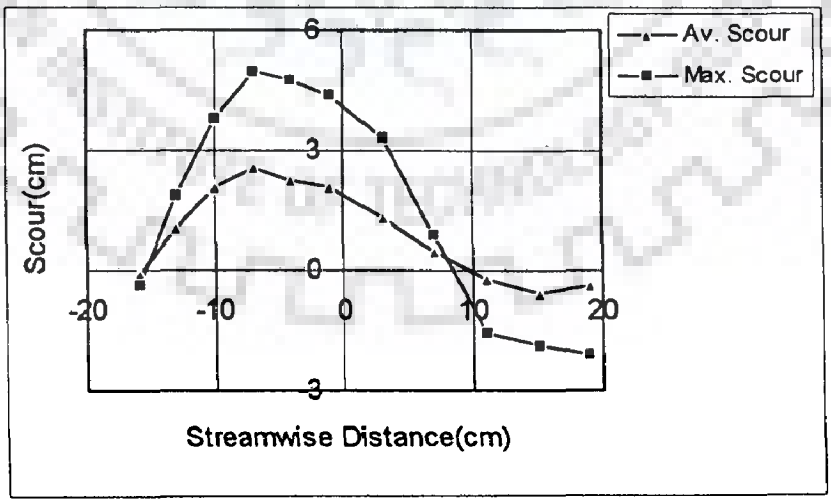

Fig. 7.8 Streamwise variation of scour around circular island (d=15 cm) at F_r =0.16 & h=15 cm with V-shaped deflector (limb length =3 cm) at 30 cm upstream of island (RunE4)

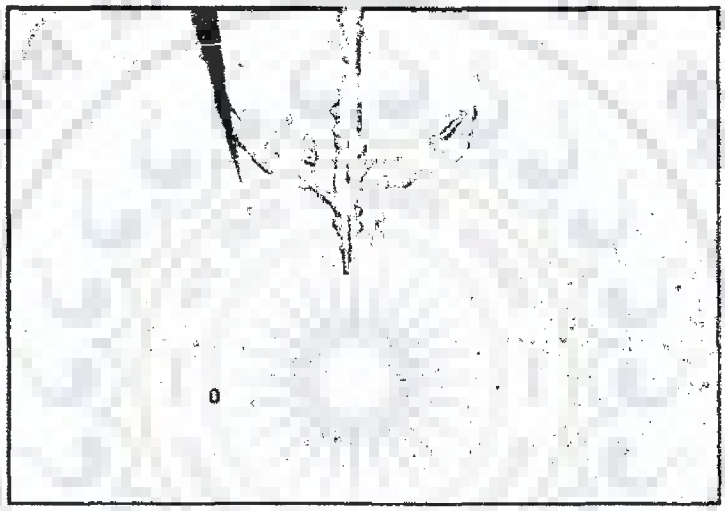

Plate 7.5 Scour around circular island (d=15 cm) at Fr=0.19 and h=15 cm with V-shaped deflector (limb length =3 cm) at 11.25 cm upstream of island (RunE5)

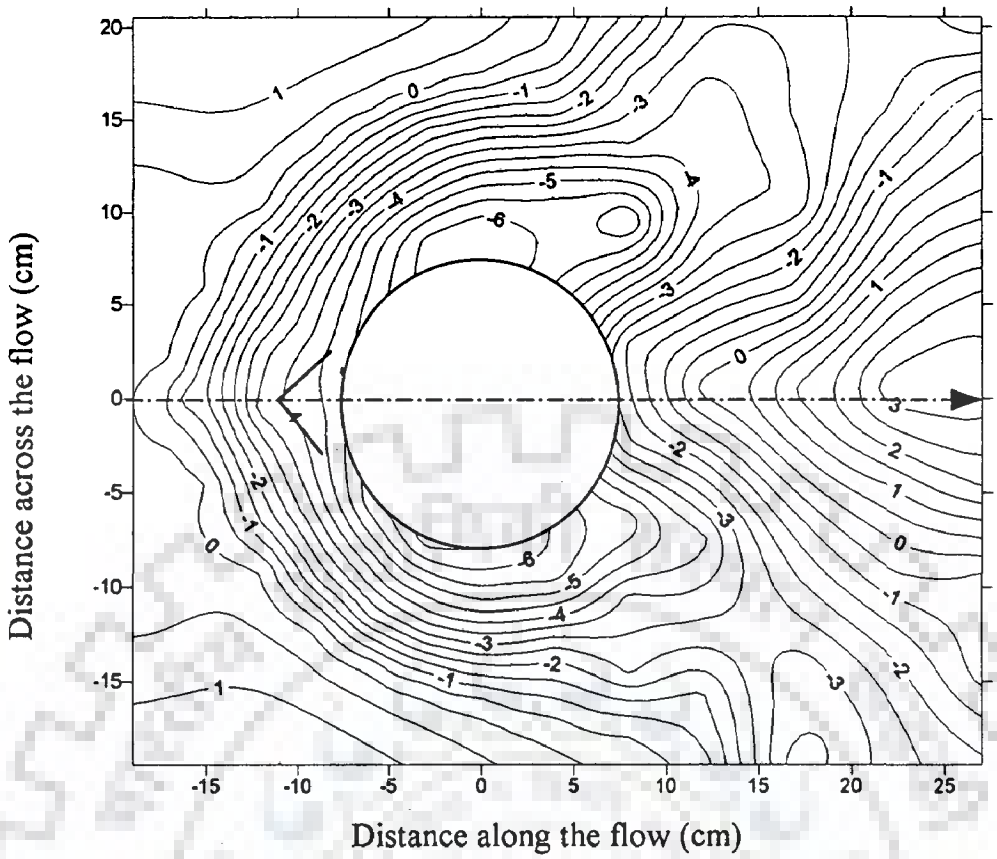

Fig. 7.9 Scour pattern around circular island (d=15 cm) at F_r=0.19 & h=15 cm with V-shaped deflector (limb length =3 cm) at 11.25 cm upstream of island (contour interval in cm) (RunE5)

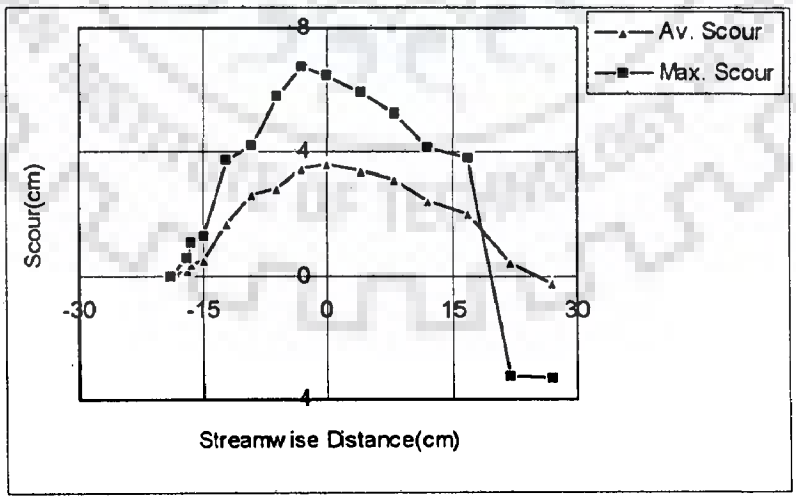

Fig. 7.10 Streamwise variation of scour around circular island (d=15 cm) at F_r =0.19 & h=15 cm with V-shaped deflector (limb length =3 cm) at 11.25 cm upstream of island (RunE5)

Plate 7.6 Scour around circular island (d=15 cm) at Fr=0.19 and h=15 cm with V-shaped deflector (limb length =3 cm) at 15 cm upstream of island (RunE6)

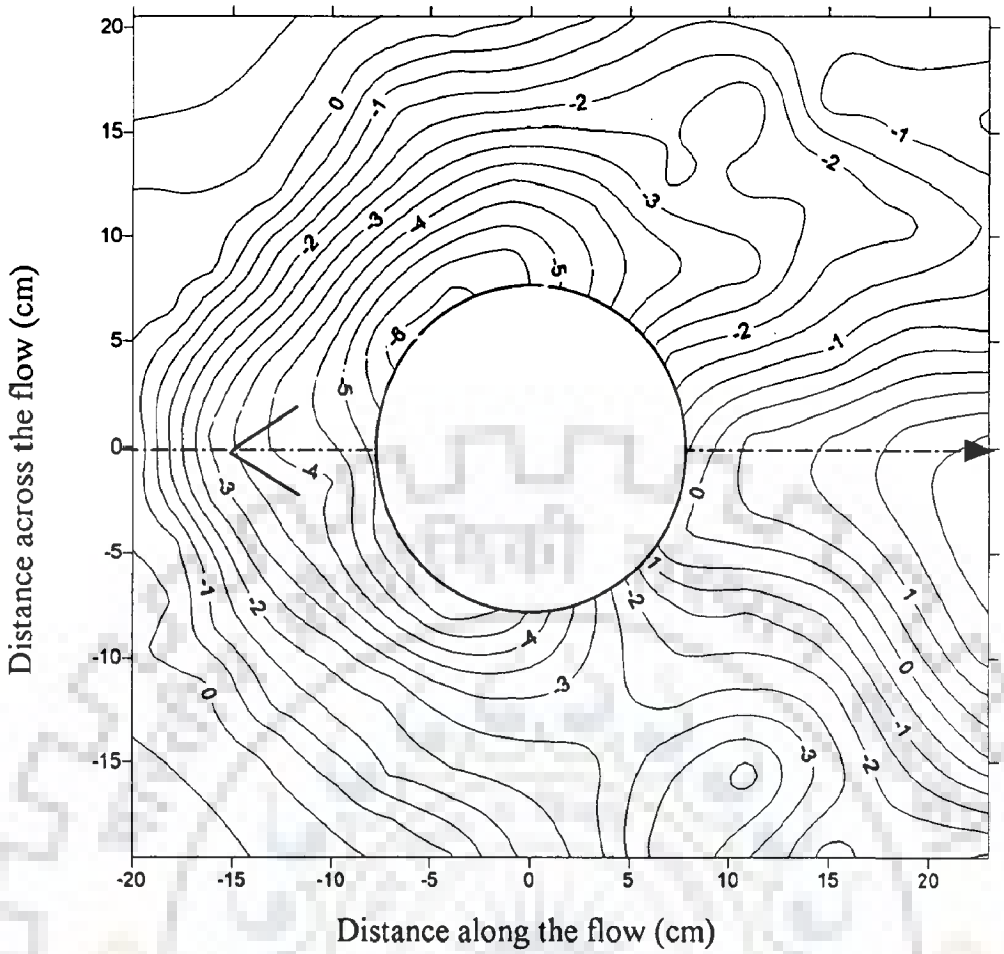

Fig. 7.11 Scour pattern around circular island (d=15 cm) at F_r=0.19 & h=15 cm with V-shaped deflector (limb length =3 cm) at 15 cm upstream of island (contour interval in cm) (RunE6)

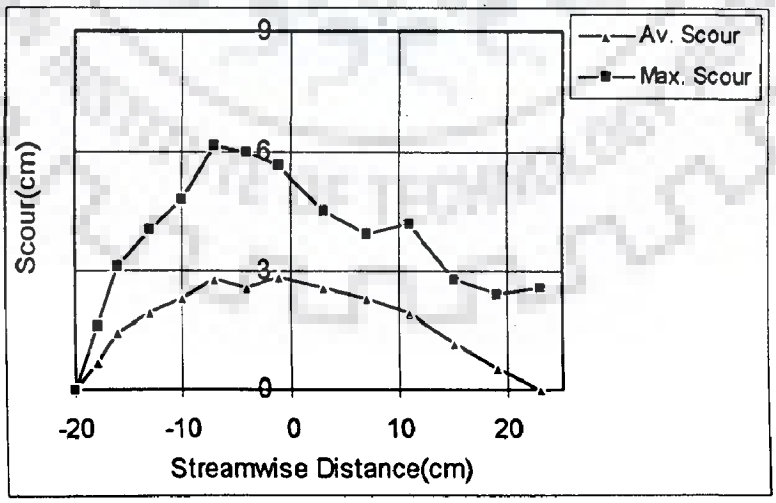

Fig. 7.12 Streamwise variation of scour around circular island (d=15 cm) at F_r =0.19 & h=15 cm with V-shaped deflector (limb length =3 cm) at 15 cm upstream of island (RunE6)

Plate 7.7 Scour around circular island (d=15 cm) at Fr=0.19 and h=15 cm with V-shaped deflector (limb length =3 cm) at 22.5 cm upstream of island (RunE7)

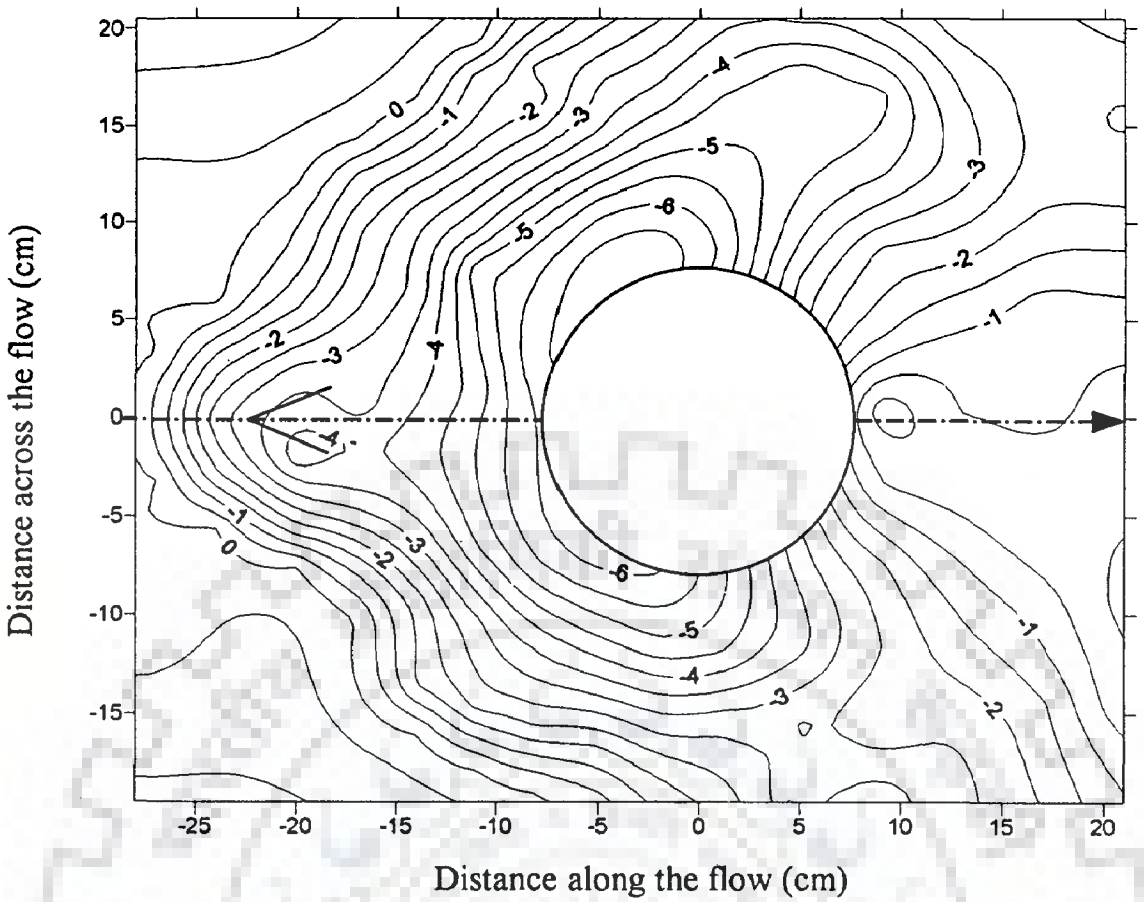

Fig. 7.13 Scour pattern around circular island (d=15 cm) at F_r=0.19 & h=15 cm with V-shaped deflector (limb length =3 cm) at 22.5 cm upstream of island (contour interval in cm) (RunE7)

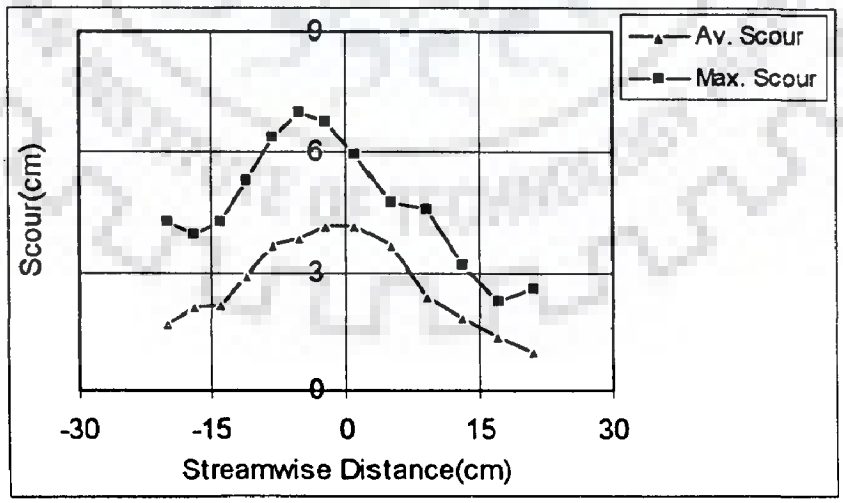

Fig. 7.14 Streamwise variation of scour around circular island (d=15 cm) at F_r =0.19 & h=15 cm with V-shaped deflector (limb length =3 cm) at 22.5 cm upstream of island (RunE7)

Plate 7.8 Scour around circular island (d=15 cm) at Fr=0.19 and h=15 cm with V-shaped deflector (limb length =3 cm) at 30 cm upstream of island (RunE8)

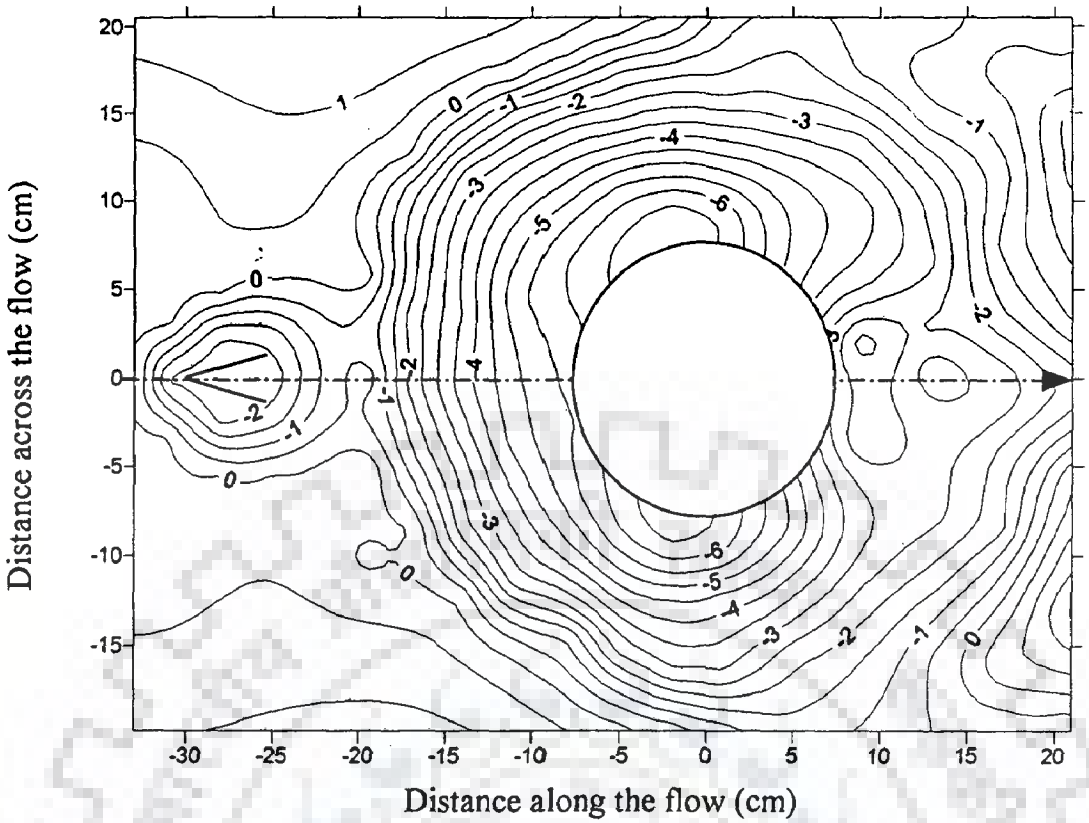

Fig. 7.15 Scour pattern around circular island (d=15 cm) at F_r=0.19 & h=15 cm with V-shaped deflector (limb length =3 cm) at 30 cm upstream of island (contour interval in cm) (RunE8)

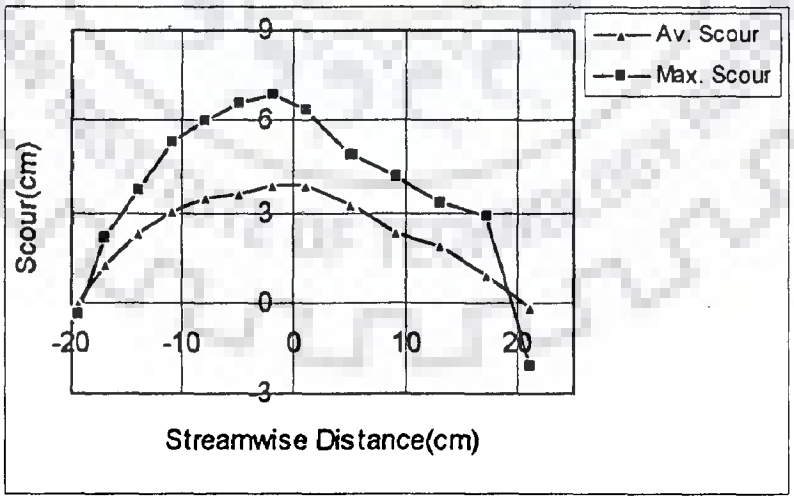

Fig. 7.16 Streamwise variation of scour around circular island (d=15 cm) at F_r =0.19 & h=15 cm with V-shaped deflector (limb length =3 cm) at 30 cm upstream of island (RunE8)

7.3 EXPERIMENTS WITH V-SHAPED DEFLECTOR HAVING LENGTH OF EACH LIMB, l= 0.3d=4.5 cm

At the second attempt, length of each limb of the V-shaped deflector was increased to 0.3d=4.5 cm. The deflector was kept at four different locations i.e., 15 cm (1.0 d), 18.75 cm (1.25 d), 22.5 cm (1.5 d) and 30 cm (2.0 d) upstream of the centre of the circular island with different included angles (Plate 7.9 to Plate 7.12 and Fig. 7.17 to Fig. 7.24). The runs were carried out at a Froude number of 0.16. From Fig. 7.20, it is clear that the scour reduced to a minimum when the deflector was placed at 18.75 cm (1.25 d) upstream of the centre of the island. Another set of four experimental runs was conducted placing the V-shaped deflectors at the same four locations at Froude number of 0.19 (Plate 7.13 to Plate 7.16 and Fig. 7.25 to Fig. 7.32). It can be seen from Fig. 7.28 that in this case also the scour reduced to a minimum when the deflector was placed at 18.75 cm (1.25 d) upstream of the center of the island.

Plate 7.9 Scour around circular island (d=15 cm) at Fr=0.16 and h=15 cm with V-shaped deflector (limb length =4.5 cm) at 15 cm upstream of island (RunE9)

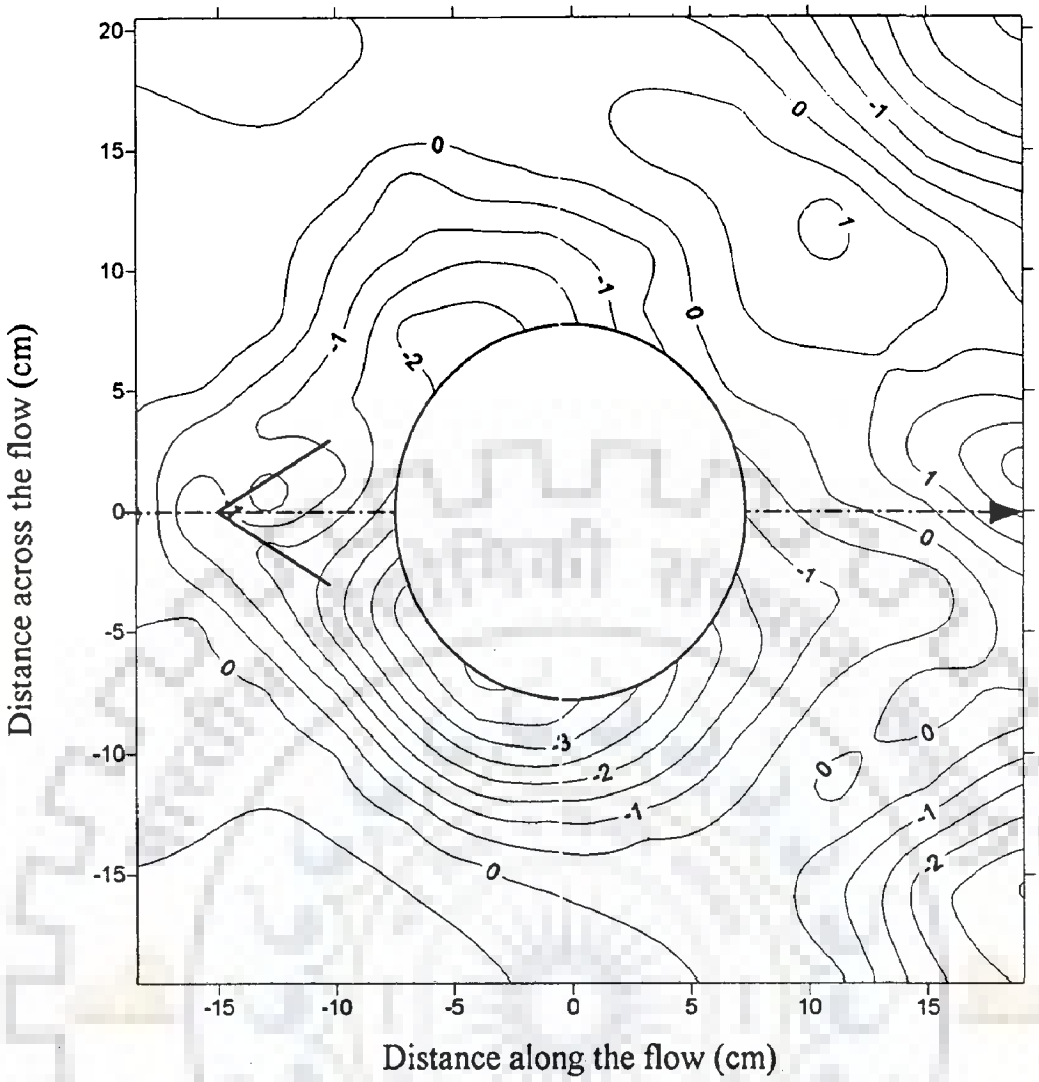

Fig. 7.17 Scour pattern around circular island (d=15 cm) at F_r=0.16 & h=15 cm with V-shaped deflector (limb length =4.5 cm) at 15 cm upstream of island (contour interval in cm) (RunE9)

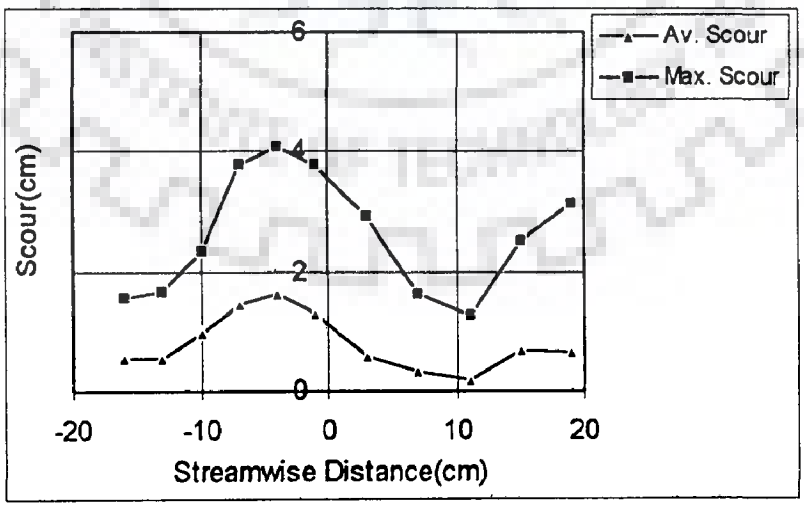

Fig. 7.18 Streamwise variation of scour around circular island (d=15 cm) at F_r =0.16 & h=15 cm with V-shaped deflector (limb length =4.5 cm) at 15 cm upstream of island (RunE9)

Plate 7.10 Scour around circular island (d=15 cm) at Fr=0.16 and h=15 cm with V-shaped deflector (limb length =4.5 cm) at 18.75 cm upstream of island (RunE10)

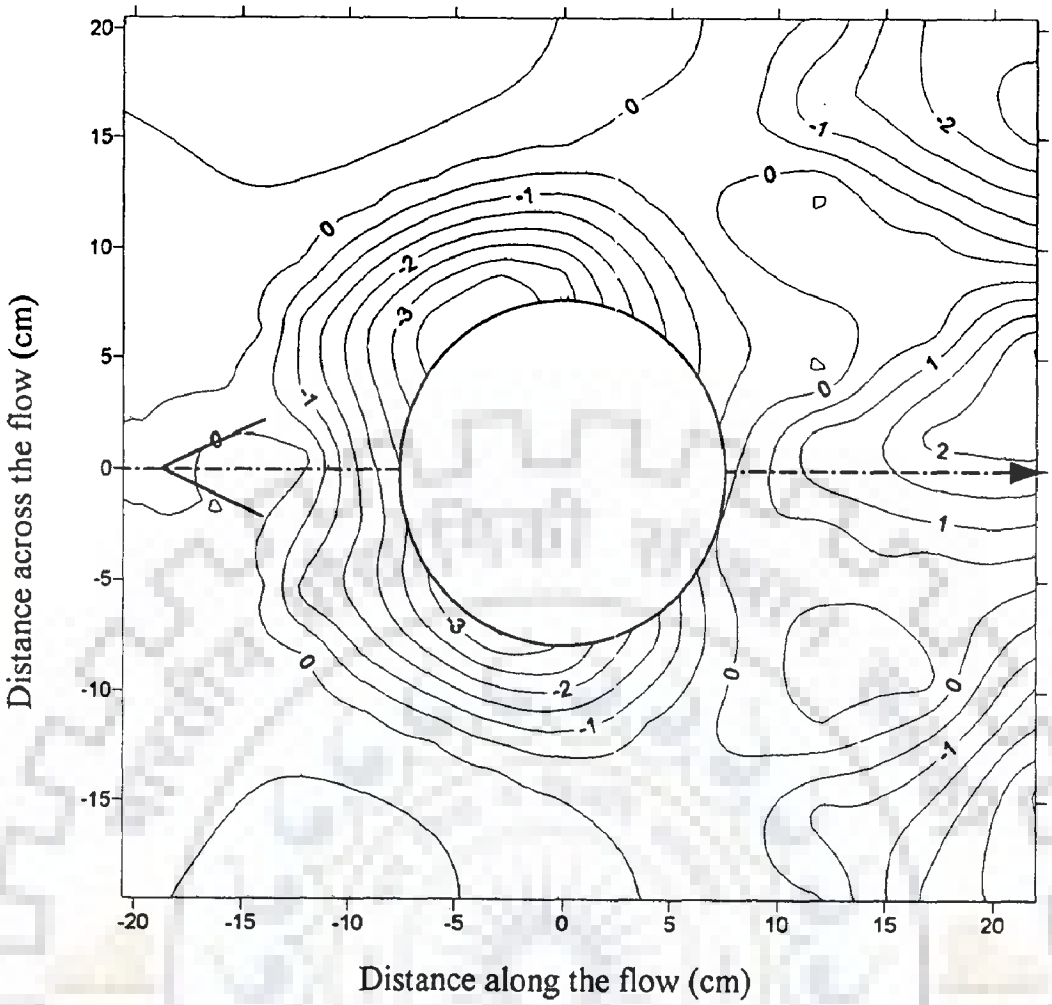

Fig. 7.19 Scour pattern around circular island (d=15 cm) at F_r=0.16 & h=15 cm with V-shaped deflector (limb length =4.5 cm) at 18.75 cm upstream of island (contour interval in cm) (RunE10)

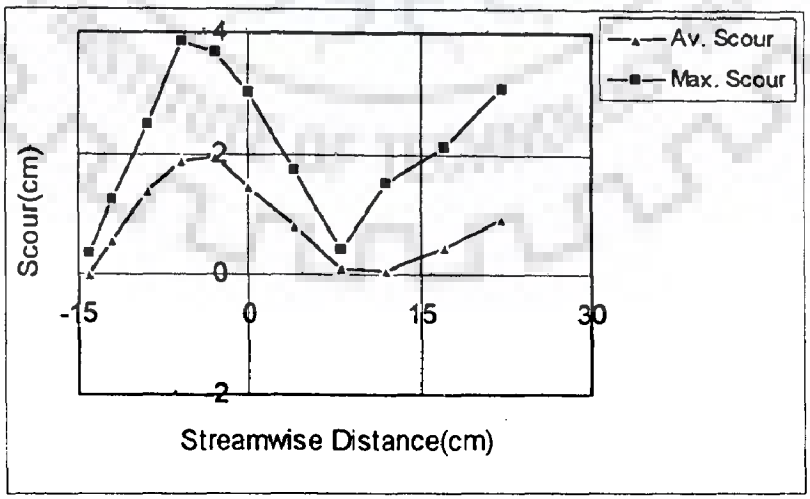

Fig. 7.20 Streamwise variation of scour around circular island (d=15 cm) at F_r =0.16 & h=15 cm with V-shaped deflector (limb length =4.5 cm) at 18.75 cm upstream of island (RunE10)

Plate 7.11 Scour around circular island (d=15 cm) at Fr=0.16 and h=15 cm with V-shaped deflector (limb length =4.5 cm) at 22.5 cm upstream of island (RunE11)

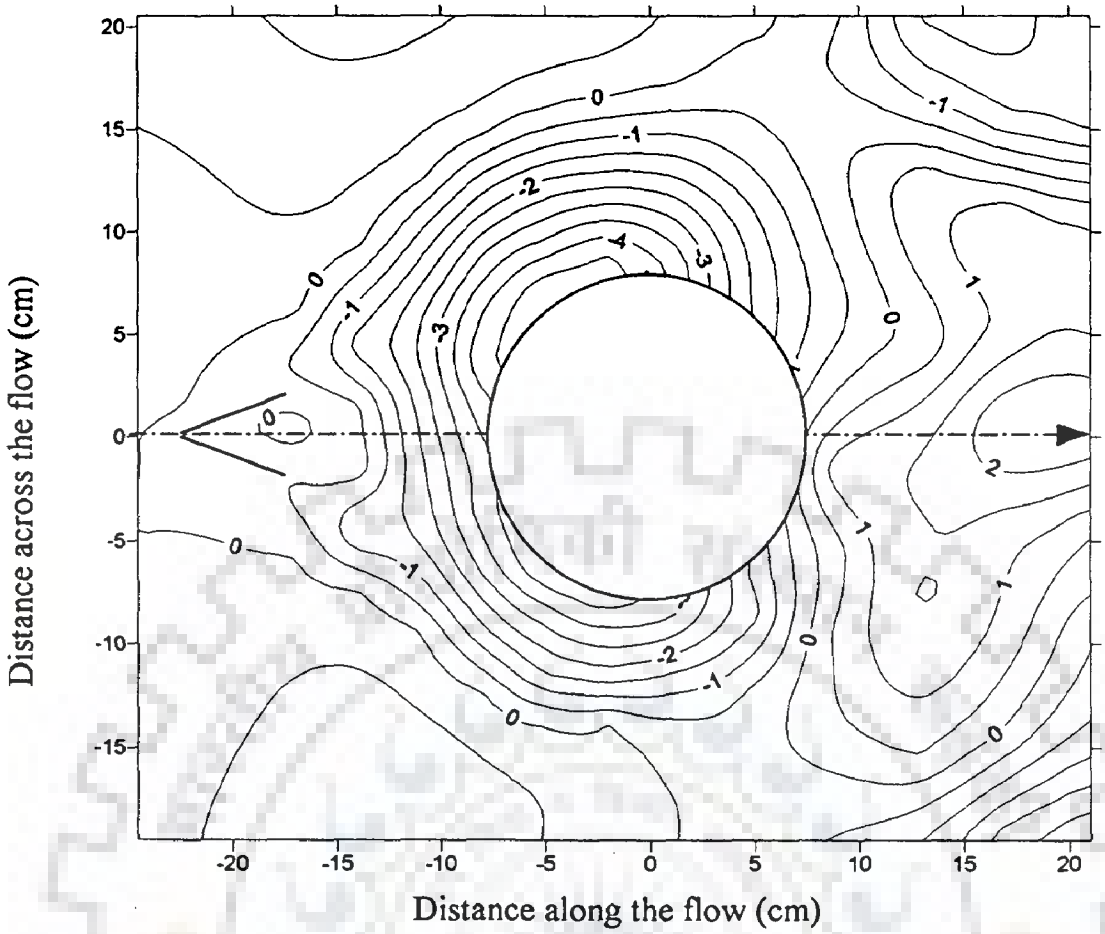

Fig. 7.21 Scour pattern around circular island (d=15 cm) at F_r=0.16 & h=15 cm with V-shaped deflector (limb length =4.5 cm) at 22.5 cm upstream of island (contour interval in cm) (RunE11)

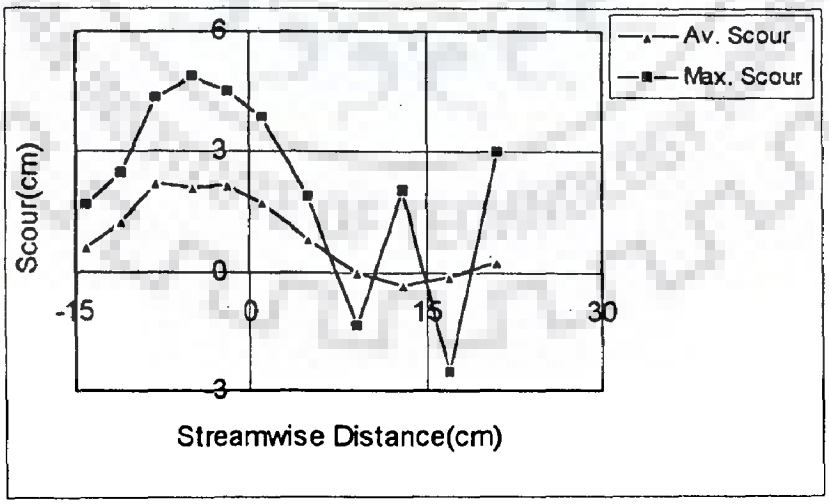

Fig. 7.22 Streamwise variation of scour around circular island (d=15 cm) at F_r =0.16 & h=15 cm with V-shaped deflector (limb length =4.5 cm) at 22.5 cm upstream of island (RunE11)

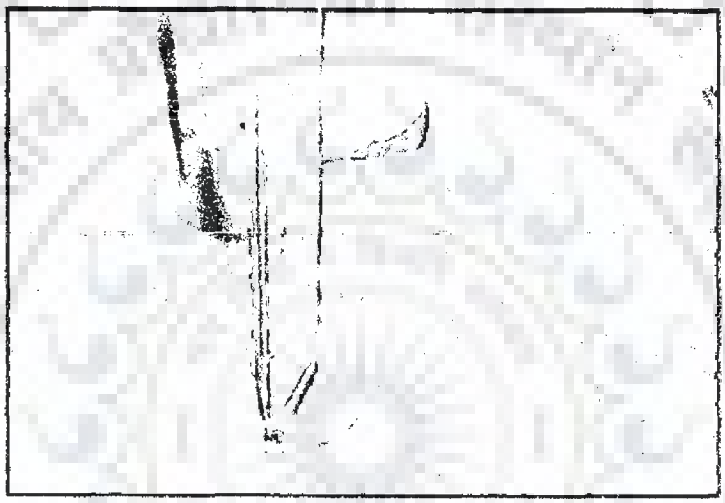

Plate 7.12 Scour around circular island (d=15 cm) at Fr=0.16 and h=15 cm with V-shaped deflector (limb length =4.5 cm) at 30 cm upstream of island (RunE12)

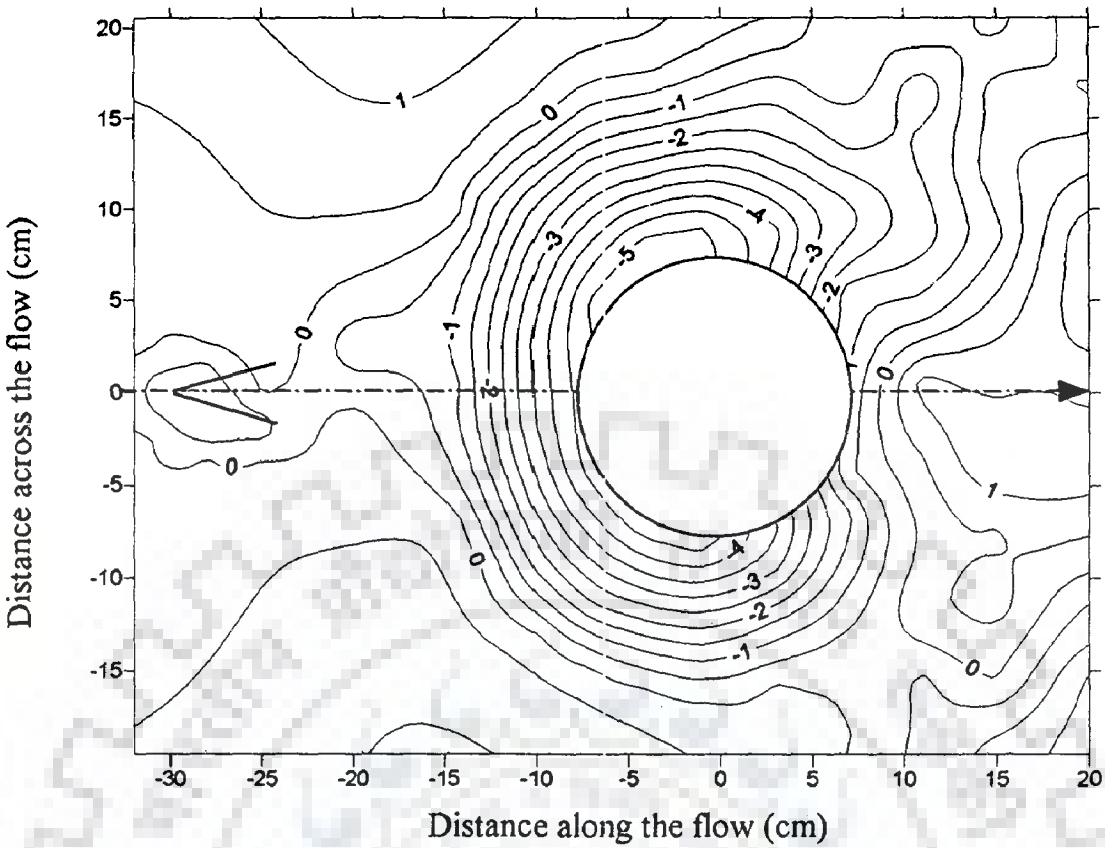

Fig. 7.23 Scour pattern around circular island (d=15 cm) at F_r=0.16 & h=15 cm with V-shaped deflector (limb length =4.5 cm) at 30 cm upstream of island (contour interval in cm) (RunE12)

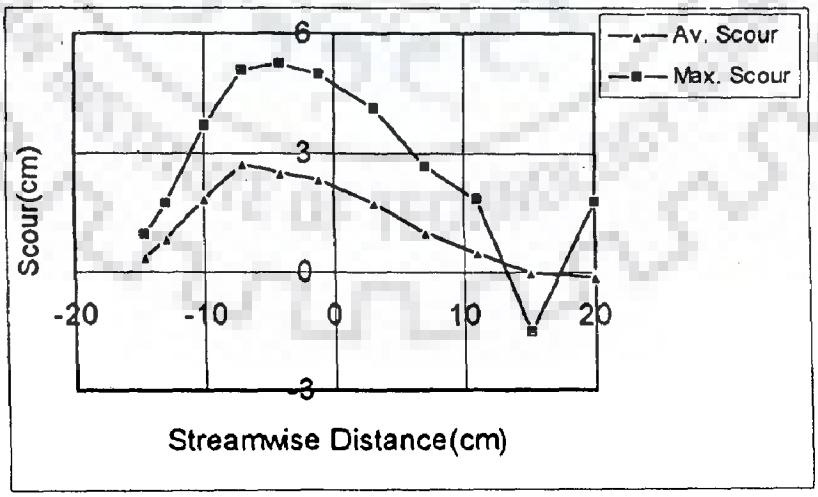

Fig. 7.24 Streamwise variation of scour around circular island (d=15 cm) at F_r =0.16 & h=15 cm with V-shaped deflector (limb length =4.5 cm) at 30 cm upstream of island (RunE12)

Plate 7.13 Scour around circular island (d=15 cm) at Fr=0.19 and h=15 cm with V-shaped deflector (limb length =4.5 cm) at 15 cm upstream of island (RunE13)

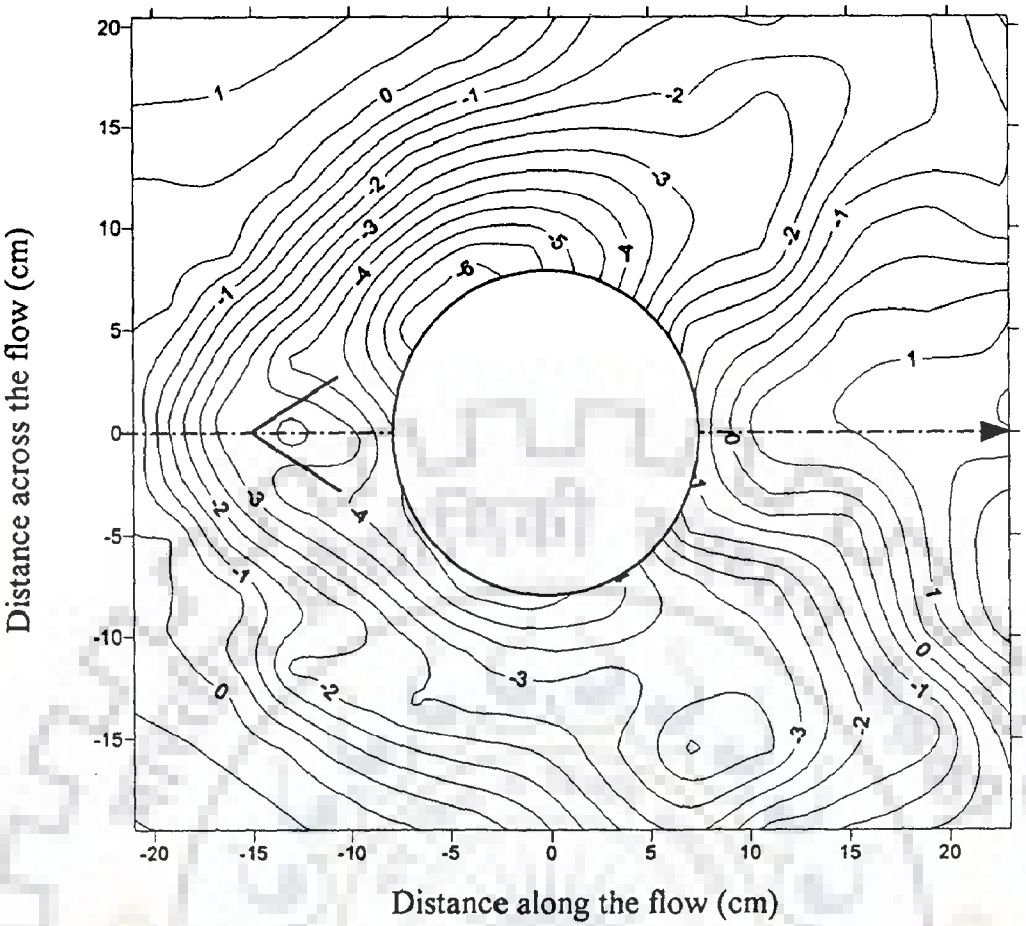

Fig. 7.25 Scour pattern around circular island (d=15 cm) at F_r=0.19 & h=15 cm with V-shaped deflector (limb length =4.5 cm) at 15 cm upstream of island (contour interval in cm) (RunE13)

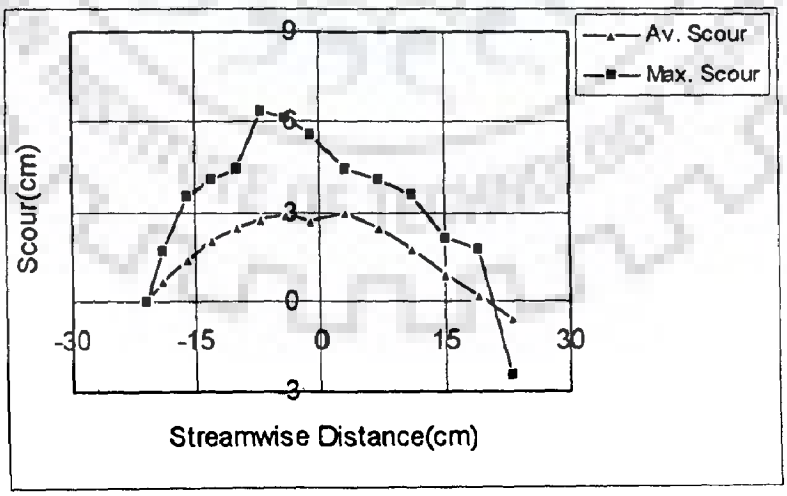

Fig. 7.26 Streamwise variation of scour around circular island (d=15 cm) at F_r =0.19 & h=15 cm with V-shaped deflector (limb length =4.5 cm) at 15 cm upstream of island (RunE13)

Plate 7.14 Scour around circular island (d=15 cm) at Fr=0.19 and h=15 cm with V-shaped deflector (limb length =4.5 cm) at 18.75 cm upstream of island (RunE14)

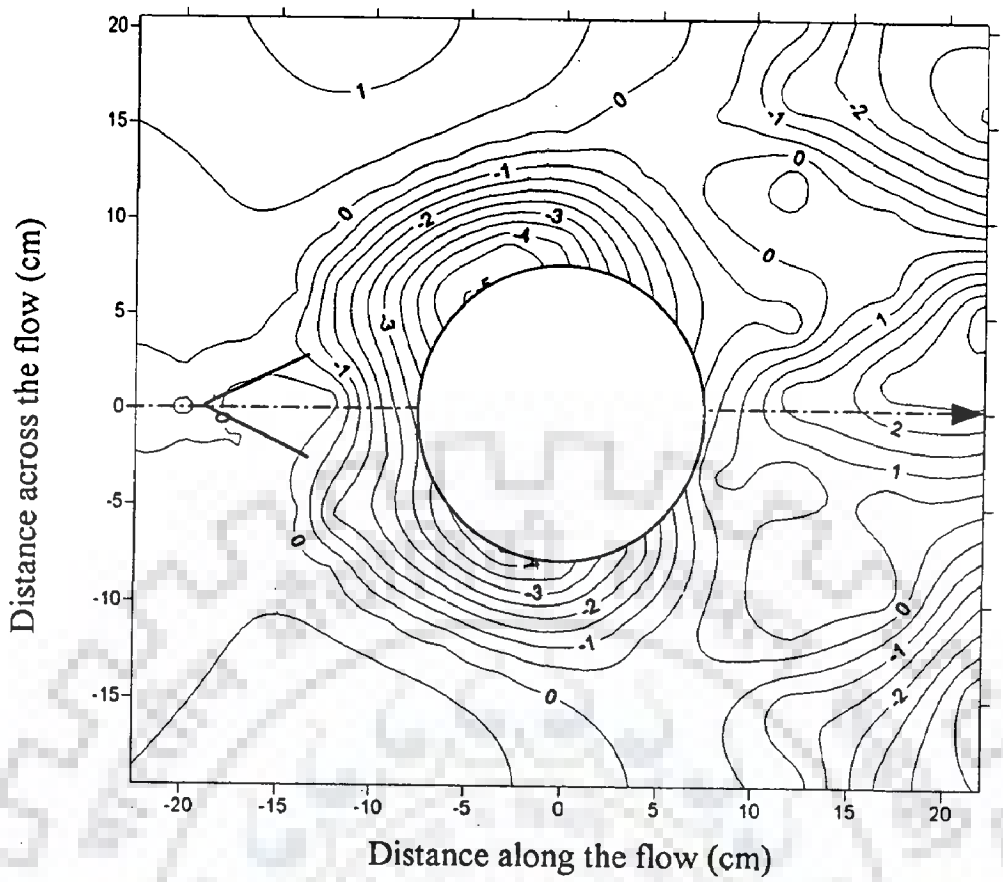

Fig. 7.27 Scour pattern around circular island (d=15 cm) at F_r=0.19 & h=15 cm with V-shaped deflector (limb length =4.5 cm) at 18.75 cm upstream of island (contour interval in cm) (RunE14)

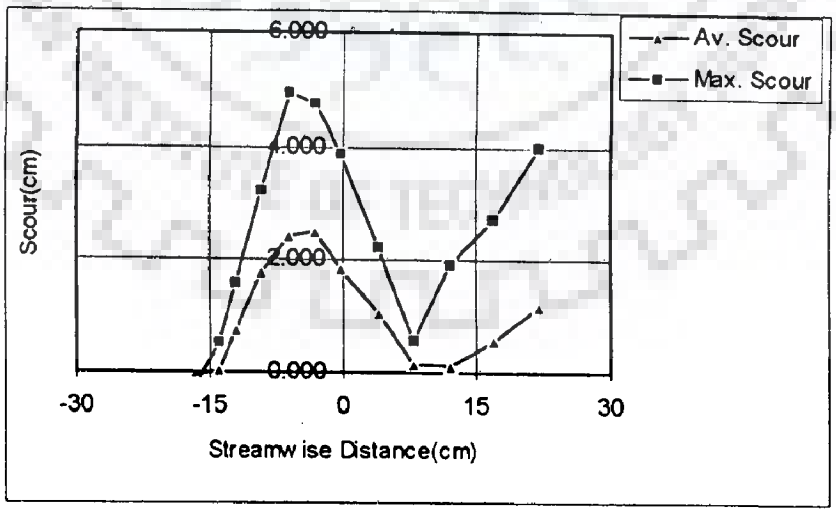

Fig. 7.28 Streamwise variation of scour around circular island (d=15 cm) at F_r =0.19 & h=15 cm with V-shaped deflector (limb length =4.5 cm) at 18.75 cm upstream of island (RunE14)

Plate 7.15 Scour around circular island (d=15 cm) at Fr=0.19 and h=15 cm with V-shaped deflector (limb length =4.5 cm) at 22.5 cm upstream of island (RunE15)

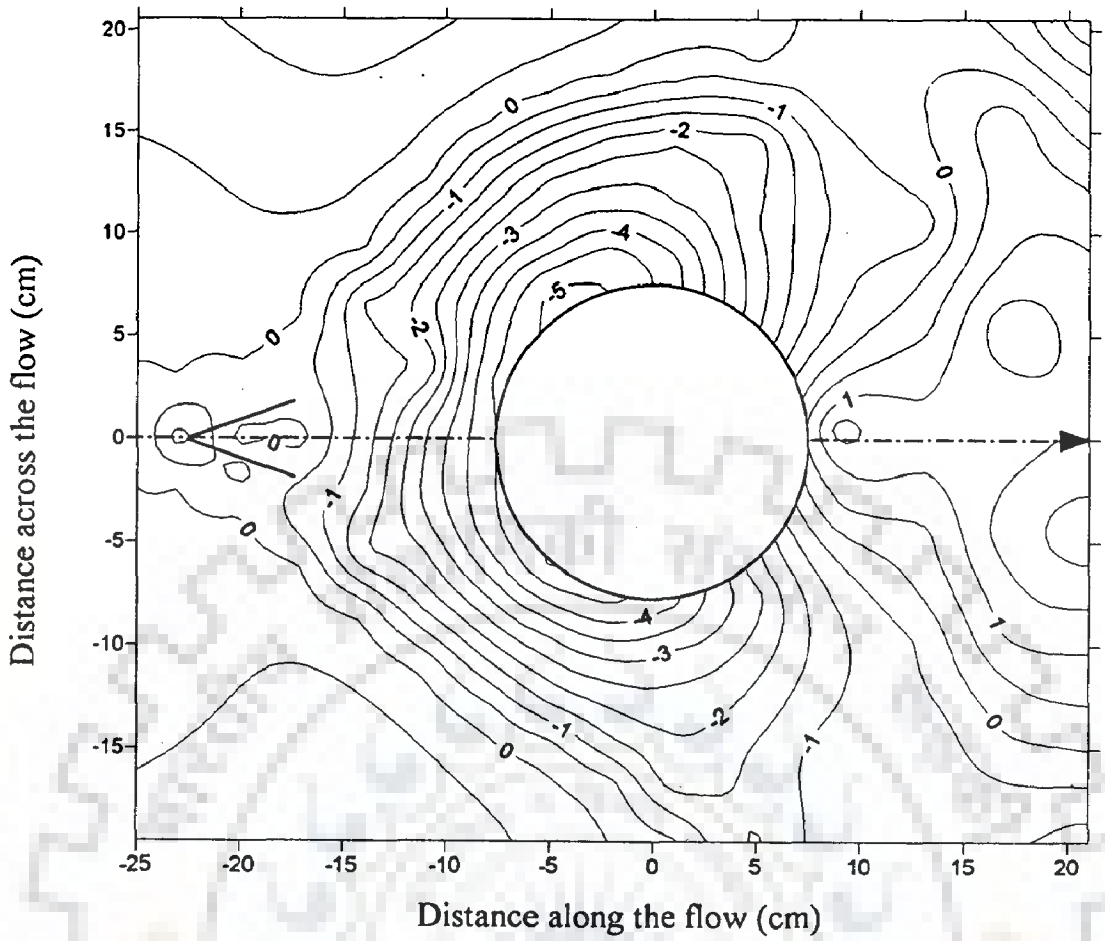

Fig. 7.29 Scour pattern around circular island (d=15 cm) at F_r=0.19 & h=15 cm with V-shaped deflector (limb length =4.5 cm) at 22.5 cm upstream of island (contour interval in cm) (RunE15)

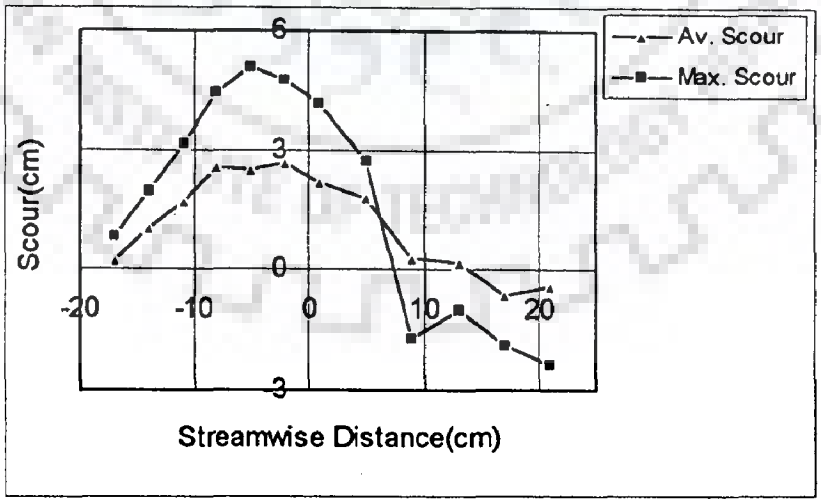

Fig. 7.30 Streamwise variation of scour around circular island (d=15 cm) at F_r =0.19 & h=15 cm with V-shaped deflector (limb length =4.5 cm) at 22.5 cm upstream of island (RunE15)

Plate 7.16 Scour around circular island (d=15 cm) at Fr=0.19 and h=15 cm with V-shaped deflector (limb length =4.5 cm) at 30 cm upstream of island (RunE16)

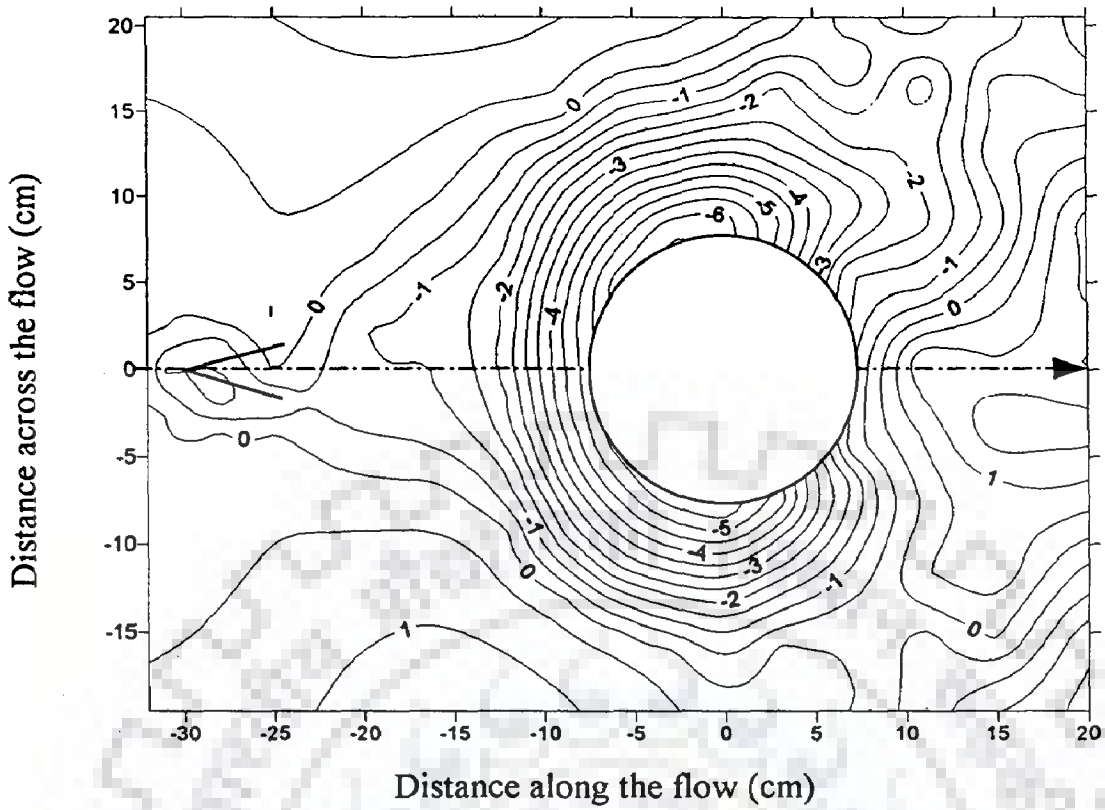

Fig. 7.31 Scour pattern around circular island (d=15 cm) at F_r=0.19 & h=15 cm with V-shaped deflector (limb length =4.5 cm) at 30 cm upstream of island (contour interval in cm) (RunE16)

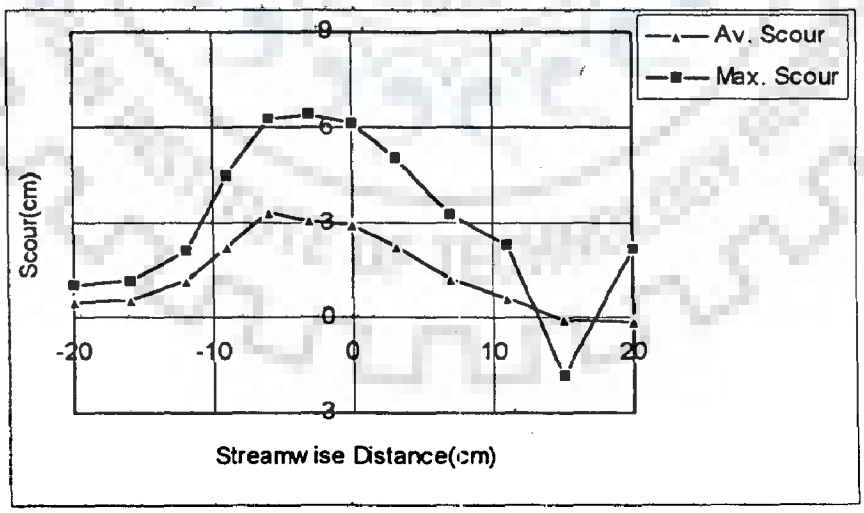

Fig. 7.32 Streamwise variation of scour around circular island (d=15 cm) at F_r =0.19 & h=15 cm with V-shaped deflector (limb length =4.5 cm) at 30 cm upstream of island (RunE16)

7.4 RESULTS

The results of the above study have been summarised in Table 7.1 through Table 7.4 and in Fig. 7.33 through Fig. 7.36. It can be observed from Table 7.1 that at F_r=0.16 with V-shaped deflector having length of each limb= 3.0 cm (0.2d) and located at 15 cm (1.0d) upstream of the centre of the circular island, the scour reduced to a minimum value of 3.58 cm which is about 57% of the maximum scour (6.25 cm) without V-shaped deflector under similar flow condition.. In this case the effective b/a ratio reduced to 0.37 from 1.0. Using the V-shaped deflector of same limb length (3.0 cm) at F_r=0.19, the scour reduced to a minimum value of 6.15 cm, which is about 66% of the maximum scour depth (9.3 cm) without V-shaped deflector, when the deflector was placed 15 cm (1.0 d) upstream of the centre of the island (Table 7.2 and Fig. 7.34). In this case the effective b/a ratio reduced to 0.51 from 1.0.

As the length of each limb of the V-shaped deflector was increased from 3.0 cm (0.2 d) to 4.5 cm (0.3 d), the location of the deflector corresponding to minimum scour shifted to 18.75 cm (1.25 d) upstream of the centre of the island (Fig. 7.35 and Fig. 7.36). At F_r=0.16, the value of maximum scour reduced to about 61% of that without deflector and in this case the effective b/a ratio reduced to 0.42 from 1.0 (Table 7.3). Similarly, at F_r=0.19, the maximum scour corresponding to optimum location of the deflector reduced to about 53% of the maximum scour without deflector. In this case the effective b/a ratio reduced to 0.30 from 1.0 (Table 7.4).

It is pertinent to mention here the utility of Fig. 5.44(a) to Fig. 5.44(c) in estimating maximum scour depth. For experimental run C15 (F_r=0.16, b/a=1.0), using equation (5.9), $\Delta E/a$ is estimated as 0.0268. Using this and Fig. 5.44(a), estimated

maximum scour depth, $d_{s(max)}$ is obtained as 6.82 cm. It can be seen that this estimate does not differ largely from observed maximum scour depth of 6.25 cm. Similar observation holds good for experimental run C16 for which F_r = 0.19 and b/a=1.0. In this case, using equation (5.9), $\Delta E/a$ is estimated as 0.0376 and from Fig. 5.44(b), maximum scour depth, $d_{s(max)}$ is obtained as 9.39 cm. The estimated maximum scour depth is again found close to the observed scour depth of 9.3 cm.

Thus, this study indicates that deflectors of V-shape can be used to protect the islands. Based on limited experiments, the role of deflectors has been emphasized. However, more work will be needed to quantify the optimum location of V-shaped deflector, included angle of deflector and placement distance from nose of island for varying flow conditions.

Table 7.1 Scour around circular island (d=15cm) at h=15cm & F_r=0.16 with V-shaped deflector having limb length of 0.2 d=3 cm

Distance of V-shaped deflector from centre of island, L (cm)	Included angle, θ	Effective b/a ratio	Maximum scour (cm)	Average scour (cm)
0.75d=11.25	84°	0.64	4.98	1.7880
1d=15	60°	0.37	3.58	0.6998
1.5d=22.5	40°	0.53	4.45	1.2440
2d=30	30°	0.64	5.00	1.6251
Maximum scour without V-shaped deflector [from Fig. 5.44(a)] = 6.82 cm **Observed maximum scour without V-shaped deflector = 6.25 cm**				

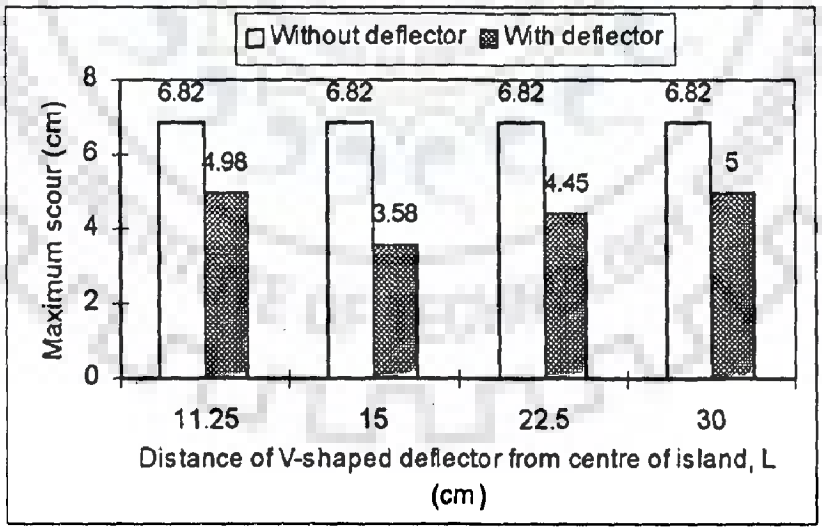

Fig. 7.33 Maximum scour around circular island (d=15cm) with V-shaped deflector (limb length =3cm) upstream of island at F_r=0.16 & h=15cm

Table 7.2 Scour around circular island (d=15cm) at h=15cm & F_r=0.19 with V-shaped deflector having limb length of 0.2d=3cm

Distance of V-shaped deflector from centre of island, L (cm)	Included angle, θ	Effective b/a ratio	Maximum scour (cm)	Average scour (cm)
0.75d=11.25	84°	0.62	6.76	2.2853
1d=15	60°	0.51	6.15	1.8184
1.5d=22.5	40°	0.66	6.98	2.6885
2d=30	30°	0.64	6.9	2.5732
Maximum scour without V-shaped deflector [from Fig. 5.44(b)] = 9.39 cm **Observed maximum scour without V-shaped deflector = 9.3 cm**				

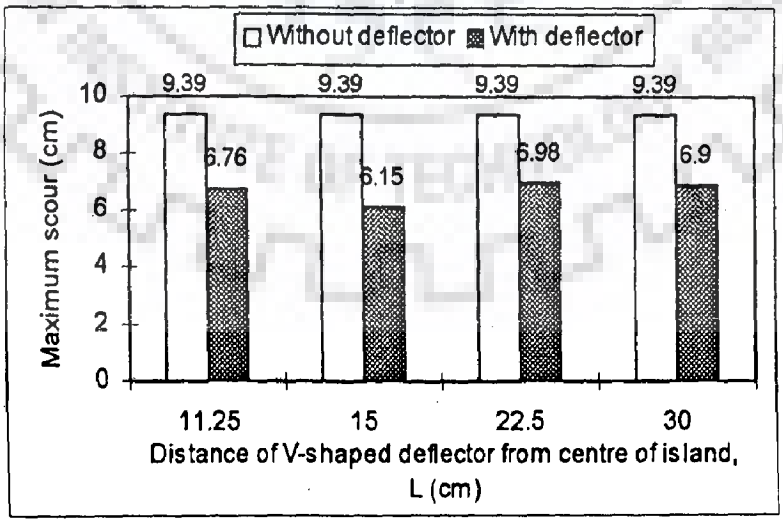

Fig. 7.34 Maximum scour around circular island (d=15cm) with V-shaped deflector (limb length =3cm) upstream of island at F_r=0.19 & h=15cm

Table 7.3 Scour around circular island (d=15cm) at h=15cm & F_r=0.16 with V-shaped deflector having limb length of 0.3d=4.5cm

Distance of V-shaped deflector from centre of island, L (cm)	Included angle, θ	Effective b/a ratio	Maximum scour (cm)	Average scour (cm)
1d=15	60°	0.47	4.1	0.7813
1.25d=18.75	48°	0.42	3.85	0.8919
1.5d=22.5	40°	0.62	4.88	1.3449
2d=30	30°	0.69	5.25	1.5583
Maximum scour without V-shaped deflector [from Fig. 5.44(a)] = 6.82 cm Observed maximum scour without V-shaped deflector = 6.25 cm				

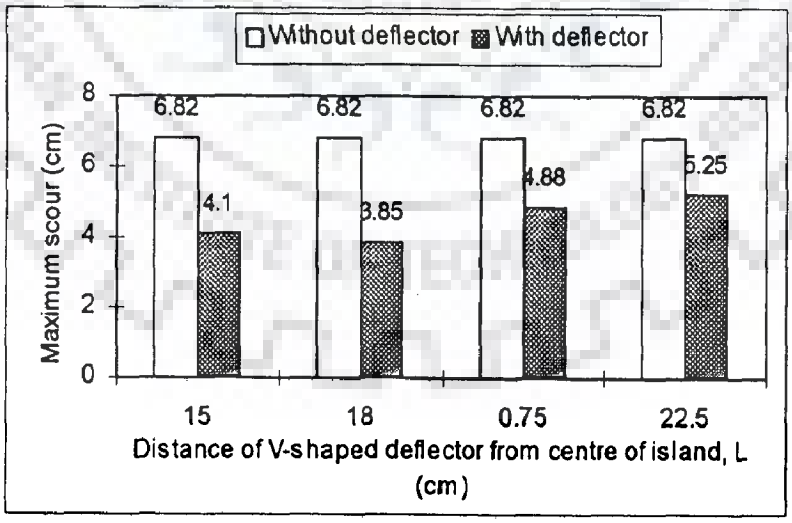

Fig. 7.35 Maximum scour around circular island (d=15cm) with V-shaped deflector (limb length =4.5cm) upstream of island at F_r=0.16 & h=15cm

Table 7.4 Scour Around Circular Island (d=15cm) at h=15cm & F_r=0.19 with V-shaped deflector having limb length of 0.3d=4.5cm

Distance of V-shaped vane from centre of island, L	Included angle, θ	Effective b/a ratio	Maximum scour (cm)	Average scour (cm)
1d=15	60°	0.54	6.3	2.0329
1.25d=18.75	48°	0.30	4.95	1.0314
1.5d=22.5	40°	0.32	5.1	1.5749
2d=30	30°	0.56	6.42	1.8636
Maximum scour without V-shaped deflector [from Fig. 5.44(b)] = 9.39 cm Observed maximum scour without V-shaped deflector = 9.3 cm				

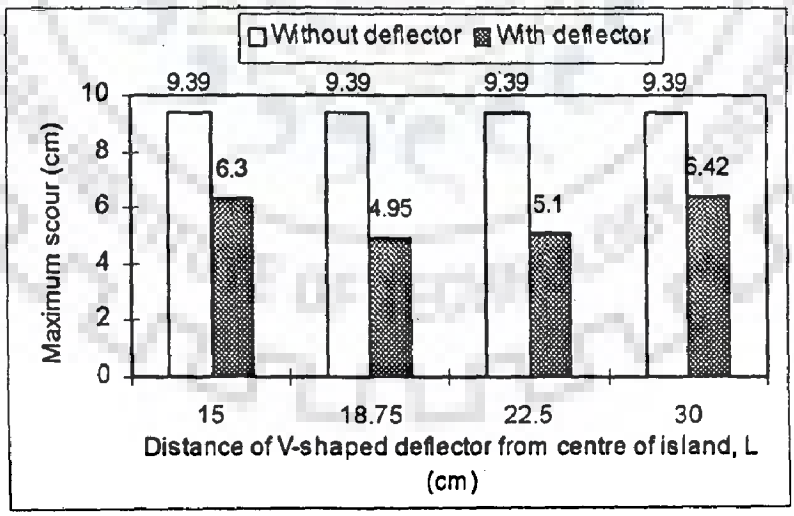

Fig. 7.36 Maximum scour around circular island (d=15cm) with V-shaped deflector (limb length =4.5cm) upstream of island at F_r=0.19 & h=15cm

CONCLUSIONS AND SCOPE FOR FUTURE WORK

8.1 CONCLUSIONS

Based on the present study, the following conclusions are drawn:

1. A set of 45 experimental runs was performed under rigid bed flow conditions with six model islands having width to length ratio of 0.15, 0.2, 0.3, 0.4, 0.6 and 1.0, placing the islands at three different eccentricities (i.e., e=0%, e=20% and e=40%). The Froude number varied from 0.105 to 0.19. A relationship for flow division around island has been developed based on 31 arbitrarily selected experimental runs out of the above 45 runs. The remaining 14 runs have been used to validate the relationship. It has been observed that the flow division computed by the above relationship agrees with the experimental data.

   The applicability of the above relationship has been also tested for mobile bed flow conditions and it is found that the discharge values obtained by the proposed relationship show good agreement with the corresponding experimental data.

2. Based on the experiments under mobile bed flow conditions with five elliptical model islands having different width to length ratio and one circular island, it has been observed that for all the islands, the scour pattern at the leading edge, i.e., in the difluence zone is similar at the three Froude numbers, F_r=0.16,

F_r=0.19 and F_r=0.20. Also, in each case, deposition was found to occur at the tail end of the island, i.e., in the confluence zone.

3. For a given Froude number, it is observed from the experiments that as the width to length ratio of island increases the scour around the island also increases. This fact is also supported from a theoretically developed model based on the concept of specific energy. Theoretical model indicates that energy loss per unit length increases with the increase in Froude number as well as b/a ratio. Furthermore, scour is related with the energy loss, and higher energy loss is well correlated with the larger scour values. Although the experiments did not include a wider range of Froude number, yet the variation of the parameter $\Delta E/\Delta x$ indicates that more scour is likely to be expected with an increase in Froude number. Nevertheless, islands with lesser value of b/a can be considered less vulnerable to scour.

4. The variation of strength of secondary current along the flow direction around the island in terms of moment of momentum (MOM) has been studied at three different Froude numbers F_r=0.14, F_r=0.16 and F_r=0.19. It has been observed that the variation of MOM along the island with respect to Froude number as well as with respect to width to length ratio of island is not consistent. The reason behind this observation has been found to be due to the fact that while computing the MOM in the transition zone, the area covered by the island was neglected. Later, instead of MOM, MOM per unit flow width (MOM/B) has been considered as a representative parameter to study the variation of strength of secondary current along the island. The study indicates an increasing trend of variation of MOM/B towards the middle of the transition zone and then the MOM/B decreases towards the confluence zone.

It has been also tried to find the effect of Froude number and b/a ratio of island on the growth of secondary flow around the island. The trend of this study shows that total MOM per unit length of island increases with the increase in Froude number as well as b/a ratio of island, depicting the pattern of secondary current growth.

5. Based on the limited experiments, the study indicates that deflectors of V-shape can be used for overall protection of island. The circular model island was included in the study, as the scour around the circular island was found to be maximum.

Experiments were carried out using V-shaped deflectors of side width of 0.2d and 0.3d (d is the diameter of the island) placing the deflectors at different locations upstream of the centre of island at Froude numbers, F_r=0.16 and F_r=0.19. The included angle of the deflector was so adjusted that the two limbs of the deflector were tangential to the periphery of the island. The scour around the island has been found to reduce when the deflector is placed upstream of the island. For V-shaped deflector of side width 0.2d, the optimum location has been found to be at 1.0d upstream of the centre of the island with an included angle of 60°. At F_r=0.16, the maximum scour around the island reduced to about 57% of that without deflector and at F_r=0.19, the value of maximum scour reduced to about 66% of that without deflector. The optimum location of V-shaped deflector of side width 0.3d has been found to be at 1.25d upstream of the centre of the island with an included angle of 48°. In this case, the maximum scour around island reduced to about 61% and 53% of that without deflector at F_r=0.16 and F_r=0.19 respectively.

Prediction of maximum scour was found close to observed scour for experiments without deflector. This indicates that the relationship between dimensionless scour depth and energy gradient [Fig. 5.44(a) to Fig. 5.44(c)] is useful.

8.2 SCOPE FOR FUTURE WORK

1. Model islands of elliptical shape and circular shape have been used for the present investigation. Future work may be carried out with model islands of other shapes.

2. As far as scour around island is concerned, experimentation may be conducted using a number of bed material sizes and covering a wider range of Froude numbers.

3. Study related to scour around island may be extended for eccentric location of island. In the present work, only the scour around islands with zero eccentricity has been considered because of certain constraints.

4. Future experiments to evaluate the potential of Fig. 5.44 can be undertaken.

5. Sediment concentration may influence the density of fluid to be used in MOM computations. This aspect needs further considerations.

6. More work is needed to quantify the optimum location of V-shaped deflector with respect to island and the included angle of V-shaped deflector for varying flow conditions.

7. Further studies related to flow hydraulics around island may be carried out under submerged flow conditions to reflect prototype fluvial scenario of an island.

8. Field testing of the findings of this work still needs to be taken through some major research proposal. The same has not been done due to budget constraints.

REFERENCES

1. Ackers, P. and Charlton, F. G. (1971). "The geometry of small meandering streams." Proceedings of the Institution of Civil Engineers, Supplement XII, 289-317.

2. Ahmed, M. (1953). "Experiments on design behaviour of spur-dikes." Proc., IAHR conference, Minnesota, 145-159.

3. Ashmore, P. E. (1982). "Laboratory modeling of gravel braided stream morphology." Earth Surface Processes, 7, 201-225.

4. Ashmore, P. E. (1991). "How do gravel-bed river braid?" Canadian Journal of Earth Sciences, 28, 326-341.

5. Ashmore, P. E. and Parker, G. (1983). " Confluence scour in coarse braided streams." Water Resources Research, 19, 392-402.

6. Ashmore, P. E., Ferguson, R. I., Prestegaard, K. L., Ashworth, P. J. & Paola, C. (1992). "Secondary flow in anabranch confluences of a braided, gravel-bed stream." Earth Surface Processes and Landforms, 17, 299-311.

7. Ashworth, P. J. (1996). "Mid-channel bar growth and its relationship to local flow strength and direction." Earth Surface Process Landforms, Vol. 21, pp.103-124.

8. Ashworth, P. J., Ferguson, R. I. & Powell, M. (1992). "Bedload transport and sorting in braided channels." In:Billi, P., Hey, R. D., Thorne, C. R. & Tacconi, P. (eds) *Dynamics of Gravel Bed Rivers*. Wiley and Sons, 497-513.

9. Baker, C. J. (1980). " Theoretical approach to prediction of local scour around bridge piers." JHR, Vol. 18, No. 1.

10. Barbe, D. E., Cruise, J. F. and Singh, V. P. (1992). "Probabilistic approach to local bridge pier scour." Transportation Research Record No. 1350, 28-33.

11. Best, J. L. (1986). " The morphology of river channel confluences." Progress in Physical Geography, 10, 157-174.

12. Best, J. L. (1988). " Sediment transport and bed morphology at river channel confluences." Sedimentology, 35, 481-498.

13. Best, J. L. and Roy, A. G. (1991). " Mixing-layer distortion at the confluence of channels of different depth." Nature, 350, 411-413.

14. Blondeaux, P. and Seminara, G. (1985). "A unified bar-bend theory of river meanders." Journal of Fluid Mechanics, 157, 449-470.

15. Bluck, B. J. (1979). " Structure of coarse grained braided alluvium." Transactions Royal Society of Edinburgh, 70, 181-221.

16. Breusers, H. N. C. and Raudkivi, A. J. (1991). " Scouring." Hydraulic structure design manual, IAHR.

17. Brice, J. C. (1964). "Channel patterns and terraces of the loup rivers in Nebraska." US Geological Survey Professional Paper 422D.

18. Bridge, J. S. (1985). "Paleochannels inferred from alluvial deposits: a critical evaluation." Journal of Sedimentary Petrology, 55, 579-589.

19. Bridge, J. S. (1993). "The interaction between channel geometry, water flow, sediment transport and deposition in braided rivers." In: Best, J. L. & Bristow, C. S. (eds), 1993, *Braided Rivers*, Geological Society Special Publication No. 75, pp. 13-71.

20. Bridge, J. S. & Gabel, S. L. (1992). "Flow and sediment dynamics in a low-sinuosity river: Calamus River, Nebraska Sandhills." Sedimentology, 39, 125-142.

21. Bridge, J. S., Smith, N. D., Trent, F., Gabel, S. L. & Bernstein, P. (1986). "Sedimentology and morphology of a low-sinuosity river: Calamus River, Nebraska Sandhills." Sedimentology, 33, 851-870.

22. Bristow, C. S. (1987). "Brahmaputra River: channel migration and deposition." *In: Ethridge, F. G.,Flores, R. M. and Harvey, M. D. (eds.) Recent Development of Sedimentology. Soc. Of Eco. Pale. And Mine. Special Publication, Vol. 39, pp. 63-74.*

23. Bristow, C. S. & Best, J. L. (1993). "Braided rivers: perspective and problems." In: Best, J. L. & Bristow, C. S. (eds), 1993, *Braided Rivers*, Geological Society Special Publication No. 75, pp. 1-11.

24. Cant, D. J. and Walker, R. G. (1978). " Fluvial processes and facies sequences in the sandy braided South Saskatchewan River, Canada." Sedimentology, 25, 625-648.

25. Carson, M. A. (1984). "The meandering-braided river threshold: a reappraisal." Journal of Hydrology, Vol. 73, pp. 315-334.

26. Chow, V. T. (1959). " Open Channel Hydraulics." MC Graw-Hill Book Company. Inc., New York.

27. Church, M. and Jones, D. (1982). "Channel bars in gravel-bed rivers." In: Hey, R. D., Bathurst, J. C. & Thorne, C. R. (eds) Gravel-*bed rivers*, Wiley, Chichester, 291-324.

28. Coleman, J. M. (1969). "Brahmaputra River: Channel process and sedimentation." Sedimentary Geology, Vol. 181, pp. 213-232.

29. Deng, Z. Q. and Singh, V. P. (1999). "Mechanism and conditions for change in channel pattern." Journal of Hydraulic Research, Vol. 37, No. 4, pp. 465-478.

30. Doeglas, D. J. (1951). "Meanderende en verwilderde Rivieren" Geologie en Mijnbouw, v. 13, p. 297-299.

31. Einstein, H. A. and Li, H. (1958). " Secondary currents in straight channel." Trans, AGU, Vol. 39, Dec.

32. Engelund, F. and Skovgaard, O. (1973). "On the origin of meandering and braiding in alluvial streams." Journal of Fluid Mechanics, 57, 289-302.

33. Ettema, R. (1980). " Scour at bridge piers." Deptt. of Civil Engineering, University of Auckland, New Zealand, Report No. 216, Feb.

34. Ferguson, R. I. (1984). "The threshold between meandering and braiding." *In: Smith, K. V. H. (ed) Proceedings of the 1st International Conference on Hydraulic Design.* Springer, 6.15-6.29.

35. Ferguson, R. I. (1987). "Hydraulic and sedimentary controls of channel pattern." *In: Richards, K. S. (ed) River Channels: Environment and Process.* Blackwell, 125-158.

36. Ferguson, R. I. and Ashworth, P. (1991). "Slope induced changes in channel character along a gravel bed stream: the Allt Dubhaig, Scotland." Earth Surface Processes and Landforms, 16, 65-82.

37. Fisk, H. N. (1944). " Geological investigation of the alluvial valley of the lower Mississippi River." Vicksburg, Miss., U. S. Army Corps Engineers, Waterways Experiment Station, 78 p.

38. Fredsoe, J. (1978). "Meandering and braiding of rivers." Journal of Fluid Mechanics, 84, 609-624.

39. Friedkin, J. F. (1945). "A laboratory study of meandering of alluvial rivers: Vicksburg, Miss." U. S. Army Corps Engineers, Waterways Experiment Station, 40 p.

40. Fukuoka, S. (1989). "Finite amplitude development of alternate bars." In: Ikeda, S. & Parker, G. (eds) *River Meandering*. American Geophysical Union, Water Resources Monographs, 12, 237-265.

41. Garde, R. J., Subramanya, K. and Nambudripad, K. D. (1961). " Study of scour around spur-dikes." Journal of Hydraulic Division, ASCE, Vol. 87, No. Hy-6, 23-37.

42. Hayashi, T. and Ozaki, S. (1980). "Alluvial bedforms analysis. I. Formation of alternating bars and braids." In: Shen, H. W. & Kikkawa, H. (eds) *Application of Stochastic Processes in Sediment Transport*. Water Resources Publications, Colorado, Ch7, 1-40.

43. Henderson, F. M. (1961). "Stability of alluvial channels." Journal of Hydraulic Division, ASCE, Vol. 87, 109-138.

44. Henderson, F. M. (1966). "Open Channel Flow." Macmillan, New York.

45. Hjorth, P. (1975). " Studies on the nature of local scour." Department of Water Resources Engineering, University of Lund, Bull. Series A, No. 16.

46. Holmes, Pat and Baldock, Tom (1999). " Seepage effects of sediment transport by waves and currents." In: Elsevier 26th International Conference on Coastal Engineering, Copenhagen, Denmark, Vol. 3, pp. 3601-3614.

47. Ikeda, H. (1973). "A study of the formation of sand bars in an experimental flume." Geographical Review of Japan, 46, 435-452.

48. Ikeda, H. (1975). "On the bed configuration in alluvial channels; their types and condition of formation with reference to bars." Geographical Review of Japan, 48, 712-730.

49. Inglis, C. C. (1949). "Behaviour and control of rivers and canals with aids of models." Research Publication No. 13, Part II, C. W. I. & N. R. S. Poona, India.

50. Jain, S. C. (1981). " Maximum clear-water scour around circular piers." Journal of Hydraulic Division, Proc. ASCE, Vol. 107, No. HY-5, May.

51. Johnson, P. A. and Ayyub, B. M. (1992). " Assessing time-variant bridge reliability due to pier scour." Journal of Hydraulic Engineering, Proc. ASCE, Vol. 118, No. 6, June.

52. Johnson, P. A., Hey, R. D., Tessier, M. and Rosgen, D. L. (2001). " Use of vanes for control of scour at vertical wall abutments." Journal of Hydraulic Engineering, ASCE, Vol. 127, No. 9, pp772-778.

53. Julien, P. Y. (2002). " River Mechanics." Cambridge University Press, Cambridge, U. K., pp 214-215.

54. Kandasami, J. K. (1989). " Abutment scour." University of Auckland, Dept. of Civil Engineering, Rep. No. 458.

55. Kothyari, U. C., Garde, R. J. and Ranga Raju, K. G. (1992a). " Temporal variation of scour around circular bridge piers." Journal of Hydraulic Engineering, ASCE, Vol. 118, No. 8, 1091-1106.

56. Kothyari, U. C., Garde, R. J. and Ranga Raju, K. G. (1992b). "Live-bed scour around cylindrical bridge piers." Journal of Hydraulic Res., IAHR, Vol. 30, No. 5, 701-715.

57. Kumar, V., Ranga Raju, K. G. and Vittal, N (1995). " Jet-flow model for equilibrium scour depth around cylindrical piers." Proc. of 6th International Symposium on River Sedimentation, New Delhi, India.

58. Kwan, T. F. (1984). " Study of abutment scour." University of Auckland, Dept. of Civil Engineering, Rep. No. 328.

59. Lane, E. W. (1957). "A study of the shape of channels formed by natural streams flowing in erodible material." Missouri River Division Sediment Series No. 9, U. S. Army Engineer Division, Missoiri River, Corps of Engineers, Omaha, Nebraska.

60. Laursen, E. M. (1958). " Scours at bridge crossings." Iowa Highway Research Board, Bull. No. 8.

61. Laursen, E. M. (1963). " An analysis of bridge relief scour." Proc., Journal of Hydraulic Division, ASCE, Vol. 89, No. HY3, 93-117.

62. Laursen, E. M. and Toch, A. (1953). " A generalized model study of scour around bridge piers and abutments." Proc., Minnesota International Hydraulic Convention, Minneapolis, Minnesota, Sept., 123-131.

63. Laursen, E. M. and Toch, A. (1956). " Scours around bridge piers and abutments." Iowa Highway Research Board, Bull. No. 4.

64. Leopold, L. B. and Wolman, M. G. (1957). "River channel patterns: braided, meandering and straight." US Geological Survey Professional Paper 282-B, 39-85.

65. Liu, H. K. G. and Skinner, M. M. (1960). " Laboratory observations of scour at bridge abutments." Highway Res. Board, Bull. No. 242.

66. Liu, H. K. G., Chang, F. M. and Skinner, M. M. (1961). " Effect on bridge construction on scour and backwater." Colorado State University, Civil Engineering Section, Ft. Collins, CER 60 HKL 22.

67. Mackin, J. H. (1956). "Cause of braiding by a graded river [abs.]." Geological Society of America Bulletin, Vol. 67, p. 1717-1718.

68. Marelius, F. and Sinha, S. K. (1998). " Experimental investigation of flow past submerged vanes." Journal of Hydraulic Engineering, ASCE, Vol. 124, No. 5, pp542-545.

69. Mazumdar, S. K. (1988). "Effectiveness of impervious type groins in river bank protection with particular reference to river Kosi in India." International Conference on Hydraulics of floods and flood control.

70. Melville, B. W. (1975). " Local scour at bridge sites." Report No. 117, University of Auckland, School of Engg., Auckland, New Zealand.

71. Melville, B. W. and Roudkivi, A. J. (1984). " Local scour at bridge abutments." Nat. Roads Board New Zealand, R R U seminar on bridge design and research, Auckland.

72. Melville, B. W. and Sutherland, A. J. (1988). "Design method for local scour of bridge piers," Journal of Hydraulic Engineering, Proc. ASCE, Vol. 114, No. HY-11, Nov.

73. Melville, B. W. and Chiew, Y. M. (1999). " Time scale for local scour at bridge pier." Journal of Hydraulic Engineering, ASCE, Vol. 125, No. 1, 59-65.

74. Mia, M. F. and Nago, H. (2003). " Design method of time-dependent local scour at circular bridge pier." Journal of Hydr. Engg., ASCE, Vol. 129, No. 6, pp420-427.

75. Miall, A. D. (1977). "A review of the braided river depositional environment." Earth Science Reviews, Vol. 13, pp. 1-62.

76. Mosley, M. P. (1976). " An experimental study of channel confluences." Journal of Geology, 84, 535-562.

77. Mosley, M. P. (1982). "Scour depths in branch channel confluences, Oahu River, Otago, New Zealand." Proceedings of the New Zealand Society of Civil Engineers, 9, 17-24.

78. Muzzammil, M. and Gangadharaiah, T. (1995). " A study of scouring horseshoe vortex." Proc. of 6th International Symposium on River Sedimentation, New Delhi, India.

79. Nwachukwu, B. A. and Rajaratnam, W. (1980). " Flow and erosion near groyane-like structures." Dept. of Civil Engineering, University of Alberta, Edmonton, Alberta.

80. Odgaard, A. J. and Kennedy, J. F. (1983). " River-bend bank protection by submerged vanes." Journal of Hydraulic Engineering, ASCE, Vol. 109, No. 9, pp 1161-1173.

81. Odgaard, A. J. and Mosconi, C. E. (1987). " Stream bank protection by submerged vanes." Journal of Hydraulic Engineering, ASCE, Vol. 113, No. 4, pp520-536.

82. Odgaard, A. J. and Spoljaric, A. (1986). " Sediment control by submerged vanes." Journal of Hydraulic Engineering, ASCE, Vol. 112, No. 12, pp1164-1181.

83. Odgaard, A. J. and Wang, Y. (1991a). "Sediment management with submerged vanes. I: Theory." Journal of Hydraulic Engineering, ASCE, Vol. 117, No. 3, pp267-283.

84. Odgaard, A. J. and Wang, Y. (1991b). "Sediment management with submerged vanes. II: Applications." Journal of Hydraulic Engineering, ASCE, Vol. 117, No. 3, pp284-302.

85. Oliveto, G. and Hager, W. H. (2002). " Temporal variation of clear-water pier and abutment scour." J. of Hydr. Engg., ASCE, Vol. 128, No. 9, pp811-820.

86. Osterkamp, W. R. (1978). "Gradient, discharge and particle size relations of alluvial channels in Kansas, with observations on braiding." American Journal of Science, 278, 1253-1268.

87. Parker, G. (1976). "On the cause and characteristic scales of meandering and braiding in rivers." Journal of Fluid Mechanics, Vol. 76, pp. 459-480.

88. Pattabhiramiah, K. R. and Rajaratnam, N. (1960). " A new method to predict flow in a branch channel." Journal of C. B. I. P., Vol.-17, No.-1, January, pp 48-51.

89. Prandtl, L. (1952). " Essentials of fluid dynamics." London, Blackie and Sons.

90. Rajaratnam, N. (1962). "Constant velocity concept for supercritical branch channel flow." Journal of C. B. I. P., Vol. 19, No. 1, January, pp. 17-21.

91. Richards, K. S. (1980). " Rivers: forms and process in alluvial channels." Methuen, London.

92. Richardson, E. V., Stevens, M. A. and Simons, D. B. (1975). " The design of spurs for river training." Proc. 16th IAHR Congress, Sao Paulo, 2, 382-388.

93. Richardson, W. R. and Thorne, C. R. (2001). " Multiple thread flow and channel bifurcation in a braided river: Brahmaputra-Jamuna River." Bangladesh: Geomorphology, Vol. 38, No. (3-4), pp. 185-196.

94. Roy, A. G. and Bergeron, N. (1990). " Flow and particle paths at a natural river confluence with coarse bed material." Geomorphology, 3, 99-112.

95. Rudra, R. P. and Dickinson, W. T. (1985). "Soil erosion and fluvial sediment research at Guelph." Seminar delivered to researchers at the USDA National Soil Erosion Laboratory, W. Lafayette, Indiana.

96. Rust, B. R. (1978). "A classification of alluvial channel systems." In: Miall, A. D., (Ed) Fluvial Sedimentology, Canadian Society of Petroleum Geologists Memories, Vol. 5, pp. 187-198.

97. Schleiss, A. (2002). "Scour formulae and their applicability to coarse gravel alpine rivers." International Conference on Fluvial Hydraulics, Erik Bollaert, Switzerland.

98. Schumm, S. A. and Khan, H. R. (1972). "Experimental study of channel patterns." Geological Society of America Bulletin, 83, 1755-1770.

99. Sen, D. J. and Garg, N. K. (2004). " Efficient algorithm for gradually varied flows in channel networks." Journal of Irrigation and Drainage, ASCE, Vol. 130, 5, pp. 351-357.

100. Shen, H. W., Schneider, V. R. and Karaki, S. S. (1966). " Mechanics of local scour." CSU Report, No. CER66, HWS 22, June.

101. Smith, N. D. (1970). " The braided stream depositional environment: comparison of the Platte River with some Silurian clastic rocks, north-central Appalachians." Geological Society of America Bulletin, 81, 2993-3014.

102. Smith, N. D. (1974). " Sedimentology and bar formation in the Upper Kicking Horse River, a braided outwash stream." Journal of Geology, 82,205-223.

103. Sridharan, K. and Lakshman Rao, N. S. (1966). " Division and combination of flow in open channels." Journal of Instt. Of Engineers (India), Civil Engineering Division, Vol. 46, March, pp. 337-355.

104. Stebbings, J. (1964). "The shape of self-formed model alluvial channels." Institute of Civil Engineering, London, Proceedings, Vol. 25, p. 485-510.

105. Tey, C. B. (1984). " Local scour at bridge abutments." University of Auckland, Dept. of Civil Engineering, Rep. No. 329.

106. Thorne, C. R., Russel, A. P. G. & Alam, M. G. (1993). "Planform pattern and channel evolution of the Brahmaputra River, Bangladesh." In: Best, J. L. & Bristow, C. S. (eds), 1993, *Braided Rivers*, Geological Society Special Publication No. 75.

107. Williams, P. F. and Rust, B. R. (1969). "The sedimentology of a braided river". *J. Sediment. Petrol.*, 39, 649-679.

108. Wong, H. H. (1982). " Scour at bridge abutments." University of Auckland, Dept. of Civil Engineering, Rep. No. 275.

APPENDIX-A

EXPERIMENTAL DATA RELATING TO FLOW DIVISION AROUND ISLAND (RIGID BED CONDITION)

Table A.1: Discharge Values for Experimental Run A1
[Elliptical Island I_1 (b/a=0.15), F_r=0.14,h=15cm, Q=0.0127m^3/sec,e=0%]

x(cm)		V_{av}(m/s)	q_{av}(m^2/s)	Q_{av}(m^3/s)
-40	Right channel	0.1936	0.02904	0.00621
	Left channel	0.1876	0.02814	0.00602
-30	Right channel	0.2068	0.03102	0.00611
	Left channel	0.2102	0.03153	0.00621
-20	Right channel	0.2166	0.03249	0.00608
	Left channel	0.2184	0.03276	0.00613
-10	Right channel	0.2285	0.034275	0.00624
	Left channel	0.2298	0.03447	0.00627
0	Right channel	0.2334	0.03501	0.00630
	Left channel	0.2316	0.03474	0.00625
10	Right channel	0.2238	0.03357	0.00611
	Left channel	0.23	0.0345	0.00628
20	Right channel	0.2188	0.03282	0.00614
	Left channel	0.2287	0.034305	0.00641
30	Right channel	0.2125	0.031875	0.00628
	Left channel	0.2193	0.032895	0.00648
40	Right channel	0.197	0.02955	0.00632
	Left channel	0.2047	0.030705	0.00657

Table A.2: Discharge Values for Experimental Run A2
[Elliptical Island I_1 (b/a=0.15), F_r=0.14,h=18cm, Q=0.01634m^3/sec,e=0%]

x(cm)		V_{av}(m/s)	q_{av}(m^2/s)	Q_{av}(m^3/s)
-40	Right channel	0.2297	0.041346	0.00886
	Left channel	0.2346	0.042228	0.009049
-30	Right channel	0.2431	0.043758	0.008598
	Left channel	0.2506	0.045108	0.008864
-20	Right channel	0.2574	0.046332	0.008655
	Left channel	0.2629	0.047322	0.00884
-10	Right channel	0.2674	0.048132	0.008741
	Left channel	0.2681	0.048258	0.008764
0	Right channel	0.2701	0.048618	0.008751
	Left channel	0.2669	0.048042	0.008648
10	Right channel	0.2624	0.047232	0.008577
	Left channel	0.2691	0.048438	0.008796
20	Right channel	0.2556	0.046008	0.008594
	Left channel	0.2685	0.04833	0.009028
30	Right channel	0.249	0.04482	0.008807
	Left channel	0.2535	0.04563	0.008966
40	Right channel	0.2356	0.042408	0.009088
	Left channel	0.2402	0.043236	0.009265

Table A.3: Discharge Values for Experimental Run A3
[Elliptical Island I_1 (b/a=0.15), F_r=0.16,h=15cm, Q=0.0146m^3/sec,e=0%]

x(cm)		V_{av} (m/s)	q_{av} (m^2/s)	Q_{av}(m^3/s)
-40	Right channel	0.2297	0.034455	0.00737
	Left channel	0.2327	0.034905	0.00747
-30	Right channel	0.2428	0.03642	0.00717
	Left channel	0.2489	0.037335	0.00735
-20	Right channel	0.2574	0.03861	0.00722
	Left channel	0.2609	0.039135	0.00732
-10	Right channel	0.2674	0.04011	0.00730
	Left channel	0.2666	0.03999	0.00728
0	Right channel	0.2715	0.040725	0.00733
	Left channel	0.2656	0.03984	0.00717
10	Right channel	0.2623	0.039345	0.00716
	Left channel	0.268	0.0402	0.00732
20	Right channel	0.2552	0.03828	0.00716
	Left channel	0.2635	0.039525	0.00739
30	Right channel	0.2474	0.03711	0.00731
	Left channel	0.2516	0.03774	0.00743
40	Right channel	0.234	0.0351	0.00751
	Left channel	0.2387	0.035805	0.00766

Table A.4: Discharge Values for Experimental Run A4
[Elliptical Island I_2 (b/a=0.2), F_r=0.105,h=23cm, Q=0.0182m^3/sec,e=0%]

x(cm)		V_{av} (m/s)	q_{av} (m^2/s)	Q_{av}(m^3/s)
-30	Right channel	0.1677	0.038571	0.00825
	Left channel	0.1846	0.042458	0.00909
-20	Right channel	0.197	0.04531	0.00874
	Left channel	0.2097	0.048231	0.00931
-10	Right channel	0.1989	0.045747	0.00837
	Left channel	0.2151	0.049473	0.00905
0	Right channel	0.2123	0.048829	0.00879
	Left channel	0.2218	0.051014	0.00918
10	Right channel	0.2046	0.047058	0.00861
	Left channel	0.2211	0.050853	0.00170
20	Right channel	0.2079	0.047817	0.00923
	Left channel	0.2131	0.049013	0.00946
30	Right channel	0.1901	0.043723	0.00936
	Left channel	0.1974	0.045402	0.00972

Table A.5: Discharge Values for Experimental Run A5
[Elliptical Island I_2 (b/a=0.2), F_r=0.12,h=20cm, Q=0.0167m^3/sec,e=0%]

x(cm)		V_{av} (m/s)	q_{av} (m^2/s)	Q_{av}(m^3/s)
-30	Right channel	0.1838	0.03676	0.00787
	Left channel	0.1978	0.03956	0.00847
-20	Right channel	0.2113	0.04226	0.00816
	Left channel	0.2221	0.04442	0.00857
-10	Right channel	0.2165	0.0433	0.00792
	Left channel	0.2291	0.04582	0.00838
0	Right channel	0.2248	0.04496	0.00809
	Left channel	0.2289	0.04578	0.00838
10	Right channel	0.2203	0.04406	0.00806
	Left channel	0.2221	0.04442	0.00813
20	Right channel	0.2225	0.0445	0.00859
	Left channel	0.2171	0.04342	0.00838
30	Right channel	0.2003	0.04006	0.00857
	Left channel	0.1978	0.03956	0.00847

Table A.6: Discharge Values for Experimental Run A6
[Elliptical Island I_2 (b/a=0.2), F_r=0.13,h=17cm, Q=0.0146m^3/sec,e=0%]

x(cm)		V_{av} (m/s)	q_{av} (m^2/s)	Q_{av}(m^3/s)
-30	Right channel	0.1973	0.033541	0.00718
	Left channel	0.2067	0.035139	0.00752
-20	Right channel	0.2235	0.037995	0.00733
	Left channel	0.228	0.03876	0.00748
-10	Right channel	0.234	0.03978	0.00728
	Left channel	0.2316	0.039372	0.00720
0	Right channel	0.2421	0.041157	0.00741
	Left channel	0.2414	0.041038	0.00739
10	Right channel	0.2392	0.040664	0.00744
	Left channel	0.2392	0.040664	0.00744
20	Right channel	0.227	0.03859	0.00745
	Left channel	0.2243	0.038131	0.00736
30	Right channel	0.212	0.03604	0.00771
	Left channel	0.2047	0.034799	0.00745

Table A.7: Discharge Values for Experimental Run A7
[Elliptical Island I_2 (b/a=0.2), F_r=0.14,h=15cm, Q=0.0127m^3/sec,e=0%]

x(cm)		V_{av} (m/s)	q_{av} (m^2/s)	Q_{av}(m^3/s)
-30	Right channel	0.1831	0.027465	0.00588
	Left channel	0.1938	0.02907	0.00622
-20	Right channel	0.203	0.03045	0.00588
	Left channel	0.2135	0.032025	0.00618
-10	Right channel	0.2169	0.032535	0.00595
	Left channel	0.2259	0.033885	0.00620
0	Right channel	0.2174	0.03261	0.00587
	Left channel	0.2266	0.03399	0.00612
10	Right channel	0.213	0.03195	0.00585
	Left channel	0.2255	0.033825	0.00619
20	Right channel	0.2093	0.031395	0.00606
	Left channel	0.2227	0.033405	0.00645
30	Right channel	0.1939	0.029085	0.00622
	Left channel	0.2015	0.030225	0.00647

Table A.8: Discharge Values for Experimental Run A8
[Elliptical Island I_2 (b/a=0.2), F_r=0.16,h=15cm, Q=0.0147m^3/sec,e=0%]

x(cm)		V_{av} (m/s)	q_{av} (m^2/s)	Q_{av}(m^3/s)
-30	Right channel	0.2023	0.030345	0.00649
	Left channel	0.2042	0.03063	0.00655
-20	Right channel	0.2252	0.03378	0.00652
	Left channel	0.2313	0.034695	0.00670
-10	Right channel	0.2394	0.03591	0.00657
	Left channel	0.2416	0.03624	0.00663
0	Right channel	0.2396	0.03594	0.00647
	Left channel	0.2443	0.036645	0.00660
10	Right channel	0.2334	0.03501	0.00641
	Left channel	0.2446	0.03669	0.00671
20	Right channel	0.2268	0.03402	0.00657
	Left channel	0.2386	0.03579	0.00691
30	Right channel	0.207	0.03105	0.00664
	Left channel	0.2168	0.03252	0.00696

Table A.9: Discharge Values for Experimental Run A9
[Elliptical Island I_2 (b/a=0.2), F_r=0.105,h=23cm, Q=0.0182m^3/sec,e=20%]

x(cm)		V_{av} (m/s)	q_{av} (m^2/s)	Q_{av}(m^3/s)
-30	Right channel	0.1794	0.041262	0.01089
	Left channel	0.1782	0.040986	0.00672
-20	Right channel	0.2079	0.047817	0.01162
	Left channel	0.2047	0.047081	0.00673
-10	Right channel	0.2107	0.048461	0.01129
	Left channel	0.2268	0.052164	0.00694
0	Right channel	0.2114	0.048622	0.01118
	Left channel	0.2254	0.051842	0.00674
10	Right channel	0.2114	0.048622	0.01133
	Left channel	0.2248	0.051704	0.00688
20	Right channel	0.2114	0.048622	0.01181
	Left channel	0.2175	0.050025	0.00715
30	Right channel	0.1883	0.043309	0.01143
	Left channel	0.1949	0.044827	0.00735

Table A.10: Discharge Values for Experimental Run A10
[Elliptical Island I_2 (b/a=0.2), F_r=0.12,h=20cm, Q=0.0167m^3/sec,e=20%]

x(cm)		V_{av} (m/s)	q_{av} (m^2/s)	Q_{av}(m^3/s)
-30	Right channel	0.1863	0.03726	0.00984
	Left channel	0.1803	0.03606	0.00591
-20	Right channel	0.2122	0.04244	0.01031
	Left channel	0.2125	0.0425	0.00608
-10	Right channel	0.2145	0.0429	0.01000
	Left channel	0.2334	0.04668	0.00621
0	Right channel	0.2131	0.04262	0.00980
	Left channel	0.2341	0.04682	0.00609
10	Right channel	0.2153	0.04306	0.01003
	Left channel	0.233	0.0466	0.00620
20	Right channel	0.2142	0.04284	0.01041
	Left channel	0.2268	0.04536	0.00649
30	Right channel	0.1935	0.0387	0.01022
	Left channel	0.2085	0.0417	0.00684

Table A.11: Discharge Values for Experimental Run A11
[Elliptical Island I_2 (b/a=0.2), F_r=0.13,h=17cm, Q=0.0146m^3/sec,e=20%]

x(cm)		V_{av} (m/s)	q_{av} (m^2/s)	Q_{av}(m^3/s)
-30	Right channel	0.1994	0.033898	0.00895
	Left channel	0.1939	0.032963	0.00541
-20	Right channel	0.2181	0.037077	0.00901
	Left channel	0.2255	0.038335	0.00548
-10	Right channel	0.2279	0.038743	0.00903
	Left channel	0.2423	0.04119	0.00548
0	Right channel	0.2317	0.039389	0.00906
	Left channel	0.2486	0.042262	0.00549
10	Right channel	0.226	0.03842	0.00895
	Left channel	0.2449	0.041633	0.00554
20	Right channel	0.222	0.03774	0.00917
	Left channel	0.2336	0.039712	0.00568
30	Right channel	0.2051	0.034867	0.00920
	Left channel	0.2053	0.034901	0.00572

Table A.12: Discharge Values for Experimental Run A12
[Elliptical Island I_2 (b/a=0.2), F_r=0.105,h=23cm, Q=0.0182m^3/sec,e=40%]

x(cm)		V_{av} (m/s)	q_{av} (m^2/s)	Q_{av}(m^3/s)
-30	Right channel	0.1865	0.042895	0.013465
	Left channel	0.16	0.0368	0.004192
-20	Right channel	0.1971	0.045333	0.013264
	Left channel	0.2087	0.048001	0.004445
-10	Right channel	0.2012	0.046276	0.013091
	Left channel	0.2264	0.052072	0.004317
0	Right channel	0.202	0.04646	0.013009
	Left channel	0.2255	0.051865	0.004149
10	Right channel	0.1964	0.045172	0.012779
	Left channel	0.2286	0.052578	0.004359
20	Right channel	0.1949	0.044827	0.013116
	Left channel	0.205	0.04715	0.004366
30	Right channel	0.182	0.04186	0.01314
	Left channel	0.1837	0.042251	0.004812

Table A.13: Discharge Values for Experimental Run A13
[Elliptical Island I_2 (b/a=0.2), F_r=0.117,h=20cm, Q=0.01634m^3/sec,e=40%]

x(cm)		V_{av} (m/s)	q_{av} (m^2/s)	Q_{av}(m^3/s)
-30	Right channel	0.1921	0.03842	0.01206
	Left channel	0.1765	0.0353	0.004021
-20	Right channel	0.206	0.0412	0.012055
	Left channel	0.2155	0.0431	0.003991
-10	Right channel	0.2077	0.04154	0.011752
	Left channel	0.2295	0.0459	0.003805
0	Right channel	0.2156	0.04312	0.012074
	Left channel	0.2221	0.04442	0.003554
10	Right channel	0.207	0.0414	0.011712
	Left channel	0.2363	0.04726	0.003918
20	Right channel	0.2053	0.04106	0.012014
	Left channel	0.2153	0.04306	0.003987
30	Right channel	0.1929	0.03858	0.01211
	Left channel	0.1932	0.03864	0.004401

Table A.14: Discharge Values for Experimental Run A14
[Elliptical Island I_2 (b/a=0.2), F_r=0.13,h=17cm, Q=0.0146m^3/sec,e=40%]

x(cm)		V_{av} (m/s)	q_{av} (m^2/s)	Q_{av}(m^3/s)
-30	Right channel	0.2076	0.035292	0.011078
	Left channel	0.183	0.03111	0.003543
-20	Right channel	0.2218	0.037706	0.011033
	Left channel	0.23	0.0391	0.003621
-10	Right channel	0.2231	0.037927	0.01073
	Left channel	0.2506	0.042602	0.003532
0	Right channel	0.229	0.03893	0.0109
	Left channel	0.2532	0.043044	0.003444
10	Right channel	0.2239	0.038063	0.010768
	Left channel	0.2607	0.044319	0.003674
20	Right channel	0.2143	0.036431	0.01066
	Left channel	0.2473	0.042041	0.003893
30	Right channel	0.1978	0.033626	0.010555
	Left channel	0.2103	0.035751	0.004072

Table A.15: Discharge Values for Experimental Run A15
[Elliptical Island I_3 (b/a=0.3), F_r=0.14,h=15cm, Q=0.0127m^3/sec,e=0%]

x(cm)		V_{av}(m/s)	q_{av}(m^2/s)	Q_{av}(m^3/s)
-20	Right channel	0.2251	0.033765	0.00618
	Left channel	0.2205	0.033075	0.00605
-10	Right channel	0.2518	0.03777	0.00623
	Left channel	0.2517	0.037755	0.00623
0	Right channel	0.2588	0.03882	0.00621
	Left channel	0.2629	0.039435	0.00631
10	Right channel	0.2471	0.037065	0.00612
	Left channel	0.2596	0.03894	0.00642
20	Right channel	0.2294	0.03441	0.00630
	Left channel	0.2348	0.03522	0.00644

Table A.16: Discharge Values for Experimental Run A16
[Elliptical Island I_3 (b/a=0.3), F_r=0.14,h=18cm, Q=0.01634m^3/sec,e=0%]

x(cm)		V_{av}(m/s)	q_{av}(m^2/s)	Q_{av}(m^3/s)
-20	Right channel	0.2481	0.044658	0.008168
	Left channel	0.2284	0.041112	0.007519
-10	Right channel	0.2745	0.04941	0.008029
	Left channel	0.2567	0.046206	0.007508
0	Right channel	0.2835	0.05103	0.008165
	Left channel	0.274	0.04932	0.007891
10	Right channel	0.2816	0.050688	0.008237
	Left channel	0.2664	0.047952	0.007792
20	Right channel	0.257	0.04626	0.008461
	Left channel	0.24	0.0432	0.007901

Table A.17: Discharge Values for Experimental Run A17
[Elliptical Island I_3 (b/a=0.3), F_r=0.16,h=15cm, Q=0.0146m^3/sec,e=0%]

x(cm)		V_{av}(m/s)	q_{av}(m^2/s)	Q_{av}(m^3/s)
-20	Right channel	0.2549	0.038235	0.00700
	Left channel	0.2466	0.03699	0.00677
-10	Right channel	0.2852	0.04278	0.00706
	Left channel	0.2814	0.04221	0.00696
0	Right channel	0.2899	0.043485	0.00696
	Left channel	0.2939	0.044085	0.00705
10	Right channel	0.2908	0.04362	0.00720
	Left channel	0.293	0.04395	0.00725
20	Right channel	0.2643	0.039645	0.00725
	Left channel	0.2579	0.038685	0.00708

Table A.18: Discharge Values for Experimental Run A18
[Elliptical Island I_3 (b/a=0.3), F_r=0.18,h=15cm, Q=0.01634m^3/sec,e=0%]

x(cm)		V_{av}(m/s)	q_{av}(m^2/s)	Q_{av}(m^3/s)
-20	Right channel	0.287	0.04305	0.00788
	Left channel	0.291	0.04365	0.00799
-10	Right channel	0.3285	0.049275	0.00813
	Left channel	0.3245	0.048675	0.00803
0	Right channel	0.3411	0.051165	0.00819
	Left channel	0.3367	0.050505	0.00808
10	Right channel	0.3381	0.050715	0.00837
	Left channel	0.3362	0.05043	0.00832
20	Right channel	0.3146	0.04719	0.00864
	Left channel	0.3066	0.04599	0.00842

Table A.19: Discharge Values for Experimental Run A19
[Elliptical Island I_3 (b/a=0.3), F_r=0.16,h=17cm, Q=0.0179m^3/sec,e=20%]

x(cm)		V_{av}(m/s)	q_{av}(m^2/s)	Q_{av}(m^3/s)
-20	Right channel	0.2831	0.048127	0.01121
	Left channel	0.2943	0.050031	0.00665
-10	Right channel	0.3112	0.052904	0.01137
	Left channel	0.3463	0.058871	0.00677
0	Right channel	0.3213	0.054621	0.01147
	Left channel	0.353	0.06001	0.00660
10	Right channel	0.3171	0.053907	0.01159
	Left channel	0.3462	0.058854	0.00677
20	Right channel	0.2976	0.050592	0.01179
	Left channel	0.3163	0.053771	0.00715

Table A.20: Discharge Values for Experimental Run A20
[Elliptical Island I_3 (b/a=0.3), F_r=0.18,h=15cm, Q=0.01634m^3/sec,e=20%]

x(cm)		V_{av}(m/s)	q_{av}(m^2/s)	Q_{av}(m^3/s)
-20	Right channel	0.2851	0.042765	0.00996
	Left channel	0.2826	0.04239	0.00564
-10	Right channel	0.3174	0.04761	0.01024
	Left channel	0.3237	0.048555	0.00558
0	Right channel	0.3339	0.050085	0.01052
	Left channel	0.3447	0.051705	0.00569
10	Right channel	0.3296	0.04944	0.01063
	Left channel	0.3281	0.049215	0.00566
20	Right channel	0.3042	0.04563	0.01063
	Left channel	0.2905	0.043575	0.00580

Table A.21: Discharge Values for Experimental Run A21
[Elliptical Island I_4 (b/a=0.4), F_r=0.11,h=23cm, Q=0.0196m^3/sec,e=0%]

x(cm)		V_{av}(m/s)	q_{av}(m^2/s)	Q_{av}(m^3/s)
-10	Right channel	0.2292	0.052716	0.00986
	Left channel	0.2274	0.052302	0.00978
0	Right channel	0.2539	0.058397	0.01022
	Left channel	0.2491	0.057293	0.01003
10	Right channel	0.2378	0.054694	0.01023
	Left channel	0.2356	0.054188	0.01013

Table A.22: Discharge Values for Experimental Run A22
[Elliptical Island I_4 (b/a=0.4), F_r=0.13,h=20cm, Q=0.0182m^3/sec,e=0%]

x(cm)		V_{av}(m/s)	q_{av}(m^2/s)	Q_{av}(m^3/s)
-10	Right channel	0.2301	0.04602	0.00861
	Left channel	0.2296	0.04592	0.00859
0	Right channel	0.2558	0.05116	0.00895
	Left channel	0.26	0.052	0.00910
10	Right channel	0.2405	0.0481	0.00899
	Left channel	0.2479	0.04958	0.00927

Table A.23: Discharge Values for Experimental Run A23
[Elliptical Island I_4 (b/a=0.4), F_r=0.14,h=15cm, Q=0.0127m^3/sec,e=0%]

x(cm)		V_{av}(m/s)	q_{av}(m^2/s)	Q_{av}(m^3/s)
-10	Right channel	0.2277	0.034155	0.00639
	Left channel	0.2162	0.03243	0.00606
0	Right channel	0.2424	0.03636	0.00636
	Left channel	0.2333	0.034995	0.00612
10	Right channel	0.2271	0.034065	0.00637
	Left channel	0.2206	0.03309	0.00619

Table A.24: Discharge Values for Experimental Run A24
[Elliptical Island I_4 (b/a=0.4), F_r=0.145,h=17cm, Q=0.0159m^3/sec,e=0%]

x(cm)		V_{av}(m/s)	q_{av}(m^2/s)	Q_{av}(m^3/s)
-10	Right channel	0.2433	0.041361	0.00773
	Left channel	0.2476	0.042092	0.00787
0	Right channel	0.2662	0.045254	0.00792
	Left channel	0.2633	0.044761	0.00783
10	Right channel	0.2472	0.042024	0.00786
	Left channel	0.2509	0.042653	0.00798

Table A.25: Discharge Values for Experimental Run A25
[Elliptical Island I_4 (b/a=0.4), F_r=0.16,h=15cm, Q=0.0146m^3/sec,e=0%]

x(cm)		V_{av}(m/s)	q_{av}(m^2/s)	Q_{av}(m^3/s)
-10	Right channel	0.2682	0.04023	0.00752
	Left channel	0.2378	0.03567	0.00667
0	Right channel	0.2887	0.043305	0.00758
	Left channel	0.2628	0.03942	0.00690
10	Right channel	0.2715	0.040725	0.00761
	Left channel	0.2518	0.03777	0.00706

Table A.26: Discharge Values for Experimental Run A26
[Elliptical Island I_4 (b/a=0.4), F_r=0.11,h=23cm, Q=0.0196m^3/sec,e=20%]

x(cm)		V_{av}(m/s)	q_{av}(m^2/s)	Q_{av}(m^3/s)
-10	Right channel	0.2217	0.050991	0.01208
	Left channel	0.2115	0.048645	0.00666
0	Right channel	0.2351	0.054073	0.01217
	Left channel	0.2431	0.055913	0.00699
10	Right channel	0.2243	0.051589	0.01223
	Left channel	0.2056	0.047288	0.00648

Table A.27: Discharge Values for Experimental Run A27
[Elliptical Island I_4 (b/a=0.4), F_r=0.12,h=20cm, Q=0.0167m^3/sec,e=20%]

x(cm)		V_{av}(m/s)	q_{av}(m^2/s)	Q_{av}(m^3/s)
-10	Right channel	0.2357	0.04714	0.01117
	Left channel	0.2111	0.04222	0.00578
0	Right channel	0.2546	0.05092	0.01146
	Left channel	0.2502	0.05004	0.00625
10	Right channel	0.2307	0.04614	0.01093
	Left channel	0.2284	0.04568	0.00626

Table A.28: Discharge Values for Experimental Run A28
[Elliptical Island I_4 (b/a=0.4), F_r=0.13,h=17cm, Q=0.0146m^3/sec,e=20%]

x(cm)		V_{av}(m/s)	q_{av}(m^2/s)	Q_{av}(m^3/s)
-10	Right channel	0.2367	0.040237	0.00952
	Left channel	0.2208	0.037536	0.00514
0	Right channel	0.2471	0.042	0.00945
	Left channel	0.2589	0.044013	0.00550
10	Right channel	0.2342	0.039814	0.00942
	Left channel	0.232	0.03944	0.00540

Table A.29: Discharge Values for Experimental Run A29
[Elliptical Island I_4 (b/a=0.4), F_r=0.105,h=23cm, Q=0.0182m^3/sec,e=40%]

x(cm)		V_{av} (m/s)	q_{av} (m^2/s)	Q_{adv}(m^3/s)
-10	Right channel	0.2088	0.048024	0.013764
	Left channel	0.207	0.04761	0.004123
0	Right channel	0.2163	0.049749	0.013681
	Left channel	0.2466	0.056718	0.004254
10	Right channel	0.2059	0.047357	0.013573
	Left channel	0.2158	0.049634	0.004298

Table A.30: Discharge Values for Experimental Run A30
[Elliptical Island I_4 (b/a=0.4), F_r=0.117,h=20cm, Q=0.01634m^3/sec,e=40%]

x(cm)		V_{av} (m/s)	q_{av} (m^2/s)	Q_{adv}(m^3/s)
-10	Right channel	0.2084	0.04168	0.011945
	Left channel	0.216	0.0432	0.003741
0	Right channel	0.2311	0.04622	0.012711
	Left channel	0.2534	0.05068	0.003801
10	Right channel	0.2118	0.04236	0.01214
	Left channel	0.2278	0.04556	0.003945

Table A.31: Discharge Values for Experimental Run A31
[Elliptical Island I_4 (b/a=0.4), F_r=0.13,h=17cm, Q=0.0146m^3/sec,e=40%]

x(cm)		V_{av} (m/s)	q_{av} (m^2/s)	Q_{adv}(m^3/s)
-10	Right channel	0.2231	0.037927	0.01088
	Left channel	0.2328	0.039576	0.00344
0	Right channel	0.2394	0.040698	0.01119
	Left channel	0.2796	0.047532	0.00356
10	Right channel	0.2244	0.038148	0.01095
	Left channel	0.2416	0.041072	0.00357

Table A.32: Discharge Values for Experimental Run A32
[Elliptical Island I_5 (b/a=0.6), F_r=0.13,h=17cm, Q=0.0146m^3/sec,e=0%]

x(cm)		V_{av} (m/s)	q_{av} (m^2/s)	Q_{av}(m^3/s)
-10	Right channel	0.1971	0.033512	0.00687
	Left channel	0.2055	0.034932	0.007161
0	Right channel	0.2372	0.040324	0.00706
	Left channel	0.249	0.04233	0.00741
10	Right channel	0.2080	0.035366	0.00725
	Left channel	0.2198	0.03736	0.007659

Table A.33: Discharge Values for Experimental Run A33
[Elliptical Island I_5 (b/a=0.6), F_r=0.14,h=15cm, Q=0.0127m^3/sec,e=0%]

x(cm)		V_{av} (m/s)	q_{av} (m^2/s)	Q_{av}(m^3/s)
-10	Right channel	0.2025	0.030375	0.00623
	Left channel	0.1856	0.02784	0.00571
0	Right channel	0.2363	0.035445	0.00620
	Left channel	0.2208	0.03312	0.00580
10	Right channel	0.2197	0.032955	0.00676
	Left channel	0.2214	0.03321	0.00681

Table A.34: Discharge Values for Experimental Run A34
[Elliptical Island I_5 (b/a=0.6), F_r=0.16,h=15cm, Q=0.0146m^3/sec,e=0%]

x(cm)		V_{av} (m/s)	q_{av} (m^2/s)	Q_{av}(m^3/s)
-10	Right channel	0.2119	0.031785	0.00652
	Left channel	0.2319	0.034785	0.00713
0	Right channel	0.2513	0.037695	0.00660
	Left channel	0.2731	0.040965	0.00717
10	Right channel	0.2483	0.037245	0.00763
	Left channel	0.265	0.03975	0.00815

Table A.35: Discharge Values for Experimental Run A35
[Elliptical Island I_5 (b/a=0.6), F_r=0.105,h=23cm, Q=0.0182m^3/sec,e=40%]

x(cm)		V_{av} (m/s)	q_{av} (m^2/s)	Q_{av}(m^3/s)
-10	Right channel	0.2108	0.04848	0.014786
	Left channel	0.1882	0.043286	0.004545
0	Right channel	0.2274	0.052302	0.014383
	Left channel	0.2711	0.062353	0.004676
10	Right channel	0.1993	0.045836	0.01398
	Left channel	0.1990	0.04578	0.004807

Table A.36: Discharge Values for Experimental Run A36
[Elliptical Island I_5 (b/a=0.6), F_r=0.117,h=20cm, Q=0.016344m^3/sec,e=40%]

x(cm)		V_{av} (m/s)	q_{av} (m^2/s)	Q_{av}(m^3/s)
-10	Right channel	0.2013	0.04027	0.012282
	Left channel	0.1862	0.037238	0.003910
0	Right channel	0.2274	0.04548	0.012507
	Left channel	0.2735	0.0547	0.004103
10	Right channel	0.2087	0.041744	0.012732
	Left channel	0.2046	0.040914	0.004296

Table A.37: Discharge Values for Experimental Run A37
[Elliptical Island I_5 (b/a=0.6), F_r=0.13,h=17cm, Q=0.0146m^3/sec,e=40%]

x(cm)		V_{av} (m/s)	q_{av} (m^2/s)	Q_{av}(m^3/s)
-10	Right channel	0.1997	0.033951	0.010355
	Left channel	0.1837	0.031238	0.00328
0	Right channel	0.2323	0.039491	0.01086
	Left channel	0.3090	0.052533	0.00394
10	Right channel	0.2007	0.034115	0.010405
	Left channel	0.18888	0.032095	0.00337

Table A.38: Discharge Values for Experimental Run A38
[Elliptical Island I_6 (d=15cm), F_r=0.13,h=17cm, Q=0.0146m^3/sec,e=0%]

x(cm)		V_{adv} (m/s)	q_{adv} (m^2/s)	Q_{adv}(m^3/s)
-5	Right channel	0.2158	0.036682	0.00712
	Left channel	0.2094	0.03559	0.006908
0	Right channel	0.2582	0.043897	0.007682
	Left channel	0.2408	0.04093	0.007163
5	Right channel	0.2306	0.039196	0.007608
	Left channel	0.2163	0.03678	0.007139

Table A.39: Discharge Values for Experimental Run A39
[Elliptical Island I_6 (d=15cm), F_r=0.14,h=15cm, Q=0.0127m^3/sec,e=0%]

x(cm)		V_{adv} (m/s)	q_{adv} (m^2/s)	Q_{adv}(m^3/s)
-5	Right channel	0.2104	0.031566	0.006127
	Left channel	0.1986	0.029794	0.005783
0	Right channel	0.2422	0.03633	0.006358
	Left channel	0.2293	0.0344	0.00602
5	Right channel	0.2005	0.030082	0.005839
	Left channel	0.2116	0.031741	0.006161

Table A.40: Discharge Values for Experimental Run A40
[Elliptical Island I_6 (d=15cm), F_r=0.16,h=15cm, Q=0.0146m^3/sec,e=0%]

x(cm)		V_{adv} (m/s)	q_{adv} (m^2/s)	Q_{adv}(m^3/s)
-5	Right channel	0.2449	0.036733	0.007128
	Left channel	0.2448	0.036723	0.007128
0	Right channel	0.2772	0.04158	0.007277
	Left channel	0.2735	0.041025	0.007179
5	Right channel	0.2551	0.03826	0.007426
	Left channel	0.2522	0.037826	0.007342

Table A.41: Discharge Values for Experimental Run A41
[Elliptical Island I_6 (d=15cm), F_r=0.14,h=15cm, Q=0.0127m^3/sec,e=20%]

x(cm)		V_{adv} (m/s)	q_{adv} (m^2/s)	Q_{adv}(m^3/s)
-5	Right channel	0.2035	0.030525	0.007451
	Left channel	0.1998	0.02997	0.004319
0	Right channel	0.2329	0.034935	0.00786
	Left channel	0.245	0.03675	0.004594
5	Right channel	0.2465	0.036975	0.009026
	Left channel	0.2615	0.039225	0.005652

Table A.42: Discharge Values for Experimental Run A42
[Elliptical Island I_6 (d=15cm), F_r=0.16,h=15cm, Q=0.0146m^3/sec,e=20%]

x(cm)		V_{adv} (m/s)	q_{adv} (m^2/s)	Q_{adv}(m^3/s)
-5	Right channel	0.236	0.0354	0.008641
	Left channel	0.2331	0.034965	0.005038
0	Right channel	0.264	0.0396	0.00891
	Left channel	0.2771	0.041565	0.005196
5	Right channel	0.2751	0.041265	0.010073
	Left channel	0.2956	0.04434	0.006389

Table A.43: Discharge Values for Experimental Run A43
[Elliptical Island I_6 (d=15cm), F_r=0.105,h=23cm, Q=0.0182m^3/sec,e=40%]

x(cm)		V_{av} (m/s)	q_{av} (m^2/s)	Q_{av}(m^3/s)
-5	Right channel	0.1993	0.045835	0.01348
	Left channel	0.1890	0.043464	0.00409
0	Right channel	0.2149	0.049427	0.013592
	Left channel	0.2389	0.054947	0.004121
5	Right channel	0.2026	0.046596	0.013704
	Left channel	0.1918	0.044123	0.004152

Table A.44: Discharge Values for Experimental Run A44
[Elliptical Island I_6 (d=15cm), F_r=0.117,h=20cm, Q=0.01634m^3/sec,e=40%]

x(cm)		V_{av} (m/s)	q_{av} (m^2/s)	Q_{av}(m^3/s)
-5	Right channel	0.23465	0.043693	0.01285
	Left channel	0.18825	0.03765	0.003543
0	Right channel	0.23745	0.04749	0.01306
	Left channel	0.2587	0.051733	0.00388
5	Right channel	0.2176	0.04352	0.012799
	Left channel	0.2027	0.040542	0.003815

Table A.45: Discharge Values for Experimental Run A45
[Elliptical Island I_6 (d=15cm), F_r=0.13,h=17cm, Q=0.0146m^3/sec,e=40%]

x(cm)		V_{av} (m/s)	q_{av} (m^2/s)	Q_{av}(m^3/s)
-5	Right channel	0.2162	0.036756	0.01081
	Left channel	0.2113	0.03592	0.00338
0	Right channel	0.2351	0.039967	0.01099
	Left channel	0.2682	0.0456	0.00342
5	Right channel	0.2234	0.03798	0.01117
	Left channel	0.1975	0.03358	0.00316

APPENDIX-B

EXPERIMENTAL DATA RELATING TO FLOW DIVISION AROUND ISLAND (MOBILE BED CONDITION)

Table B.1: Discharge Values for Experimental Run B1
[Elliptical Island I_1 (b/a=0.15), F_r=0.16,h=15cm, Q=0.0146m^3/sec,e=0%]

x(cm)		V_{av}(m/s)	q_{av}(m^2/s)	Q_{av}(m^3/s)
-40	Right channel	0.2419	0.036285	0.00776
	Left channel	0.2162	0.03243	0.00694
-30	Right channel	0.2613	0.039195	0.00772
	Left channel	0.2415	0.036225	0.00714
-20	Right channel	0.2599	0.038985	0.00729
	Left channel	0.2604	0.03906	0.00730
-10	Right channel	0.2664	0.03996	0.00727
	Left channel	0.2633	0.039495	0.00719
0	Right channel	0.2728	0.04092	0.00737
	Left channel	0.2598	0.03897	0.00701
10	Right channel	0.2633	0.039495	0.00719
	Left channel	0.2612	0.03918	0.00713
20	Right channel	0.2559	0.038385	0.00718
	Left channel	0.2523	0.037845	0.00708
30	Right channel	0.2488	0.03732	0.00735
	Left channel	0.2462	0.03693	0.00727
40	Right channel	0.2327	0.034905	0.00747
	Left channel	0.2323	0.034845	0.00746

Table B.2: Discharge Values for Experimental Run B2
[Elliptical Island I_1 (b/a=0.15), F_r=0.19,h=15cm, Q=0.0173m^3/sec,e=0%]

x(cm)		V_{av}(m/s)	q_{av}(m^2/s)	Q_{av}(m^3/s)
-30	Right channel	0.2628	0.039415	0.007745
	Left channel	0.2703	0.040539	0.007966
-20	Right channel	0.2841	0.042612	0.00796
	Left channel	0.2741	0.041113	0.00768
-10	Right channel	0.32845	0.049268	0.008947
	Left channel	0.2880	0.043199	0.007845
0	Right channel	0.3044	0.04566	0.00828
	Left channel	0.2944	0.04416	0.00795
10	Right channel	0.3069	0.046035	0.00836
	Left channel	0.3027	0.045407	0.008246
20	Right channel	0.3030	0.04545	0.00849
	Left channel	0.2891	0.043362	0.0081
30	Right channel	0.2772	0.041588	0.008172
	Left channel	0.2668	0.040015	0.007863

Table B.3: Discharge Values for Experimental Run B3
[Elliptical Island I_1 (b/a=0.15), F_r=0.2,h=15cm, Q=0.0182m^3/sec,e=0%]

x(cm)		V_{av} (m/s)	q_{av} (m^2/s)	Q_{av}(m^3/s)
-40	Right channel	0.3031	0.045465	0.00973
	Left channel	0.2598	0.03897	0.00834
-30	Right channel	0.342	0.0513	0.01011
	Left channel	0.2918	0.04377	0.00862
-20	Right channel	0.3634	0.05451	0.01019
	Left channel	0.3004	0.04506	0.00843
-10	Right channel	0.3404	0.05106	0.00929
	Left channel	0.2926	0.04389	0.00799
0	Right channel	0.3173	0.047595	0.00857
	Left channel	0.287	0.04305	0.00775
10	Right channel	0.3168	0.04752	0.00865
	Left channel	0.2887	0.043305	0.00788
20	Right channel	0.3134	0.04701	0.00879
	Left channel	0.2878	0.04317	0.00807
30	Right channel	0.3252	0.04878	0.00961
	Left channel	0.295	0.04425	0.00871
40	Right channel	0.3262	0.04893	0.01047
	Left channel	0.3026	0.04539	0.00971

Table B.4: Discharge Values for Experimental Run B4
[Elliptical Island I_2 (b/a=0.2), F_r=0.16,h=15cm, Q=0.0146m^3/sec,e=0%]

x(cm)		V_{av} (m/s)	q_{av} (m^2/s)	Q_{av}(m^3/s)
-30	Right channel	0.2400	0.036012	0.007703
	Left channel	0.2378	0.035671	0.00763
-20	Right channel	0.2663	0.039945	0.007693
	Left channel	0.26	0.039	0.007511
-10	Right channel	0.2748	0.041225	0.00754
	Left channel	0.2693	0.040399	0.007389
0	Right channel	0.274	0.0411	0.007398
	Left channel	0.2728	0.04092	0.007366
10	Right channel	0.2788	0.041826	0.00765
	Left channel	0.2664	0.039967	0.00731
20	Right channel	0.2862	0.04293	0.008268
	Left channel	0.2636	0.03954	0.007615
30	Right channel	0.5713	0.03857	0.00825
	Left channel	0.2387	0.035802	0.007658

Table B.5: Discharge Values for Experimental Run B5
[Elliptical Island I_2 (b/a=0.2), F_r=0.19,h=15cm, Q=0.0173m^3/sec,e=0%]

x(cm)		V_{av} (m/s)	q_{av} (m^2/s)	Q_{av}(m^3/s)
-30	Right channel	0.2759	0.041385	0.00886
	Left channel	0.2598	0.03897	0.00834
-20	Right channel	0.3123	0.046845	0.00904
	Left channel	0.2988	0.04482	0.00865
-10	Right channel	0.3247	0.048705	0.00891
	Left channel	0.309	0.04635	0.00848
0	Right channel	0.304	0.0456	0.00821
	Left channel	0.2833	0.042495	0.00765
10	Right channel	0.2988	0.04482	0.00820
	Left channel	0.2897	0.043455	0.00795
20	Right channel	0.3043	0.045645	0.00881
	Left channel	0.2919	0.043785	0.00845
30	Right channel	0.3207	0.048105	0.01029
	Left channel	0.2903	0.043545	0.00932

Table B.6: Discharge Values for Experimental Run B6
[Elliptical Island I_2 (b/a=0.2), F_r=0.2,h=15cm, Q=0.0182m^3/sec,e=0%]

x(cm)		V_{av} (m/s)	q_{av} (m^2/s)	Q_{av}(m^3/s)
-30	Right channel	0.2807	0.042105	0.00901
	Left channel	0.2737	0.041055	0.00879
-20	Right channel	0.3005	0.045075	0.00870
	Left channel	0.2985	0.044775	0.00864
-10	Right channel	0.3061	0.045915	0.00840
	Left channel	0.3077	0.046155	0.00845
0	Right channel	0.3099	0.046485	0.00837
	Left channel	0.3066	0.04599	0.00828
10	Right channel	0.3152	0.04728	0.00865
	Left channel	0.3155	0.047325	0.00866
20	Right channel	0.3224	0.04836	0.00933
	Left channel	0.3078	0.04617	0.00891
30	Right channel	0.3277	0.049155	0.01052
	Left channel	0.2885	0.043275	0.00926

Table B.7: Discharge Values for Experimental Run B7
[Elliptical Island I_2 (b/a=0.2), F_r=0.16,h=15cm, Q=0.0146m^3/sec,e=20%]

x(cm)		V_{av} (m/s)	q_{av} (m^2/s)	Q_{av}(m^3/s)
-30	Right channel	0.2331	0.034965	0.00923
	Left channel	0.224	0.0336	0.00551
-20	Right channel	0.2538	0.03807	0.00925
	Left channel	0.272	0.0408	0.00583
-10	Right channel	0.2531	0.037965	0.00885
	Left channel	0.2724	0.04086	0.00543
0	Right channel	0.2556	0.03834	0.00882
	Left channel	0.2571	0.038565	0.00501
10	Right channel	0.258	0.0387	0.00902
	Left channel	0.2637	0.039555	0.00526
20	Right channel	0.2536	0.03804	0.00924
	Left channel	0.2538	0.03807	0.00544
30	Right channel	0.2532	0.03798	0.01003
	Left channel	0.2706	0.04059	0.00666

Table B.8: Discharge Values for Experimental Run B8
[Elliptical Island I_2 (b/a=0.2), F_r=0.19,h=15cm, Q=0.0173m^3/sec,e=20%]

x(cm)		V_{av} (m/s)	q_{av} (m^2/s)	Q_{av}(m^3/s)
-30	Right channel	0.273	0.04095	0.01081
	Left channel	0.2506	0.03759	0.00616
-20	Right channel	0.3044	0.04566	0.01109
	Left channel	0.2975	0.044625	0.00638
-10	Right channel	0.302	0.0453	0.01055
	Left channel	0.3188	0.04782	0.00636
0	Right channel	0.2864	0.04296	0.00988
	Left channel	0.291	0.04365	0.00567
10	Right channel	0.2799	0.041985	0.00978
	Left channel	0.3019	0.045285	0.00602
20	Right channel	0.293	0.04395	0.01068
	Left channel	0.2852	0.042777	0.00610
30	Right channel	0.3032	0.04548	0.01201
	Left channel	0.2775	0.041625	0.00683

Table B.9: Discharge Values for Experimental Run B9
[Elliptical Island I_3 (b/a=0.3), F_r=0.16,h=15cm, Q=0.0146m^3/sec,e=0%]

x(cm)		V_{av} (m/s)	q_{av} (m^2/s)	Q_{av}(m^3/s)
-20	Right channel	0.2912	0.04368	0.00799
	Left channel	0.2597	0.038955	0.00713
-10	Right channel	0.3204	0.04806	0.00793
	Left channel	0.2863	0.042945	0.00709
0	Right channel	0.3146	0.04719	0.00755
	Left channel	0.2837	0.042555	0.00681
10	Right channel	0.3102	0.04653	0.00768
	Left channel	0.282	0.0423	0.00698
20	Right channel	0.3035	0.045525	0.00833
	Left channel	0.2925	0.043875	0.00803

Table B.10: Discharge Values for Experimental Run B10
[Elliptical Island I_3 (b/a=0.3), F_r=0.19,h=15cm, Q=0.0173m^3/sec,e=0%]

x(cm)		V_{av} (m/s)	q_{av} (m^2/s)	Q_{av}(m^3/s)
-20	Right channel	0.3347	0.050205	0.00919
	Left channel	0.2692	0.04038	0.00739
-10	Right channel	0.347	0.05205	0.00859
	Left channel	0.2733	0.040995	0.00676
0	Right channel	0.3277	0.049155	0.00786
	Left channel	0.3027	0.045405	0.00726
10	Right channel	0.3382	0.05073	0.00837
	Left channel	0.2692	0.04038	0.00666
20	Right channel	0.3224	0.04836	0.00885
	Left channel	0.2471	0.037065	0.00678

Table B.11: Discharge Values for Experimental Run B11
[Elliptical Island I_3 (b/a=0.3), F_r=0.16,h=15cm, Q=0.0146m^3/sec,e=20%]

x(cm)		V_{av} (m/s)	q_{av} (m^2/s)	Q_{av}(m^3/s)
-20	Right channel	0.2784	0.04176	0.00973
	Left channel	0.2384	0.03576	0.00476
-10	Right channel	0.296	0.0444	0.00955
	Left channel	0.2758	0.04137	0.00476
0	Right channel	0.2824	0.04236	0.00890
	Left channel	0.3333	0.05	0.00550
10	Right channel	0.2785	0.041775	0.00898
	Left channel	0.3148	0.047222	0.00544
20	Right channel	0.2836	0.04254	0.00991
	Left channel	0.2408	0.03612	0.00480

Table B.12: Discharge Values for Experimental Run B12
[Elliptical Island I_3 (b/a=0.3), F_r=0.16,h=18cm, Q=0.0193m^3/sec,e=20%]

x(cm)		V_{av}(m/s)	q_{av}(m^2/s)	Q_{av}(m^3/s)
-20	Right channel	0.2909	0.052362	0.01220
	Left channel	0.2758	0.049644	0.00660
-10	Right channel	0.3096	0.055728	0.01198
	Left channel	0.3251	0.058518	0.00673
0	Right channel	0.3026	0.054468	0.01144
	Left channel	0.3231	0.058158	0.00640
10	Right channel	0.2873	0.051714	0.01112
	Left channel	0.4077	0.073386	0.00844
20	Right channel	0.2813	0.050634	0.01180
	Left channel	0.2939	0.052902	0.00704

Table B.13: Discharge Values for Experimental Run B13
[Elliptical Island I_3 (b/a=0.3), F_r=0.19,h=15cm, Q=0.0173m^3/sec,e=20%]

x(cm)		V_{av}(m/s)	q_{av}(m^2/s)	Q_{av}(m^3/s)
-20	Right channel	0.2899	0.043485	0.01013
	Left channel	0.3158	0.04737	0.0063
-10	Right channel	0.3037	0.045555	0.00979
	Left channel	0.3888	0.05832	0.00671
0	Right channel	0.3027	0.045405	0.00953
	Left channel	0.3481	0.052215	0.00574
10	Right channel	0.3078	0.04617	0.00993
	Left channel	0.3393	0.050895	0.00585
20	Right channel	0.3127	0.046905	0.01093
	Left channel	0.3306	0.04959	0.0066

Table B.14: Discharge Values for Experimental Run B14
[Elliptical Island I_4 (b/a=0.4), F_r=0.16,h=18cm, Q=0.0193m^3/sec,e=0%]

x(cm)		V_{av}(m/s)	q_{av}(m^2/s)	Q_{av}(m^3/s)
-10	Right channel	0.2824	0.050832	0.00951
	Left channel	0.28	0.0504	0.00942
0	Right channel	0.3141	0.056538	0.00989
	Left channel	0.3154	0.056772	0.00993
10	Right channel	0.2977	0.053586	0.01002
	Left channel	0.2954	0.053172	0.00994

Table B.15: Discharge Values for Experimental Run B15
[Elliptical Island I_4 (b/a=0.4), F_r=0.19,h=15cm, Q=0.0173m^3/sec,e=0%]

x(cm)		V_{av} (m/s)	q_{av} (m^2/s)	Q_{av}(m^3/s)
-10	Right channel	0.3102	0.04653	0.00870
	Left channel	0.2561	0.038415	0.00718
0	Right channel	0.332	0.0498	0.00871
	Left channel	0.2603	0.039045	0.00683
10	Right channel	0.3142	0.04713	0.00881
	Left channel	0.261	0.03915	0.00732

Table B.16: Discharge Values for Experimental Run B16
[Elliptical Island I_4 (b/a=0.4), F_r=0.16,h=15cm, Q=0.0146m^3/sec,e=20%]

x(cm)		V_{av} (m/s)	q_{av} (m^2/s)	Q_{av}(m^3/s)
-10	Right channel	0.268	0.0402	0.00953
	Left channel	0.2825	0.042375	0.00580
0	Right channel	0.2861	0.042915	0.00966
	Left channel	0.3159	0.047385	0.00592
10	Right channel	0.2666	0.03999	0.00948
	Left channel	0.2932	0.04398	0.00602

Table B.17: Discharge Values for Experimental Run B17
[Elliptical Island I_4 (b/a=0.4), F_r=0.16,h=18cm, Q=0.0193m^3/sec,e=20%]

x(cm)		V_{av} (m/s)	q_{av} (m^2/s)	Q_{av}(m^3/s)
-10	Right channel	0.2862	0.051516	0.01221
	Left channel	0.296	0.05328	0.00730
0	Right channel	0.3186	0.057348	0.01290
	Left channel	0.3071	0.055278	0.00691
10	Right channel	0.2963	0.053334	0.01264
	Left channel	0.293	0.05274	0.00722

Table B.18: Discharge Values for Experimental Run B18
[Elliptical Island I_4 (b/a=0.4), F_r=0.19,h=15cm, Q=0.0173m^3/sec,e=20%]

x(cm)		V_{av} (m/s)	q_{av} (m^2/s)	Q_{av}(m^3/s)
-10	Right channel	0.305	0.04575	0.01084
	Left channel	0.2843	0.042645	0.00584
0	Right channel	0.3349	0.050235	0.01130
	Left channel	0.3182	0.04773	0.00597
10	Right channel	0.329	0.04935	0.01170
	Left channel	0.3263	0.048945	0.00671

Table B.19: Discharge Values for Experimental Run B19
[Elliptical Island I_5 (b/a=0.6), F_r=0.16,h=15cm, Q=0.0146m^3/sec,e=0%]

x(cm)		V_{av} (m/s)	q_{av} (m^2/s)	Q_{av}(m^3/s)
-10	Right channel	0.2319	0.034785	0.00713
	Left channel	0.2148	0.03222	0.00660
-5	Right channel	0.2545	0.038175	0.00691
	Left channel	0.2436	0.03654	0.00661
0	Right channel	0.2609	0.039135	0.00685
	Left channel	0.2531	0.037965	0.00664
5	Right channel	0.2597	0.038955	0.00705
	Left channel	0.2451	0.036765	0.00665
10	Right channel	0.2493	0.037395	0.00767
	Left channel	0.2425	0.036375	0.00746

Table B.20: Discharge Values for Experimental Run B20
[Elliptical Island I_5 (b/a=0.6), F_r=0.19,h=15cm, Q=0.0173m^3/sec,e=0%]

x(cm)		V_{av} (m/s)	q_{av} (m^2/s)	Q_{av}(m^3/s)
-10	Right channel	0.2482	0.03723	0.00763
	Left channel	0.2463	0.036945	0.00757
-5	Right channel	0.2747	0.041205	0.00746
	Left channel	0.2749	0.041235	0.00746
0	Right channel	0.2874	0.04311	0.00754
	Left channel	0.2864	0.04296	0.00752
5	Right channel	0.2872	0.04308	0.00780
	Left channel	0.2802	0.04203	0.00761
10	Right channel	0.2816	0.04224	0.00866
	Left channel	0.2746	0.04119	0.00844

Table B.21: Discharge Values for Experimental Run B21
[Elliptical Island I_5 (b/a=0.6), F_r=0.16,h=18cm, Q=0.0193m^3/sec,e=20%]

x(cm)		V_{adv} (m/s)	q_{adv} (m^2/s)	Q_{adv}(m^3/s)
-10	Right channel	0.2669	0.048042	0.01225
	Left channel	0.2213	0.039834	0.00617
-5	Right channel	0.2971	0.053478	0.01235
	Left channel	0.2687	0.048366	0.00634
0	Right channel	0.3112	0.056016	0.01260
	Left channel	0.285	0.0513	0.00641
5	Right channel	0.3038	0.054684	0.01263
	Left channel	0.2731	0.049158	0.00644
10	Right channel	0.2891	0.052038	0.01327
	Left channel	0.2819	0.050742	0.00786

Table B.22: Discharge Values for Experimental Run B22
[Elliptical Island I_6 (d=15cm), F_r=0.15,h=15cm, Q=0.0139m^3/sec,e=0%]

x(cm)		V_{av} (m/s)	q_{av} (m^2/s)	Q_{av}(m^3/s)
-5	Right channel	0.2232	0.03348	0.00649
	Left channel	0.2092	0.03138	0.00609
0	Right channel	0.252	0.0378	0.00661
	Left channel	0.2341	0.035115	0.00614
5	Right channel	0.2579	0.038685	0.00750
	Left channel	0.2471	0.037065	0.00719

Table B.23: Discharge Values for Experimental Run B23
[Elliptical Island I_6 (d=15cm), F_r=0.17,h=15cm, Q=0.0157m^3/sec,e=0%]

x(cm)		V_{av} (m/s)	q_{av} (m^2/s)	Q_{av}(m^3/s)
-5	Right channel	0.2651	0.039773	0.00772
	Left channel	0.249	0.03735	0.00725
0	Right channel	0.2476	0.03714	0.00750
	Left channel	0.2434	0.03651	0.00739
5	Right channel	0.2586	0.038794	0.00753
	Left channel	0.2487	0.0373	0.00724

Table B.24: Discharge Values for Experimental Run B24
[Elliptical Island I_6 (d=15cm), F_r=0.19,h=15cm, Q=0.0173m^3/sec,e=0%]

x(cm)		V_{av} (m/s)	q_{av} (m^2/s)	Q_{av}(m^3/s)
-5	Right channel	0.2913	0.043689	0.00848
	Left channel	0.2837	0.042555	0.00826
0	Right channel	0.3154	0.047314	0.00828
	Left channel	0.3051	0.04577	0.00801
5	Right channel	0.287	0.04305	0.00835
	Left channel	0.2712	0.04068	0.00789

APPENDIX-C

EXPERIMENTAL DATA RELATING TO SCOUR PATTERN AROUND ISLAND

Table C.1: Scour Data for Experimental Run C1
[Elliptical Island I_1 (b/a=0.15), F_r=0.16,h=15cm]

x(cm)	y(cm)	z(cm)	x(cm)	y(cm)	z(cm)	x(cm)	y(cm)	z(cm)
-48.5	-10	0	-10	10.5	0.80	20	-7.1	1.20
-48.5	-5	0	-10	13.5	-0.87	20	6.5	0.65
-48.5	0	0	-10	16.5	-2.64	20	11.5	0.37
-48.5	5	0	-10	20.5	-1.35	20	16.5	-0.67
-48.5	10	0	-5	-19.5	-0.28	20	20.5	-0.01
-47.5	-3.7	0	-5	-16.5	-0.60	25	-19.5	-1.87
-47.5	0	-0.15	-5	-13.5	0.46	25	-14.5	0.03
-47.5	2.9	0	-5	-10.5	1.04	25	-9.5	0.50
-42	-5.5	0	-5	-8.3	1.60	25	-6.5	0.85
-42	-1.5	-0.06	-5	8	1.37	25	5.5	1.35
-42	1	-0.35	-5	10.5	0.04	25	10.5	0.03
-42	3.5	-0.02	-5	13.5	-1.40	25	15.5	-1.16
-38	-5.5	0	-5	16.5	-0.80	25	20.5	0.12
-38	-2.5	-0.23	-5	20.5	-0.70	30	-19.5	0.04
-38	3.5	-0.45	1	-19.5	-1.55	30	-14.5	-0.80
-38	4.5	-0.05	1	-16.5	-2.50	30	-9.5	0.30
-33	-7.1	0	1	-13.5	-1.48	30	-5.5	0.56
-33	-3.8	-0.75	1	-10.5	0.10	30	4.5	-0.20
-33	4.5	-0.55	1	-8.5	0.50	30	9.5	1.05
-33	7.1	0	1	8	1.35	30	14.5	0.25
-28	-8.5	0.05	1	10.5	0.23	30	20.5	0.40
-28	-5.5	-1.10	1	13.5	0.85	35	-19.5	-1.06
-28	5	-0.05	1	16.5	-0.80	35	-16	-1.97
-28	6.5	0.20	1	20.5	-2.53	35	-11	1.32
-28	8.5	-0.05	5	-19.5	-0.68	35	-6.5	0.07
-23	-10.5	0.10	5	-15.5	-1.20	35	-4.5	0.10
-23	-6.3	0.25	5	-11.5	-1.20	35	4	-0.05
-23	6.5	-0.15	5	-8	0.46	35	7.5	-0.12
-23	9.5	-1.17	5	7.7	1.87	35	12.5	0
-23	13	-0.02	5	11.5	1.00	35	17.5	-0.30
-19	-11.3	0.11	5	15.5	-0.70	35	20.5	-1.27
-19	-7	0.26	5	20.5	-2.10	40	-19.5	0
-19	6.7	-1.00	10	-19.5	0.65	40	-14.5	0.70
-19	9.5	-1.23	10	-14.5	1.22	40	-9.5	-0.25
-19	12.5	-0.88	10	-8.5	-0.58	40	-3.5	-0.37
-19	15.5	0.05	10	7.5	2.20	40	2.5	-0.54
-15	-14	0.02	10	12.5	0.62	40	5.5	-0.48
-15	-11.5	-1.20	10	17.5	-0.20	40	11.5	-0.29
-15	-7.1	-0.54	10	20.5	0.70	40	15.5	0
-15	7.5	0.12	15	-19.5	-0.73	40	20.5	0
-15	10.5	-0.15	15	-14.5	0.30	45	-19.5	0
-15	13.5	-0.30	15	-8	0.10	45	-14.5	-0.10
-15	16.5	-0.78	15	7	0.40	45	-9.5	-0.28
-15	20.5	-0.08	15	11.5	1.24	45	-4.5	-0.10
-10	-16.5	-0.04	15	16.5	0.33	45	-1	-0.25
-10	-13.5	-0.30	15	20.5	0.40	45	5.5	0
-10	-10.5	-0.06	20	-19.5	-1.60	45	11.5	0.05
-10	-8	0.30	20	-14.5	0	45	15.5	0.05
-10	8	1.60	20	-9.5	0.72	45	20.5	0.11

Table C.2: Scour Data for Experimental Run C2
[Elliptical Island I_1 (b/a=0.15), F_r=0.19,h=15cm]

x(cm)	y(cm)	z(cm)	x(cm)	y(cm)	z(cm)	x(cm)	y(cm)	z(cm)
-56.5	-10.0	0	-40	-8.0	-3.43	-20	16.0	-0.18
-56.5	-7.0	0	-40	-5.0	-3.11	-20	19.0	-0.84
-56.5	-4.0	0	-40	4.9	-3.01	-20	20.0	-1.19
-56.5	-1.0	0	-40	8.0	-2.66	-15	-20.0	-2.27
-56.5	2.0	0	-40	11.0	-1.68	-15	-17.0	-2.31
-56.5	5.0	0	-40	14.0	-0.49	-15	-14.0	-1.37
-56.5	8.0	0	-40	15.0	0.03	-15	-11.0	-0.21
-55	-7.0	0	-35	-18.5	-0.07	-15	-8.0	0.70
-55	-4.0	-0.98	-35	-17.0	-0.66	-15	7.5	0
-55	-1.0	-1.47	-35	-14.0	-0.77	-15	10.0	-0.56
-55	2.0	-1.22	-35	-11.0	-1.86	-15	13.0	-1.12
-55	5.0	-0.14	-35	-8.0	-2.24	-15	16.0	-0.80
-55	8.0	0	-35	-6.5	-2.20	-15	19.0	-1.68
-52	-10.0	0	-35	6.0	-1.54	-15	20.0	-1.99
-52	-7.0	-1.54	-35	9.0	-1.29	-10	-20.0	-2.41
-52	-4.0	-2.41	-35	12.0	-1.05	-10	-17.0	-2.24
-52	-1.0	-2.80	-35	15.0	0.04	-10	-14.0	-2.07
-52	2.0	-2.56	-30	-18.5	-0.14	-10	-11.0	-0.80
-52	5.0	-1.96	-30	-16.0	-0.21	-10	-8.0	-0.28
-52	8.0	-1.05	-30	-13.0	-1.01	-10	8.0	-0.91
-52	10.5	0	-30	-10.0	-1.26	-10	11.0	-1.16
-49	-14.0	0	-30	-7.0	-1.19	-10	14.0	-1.75
-49	-12.2	-0.14	-30	6.5	-0.59	-10	17.0	-2.41
-49	-9.0	-1.75	-30	9.0	-0.74	-10	20.0	-2.98
-49	-6.0	-3.01	-30	12.0	-0.77	-5	-20.0	-2.55
-49	-3.0	-3.78	-30	15.0	0.10	-5	-17.0	-2.94
-49	0	-4.16	-25	-20.0	-0.98	-5	-14.0	-2.45
-49	3.0	-3.50	-25	-17.0	-0.45	-5	-11.0	-2.00
-49	6.0	-2.69	-25	-14.0	-0.77	-5	-8.0	-1.54
-49	9.0	-1.65	-25	-11.0	-0.77	-5	8.0	-1.29
-49	12.4	0.07	-25	-8.0	-0.38	-5	11.0	-2.49
-46	-17.0	-0.07	-25	7.0	-0.25	-5	14.0	-3.32
-46	-14.0	-0.14	-25	10.0	-0.45	-5	17.0	-3.67
-46	-11.0	-1.82	-25	13.0	-0.63	-5	20.0	-3.36
-46	-8.0	-2.90	-25	16.0	0.07	0	-20.0	-2.87
-46	-5.0	-4.24	-25	19.0	-0.28	0	-17.0	-2.70
-46	-3.1	-4.41	-25	20.0	-0.14	0	-14.0	-2.83
-46	2.8	-4.41	-20	-20.0	-1.92	0	-11.0	-2.41
-46	5.0	-3.78	-20	-17.0	-1.29	0	-8.0	-1.89
-46	8.0	-2.59	-20	-14.0	-0.95	0	8.0	-1.02
-46	11.0	-1.64	-20	-11.0	-0.31	0	11.0	-2.52
-46	14.0	0.07	-20	-7.5	0.56	0	14.0	-2.94
-40	-17.0	-0.03	-20	7.5	-0.07	0	17.0	-2.69
-40	-14.0	-1.36	-20	10.0	-0.56	0	20.0	-2.56
-40	-11.0	-2.28	-20	13.0	-0.77	5	-20.0	-3.22

x(cm)	y(cm)	z(cm)	x(cm)	y(cm)	z(cm)	x(cm)	y(cm)	z(cm)
5	-17.0	-3.22	25	-20.0	-2.97	40	-5.0	-0.25
5	-14.0	-3.04	25	-17.0	-2.66	40	4.5	1.15
5	-11.0	-2.73	25	-14.0	-1.75	40	7.0	0.80
5	-8.0	-1.93	25	-11.0	-1.19	40	10.0	0.18
5	8.0	-0.42	25	-8.0	-1.68	40	13.0	0.03
5	11.0	-1.71	25	-6.7	-2.07	40	16.0	-0.67
5	14.0	-2.20	25	7.0	0.66	40	19.0	-0.63
5	17.0	-2.07	25	10.0	-0.35	40	20.0	-0.49
5	20.0	-1.68	25	13.0	-0.53	45	-20.0	0.14
10	-20.0	-2.83	25	16.0	-1.64	45	-16.0	-0.14
10	-17.0	-2.56	25	19.0	-1.23	45	-12.0	-0.42
10	-14.0	-2.59	25	20.0	-0.98	45	-8.0	-0.56
10	-11.0	-2.00	30	-20.0	-1.12	45	-4.0	-0.17
10	-8.0	-1.85	30	-17.0	-1.26	45	-2.0	0.07
10	8.0	0.07	30	-14.0	-2.10	45	2.0	0.46
10	11.0	-1.05	30	-11.0	-2.03	45	6.0	1.12
10	14.0	-1.50	30	-8.0	-1.61	45	10.0	0.91
10	17.0	-1.58	30	-6.2	-1.89	45	14.0	0.60
10	20.0	-1.47	30	6.5	0.77	45	18.0	0.91
15	-20.0	-2.34	30	9.0	0.14	45	20.0	1.26
15	-17.0	-2.20	30	12.0	-0.03	50	-20.0	0.35
15	-14.0	-2.59	30	15.0	-1.16	50	-15.0	0.14
15	-11.0	-2.07	30	18.0	-1.01	50	-10.0	-0.56
15	-8.0	-1.05	30	20.0	-0.70	50	-5.0	0.49
15	7.5	0.87	35	-20.0	-0.95	50	0	0
15	10.0	-0.14	35	-17.0	-1.22	50	5.0	0.17
15	13.0	-0.84	35	-14.0	-2.28	50	10.0	0.56
15	16.0	-1.93	35	-11.0	-2.52	50	15.0	1.43
15	19.0	-2.73	35	-8.0	-1.19	50	19.0	2.07
15	20.0	-2.97	35	-5.5	-1.05	50	20.0	1.68
20	-20.0	-3.22	35	5.5	0.17	60	-20.0	0.91
20	-17.0	-2.62	35	9.0	0.88	60	-15.0	1.40
20	-14.0	-2.14	35	12.0	0.49	60	-10.0	0.98
20	-11.0	-1.68	35	15.0	-0.56	60	-5.0	0
20	-8.0	-0.73	35	18.0	-1.43	60	0	0.56
20	7.5	1.23	35	20.0	-1.30	60	5.0	0.63
20	10.0	0	40	-20.0	-0.17	60	10.0	0.42
20	13.0	-1.33	40	-17.0	-0.07	60	15.0	1.12
20	16.0	-2.27	40	-14.0	-0.91	60	20.0	0.87
20	19.0	-2.70	40	-11.0	-1.26			
20	20.0	-2.73	40	-8.0	-0.63			

Table C.3: Scour Data for Experimental Run C3
[Elliptical Island I_1 (b/a=0.15), F_r=0.2,h=15cm]

x(cm)	y(cm)	z(cm)	x(cm)	y(cm)	z(cm)	x(cm)	y(cm)	z(cm)
-56.5	-10.0	0	-40	8.0	-3.80	-20	20.0	-1.70
-56.5	-7.0	0	-40	11.0	-2.40	-15	-20.0	-3.25
-56.5	-4.0	0	-40	14.0	-0.70	-15	-17.0	-3.30
-56.5	-1.0	0	-40	15.0	0.05	-15	-14.0	-1.95
-56.5	2.0	0	-35	-18.5	-0.10	-15	-11.0	-0.30
-56.5	5.0	0	-35	-17.0	-0.95	-15	-8.0	1.00
-56.5	8.0	0	-35	-14.0	-1.10	-15	7.5	0
-55	-7.0	0	-35	-11.0	-2.65	-15	10.0	-0.80
-55	-4.0	-1.40	-35	-8.0	-3.20	-15	13.0	-1.60
-55	-1.0	-2.10	-35	-6.5	-3.15	-15	16.0	-1.15
-55	2.0	-1.75	-35	6.0	-2.20	-15	19.0	-2.40
-55	5.0	-0.20	-35	9.0	-1.85	-15	20.0	-2.85
-52	-10.0	0	-35	12.0	-1.50	-10	-20.0	-3.45
-52	-7.0	-2.20	-35	15.0	0.05	-10	-17.0	-3.20
-52	-4.0	-3.45	-30	-18.5	-0.20	-10	-14.0	-2.95
-52	-1.0	-4.00	-30	-16.0	-0.30	-10	-11.0	-1.15
-52	2.0	-3.65	-30	-13.0	-1.45	-10	-8.0	-0.40
-52	5.0	-2.80	-30	-10.0	-1.80	-10	8.0	-1.30
-52	8.0	-1.50	-30	-7.0	-1.70	-10	11.0	-1.65
-52	10.5	0	-30	6.5	-0.85	-10	14.0	-2.50
-49	-12.2	-0.20	-30	9.0	-1.05	-10	17.0	-3.45
-49	-9.0	-2.50	-30	12.0	-1.10	-10	20.0	-4.25
-49	-6.0	-4.30	-30	15.0	0.15	-5	-20.0	-3.65
-49	-3.0	-5.40	-30	16.8	-0.05	-5	-17.0	-4.20
-49	0	-5.95	-25	-20.0	-1.40	-5	-14.0	-3.50
-49	3.0	-5.00	-25	-17.0	-0.65	-5	-11.0	-2.85
-49	6.0	-3.85	-25	-14.0	-1.10	-5	-8.0	-2.20
-49	9.0	-2.35	-25	-11.0	-1.10	-5	8.0	-1.85
-49	12.4	0.10	-25	-8.0	-0.55	-5	11.0	-3.55
-46	-14.0	-0.20	-25	7.0	-0.35	-5	14.0	-4.75
-46	-11.0	-2.60	-25	10.0	-0.65	-5	17.0	-5.25
-46	-8.0	-4.15	-25	13.0	-0.90	-5	20.0	-4.80
-46	-5.0	-6.05	-25	16.0	0.10	0	-20.0	-4.10
-46	-3.1	-6.30	-25	19.0	-0.40	0	-17.0	-3.85
-46	2.8	-6.30	-25	20.0	-0.20	0	-14.0	-4.05
-46	5.0	-5.40	-20	-20.0	-2.75	0	-11.0	-3.45
-46	8.0	-3.70	-20	-17.0	-1.85	0	-8.0	-2.70
-46	11.0	-2.35	-20	-14.0	-1.35	0	8.0	-1.45
-46	14.0	0.10	-20	-11.0	-0.45	0	11.0	-3.60
-40	-17.0	-0.05	-20	-7.5	0.80	0	14.0	-4.20
-40	-14.0	-1.95	-20	7.5	-0.10	0	17.0	-3.85
-40	-11.0	-3.25	-20	10.0	-0.80	0	20.0	-3.65
-40	-8.0	-4.90	-20	13.0	-1.10	5	-20.0	-4.60
-40	-5.0	-4.45	-20	16.0	-0.25	5	-17.0	-4.60
-40	4.9	-4.30	-20	19.0	-1.20	5	-14.0	-4.35

x(cm)	y(cm)	z(cm)	x(cm)	y(cm)	z(cm)	x(cm)	y(cm)	z(cm)
5	-11.0	-3.90	25	-17.0	-3.80	40	-5.0	-0.35
5	-8.0	-2.75	25	-14.0	-2.50	40	4.5	1.65
5	8.0	-0.60	25	-11.0	-1.70	40	7.0	1.15
5	11.0	-2.45	25	-8.0	-2.40	40	10.0	0.25
5	14.0	-3.15	25	-6.7	-2.95	40	13.0	0.05
5	17.0	-2.95	25	7.0	0.95	40	16.0	-0.95
5	20.0	-2.40	25	10.0	-0.50	40	19.0	-0.90
10	-20.0	-4.05	25	13.0	-0.75	40	20.0	-0.70
10	-17.0	-3.65	25	16.0	-2.35	45	-20.0	0.20
10	-14.0	-3.70	25	19.0	-1.75	45	-16.0	-0.20
10	-11.0	-2.85	25	20.0	-1.40	45	-12.0	-0.60
10	-8.0	-2.65	30	-20.0	-1.60	45	-8.0	-0.80
10	8.0	0.10	30	-17.0	-1.80	45	-4.0	-0.25
10	11.0	-1.50	30	-14.0	-3.00	45	-2.0	0.10
10	14.0	-2.15	30	-11.0	-2.90	45	2.0	0.65
10	17.0	-2.25	30	-8.0	-2.30	45	6.0	1.60
10	20.0	-2.10	30	-6.2	-2.70	45	10.0	1.30
15	-20.0	-3.35	30	6.5	1.10	45	14.0	0.85
15	-17.0	-3.15	30	9.0	0.20	45	18.0	1.30
15	-14.0	-3.70	30	12.0	-0.05	45	20.0	1.80
15	-11.0	-2.95	30	15.0	-1.65	50	-20.0	0.50
15	-8.0	-1.50	30	18.0	-1.45	50	-15.0	0.20
15	7.5	1.25	30	20.0	-1.00	50	-10.0	-0.80
15	10.0	-0.20	35	-20.0	-1.35	50	-5.0	0.70
15	13.0	-1.20	35	-17.0	-1.75	50	0	0
15	16.0	-2.75	35	-14.0	-3.25	50	5.0	0.25
15	19.0	-3.90	35	-11.0	-3.60	50	10.0	0.80
15	20.0	-4.25	35	-8.0	-1.70	50	15.0	2.05
20	-20.0	-4.60	35	-5.5	-1.50	50	19.0	2.95
20	-17.0	-3.75	35	5.5	0.25	50	20.0	2.40
20	-14.0	-3.05	35	9.0	1.25	60	-20.0	1.30
20	-11.0	-2.40	35	12.0	0.70	60	-15.0	2.00
20	-8.0	-1.05	35	15.0	-0.80	60	-10.0	1.40
20	7.5	1.75	35	18.0	-2.05	60	-5.0	0
20	10.0	0	35	20.0	-1.85	60	0	0.80
20	13.0	-1.90	40	-20.0	-0.25	60	5.0	0.90
20	16.0	-3.25	40	-17.0	-0.10	60	10.0	0.60
20	19.0	-3.85	40	-14.0	-1.30	60	15.0	1.60
20	20.0	-3.90	40	-11.0	-1.80	60	20.0	1.25
25	-20.0	-4.25	40	-8.0	-0.90			

Table C.4: Scour Data for Experimental Run C4
[Elliptical Island I_2 (b/a=0.2), F_r=0.16,h=15cm]

x(cm)	y(cm)	z(cm)	x(cm)	y(cm)	z(cm)	x(cm)	y(cm)	z(cm)
-40	-4.0	-0.05	-14	-14.0	-1.85	2	-13.0	-1.35
-40	-1.0	-1.00	-14	-11.0	-0.95	2	-10.0	-0.55
-40	2.0	-0.60	-14	-8.0	-0.25	2	-8.5	0.40
-40	3.5	0.05	-14	7.0	-0.10	2	7.5	-1.00
-37	-8.0	0	-14	10.0	-1.05	2	10.0	-2.30
-37	-5.0	-1.55	-14	13.0	-0.80	2	13.0	-2.55
-37	-2.0	-2.55	-14	15.0	-0.85	2	15.0	-2.15
-37	1.0	-2.45	-10	-23.0	-0.45	6	-25.0	-1.25
-37	4.0	-1.30	-10	-20.0	-2.05	6	-22.0	-1.30
-37	6.7	0.15	-10	-17.0	-3.05	6	-19.0	-0.55
-34	-10.0	0	-10	-14.0	-2.80	6	-16.0	0.15
-34	-7.0	-1.20	-10	-11.0	-1.60	6	-13.0	0.45
-34	-4.0	-2.80	-10	-8.0	-0.81	6	-10.0	0.85
-34	3.0	-2.65	-10	7.3	-1.45	6	-8.5	1.65
-34	6.0	-0.70	-10	10.0	-1.85	6	7.5	0.25
-34	8.0	0.25	-10	13.0	-2.15	6	10.0	-1.00
-30	-9.0	0	-10	15.0	-2.05	6	13.0	-1.00
-30	-6.0	-1.45	-6	-25.0	-0.50	6	15.0	-1.05
-30	4.7	-1.40	-6	-22.0	-1.90	10	-25.0	-2.80
-30	7.0	-0.15	-6	-19.0	-3.25	10	-22.0	-1.65
-30	10.0	0.10	-6	-16.0	-3.75	10	-19.0	-0.50
-26	-13.0	-0.05	-6	-13.0	-3.05	10	-16.0	0.80
-26	-10.0	0.60	-6	-10.0	-1.55	10	-13.0	1.45
-26	-7.0	-0.15	-6	-8.5	-0.80	10	-10.0	2.10
-26	5.5	-0.15	-6	7.5	-1.75	10	-8.5	2.90
-26	8.0	0.50	-6	10.0	-2.55	10	7.0	1.75
-26	11.0	0.15	-6	13.0	-2.95	10	10.0	0.25
-22	-14.5	-0.15	-6	15.0	-2.85	10	13.0	0
-22	-12.0	0.65	-2	-25.0	-0.90	10	15.0	-0.25
-22	-9.0	0.70	-2	-22.0	-1.85	15	-25.0	-3.55
-22	-7.0	0.95	-2	-19.0	-2.70	15	-22.0	-3.05
-22	6.4	0.55	-2	-16.0	-3.20	15	-19.0	-2.50
-22	9.0	0.85	-2	-13.0	-2.85	15	-16.0	-0.85
-22	12.0	0.05	-2	-10.0	-1.35	15	-13.0	0.65
-18	-16.0	-0.40	-2	-8.5	-0.45	15	-10.0	2.10
-18	-13.0	0.35	-2	7.5	-1.60	15	-8.0	2.35
-18	-10.0	1.05	-2	10.0	-2.75	15	6.5	3.00
-18	-7.5	1.65	-2	13.0	-3.25	15	9.0	1.70
-18	7.0	0.90	-2	15.0	-3.15	15	12.0	0.25
-18	10.0	0.95	2	-25.0	-1.10	15	15.0	-0.05
-18	13.0	0.05	2	-22.0	-1.55	20	-25.0	-1.85
-14	-20.0	-0.35	2	-19.0	-1.40	20	-22.0	-2.65
-14	-17.0	-2.05	2	-16.0	-1.40	20	-19.0	-2.40

x(cm)	y(cm)	z(cm)	x(cm)	y(cm)	z(cm)	x(cm)	y(cm)	z(cm)
20	-16.0	-2.15	30	-5.5	2.95	40	-10.0	0.55
20	-13.0	-0.45	30	3.5	1.05	40	-7.0	1.05
20	-10.0	0.90	30	6.0	2.10	40	-4.0	2.40
20	-7.5	1.35	30	9.0	2.75	40	-2.0	3.25
20	6.0	2.25	30	12.0	1.40	40	1.0	1.35
20	9.0	0.85	30	15.0	0.35	40	4.0	0.50
20	12.0	-0.55	35	-25.0	-2.95	40	7.0	0.15
20	15.0	-1.20	35	-22.0	-1.50	40	10.0	0.30
25	-25.0	-0.85	35	-19.0	-0.15	40	13.0	0.70
25	-22.0	-1.00	35	-16.0	1.15	40	15.0	0.85
25	-19.0	-1.30	35	-13.0	1.25	45	-25.0	0.65
25	-16.0	-1.45	35	-10.0	0.85	45	-22.0	0.55
25	-13.0	-0.95	35	-7.0	2.05	45	-19.0	0.05
25	-10.0	0.80	35	-4.0	3.30	45	-16.0	-0.15
25	-7.0	1.25	35	-3.0	3.50	45	-12.5	1.55
25	5.0	3.55	35	0.5	2.40	45	-10.0	0.85
25	8.0	2.30	35	2.0	1.40	45	-7.0	1.00
25	11.0	0.75	35	5.0	1.35	45	-4.0	1.55
25	14.0	0.85	35	8.0	1.15	45	-1.0	0.25
30	-25.0	-0.45	35	11.0	0.60	45	2.0	-0.30
30	-22.0	0.25	35	14.0	0.10	45	5.0	-0.05
30	-19.0	0.95	40	-25.0	-2.25	45	8.0	-0.35
30	-16.0	1.15	40	-22.0	-2.45	45	11.0	-0.75
30	-13.0	0.80	40	-18.0	-1.55	45	14.0	-0.05
30	-10.0	1.00	40	-16.0	0.35	45	15.0	0.30
30	-7.0	2.60	40	-13.0	1.05			

Table C.5: Scour Data for Experimental Run C5
[Elliptical Island I_2 (b/a=0.2), F_r=0.19,h=15cm]

x(cm)	y(cm)	z(cm)	x(cm)	y(cm)	z(cm)	x(cm)	y(cm)	z(cm)
-43	-7.0	0	-26	-5.8	-2.20	-6	-20.0	-1.95
-43	-4.0	-0.40	-26	6.0	-2.10	-6	-17.0	-0.80
-43	-1.0	-1.20	-26	9.0	-1.45	-6	-14.0	-0.10
-43	2.0	-0.90	-26	12.0	-0.20	-6	-11.0	0.70
-43	5.0	0	-26	15.0	0.15	-6	-8.0	2.00
-40	-9.2	0	-22	-17.0	0	-6	8.0	0.20
-40	-6.0	-2.10	-22	-14.0	0.20	-6	11.0	-1.05
-40	-3.0	-2.95	-22	-11.0	-1.00	-6	14.0	-2.80
-40	0	-3.20	-22	-8.0	-1.05	-6	17.0	-3.35
-40	3.0	-2.70	-22	-6.5	-0.70	-6	20.0	-3.40
-40	6.0	-1.75	-22	6.5	-0.70	-2	-20.0	-3.60
-40	9.0	0	-22	10.0	-0.55	-2	-17.0	-3.15
-36.5	-12.0	-0.05	-22	13.0	0.30	-2	-14.0	-1.95
-36.5	-9.0	-2.10	-22	16.0	0	-2	-11.0	-0.50
-36.5	-6.0	-3.55	-18	-16.0	0.20	-2	-8.0	0.25
-36.5	-3.0	-4.10	-18	-13.0	-0.30	-2	8.0	-0.30
-36.5	1.0	-4.67	-18	-10.0	-1.20	-2	11.0	-1.30
-36.5	4.0	-3.75	-18	-7.0	0.30	-2	14.0	-3.00
-36.5	7.0	-2.30	-18	7.5	0.10	-2	17.0	-3.70
-36.5	10.0	-2.20	-18	10.0	0	-2	20.0	-3.75
-36.5	12.3	0.15	-18	13.0	0.25	2	-20.0	-4.27
-33	-14.0	-0.20	-18	16.0	0.05	2	-17.0	-4.30
-33	-11.0	-1.65	-18	17.5	-0.20	2	-14.0	-2.95
-33	-8.0	-3.40	-14	-19.5	0.20	2	-11.0	-1.70
-33	-5.0	-4.50	-14	-16.0	0.30	2	-8.0	-0.60
-33	-3.5	-4.46	-14	-13.0	-0.10	2	8.0	-0.50
-33	4.0	-4.33	-14	-9.0	0.55	2	11.0	-1.55
-33	7.0	-3.20	-14	-7.5	1.10	2	14.0	-3.05
-33	10.0	-1.40	-14	8.0	0.80	2	17.0	-3.40
-33	13.5	0.15	-14	11.0	0.10	2	20.0	-3.30
-30	-15.5	-0.15	-14	14.0	0.15	6	-20.0	-4.34
-30	-12.0	-1.10	-14	17.0	-0.40	6	-17.0	-4.30
-30	-9.0	-2.95	-14	20.0	-1.10	6	-14.0	-4.00
-30	-6.0	-4.00	-10	-20.0	-0.50	6	-11.0	-2.15
-30	-5.0	-4.05	-10	-17.0	-0.05	6	-8.0	-1.25
-30	5.0	-3.65	-10	-14.0	0.10	6	7.5	-0.80
-30	8.0	-2.60	-10	-11.0	0.40	6	10.0	-1.50
-30	11.0	-0.85	-10	-8.0	1.60	6	13.0	-2.70
-30	14.0	0.10	-10	7.8	1.30	6	16.0	-3.05
-26	-16.5	-0.10	-10	11.0	-0.20	6	19.0	-2.40
-26	-13.0	-0.50	-10	14.0	-1.75	6	20.0	-2.40
-26	-10.0	-1.80	-10	17.0	-2.20	10	-20.0	-4.25
-26	-7.0	-2.40	-10	20.0	-2.50	10	-17.0	-4.55

x(cm)	y(cm)	z(cm)	x(cm)	y(cm)	z(cm)	x(cm)	y(cm)	z(cm)
10	-14.0	-4.20	22	-8.0	0.10	35	-14.0	-0.70
10	-11.0	-2.70	22	-7.0	0.75	35	-11.0	0.20
10	-8.0	-1.40	22	6.5	1.45	35	-8.0	1.25
10	7.5	-0.40	22	9.0	0.25	35	-5.0	3.00
10	10.0	-1.90	22	12.0	-1.25	35	-3.0	4.15
10	13.0	-3.15	22	15.0	-2.30	35	1.0	4.50
10	16.0	-2.90	22	18.0	-2.60	35	4.0	4.50
10	19.0	-1.60	22	20.0	-1.50	35	7.0	3.25
10	20.0	-1.55	26	-20.0	-0.40	35	10.0	2.00
14	-20.0	-3.55	26	-17.0	0.45	35	13.0	0.55
14	-17.0	-3.90	26	-14.0	0.65	35	16.0	-0.90
14	-14.0	-3.95	26	-11.0	0.45	35	19.0	-0.90
14	-11.0	-3.30	26	-8.0	1.05	35	20.0	-1.20
14	-8.0	-1.35	26	-6.0	2.15	40	-20.0	-2.75
14	7.5	-0.50	26	5.4	2.55	40	-15.0	-0.85
14	10.0	-0.85	26	8.0	1.00	40	-10.0	0.70
14	13.0	-2.05	26	11.0	-0.20	40	-5.0	2.90
14	16.0	-1.90	26	14.0	-1.30	40	-1.5	4.30
14	19.0	-1.45	26	17.0	-1.70	40	1.0	2.85
14	20.0	-1.10	26	20.0	-1.10	40	4.5	3.00
18	-20.0	-3.85	30	-20.0	-2.05	40	7.0	2.40
18	-17.0	-3.70	30	-17.0	-1.00	40	10.0	2.00
18	-14.0	-2.80	30	-14.0	-0.05	40	15.0	-0.20
18	-11.0	-2.40	30	-11.0	0.90	40	20.0	0.60
18	-8.0	-0.80	30	-8.0	1.75	45	-20.0	-1.20
18	7.0	0	30	-5.0	3.40	45	-15.0	-0.30
18	10.0	-1.35	30	4.5	3.05	45	-10.0	1.50
18	13.0	-2.50	30	7.0	2.90	45	-5.0	2.15
18	16.0	-2.85	30	10.0	1.55	45	-2.5	3.80
18	19.0	-2.35	30	13.0	0.70	45	3.0	1.90
18	20.0	-1.95	30	16.0	0.10	45	6.0	1.60
22	-20.0	-2.15	30	19.0	-1.50	45	10.0	0.75
22	-17.0	-1.45	30	20.0	-2.15	45	14.0	0.10
22	-14.0	-1.00	35	-20.0	-2.55	45	20.0	2.10
22	-11.0	-0.85	35	-17.0	-1.60			

Table C.6: Scour Data for Experimental Run C6
[Elliptical Island I_2 (b/a=0.2), F_r=0.2,h=15cm]

x(cm)	y(cm)	z(cm)	x(cm)	y(cm)	z(cm)	x(cm)	y(cm)	z(cm)
-43	-7.0	0	-26	-13.0	-0.65	-10	17.0	-2.86
-43	-4.0	-0.52	-26	-10.0	-2.34	-10	20.0	-3.25
-43	-1.0	-1.56	-26	-7.0	-3.12	-6	-20.0	-2.53
-43	2.0	-1.17	-26	-5.8	-2.86	-6	-17.0	-1.04
-43	5.0	0	-26	6.0	-2.73	-6	-14.0	-0.13
-40	-9.2	0	-26	9.0	-1.88	-6	-11.0	0.91
-40	-6.0	-2.73	-26	12.0	-0.26	-6	-8.0	2.60
-40	-3.0	-3.83	-26	15.0	0.20	-6	8.0	0.26
-40	0	-4.16	-22	-14.0	0.26	-6	11.0	-1.37
-40	3.0	-3.51	-22	-11.0	-1.30	-6	14.0	-3.64
-40	6.0	-2.28	-22	-8.0	-1.36	-6	17.0	-4.35
-40	9.0	0	-22	-6.5	-0.91	-6	20.0	-4.42
-36.5	-12.0	-0.06	-22	6.5	-0.91	-2	-20.0	-4.68
-36.5	-9.0	-2.73	-22	10.0	-0.20	-2	-17.0	-4.09
-36.5	-6.0	-4.62	-22	13.0	0.39	-2	-14.0	-2.54
-36.5	-3.0	-6.63	-22	16.0	0	-2	-11.0	-0.65
-36.5	1.0	-6.82	-18	-16.0	0.26	-2	-8.0	0.32
-36.5	4.0	-4.88	-18	-13.0	-0.39	-2	8.0	-0.39
-36.5	7.0	-2.99	-18	-10.0	-1.56	-2	11.0	-1.69
-36.5	10.0	-2.86	-18	-7.0	0.39	-2	14.0	-3.90
-36.5	12.3	0.20	-18	7.5	0.13	-2	17.0	-4.81
-33	-16.0	-0.13	-18	10.0	0	-2	20.0	-4.88
-33	-14.0	-0.26	-18	13.0	0.32	2	-20.0	-6.11
-33	-11.0	-2.14	-18	16.0	0.07	2	-17.0	-5.59
-33	-8.0	-4.42	-18	17.5	-0.26	2	-14.0	-3.83
-33	-5.0	-6.50	-14	-19.5	0.26	2	-11.0	-2.21
-33	-3.5	-6.37	-14	-16.0	0.39	2	-8.0	-0.78
-33	4.0	-6.30	-14	-13.0	-0.13	2	8.0	-0.65
-33	7.0	-4.16	-14	-9.0	0.71	2	11.0	-2.02
-33	10.0	-1.82	-14	-7.5	1.43	2	14.0	-3.96
-33	13.5	0.20	-14	8.0	1.04	2	17.0	-4.42
-30	-15.5	-0.19	-14	11.0	0.13	2	20.0	-4.29
-30	-12.0	-1.43	-14	14.0	0.20	6	-20.0	-6.37
-30	-9.0	-3.84	-14	17.0	-0.52	6	-17.0	-6.37
-30	-6.0	-5.20	-14	20.0	-1.43	6	-14.0	-5.20
-30	-5.0	-5.26	-10	-20.0	-0.65	6	-11.0	-2.80
-30	5.0	-4.75	-10	-17.0	-0.06	6	-8.0	-1.62
-30	8.0	-3.38	-10	-14.0	0.13	6	7.5	-1.04
-30	11.0	-1.10	-10	-11.0	0.52	6	10.0	-1.95
-30	14.0	0.13	-10	-8.0	2.08	6	13.0	-3.51
-30	17.0	0.26	-10	7.8	1.69	6	16.0	-3.97
-26	-19.0	0.13	-10	11.0	-0.26	6	19.0	-3.12
-26	-16.5	-0.13	-10	14.0	-2.80	6	20.0	-3.12

x(cm)	y(cm)	z(cm)	x(cm)	y(cm)	z(cm)	x(cm)	y(cm)	z(cm)
10	-20.0	-5.52	22	-11.0	-1.10	35	-14.0	-0.91
10	-17.0	-5.92	22	-8.0	0.13	35	-11.0	0.26
10	-14.0	-5.46	22	-7.0	0.98	35	-8.0	1.62
10	-11.0	-3.51	22	6.5	1.88	35	-5.0	3.90
10	-8.0	-1.82	22	9.0	0.33	35	-3.0	5.40
10	7.5	-0.52	22	12.0	-1.62	35	1.0	5.85
10	10.0	-2.47	22	15.0	-3.00	35	4.0	5.85
10	13.0	-4.09	22	18.0	-3.38	35	7.0	4.22
10	16.0	-3.77	22	20.0	-1.95	35	10.0	2.60
10	19.0	-2.08	26	-20.0	-0.52	35	13.0	0.71
10	20.0	-2.02	26	-17.0	0.58	35	16.0	-1.17
14	-20.0	-4.61	26	-14.0	0.85	35	19.0	-1.17
14	-17.0	-5.07	26	-11.0	0.58	35	20.0	-1.56
14	-14.0	-5.14	26	-8.0	1.37	40	-20.0	-3.57
14	-11.0	-4.29	26	-6.0	2.80	40	-15.0	-1.10
14	-8.0	-1.75	26	5.4	3.31	40	-10.0	0.91
14	7.5	-0.65	26	8.0	1.30	40	-5.0	3.77
14	10.0	-1.10	26	11.0	-0.26	40	-1.5	5.59
14	13.0	-2.67	26	14.0	-1.69	40	1.0	3.71
14	16.0	-2.47	26	17.0	-2.21	40	4.5	3.90
14	19.0	-1.88	26	20.0	-1.43	40	7.0	3.12
14	20.0	-1.43	30	-20.0	-2.66	40	10.0	2.60
18	-20.0	-5.00	30	-17.0	-1.30	40	15.0	-0.26
18	-17.0	-4.81	30	-14.0	-0.06	40	20.0	0.78
18	-14.0	-3.64	30	-11.0	1.17	45	-20.0	-1.56
18	-11.0	-3.12	30	-8.0	2.28	45	-15.0	-0.39
18	-8.0	-1.04	30	-5.0	4.42	45	-10.0	1.95
18	7.0	0	30	4.5	3.96	45	-5.0	2.80
18	10.0	-1.76	30	7.0	3.77	45	-2.5	4.94
18	13.0	-3.25	30	10.0	2.02	45	3.0	2.47
18	16.0	-3.70	30	13.0	0.91	45	6.0	2.08
18	19.0	-3.05	30	16.0	0.13	45	10.0	0.97
18	20.0	-2.54	30	19.0	-1.95	45	14.0	0.13
22	-20.0	-2.80	30	20.0	-2.80	45	20.0	2.73
22	-17.0	-1.88	35	-20.0	-3.31			
22	-14.0	-1.30	35	-17.0	-2.08			

Table C.7: Scour Data for Experimental Run C7
[Elliptical Island I_3 (b/a=0.3), F_r=0.16,h=15cm]

x(cm)	y(cm)	z(cm)	x(cm)	y(cm)	z(cm)	x(cm)	y(cm)	z(cm)
-35	-5.0	0	-13	17.0	-0.40	15	12.0	-0.70
-35	-2.0	-0.30	-13	20.0	-0.10	15	15.0	-1.00
-35	0	-1.42	-10	-17	-0.20	15	18.0	-2.85
-35	2.0	-1.10	-10	-14	0.25	15	21.0	-3.15
-35	5.0	-0.60	-10	-11	0.60	20	-20.0	0.15
-35	7.0	0	-10	10.5	0.45	20	-17.0	0.40
-32	-6.5	-0.20	-10	13.0	0.50	20	-14.0	0.60
-32	-3.0	-1.53	-10	16.0	-0.35	20	-11.0	0.05
-32	0	-2.15	-10	19.0	-1.50	20	-8.0	0.75
-32	3.0	-1.06	-10	20.8	-0.30	20	8.0	1.95
-32	6.0	-0.80	-5	-17.5	-2.45	20	11.0	0.50
-32	8.0	0	-5	-14	-1.32	20	14.0	0.05
-30	-9.3	0	-5	-11	-0.80	20	17.0	-0.35
-30	-7.0	-1.30	-5	11.0	-0.60	20	20.0	0.45
-30	-4.0	-1.85	-5	14.0	-1.55	25	-20.0	0.60
-30	-1.0	-3.05	-5	17.0	-2.85	25	-17.0	1.05
-30	3.0	-1.55	-5	20.0	-3.00	25	-14.0	2.15
-30	6.0	-0.70	0	-20	-3.80	25	-11.0	1.70
-30	8.0	0.20	0	-18	-3.15	25	-8.0	2.05
-25	-12	0	0	-15	-2.92	25	-6.5	2.50
-25	-9	-1.65	0	-12	-1.25	25	6.0	4.10
-25	-6.5	-2.15	0	11.5	-1.75	25	8.0	3.30
-25	6.5	-2.40	0	15.0	-3.60	25	11.0	2.80
-25	9.0	-2.20	0	18.0	-4.05	25	14.0	1.30
-25	12.0	-0.60	0	21.0	-3.85	25	17.0	1.60
-25	13.0	0	5	-20.0	-0.20	25	20.0	1.00
-22	-15.0	-0.20	5	-17.6	-0.35	30	-20.0	-0.05
-22	-14.0	-0.45	5	-15.0	-1.35	30	-17.0	-0.15
-22	-11.0	-1.12	5	-12.0	-2.00	30	-14.0	0.15
-22	-7.5	-2.35	5	-10.0	-2.05	30	-11.0	0.35
-22	7.5	-2.55	5	11.0	-2.00	30	-8.0	0.35
-22	10.0	-1.60	5	14.0	-3.30	30	-4.0	0.60
-22	13.0	-0.30	5	17.0	-3.00	30	2.3	1.30
-22	14.0	-0.10	5	20.0	-2.70	30	5.0	2.20
-17	-16	0	10	-20.0	-0.35	30	8.0	2.20
-17	-15	-0.30	10	-17.0	-1.50	30	12.0	2.35
-17	-12	-0.65	10	-14.0	-2.40	30	16.0	1.05
-17	-9	-1.20	10	-11.0	-2.45	30	19.0	-0.30
-17	9	-1.00	10	-9.5	-1.90	35	-20.0	-1.15
-17	12	-0.55	10	10.5	-0.85	35	-15.0	-0.05
-17	15.5	-0.20	10	13.0	-1.10	35	-10.0	-0.05
-17	19	-0.10	10	16.0	-0.95	35	-5.0	0.80
-13	-17	-0.45	10	19.0	-1.95	35	0.0	0.50
-13	-14	-0.20	15	-20.0	-0.10	35	6.0	2.05
-13	-12	-0.50	15	-17.0	-0.60	35	10.0	0.60
-13	-10	-0.35	15	-14.0	-1.20	35	15.0	-0.25
-13	10.0	0	15	-11.0	-1.60	35	20.0	-0.70
-13	12.0	0.35	15	-9.0	-0.95			
-13	15.0	-0.10	15	9.5	0.90			

Table C.8: Scour Data for Experimental Run C8
[Elliptical Island I_3 (b/a=0.3), F_r=0.19,h=15cm]

x(cm)	y(cm)	z(cm)	x(cm)	y(cm)	z(cm)	x(cm)	y(cm)	z(cm)
-35	-8.5	0	-20	-8.0	-2.34	5	-20.0	-1.92
-35	-5.0	-1.17	-20	8.5	-1.98	5	-17.0	-1.89
-35	1.0	-0.45	-20	12.0	-1.98	5	-14.0	-2.34
-35	5.0	-1.32	-20	15.0	-1.26	5	-11.0	-2.10
-35	8.0	-0.72	-20	18.0	-1.20	5	-9.7	-1.86
-35	9.4	0	-20	20.0	-1.62	5	11.2	0.06
-32	-17.5	-0.12	-15	-20.0	-0.75	5	14.0	-1.02
-32	-15.0	-0.66	-15	-17.0	-1.62	5	17.0	-1.68
-32	-12.0	-0.54	-15	-14.0	-1.65	5	20.0	-2.31
-32	-9.0	-1.14	-15	-11.0	-2.13	10	-20.0	-1.89
-32	-6.0	-1.92	-15	-9.0	-2.04	10	-17.0	-1.44
-32	-3.0	-1.68	-15	9.5	-2.04	10	-14.0	-1.71
-32	0	-2.61	-15	12.0	-2.34	10	-11.0	-1.59
-32	3.0	-2.70	-15	15.0	-1.71	10	-9.5	-1.56
-32	6.0	-1.98	-15	17.0	-1.62	10	10.5	-0.39
-32	9.0	-1.26	-15	20.0	-2.04	10	13.0	-1.17
-32	12.5	0	-10	-20.0	-1.41	10	16.0	-2.01
-30	-19.0	-0.15	-10	-17.0	-1.68	10	19.0	-2.79
-30	-16.0	-1.44	-10	-14.0	-2.04	10	20.0	-2.82
-30	-13.0	-0.99	-10	-11.0	-2.40	15	-20.0	-2.46
-30	-10.0	-1.26	-10	-9.5	-1.98	15	-17.0	-1.68
-30	-7.0	-1.98	-10	10.5	-2.46	15	-14.0	-1.89
-30	-4.0	-2.70	-10	13.0	0.69	15	-11.0	-1.86
-30	3.0	-3.42	-10	16.0	-3.29	15	-9.0	-1.44
-30	6.0	-2.28	-10	19.0	-1.89	15	9.5	-1.8
-30	9.0	-1.44	-10	20.0	-1.62	15	12.0	-1.8
-30	12.0	-0.84	-5	-20.0	-2.52	15	15.0	-2.73
-30	14.0	0	-5	-17.0	-4.92	15	17.0	-3.18
-25	-20.0	-0.84	-5	-14.0	-3.09	15	20.0	-3.06
-25	-17.0	-1.68	-5	-11.0	-2.76	20	-20.0	-1.89
-25	-14.0	-1.32	-5	11.3	-1.95	20	-17.0	-0.84
-25	-11.0	-1.74	-5	14.0	-2.25	20	-14.0	-0.99
-25	-8.0	-1.86	-5	17.0	-2.19	20	-11.0	-0.87
-25	-6.5	-1.86	-5	20.0	-1.80	20	-8.0	-0.06
-25	6.5	-2.19	0	-20.0	-2.61	20	8.1	-2.85
-25	9.0	-1.98	0	-17.0	-2.88	20	11.0	-2.82
-25	12.0	-1.32	0	-14.0	-3.00	20	14.0	-2.64
-25	15.0	-0.81	0	-11.0	-2.70	20	17.0	-2.16
-25	18.0	0	0	-10.0	-2.22	20	20.0	-1.44
-20	-20.0	-0.9	0	11.0	-0.84	25	-20.0	-1.83
-20	-17.0	-1.71	0	14.0	-1.02	25	-17.0	-1.35
-20	-14.0	-1.29	0	17.0	-1.05	25	-14.0	-0.33
-20	-11.0	-1.95	0	20.0	-1.35	25	-11.0	0.18

x(cm)	y(cm)	z(cm)	x(cm)	y(cm)	z(cm)	x(cm)	y(cm)	z(cm)
25	-8.0	0	30	-2.6	1.32	35	7.0	-0.03
25	-6.5	0.30	30	2.0	0.36	35	10.0	0
25	6.0	-1.89	30	5.0	0	35	15.0	0.57
25	9.0	-1.23	30	8.0	0.21	35	20.0	1.17
25	12.0	-1.02	30	11.0	0.09	40	-20.0	-0.93
25	15.0	-0.54	30	14.0	0.15	40	-15.0	-0.27
25	18.0	0.12	30	17.0	0.48	40	-10.0	0.12
25	20.0	0.39	30	20.0	0.90	40	-5.0	0.39
30	-20.0	-1.44	35	-20.0	-0.63	40	0	1.65
30	-17.0	-1.17	35	-15.0	-0.66	40	5.0	0.87
30	-14.0	-0.45	35	-10.0	-0.45	40	10.0	0.99
30	-11.0	-0.42	35	-5.0	0.69	40	15.0	1.50
30	-8.0	0	35	-0.5	1.89	40	20.0	1.92
30	-5.0	0.87	35	3.0	0.75			

Table C.9: Scour Data for Experimental Run C9
[Elliptical Island I_4 (b=15cm,b/a=0.4), F_r=0.16,h=15cm]

x(cm)	y(cm)	z(cm)	x(cm)	y(cm)	z(cm)	x(cm)	y(cm)	z(cm)
-24	-6.5	0	-11	7.2	-2.40	7	19.5	-1.02
-24	-3.5	-0.84	-11	9.5	-1.56	12	-19.5	-1.44
-24	-0.5	-1.44	-11	11.5	-0.30	12	-16.5	-2.40
-24	2.5	-1.56	-11	14.5	-0.78	12	-13.5	-2.82
-24	5.5	-0.42	-11	17.5	-1.02	12	-10.5	-1.68
-24	8.5	0	-11	19.5	-0.12	12	-7.5	1.26
-22	-8.5	0	-8	-14.5	-0.30	12	6.3	2.76
-22	-6.5	-0.42	-8	-12.7	-0.42	12	8.5	1.14
-22	-3.5	-2.28	-8	-10.5	-0.06	12	11.5	-0.36
-22	-0.5	-3.42	-8	-8.5	-0.96	12	14.5	-0.24
-22	2.5	-3.12	-8	7.8	-1.68	12	17.5	-1.08
-22	5.5	-1.80	-8	9.5	-1.44	12	20.5	-2.70
-22	8.5	-1.02	-8	12.0	-0.24	17	-19.5	-0.06
-22	11.5	0	-8	14.5	-1.26	17	-16.5	0.24
-20	-10.5	-0.18	-8	17.5	-2.88	17	-13.5	0.48
-20	-8.5	-0.18	-8	19.5	-1.92	17	-10.5	0.30
-20	-6.5	-1.26	-3	-17.5	-0.24	17	-7.5	0.78
-20	-3.5	-3.66	-3	-14.5	-0.54	17	-4.5	3.00
-20	-0.5	-4.56	-3	-13.5	-0.78	17	3.5	4.74
-20	2.5	-4.50	-3	-11.6	0.36	17	6.5	1.68
-20	5.5	-2.82	-3	-8.5	0.24	17	9.5	-0.12
-20	8.5	-1.44	-3	8.5	-0.24	17	12.5	0.06
-20	11.5	-0.06	-3	10.5	-1.08	17	15.5	-2.40
-17	-10.5	-0.18	-3	13.5	-2.46	17	18.5	-3.36
-17	-8.5	-0.60	-3	16.5	-3.78	22	-19.5	-0.12
-17	-5.5	-3.24	-3	18.5	-4.02	22	-15.5	0.36
-17	-3.8	-3.60	2	-19.5	-0.72	22	-11.5	0.78
-17	5.0	-4.14	2	-16.5	-1.98	22	-7.5	1.74
-17	6.5	-3.24	2	-13.5	-1.68	22	-3.5	1.92
-17	8.5	-1.14	2	-10.5	0.36	22	-1.0	2.52
-17	11.5	-0.66	2	-8.5	1.32	22	2.5	1.50
-17	14.5	0	2	8.3	-0.36	22	5.8	2.58
-14	-11.5	-0.36	2	11.5	-2.70	22	8.5	1.08
-14	-9.5	-0.42	2	14.5	-4.14	22	11.5	1.32
-14	-7.5	-1.86	2	17.5	-2.76	22	14.5	0.90
-14	-5.5	-2.64	2	20.5	-2.46	22	18.5	-1.20
-14	6.5	-3.42	7	-19.5	-2.34	27	-19.5	-0.12
-14	8.5	-2.04	7	-16.5	-3.36	27	-15.5	0.60
-14	10.5	-0.66	7	-13.5	-2.82	27	-11.5	1.20
-14	13.5	-0.24	7	-10.5	-0.96	27	-7.5	1.62
-14	16.5	0	7	-8.0	0.84	27	-3.5	1.32
-11	-13.5	-0.30	7	8.0	0.36	27	0.5	0.90
-11	-10.5	-0.30	7	10.5	-1.56	27	1.4	0.48
-11	-8.5	-1.20	7	13.5	-1.80	27	3.5	0.84
-11	-7.0	-1.74	7	16.5	-0.60	27	7.5	0.84

x(cm)	y(cm)	z(cm)	x(cm)	y(cm)	z(cm)	x(cm)	y(cm)	z(cm)
27	11.5	1.32	32	15.5	0.60	37	21.5	-3.12
27	13.5	1.38	32	19.5	-0.24	42	-19.5	-2.04
27	16.5	0.18	37	-19.5	-2.40	42	-15.5	0.54
27	20.5	-0.90	37	-15.5	-0.30	42	-9.5	0.72
32	-19.5	-0.72	37	-11.5	0.96	42	-5.0	0.36
32	-15.5	0.24	37	-7.5	0.72	42	-2.5	-1.32
32	-11.5	1.44	37	-5.0	0.42	42	2.5	-0.78
32	-7.5	1.44	37	-1.5	-1.38	42	6.5	-0.48
32	-3.5	0.84	37	2.5	-1.08	42	9.5	0.66
32	-0.5	-0.36	37	6.5	-0.42	42	12.5	0.84
32	3.5	0.36	37	9.0	1.08	42	15.5	-0.48
32	7.5	0.96	37	13.5	1.26	42	18.5	-0.66
32	11.5	1.56	37	17.5	-0.78			

Table C.10: Scour Data for Experimental Run C10
[Elliptical Island I_4 (b/a=0.4), F_r=0.19,h=15cm]

x(cm)	y(cm)	z(cm)	x(cm)	y(cm)	z(cm)	x(cm)	y(cm)	z(cm)
-25	-10.0	0	-4	-15.0	0	16	-8.0	-0.05
-25	-5.0	0	-4	-12.0	-0.30	16	-5.0	1.35
-25	0	0	-4	-9.0	-1.20	16	5.5	1.55
-25	5.0	0	-4	8.4	-0.90	16	8.0	0.55
-25	10.0	0	-4	11.0	-1.15	16	11.0	-0.65
-23	-10.0	0	-4	14.0	-2.30	16	14.0	-1.95
-23	-6.6	-0.30	-4	17.0	-3.30	16	17.0	-3.35
-23	-4.0	-1.45	-4	20.0	-1.50	16	20.0	-4.60
-23	-1.0	-1.55	0	-19.0	-0.05	20	-20.0	-2.65
-23	2.0	-1.45	0	-16.0	0.15	20	-16.0	-3.00
-23	5.0	-0.25	0	-13.0	0.35	20	-12.0	-1.80
-23	8.0	0	0	-10.0	-0.45	20	-8.0	0
-20	-11.0	-1.35	0	-8.4	-0.60	20	-4.0	1.90
-20	-8.0	-1.80	0	8.8	-1.10	20	0	4.25
-20	-5.0	-2.90	0	11.0	-2.35	20	4.0	1.85
-20	-2.0	-3.40	0	14.0	-4.00	20	8.0	0.80
-20	1.0	-3.10	0	17.0	-4.15	20	12.0	-1.00
-20	4.0	-2.25	0	20.0	-2.70	20	16.0	-2.65
-20	7.0	-1.20	4	-17.0	-0.05	20	20.0	-2.80
-20	10.0	0	4	-14.0	0.90	24	-20.0	-1.30
-17	-13.0	0	4	-11.0	0.35	24	-16.0	-1.85
-17	-10.0	-2.35	4	-8.0	0.20	24	-12.0	-1.45
-17	-7.0	-3.90	4	8.3	-1.85	24	-8.0	0.50
-17	-4.0	-5.15	4	11.0	-2.65	24	-4.0	3.60
-17	4.5	-3.75	4	14.0	-3.35	24	0	4.05
-17	7.0	-2.85	4	17.0	-2.65	24	4.0	4.10
-17	10.0	-0.90	4	20.0	-2.15	24	8.0	1.70
-17	13.0	0.15	8	-20.0	-0.45	24	12.0	0.45
-14	-14.8	0	8	-17.0	-0.90	24	16.0	0.85
-14	-12.0	-1.10	8	-14.0	0.75	24	20.0	1.05
-14	-9.0	-2.65	8	-11.0	0.65	28	-20.0	0.15
-14	-6.0	-3.50	8	-9.0	0.85	28	-16.0	-0.35
-14	6.2	-2.80	8	-7.2	1.10	28	-12.0	-0.90
-14	9.0	-1.15	8	8.3	0.35	28	-8.0	0.55
-14	12.0	-0.40	8	11.0	-2.50	28	-4.0	1.75
-14	15.0	0.20	8	14.0	-1.20	28	0	3.45
-11	-16.0	0	8	17.0	-1.15	28	4.0	4.00
-11	-13.0	-0.60	8	20.0	-1.75	28	8.0	2.00
-11	-10.0	-1.30	12	-20.0	-1.95	28	12.0	1.90
-11	-7.0	-2.30	12	-17.0	-2.00	28	16.0	2.80
-11	7.0	-1.85	12	-14.0	-1.10	28	20.0	2.95
-11	10.0	-0.95	12	-11.0	-0.25	32	-20.0	1.00
-11	13.0	-0.50	12	-8.0	0.65	32	-16.0	0.65
-11	16.0	0.15	12	6.6	-0.30	32	-12.0	-0.15
-8	-17.0	0	12	9.0	-0.70	32	-8.0	0.30
-8	-14.0	-0.25	12	12.0	-0.20	32	-4.0	0.15
-8	-11.0	-0.75	12	15.0	-0.75	32	0	2.25
-8	-8.0	-1.85	12	15.0	-2.00	32	4.0	4.20
-8	7.8	-1.40	12	20.0	-2.55	32	8.0	2.60
-8	10.0	-0.90	16	-20.0	-2.75	32	12.0	3.35
-8	13.0	-0.70	16	-17.0	-2.90	32	16.0	1.55
-8	16.0	-1.85	16	-14.0	-2.20	32	20.0	1.05
-8	19.0	0.10	16	-11.0	-1.05			

Table C.11: Scour Data for Experimental Run C11
[Elliptical Island I_4 (b/a=0.4), F_r=0.2,h=15cm]

x(cm)	y(cm)	z(cm)	x(cm)	y(cm)	z(cm)	x(cm)	y(cm)	z(cm)
-33	-6.5	-0.05	-21	-7.5	-6.40	-6	8.2	-3.95
-33	-4.5	-0.55	-21	-4.5	-7.50	-6	10.5	-3.85
-33	-2.5	-1.55	-21	-1.5	-8.50	-6	13.5	-3.20
-33	-0.5	-1.25	-21	1.5	-8.45	-6	16.5	-2.45
-33	1.5	-1.00	-21	4.5	-7.50	-6	19.5	-0.65
-33	3.5	-0.40	-21	7.5	-6.25	-2	-19.5	-1.30
-33	5.5	-0.15	-21	10.5	-4.70	-2	-16.5	-2.90
-33	7.5	0	-21	13.5	-3.25	-2	-13.5	-3.25
-30	-12.0	-0.05	-21	16.5	-2.15	-2	-10.5	-3.60
-30	-10.5	-0.80	-21	19.5	-0.15	-2	-8.5	-3.35
-30	-8.5	-1.70	-18	-19.5	-1.80	-2	8.5	-2.25
-30	-6.5	-2.40	-18	-16.5	-3.30	-2	11.5	-2.30
-30	-3.5	-3.00	-18	-13.5	-4.45	-2	14.5	-2.10
-30	-0.5	-3.25	-18	-10.5	-2.65	-2	17.5	-1.70
-30	2.5	-3.10	-18	-7.5	-7.90	-2	20.5	-0.10
-30	5.5	-2.50	-18	-4.5	-7.95	2	-19.5	-1.00
-30	8.5	-1.50	-18	4.3	-7.85	2	-16.5	-2.30
-30	11.5	-0.25	-18	6.5	-7.80	2	-13.5	-2.30
-30	14.5	0	-18	9.5	-6.10	2	-10.5	-2.30
-27	-15.5	-0.10	-18	12.5	-4.30	2	-8.5	-1.90
-27	-12.5	-1.95	-18	15.5	-2.65	2	8.3	-0.75
-27	-9.5	-3.25	-18	18.5	-1.85	2	10.5	-1.10
-27	-6.5	-4.00	-14	-19.5	-2.45	2	13.5	-1.20
-27	-3.5	-4.70	-14	-16.5	-3.35	2	16.5	-1.40
-27	-0.5	-4.95	-14	-13.5	-5.30	2	19.5	-0.80
-27	2.5	-4.65	-14	-10.5	-6.95	7	-19.5	-0.60
-27	5.5	-4.05	-14	-7.5	-7.50	7	-16.5	-1.75
-27	8.5	-3.25	-14	-6.0	-7.05	7	-13.5	-1.50
-27	11.5	-2.25	-14	6.4	-6.75	7	-10.5	-1.30
-27	14.5	-0.45	-14	9.5	-6.50	7	-8.0	-0.30
-27	16.5	0	-14	12.5	-4.10	7	7.5	1.10
-24	-19.5	-0.10	-14	15.5	-3.10	7	10.5	0.30
-24	-17.5	-0.65	-14	18.5	-1.75	7	13.5	-0.25
-24	-14.5	-2.50	-10	-19.5	-1.95	7	16.5	-0.95
-24	-11.5	-3.70	-10	-16.5	-3.55	7	19.5	-0.75
-24	-8.5	-4.60	-10	-13.5	-5.15	12	-19.5	-0.25
-24	-5.5	-5.75	-10	-10.5	-6.10	12	-16.5	-1.35
-24	-2.5	-6.50	-10	-9.5	-6.30	12	-13.5	-1.10
-24	0.5	-6.65	-10	-7.5	-6.20	12	-10.5	-0.45
-24	3.5	-6.10	-10	7.8	-5.40	12	-6.8	0.75
-24	6.5	-5.30	-10	10.5	-5.10	12	6.0	2.90
-24	9.5	-3.90	-10	13.5	-4.15	12	7.5	2.00
-24	12.5	-2.90	-10	16.5	-2.65	12	10.5	1.20
-24	15.5	-1.40	-10	19.5	-1.05	12	13.5	0.20
-24	18.5	0	-6	-19.5	-1.60	12	16.5	-0.55
-21	-19.5	-0.90	-6	-16.5	-3.45	12	19.5	-1.20
-21	-16.5	-2.75	-6	-13.5	-4.40	17	-19.5	0.25
-21	-13.5	-3.85	-6	-10.5	-5.00	17	-16.5	-1.00
-21	-10.5	-5.05	-6	-8.5	-4.90	17	-13.5	-1.15

x(cm)	y(cm)	z(cm)	x(cm)	y(cm)	z(cm)	x(cm)	y(cm)	z(cm)
17	-10.5	-0.40	22	16.5	-1.70	32	-1.5	0.60
17	-7.5	0.60	22	19.5	-1.70	32	1.5	1.00
17	-4.5	0.70	27	-19.5	0.20	32	4.5	1.20
17	3.9	2.10	27	-16.5	-0.40	32	7.5	0.80
17	5.5	2.10	27	-13.5	-1.15	32	10.5	0.10
17	8.5	1.90	27	-10.5	-1.00	32	13.5	0.20
17	11.5	0.80	27	-7.5	-0.25	32	16.5	0.20
17	14.5	-0.90	27	-4.5	0.35	32	19.5	0.30
17	17.5	-1.85	27	-1.5	0.85	37	-19.5	0.90
17	20.5	-2.15	27	1.5	1.45	37	-16.5	0.90
22	-19.5	0.30	27	4.5	0.80	37	-13.5	0.75
22	-16.5	-0.65	27	7.5	0.45	37	-10.5	0.65
22	-13.5	-1.10	27	10.5	-0.35	37	-7.5	0.70
22	-10.5	-0.70	27	13.5	-1.10	37	-4.5	0.50
22	-7.5	0.25	27	16.5	-1.10	37	-1.5	0.80
22	-4.5	0.25	27	19.5	-0.80	37	1.5	0.10
22	-1.5	1.15	32	-19.5	0.60	37	4.5	0.65
22	1.5	2.00	32	-16.5	-0.70	37	7.5	-0.35
22	4.5	1.10	32	-13.5	-0.50	37	10.5	-0.10
22	7.5	1.00	32	-10.5	-0.10	37	13.5	-0.20
22	10.5	0.90	32	-7.5	0.30	37	16.5	0.65
22	13.5	-1.25	32	-4.5	0.50	37	19.5	1.60

Table C.12: Scour Data for Experimental Run C12
[Elliptical Island I_5 (b/a=0.6), F_r=0.16,h=15cm]

x(cm)	y(cm)	z(cm)	x(cm)	y(cm)	z(cm)	x(cm)	y(cm)	z(cm)
-17	-3.0	-0.14	4	-13.6	-0.57	13	20.0	-0.91
-17	0	-0.56	4	-13.0	1.04	16	-20.0	-2.94
-17	4.0	-0.14	4	-11.5	3.50	16	-16.0	-5.04
-14	-8.2	0	4	-9.0	1.04	16	-12.0	-4.48
-14	-5.0	-2.80	4	-8.5	1.32	16	-8.0	1.40
-14	-2.0	-4.40	4	7.7	-0.19	16	-4.0	4.48
-14	1.0	-4.00	4	9.5	0.38	16	-1.5	3.78
-14	4.0	-2.20	4	11.0	0.66	16	1.0	5.60
-14	7.5	-0.40	4	13.0	-2.08	16	4.0	2.94
-14	9.0	-0.40	4	16.0	-1.23	16	8.0	1.12
-11	-10.0	-0.10	4	17.5	-0.09	16	12.0	-2.24
-11	-7.0	-3.25	7	-20.0	-0.20	16	16.0	-0.56
-11	-4.5	-5.13	7	-18.5	-0.30	16	20.0	0.28
-11	4.0	-4.93	7	-16.0	-2.12	19	-20.0	0.20
-11	7.0	-2.27	7	-13.0	-0.20	19	-16.0	-0.10
-11	8.6	-0.69	7	-10.0	1.41	19	-12.0	-0.40
-11	11.0	-0.39	7	-8.0	0.91	19	-8.0	1.01
-8	-12.0	-0.20	7	7.0	1.91	19	-4.0	2.82
-8	-9.0	-2.07	7	9.5	0.60	19	0	2.42
-8	-6.5	-4.34	7	12.0	-1.41	19	4.0	2.01
-8	6.4	-4.73	7	15.0	-3.63	19	8.0	0.60
-8	9.0	-1.38	7	18.0	-2.01	19	12.0	1.31
-8	10.0	-0.49	7	20.0	0.20	19	16.0	2.01
-8	13.0	-0.39	10	-20.0	-1.71	19	20.0	1.11
-5	-17.0	-0.20	10	-17.0	-3.53	22	-20.0	1.31
-5	-12.5	-0.30	10	-14.0	-2.52	22	-16.0	1.81
-5	-10.5	-0.40	10	-11.0	-0.20	22	-12.0	0.20
-5	-9.0	-2.62	10	-8.0	-0.10	22	-8.0	-0.20
-5	-8.0	-4.03	10	-6.5	0.81	22	-4.0	2.62
-5	7.5	-3.93	10	5.0	1.81	22	0	0.91
-5	10.0	-0.81	10	8.0	0.91	22	4.0	1.41
-5	13.0	-0.30	10	12.0	-1.81	22	8.0	2.62
-2	-15.0	-0.20	10	15.0	-3.83	22	12.0	2.62
-2	-13.5	-0.20	10	19.0	-3.53	22	16.0	1.01
-2	-11.5	0.71	10	20.0	-1.31	22	20.0	0.60
-2	-9.0	-1.61	13	-20.0	-2.92	25	-20.0	1.81
-2	8.3	-2.72	13	-16.0	-4.43	25	-16.0	1.11
-2	10.9	0.10	13	-12.0	-2.12	25	-12.0	2.82
1	-17.0	0.00	13	-8.0	0.10	25	-8.0	-0.71
1	-14.0	-0.19	13	-4.5	3.02	25	-4.0	2.52
1	-11.5	1.54	13	-3.5	2.42	25	0	-0.20
1	-9.0	-0.29	13	2.3	3.12	25	4.0	0.40
1	8.5	-1.45	13	5.0	1.71	25	8.0	1.21
1	10.0	-0.39	13	8.0	1.41	25	12.0	1.61
1	11.0	0.39	13	12.0	-1.81	25	16.0	0.30
1	13.0	-0.97	13	15.0	-3.02	25	20.0	-1.91
4	-17.0	-0.09	13	19.0	-1.61			

Table C.13: Scour Data for Experimental Run C13
[Elliptical Island I_5 (b/a=0.6), F_r=0.19,h=15cm]

x(cm)	y(cm)	z(cm)	x(cm)	y(cm)	z(cm)	x(cm)	y(cm)	z(cm)
-25	-15.0	0	-11	4.5	-5.75	5	-20.0	-2.05
-25	-10.0	0	-11	7.0	-4.95	5	-17.0	-0.70
-25	-5.0	0	-11	10.0	-2.85	5	-14.0	0.05
-25	0	0	-11	13.0	-1.40	5	-12.0	-0.85
-25	5.0	0	-11	16.7	0.10	5	-9.0	-1.25
-25	10.0	0	-8	-17.7	-0.15	5	7.9	-1.30
-23	-5.0	-0.10	-8	-15.0	-1.45	5	11.0	-1.00
-23	-2.0	-0.75	-8	-12.0	-2.80	5	14.0	-0.10
-23	1.0	-0.65	-8	-9.0	-4.85	5	17.0	-1.75
-23	4.0	0	-8	-7.0	-5.45	5	20.0	-1.90
-20	-10.5	0	-8	6.4	-5.35	9	-20.0	-1.50
-20	-8.0	-1.35	-8	9.0	-4.30	9	-17.0	-0.85
-20	-5.0	-2.40	-8	12.0	-2.05	9	-14.0	0.50
-20	-2.0	-2.55	-8	15.0	-0.95	9	-11.0	0.30
-20	1.0	-2.60	-8	18.5	0.10	9	-8.0	0.60
-20	4.0	-2.25	-5	-18.5	-0.20	9	6.0	0.70
-20	7.0	-1.50	-5	-16.0	-1.00	9	9.0	-0.05
-20	10.0	0	-5	-13.0	-2.05	9	12.0	0.50
-17	-13.5	-0.05	-5	-10.0	-4.20	9	15.0	0.10
-17	-10.0	-2.20	-5	-8.0	-4.70	9	18.0	-1.20
-17	-7.0	-2.80	-5	8.0	-4.60	9	20.0	-2.00
-17	-4.0	-3.20	-5	11.0	-3.05	13	-20.0	-1.70
-17	-1.0	-3.25	-5	14.0	-1.15	13	-17.0	-0.55
-17	2.0	-3.90	-5	17.0	-0.80	13	-14.0	0.25
-17	5.0	-3.05	-5	20.0	0.10	13	-11.0	1.50
-17	8.0	-2.30	-2	-19.5	-0.20	13	-8.0	2.10
-17	11.0	-1.30	-2	-17.0	-0.50	13	-3.5	3.55
-17	13.0	0	-2	-14.0	-1.90	13	2.0	2.45
-14	-15.5	-0.10	-2	-11.0	-3.30	13	5.0	1.40
-14	-13.0	-1.75	-2	-8.5	-3.90	13	8.0	1.40
-14	-10.0	-2.65	-2	8.3	-3.80	13	11.0	1.35
-14	-7.0	-4.20	-2	11.0	-2.75	13	14.0	-0.05
-14	-4.0	-5.65	-2	14.0	-1.10	13	17.0	-0.75
-14	-1.0	-6.10	-2	17.0	-0.95	13	20.0	-1.30
-14	2.0	-5.85	-2	20.0	-1.05	17	-20.0	-1.40
-14	5.0	-4.70	1	-20.0	-0.65	17	-17.0	-0.60
-14	8.0	-3.10	1	-18.0	-0.90	17	-14.0	0.75
-14	11.0	-1.90	1	-15.0	-0.30	17	-11.0	1.45
-14	14.0	-0.65	1	-12.0	-2.00	17	-8.0	3.30
-14	15.0	0.05	1	-9.0	-2.80	17	-5.0	3.70
-11	-17.0	-0.15	1	8.0	-2.70	17	-2.0	2.75
-11	-14.0	-1.80	1	11.0	-2.15	17	1.0	2.75
-11	-11.0	-2.90	1	14.0	-0.85	17	4.0	2.60
-11	-8.0	-5.00	1	17.0	-1.50	17	7.0	2.25
-11	-5.0	-5.90	1	20.0	-1.80	17	10.0	1.45

x(cm)	y(cm)	z(cm)	x(cm)	y(cm)	z(cm)	x(cm)	y(cm)	z(cm)
17	13.0	1.25	21	2.0	1.85	25	-8.0	2.70
17	16.0	0.65	21	6.0	2.20	25	-4.0	1.65
17	19.0	-0.55	21	10.0	1.20	25	0	0.90
17	20.0	-1.20	21	14.0	1.00	25	4.0	1.35
21	-20.0	-1.20	21	18.0	-0.35	25	8.0	1.55
21	-16.0	0	21	20.0	-0.55	25	12.0	1.60
21	-12.0	0.55	25	-20.0	-1.15	25	16.0	1.15
21	-6.0	3.35	25	-16.0	0.35	25	20.0	-0.70
21	-2.0	1.55	25	-12.0	1.85			

Table C.14 Scour Data for Experimental Run C14
[Elliptical Island I_5 (b/a=0.6), F_r=0.2,h=15cm]

x(cm)	y(cm)	z(cm)	x(cm)	y(cm)	z(cm)	x(cm)	y(cm)	z(cm)
-25	-15.0	0	-11	-5.0	-8.03	1	20.0	-3.06
-25	-10.0	0	-11	4.5	-8.77	5	-20.0	-3.48
-25	-5.0	0	-11	7.0	-6.42	5	-17.0	-1.19
-25	0	0	-11	10.0	-3.84	5	-14.0	0.09
-25	5.0	0	-11	13.0	-2.38	5	-12.0	-1.44
-25	10.0	0	-11	16.7	0.17	5	-9.0	-2.13
-23	-8.0	0	-8	-17.7	-0.25	5	7.9	-2.21
-23	-5.0	-0.17	-8	-15.0	-2.47	5	11.0	-1.70
-23	-2.0	-1.27	-8	-12.0	-4.76	5	14.0	-0.17
-23	1.0	-1.10	-8	-9.0	-8.24	5	17.0	-2.97
-23	4.0	0	-8	-7.0	-9.26	5	20.0	-3.23
-20	-10.5	0	-8	6.4	-9.09	9	-20.0	-2.55
-20	-8.0	-2.30	-8	9.0	-7.31	9	-17.0	-1.44
-20	-5.0	-4.08	-8	12.0	-3.49	9	-14.0	0.85
-20	-2.0	-4.33	-8	15.0	-1.61	9	-11.0	0.51
-20	1.0	-4.42	-8	18.5	0.17	9	-8.0	1.02
-20	4.0	-3.82	-5	-18.5	-0.34	9	6.0	1.19
-20	7.0	-2.55	-5	-16.0	-1.70	9	9.0	-0.09
-20	10.0	0	-5	-13.0	-3.48	9	12.0	0.85
-17	-13.5	-0.08	-5	-10.0	-7.14	9	15.0	0.17
-17	-10.0	-3.74	-5	-8.0	-7.99	9	18.0	-2.04
-17	-7.0	-4.76	-5	8.0	-7.82	9	20.0	-3.4
-17	-4.0	-5.44	-5	11.0	-5.19	13	-20.0	-2.89
-17	-1.0	-5.53	-5	14.0	-1.95	13	-17.0	-0.93
-17	2.0	-6.63	-5	17.0	-1.36	13	-14.0	0.43
-17	5.0	-5.18	-5	20.0	0.17	13	-11.0	2.55
-17	8.0	-3.91	-2	-19.5	-0.34	13	-8.0	3.57
-17	11.0	-2.21	-2	-17.0	-0.85	13	-3.5	6.03
-17	13.0	0	-2	-14.0	-3.23	13	2.0	4.17
-14	-15.5	-0.17	-2	-11.0	-5.61	13	5.0	2.38
-14	-13.0	-2.97	-2	-8.5	-6.63	13	8.0	2.38
-14	-10.0	-4.51	-2	8.3	-6.46	13	11.0	2.30
-14	-7.0	-5.14	-2	11.0	-4.67	13	14.0	-0.08
-14	-4.0	-7.60	-2	14.0	-1.87	13	17.0	-1.27
-14	-1.0	-8.37	-2	17.0	-1.62	13	20.0	-2.21
-14	2.0	-8.94	-2	20.0	-1.78	17	-20.0	-2.38
-14	5.0	-7.99	1	-20.0	-1.10	17	-17.0	-1.02
-14	8.0	-5.27	1	-18.0	-1.53	17	-14.0	1.27
-14	11.0	-3.23	1	-15.0	-0.51	17	-11.0	2.47
-14	14.0	-1.10	1	-12.0	-3.40	17	-8.0	5.61
-14	15.0	0.09	1	-9.0	-4.76	17	-5.0	6.29
-11	-17.0	-0.25	1	8.0	-4.59	17	-2.0	4.67
-11	-14.0	-1.06	1	11.0	-3.66	17	1.0	4.68
-11	-11.0	-3.93	1	14.0	-1.44	17	4.0	4.42
-11	-8.0	-5.50	1	17.0	-2.55	17	7.0	3.82

x(cm)	y(cm)	z(cm)	x(cm)	y(cm)	z(cm)	x(cm)	y(cm)	z(cm)
17	10.0	2.46	21	-2.0	2.63	25	-12.0	3.14
17	13.0	2.13	21	2.0	3.15	25	-8.0	4.59
17	16.0	1.10	21	6.0	3.74	25	-4.0	2.80
17	19.0	-0.94	21	10.0	2.04	25	0	1.53
17	20.0	-2.04	21	14.0	1.70	25	4.0	2.30
21	-20.0	-2.04	21	18.0	-0.59	25	8.0	2.63
21	-16.0	0	21	20.0	-0.94	25	12.0	2.72
21	-12.0	0.93	25	-20.0	-1.95	25	16.0	1.96
21	-6.0	5.70	25	-16.0	0.60	25	20.0	-1.19

Table C.15: Scour Data for Experimental Run C15
[Circular Island I_6 (d=15cm), F_r=0.16,h=15cm]

x(cm)	y(cm)	z(cm)	x(cm)	y(cm)	z(cm)	x(cm)	y(cm)	z(cm)
-18	-10	0	-4	-15.5	-1.60	11	-1.5	0.25
-18	-5	0	-4	-12.5	-2.75	11	2	0.30
-18	0	0	-4	-9.5	-4.53	11	5.5	-1.83
-18	5	0	-4	-6.9	-6.10	11	9.5	-2.95
-18	10	0	-4	8	-6.25	11	13.5	-2.80
-16	-7.5	0	-4	10.5	-4.95	11	17.5	-1.15
-16	-4.5	-0.90	-4	13.5	-3.03	11	20.5	-2.40
-16	-1.5	-1.55	-4	16.5	-1.75	15	-19.5	-1.35
-16	1.5	-1.55	-4	19.5	-0.15	15	-15.5	-0.53
-16	4.5	-1.13	-1	-19.5	-0.83	15	-11.5	-0.50
-16	7.5	-0.35	-1	-16.5	-1.80	15	-7.5	-0.75
-16	8.3	-0.05	-1	-13.5	-2.57	15	-3.5	-0.25
-13	-11.3	-0.05	-1	-10.5	-4.35	15	-0.5	1.00
-13	-8.5	-1.57	-1	-8	-5.85	15	2.5	0.73
-13	-5.5	-2.23	-1	9	-6.25	15	6.5	0.05
-13	-2.5	-2.73	-1	11.5	-4.85	15	10.5	-1.00
-13	0.5	-2.93	-1	14.5	-2.95	15	14.5	-1.25
-13	3.5	-2.70	-1	17.5	-2.15	15	16	-0.35
-13	6.5	-2.22	-1	20.5	-0.97	15	20.5	-2.23
-13	9.5	-1.60	3	-19.5	-1.95	19	-19.5	-1.93
-13	12.5	-0.03	3	-16.5	-2.83	19	-15.5	-1.15
-10	-14.3	-0.05	3	-13.5	-3.05	19	-11.5	-0.10
-10	-11.5	-1.73	3	-10.5	-4.15	19	-7.5	0.27
-10	-8.5	-2.60	3	-7.7	-5.05	19	-3.5	2.08
-10	-5.5	-3.70	3	8.5	-5.30	19	-1.9	2.55
-10	-2.5	-4.35	3	11.5	-4.45	19	0.7	1.00
-10	0.5	-4.35	3	14.5	-2.83	19	2.9	1.70
-10	3.5	-4.35	3	17.5	-2.85	19	6.5	0.45
-10	6.5	-3.85	3	20.5	-1.43	19	10.5	-0.80
-10	9.5	-2.75	7	-19.5	-1.75	19	14.5	-0.55
-10	12.5	-1.75	7	-15.5	-3.20	19	18.5	-1.05
-10	15.5	-0.15	7	-11.5	-3.90	19	20.5	-1.40
-7	-16.2	-0.15	7	-7.5	-3.55	23	-19.5	-0.75
-7	-13.5	-1.80	7	-4.7	-2.15	23	-14.5	-0.40
-7	-10.5	-2.87	7	5.2	-2.25	23	-9.5	0.40
-7	-7.5	-4.43	7	8.5	-3.45	23	-4.5	2.00
-7	-4.1	-5.55	7	12.5	-3.55	23	-2.9	2.43
-7	4.8	-5.80	7	16.5	-2.90	23	0.5	1.75
-7	7.5	-5.10	7	20.5	-1.25	23	5.5	2.25
-7	10.5	-3.77	11	-19.5	-1.75	23	10.5	0.75
-7	13.5	-2.37	11	-17.5	-1.60	23	15.5	-0.20
-7	16.5	-1.05	11	-13.5	-3.05	23	20.5	-0.63
-7	18.1	-0.15	11	-9.5	-3.55			
-4	-17.8	-0.25	11	-5.5	-1.95			

Table C.16: Scour Data for Experimental Run C16
[Circular Island I_6 (d=15cm), F_r=0.19,h=15cm]

x(cm)	y(cm)	z(cm)	x(cm)	y(cm)	z(cm)	x(cm)	y(cm)	z(cm)
-24	-6.0	0	-11	-10.0	-5.15	0	14.0	-5.60
-24	-3.0	0	-11	-7.0	-6.30	0	17.0	-3.70
-24	0	0	-11	-4.0	-6.40	0	20.0	-2.45
-24	3.0	0	-11	-1.0	-6.55	4	-20.0	-2.40
-24	6.0	0	-11	2.0	-6.55	4	-17.0	-4.15
-22.5	-7.0	0	-11	5.0	-6.45	4	-14.0	-5.95
-22.5	-4.0	-0.90	-11	8.0	-5.60	4	-11.0	-7.30
-22.5	-1.0	-1.15	-11	11.0	-3.50	4	-8.0	-8.65
-22.5	2.0	-0.95	-11	14.0	-2.95	4	7.0	-8.60
-22.5	5.0	0	-11	17.0	-1.50	4	10.0	-7.75
-20	-10.6	0	-11	19.2	0.20	4	13.0	-6.20
-20	-8.0	-1.70	-8	-20.0	-0.40	4	16.0	-4.90
-20	-5.0	-2.50	-8	-17.0	-3.00	4	19.0	-3.25
-20	-2.0	-2.90	-8	-14.0	-4.30	4	20.0	-2.55
-20	1.0	-2.80	-8	-11.0	-6.25	8	-20.0	-2.15
-20	4.0	-2.40	-8	-8.0	-6.90	8	-17.0	-3.85
-20	7.0	-1.85	-8	-5.0	-7.40	8	-14.0	-5.15
-20	10.8	0.05	-8	-2.0	-7.05	8	-11.0	-6.50
-17	-14.5	0	-8	1.0	-7.55	8	-8.0	-7.15
-17	-12.0	-1.95	-8	4.0	-7.75	8	-5.0	-6.05
-17	-9.0	-3.20	-8	7.0	-7.15	8	-2.0	-5.15
-17	-6.0	-3.65	-8	10.0	-5.80	8	1.0	-5.10
-17	-3.0	-3.85	-8	13.0	-4.05	8	4.0	-5.85
-17	0	-4.00	-8	16.0	-2.85	8	7.0	-6.65
-17	3.0	-3.80	-8	19.0	-1.00	8	10.0	-6.05
-17	6.0	-3.35	-8	20.0	-0.30	8	13.0	-5.90
-17	9.0	-2.70	-4	-20.0	-1.40	8	16.0	-4.85
-17	12.0	-1.50	-4	-17.0	-3.70	8	19.0	-2.75
-17	14.6	0.10	-4	-14.0	-5.25	8	20.0	-2.15
-14	-17.0	-0.20	-4	-11.0	-7.10	12	-20.0	-1.90
-14	-14.0	-2.45	-4	-8.0	-8.70	12	-16.0	-3.55
-14	-11.0	-3.65	-4	-6.2	-8.70	12	-12.0	-5.35
-14	-8.0	-4.45	-4	7.0	-9.25	12	-8.0	-6.00
-14	-5.0	-5.35	-4	10.0	-7.40	12	-4.0	-4.80
-14	-2.0	-5.80	-4	13.0	-5.35	12	0	-5.40
-14	1.0	-5.75	-4	16.0	-3.75	12	4.0	-5.75
-14	4.0	-5.50	-4	19.0	-2.40	12	8.0	-5.75
-14	7.0	-4.35	-4	20.0	-1.70	12	12.0	-5.15
-14	10.0	-3.40	0	-20.0	-2.20	12	16.0	-3.10
-14	13.0	-2.45	0	-17.0	-3.95	12	20.0	-2.20
-14	16.0	-0.85	0	-14.0	-6.00	16	-20.0	-2.25
-14	17.2	0.20	0	-11.0	-7.95	16	-16.0	-1.95
-11	-19.0	-0.20	0	-8.3	-9.30	16	-12.0	-2.85
-11	-16.0	-2.55	0	8.0	-9.20	16	-8.0	-3.20
-11	-13.0	-3.90	0	11.0	-7.40	16	-4.0	-3.60

x(cm)	y(cm)	z(cm)	x(cm)	y(cm)	z(cm)	x(cm)	y(cm)	z(cm)
16	0	-4.25	20	-4.0	-3.35	24	-8.0	-0.65
16	4.0	-3.30	20	0	-3.40	24	-4.0	-1.20
16	8.0	-3.35	20	4.0	-1.95	24	0	-1.90
16	12.0	-2.80	20	8.0	-2.35	24	4.0	-0.70
16	16.0	-2.55	20	12.0	-2.40	24	8.0	-0.35
16	20.0	-1.45	20	16.0	-1.40	24	12.0	-0.25
20	-20.0	-1.15	20	20.0	-0.30	24	16.0	-0.20
20	-16.0	-1.90	24	-20.0	-0.95	24	20.0	-0.45
20	-12.0	-2.65	24	-16.0	-0.75			
20	-8.0	-2.45	24	-12.0	-0.65			

APPENDIX-D

EXPERIMENTAL DATA RELATING TO VARIATION OF STRENGTH OF SECONDAEY CURRENT AROUND ISLAND

Table D.1: 3D Velocity Components for Experimental Run D1
[Elliptical Island I_1 (b/a=0.15), F_r=0.14,h=15cm]

Coordinates (cm)	Vx (cm/sec)	Vy (cm/sec)	Vz (cm/sec)	Coordinates (cm)	Vx (cm/sec)	Vy (cm/sec)	Vz (cm/sec)
(-70, -20,3.0)	15.36	2.45	-0.71	(-40, -20,3.0)	18.01	2.46	-0.92
(-70, -20,6.0)	16.63	2.90	-0.85	(-40, -20,6.0)	18.96	2.34	-1.09
(-70, -20,9.0)	15.76	2.66	-0.51	(-40, -20,9.0)	19.07	2.32	-0.66
(-70, -10,3.0)	15.09	3.20	-0.48	(-40, -10,3.0)	18.93	0.91	-0.83
(-70, -10,6.0)	15.65	2.51	-0.73	(-40, -10,6.0)	19.77	0.46	-1.01
(-70, -10,9.0)	17.06	3.11	-0.64	(-40, -10,9.0)	20.32	0.76	-0.71
(-70, 0,3.0)	15.08	3.58	-0.61	(-40, 10,3.0)	18.08	6.58	-1.07
(-70, 0,6.0)	15.91	3.20	-0.72	(-40, 10,6.0)	18.61	7.72	-1.47
(-70, 0,9.0)	16.56	3.04	-0.45	(-40, 10,9.0)	19.62	6.91	-1.13
(-70, 10,3.0)	14.58	3.22	-0.43	(-40, 20,3.0)	18.53	4.70	-0.75
(-70, 10,6.0)	16.18	3.86	-0.39	(-40, 20,6.0)	18.91	4.29	-0.69
(-70, 10,9.0)	17.05	3.90	-0.45	(-40, 20,9.0)	19.22	5.30	-0.70
(-70, 20,3.0)	15.93	2.81	-0.66	(-30, -20,3.0)	19.41	2.97	-0.86
(-70, 20,6.0)	16.97	2.89	-0.71	(-30, -20,6.0)	20.56	2.91	-0.97
(-70, 20,9.0)	16.99	3.43	-0.62	(-30, -20,9.0)	20.44	2.86	-0.56
(-60, -20,3.0)	15.77	2.78	-0.79	(-30, -10,3.0)	19.96	2.36	-0.89
(-60, -20,6.0)	16.49	2.91	-0.96	(-30, -10,6.0)	20.80	2.13	-0.82
(-60, -20,9.0)	16.37	2.78	-0.60	(-30, -10,9.0)	22.01	1.98	-0.63
(-60, -10,3.0)	14.72	2.62	-0.58	(-30, 10,3.0)	20.51	5.92	-1.00
(-60, -10,6.0)	15.35	2.32	-0.93	(-30, 10,6.0)	20.60	6.95	-1.37
(-60, -10,9.0)	16.68	2.45	-0.70	(-30, 10,9.0)	21.70	6.22	-0.98
(-60, 0,3.0)	15.26	3.44	-0.93	(-30, 20,3.0)	21.02	4.35	-0.60
(-60, 0,6.0)	16.03	2.73	-0.54	(-30, 20,6.0)	21.45	3.96	-0.53
(-60, 0,9.0)	16.62	2.63	-0.51	(-30, 20,9.0)	20.97	5.22	-0.63
(-60, 10,3.0)	15.05	3.68	-0.19	(-20, -20,3.0)	20.77	3.34	-0.95
(-60, 10,6.0)	16.34	4.39	-0.22	(-20, -20,6.0)	21.37	3.07	-1.12
(-60, 10,9.0)	17.12	4.09	-0.21	(-20, -20,9.0)	21.29	2.96	-0.65
(-60, 20,3.0)	16.99	3.03	-0.69	(-20, -10,3.0)	20.91	2.80	-0.90
(-60, 20,6.0)	17.83	2.92	-0.69	(-20, -10,6.0)	21.96	2.58	-0.95
(-60, 20,9.0)	17.68	3.39	-0.61	(-20, -10,9.0)	22.35	2.35	-0.67
(-50, -20,3.0)	16.63	2.61	-0.69	(-20, 10,3.0)	21.33	5.38	-1.30
(-50, -20,6.0)	17.39	2.39	-0.86	(-20, 10,6.0)	21.79	6.20	-1.81
(-50, -20,9.0)	17.34	2.40	-0.55	(-20, 10,9.0)	22.62	5.58	-1.25
(-50, -10,3.0)	16.12	1.09	-0.57	(-20, 20,3.0)	21.77	4.51	-0.66
(-50, -10,6.0)	16.89	1.29	-0.95	(-20, 20,6.0)	21.89	4.10	-0.58
(-50, -10,9.0)	17.49	0.91	-0.62	(-20, 20,9.0)	22.03	5.41	-0.69
(-50, 0,3.0)	12.35	1.94	-1.06	(-10, -20,3.0)	22.09	3.93	-0.89
(-50, 0,6.0)	13.37	1.72	-1.24	(-10, -20,6.0)	22.72	3.44	-1.10
(-50, 0,9.0)	13.38	1.73	-0.82	(-10, -20,9.0)	23.24	3.26	-0.63
(-50, 10,3.0)	15.23	5.10	-0.53	(-10, -10,3.0)	21.73	3.68	-1.07
(-50, 10,6.0)	16.19	6.06	-0.73	(-10, -10,6.0)	22.99	3.44	-1.26
(-50, 10,9.0)	17.30	5.35	-0.64	(-10, -10,9.0)	23.41	3.10	-0.82
(-50, 20,3.0)	17.19	3.92	-0.84	(-10, 10,3.0)	22.39	4.51	-0.86
(-50, 20,6.0)	18.04	3.59	-0.79	(-10, 10,6.0)	23.22	5.08	-1.22
(-50, 20,9.0)	18.31	4.11	-0.71	(-10, 10,9.0)	23.24	4.60	-0.81

Coordinates (cm)	Vx (cm/sec)	Vy (cm/sec)	Vz (cm/sec)	Coordinates (cm)	Vx (cm/sec)	Vy (cm/sec)	Vz (cm/sec)
(-10, 20,3.0)	22.92	4.25	-0.94	(40, -10,3.0)	18.33	6.62	-0.25
(-10, 20,6.0)	22.74	3.70	-0.74	(40, -10,6.0)	19.44	5.98	-0.34
(-10, 20,9.0)	22.83	4.58	-0.53	(40, -10,9.0)	21.37	6.26	-0.31
(0, -20,3.0)	22.41	4.08	-1.03	(40, 10,3.0)	19.33	0.46	-0.48
(0, -20,6.0)	23.04	3.73	-1.27	(40, 10,6.0)	20.28	0.55	-0.60
(0, -20,9.0)	22.98	3.98	-0.81	(40, 10,9.0)	20.66	0.50	-0.36
(0, -10,3.0)	22.39	4.35	-0.85	(40, 20,3.0)	19.90	2.63	-0.68
(0, -10,6.0)	23.64	4.33	-0.98	(40, 20,6.0)	20.67	2.41	-0.90
(0, -10,9.0)	23.70	3.97	-0.58	(40, 20,9.0)	20.83	2.89	-0.91
(0, 10,3.0)	23.07	4.41	-1.06	(50, -20,3.0)	17.98	3.73	-0.69
(0, 10,6.0)	23.35	4.41	-1.04	(50, -20,6.0)	18.54	3.87	-0.62
(0, 10,9.0)	23.32	3.74	-0.81	(50, -20,9.0)	18.74	3.97	-0.38
(0, 20,3.0)	22.86	4.01	-0.50	(50, -10,3.0)	17.02	5.65	-0.20
(0, 20,6.0)	22.98	3.20	-0.56	(50, -10,6.0)	18.09	5.11	-0.27
(0, 20,9.0)	23.06	4.12	-0.39	(50, -10,9.0)	19.44	5.34	-0.25
(10, -20,3.0)	20.99	4.36	-0.78	(50, 0,3.0)	0.76	1.40	-0.14
(10, -20,6.0)	22.17	3.99	-0.96	(50, 0,6.0)	2.17	2.76	-0.41
(10, -20,9.0)	22.71	4.25	-0.61	(50, 0,9.0)	1.70	1.65	0.16
(10, -10,3.0)	21.40	5.18	-0.76	(50, 10,3.0)	17.22	1.19	-0.26
(10, -10,6.0)	22.60	5.39	-0.85	(50, 10,6.0)	18.80	1.73	-0.53
(10, -10,9.0)	22.98	4.99	-0.44	(50, 10,9.0)	18.98	1.59	-0.31
(10, 10,3.0)	22.01	3.46	-1.15	(50, 20,3.0)	18.70	2.28	-0.55
(10, 10,6.0)	22.94	3.39	-1.09	(50, 20,6.0)	19.45	2.39	-0.62
(10, 10,9.0)	23.59	2.84	-0.62	(50, 20,9.0)	19.19	2.66	-0.70
(10, 20,3.0)	23.21	3.71	-0.87	(60, -20,3.0)	17.15	3.27	-0.73
(10, 20,6.0)	23.06	2.65	-1.29	(60, -20,6.0)	17.68	3.49	-0.76
(10, 20,9.0)	23.46	3.60	-0.89	(60, -20,9.0)	17.74	3.54	-0.41
(20, -20,3.0)	20.93	4.66	-0.87	(60, -10,3.0)	16.14	4.70	-0.36
(20, -20,6.0)	21.68	4.19	-1.04	(60, -10,6.0)	18.05	4.23	-0.34
(20, -20,9.0)	21.72	4.45	-0.64	(60, -10,9.0)	18.87	4.42	-0.33
(20, -10,3.0)	20.89	6.02	-0.89	(60, 0,3.0)	6.55	2.87	-1.46
(20, -10,6.0)	22.09	5.89	-0.90	(60, 0,6.0)	9.38	2.63	-1.43
(20, -10,9.0)	22.92	5.48	-0.53	(60, 0,9.0)	10.02	1.99	-0.70
(20, 10,3.0)	22.70	2.25	-1.22	(60, 10,3.0)	16.00	1.62	-0.33
(20, 10,6.0)	23.05	2.22	-1.18	(60, 10,6.0)	18.18	2.38	-0.49
(20, 10,9.0)	23.47	1.92	-0.69	(60, 10,9.0)	18.32	2.43	-0.34
(20, 20,3.0)	22.38	3.27	-0.61	(60, 20,3.0)	17.76	2.59	-0.56
(20, 20,6.0)	22.70	2.49	-0.91	(60, 20,6.0)	18.27	2.62	-0.59
(20, 20,9.0)	22.71	3.29	-0.72	(60, 20,9.0)	18.50	2.83	-0.62
(30, -20,3.0)	20.27	4.50	-0.82	(-70, -20,3.0)	16.20	2.96	-0.56
(30, -20,6.0)	21.00	3.98	-0.95	(-70, -20,6.0)	16.91	3.27	-0.68
(30, -20,9.0)	21.12	4.22	-0.56	(-70, -20,9.0)	17.24	3.28	-0.33
(30, -10,3.0)	20.30	6.55	-0.67	(-70, -10,3.0)	14.96	4.03	-0.50
(30, -10,6.0)	21.50	6.08	-0.59	(-70, -10,6.0)	17.68	3.61	-0.40
(30, -10,9.0)	22.15	5.69	-0.42	(-70, -10,9.0)	18.31	3.77	-0.32
(30, 10,3.0)	21.51	1.65	-0.80	(-70, 0,3.0)	11.35	2.70	-1.86
(30, 10,6.0)	21.84	1.65	-0.79	(-70, 0,6.0)	12.95	2.43	-1.37
(30, 10,9.0)	22.39	1.52	-0.48	(-70, 0,9.0)	13.20	2.87	-0.67
(30, 20,3.0)	21.22	3.16	-0.56	(-70, 10,3.0)	15.06	1.67	-0.56
(30, 20,6.0)	22.02	2.59	-0.85	(-70, 10,6.0)	17.88	2.48	-0.70
(30, 20,9.0)	21.61	3.31	-0.79	(-70, 10,9.0)	18.18	2.71	-0.54
(40, -20,3.0)	19.37	4.05	-0.66	(-70, 20,3.0)	17.34	2.72	-0.58
(40, -20,6.0)	19.97	3.86	-0.69	(-70, 20,6.0)	17.84	2.67	-0.57
(40, -20,9.0)	19.95	4.03	-0.41	(-70, 20,9.0)	18.26	2.80	-0.56

Table D.2: 3D Velocity Components for Experimental Run D2
[Elliptical Island I_1 (b/a=0.15), F_r=0.16,h=15cm]

Coordinates (cm)	Vx (cm/sec)	Vy (cm/sec)	Vz (cm/sec)	Coordinates (cm)	Vx (cm/sec)	Vy (cm/sec)	Vz (cm/sec)
(-70, -20,3.0)	17.14	3.52	-0.71	(-40, -20,3.0)	21.99	3.17	0.85
(-70, -20,6.0)	19.32	3.64	-0.82	(-40, -20,6.0)	23.30	3.56	-0.41
(-70, -20,9.0)	18.82	3.27	-0.59	(-40, -20,9.0)	22.93	3.41	-0.97
(-70, -10,3.0)	17.86	3.31	-0.52	(-40, -10,3.0)	21.71	2.12	-0.82
(-70, -10,6.0)	19.15	3.08	-0.43	(-40, -10,6.0)	22.64	2.03	-0.94
(-70, -10,9.0)	20.06	3.58	-0.62	(-40, -10,9.0)	22.68	2.16	-1.01
(-70, 0,3.0)	18.30	3.67	-0.46	(-40, 10,3.0)	22.08	6.64	-0.64
(-70, 0,6.0)	19.52	3.93	-0.35	(-40, 10,6.0)	24.42	6.91	-0.72
(-70, 0,9.0)	19.73	3.77	-0.44	(-40, 10,9.0)	24.45	7.34	-0.99
(-70, 10,3.0)	17.88	3.32	-0.30	(-40, 20,3.0)	22.05	5.23	-0.80
(-70, 10,6.0)	19.29	3.77	-0.41	(-40, 20,6.0)	22.12	5.62	-0.57
(-70, 10,9.0)	19.84	4.35	-0.66	(-40, 20,9.0)	23.12	5.55	-0.46
(-70, 20,3.0)	19.17	3.73	-0.73	(-30, -20,3.0)	22.87	3.62	-0.84
(-70, 20,6.0)	19.59	3.94	-0.66	(-30, -20,6.0)	24.00	4.14	-1.04
(-70, 20,9.0)	20.18	3.83	-0.47	(-30, -20,9.0)	23.48	3.77	-0.81
(-60, -20,3.0)	18.87	3.34	-0.76	(-30, -10,3.0)	24.55	3.26	-0.41
(-60, -20,6.0)	20.72	3.33	-0.43	(-30, -10,6.0)	24.57	3.13	-0.69
(-60, -20,9.0)	20.36	3.28	-0.66	(-30, -10,9.0)	24.72	3.50	-0.81
(-60, -10,3.0)	18.30	2.75	-0.36	(-30, 10,3.0)	24.58	6.34	-1.07
(-60, -10,6.0)	19.87	2.78	-0.40	(-30, 10,6.0)	25.98	6.43	-0.78
(-60, -10,9.0)	20.29	2.90	-0.53	(-30, 10,9.0)	25.58	6.76	-0.91
(-60, 0,3.0)	18.79	3.64	-0.57	(-30, 20,3.0)	23.73	5.86	-0.72
(-60, 0,6.0)	18.10	3.95	-0.75	(-30, 20,6.0)	23.81	6.07	-0.73
(-60, 0,9.0)	18.89	3.70	-0.58	(-30, 20,9.0)	24.88	6.00	-0.71
(-60, 10,3.0)	17.23	3.91	-0.28	(-20, -20,3.0)	24.82	4.15	-0.96
(-60, 10,6.0)	18.83	4.19	-0.38	(-20, -20,6.0)	25.68	4.46	-0.79
(-60, 10,9.0)	19.86	4.58	-0.66	(-20, -20,9.0)	25.17	4.50	-0.74
(-60, 20,3.0)	19.21	4.04	-0.73	(-20, -10,3.0)	25.46	3.89	-0.73
(-60, 20,6.0)	19.34	4.61	-0.74	(-20, -10,6.0)	25.80	3.68	-0.61
(-60, 20,9.0)	20.03	4.58	-0.69	(-20, -10,9.0)	25.83	3.81	-0.62
(-50, -20,3.0)	19.09	2.95	-0.79	(-20, 10,3.0)	25.74	5.46	-0.89
(-50, -20,6.0)	20.47	3.36	-0.97	(-20, 10,6.0)	27.22	5.54	-0.95
(-50, -20,9.0)	20.28	3.27	-0.60	(-20, 10,9.0)	26.77	6.06	-1.04
(-50, -10,3.0)	18.37	1.79	-0.65	(-20, 20,3.0)	24.88	5.71	-0.83
(-50, -10,6.0)	20.19	1.81	-0.69	(-20, 20,6.0)	24.96	5.86	-0.64
(-50, -10,9.0)	20.11	2.21	-0.82	(-20, 20,9.0)	26.08	5.84	-0.53
(-50, 0,3.0)	14.80	2.53	-0.87	(-10, -20,3.0)	25.59	4.75	-0.88
(-50, 0,6.0)	15.82	2.54	-0.98	(-10, -20,6.0)	26.15	5.09	-1.00
(-50, 0,9.0)	15.83	2.46	-0.72	(-10, -20,9.0)	25.67	5.11	-1.08
(-50, 10,3.0)	17.95	5.16	-0.56	(-10, -10,3.0)	26.67	4.45	-0.57
(-50, 10,6.0)	19.86	5.53	-0.56	(-10, -10,6.0)	27.33	4.67	-0.99
(-50, 10,9.0)	19.88	6.01	-0.56	(-10, -10,9.0)	27.24	4.67	-0.85
(-50, 20,3.0)	20.48	4.86	-0.78	(-10, 10,3.0)	26.07	5.26	-0.97
(-50, 20,6.0)	20.33	4.64	-0.89	(-10, 10,6.0)	27.58	5.59	-1.09
(-50, 20,9.0)	21.17	4.97	-0.51	(-10, 10,9.0)	27.29	5.44	-0.78

Coordinates (cm)	Vx (cm/sec)	Vy (cm/sec)	Vz (cm/sec)	Coordinates (cm)	Vx (cm/sec)	Vy (cm/sec)	Vz (cm/sec)
(-10, 20,3.0)	26.30	5.96	-0.88	(40, -10,3.0)	22.75	5.99	0.04
(-10, 20,6.0)	25.74	5.81	-0.73	(40, -10,6.0)	23.78	6.62	-0.23
(-10, 20,9.0)	26.46	5.56	-0.78	(40, -10,9.0)	24.59	7.77	-0.51
(0, -20,3.0)	25.84	5.06	-1.18	(40, 10,3.0)	22.42	1.60	-0.25
(0, -20,6.0)	26.72	5.23	-1.15	(40, 10,6.0)	23.59	1.76	-0.34
(0, -20,9.0)	26.77	5.28	-0.95	(40, 10,9.0)	23.83	2.07	-0.38
(0, -10,3.0)	26.64	5.28	-0.77	(40, 20,3.0)	23.06	3.89	-0.59
(0, -10,6.0)	27.28	5.39	-0.71	(40, 20,6.0)	24.16	3.93	-0.85
(0, -10,9.0)	27.01	5.57	-0.60	(40, 20,9.0)	24.83	3.94	-0.78
(0, 10,3.0)	26.56	4.90	-1.38	(50, -20,3.0)	21.11	4.61	-0.72
(0, 10,6.0)	27.76	5.17	-1.04	(50, -20,6.0)	21.72	5.08	-0.74
(0, 10,9.0)	27.23	5.25	-0.71	(50, -20,9.0)	21.85	4.30	-0.68
(0, 20,3.0)	25.74	5.91	-0.82	(50, -10,3.0)	20.44	5.06	-0.25
(0, 20,6.0)	25.37	5.45	-0.87	(50, -10,6.0)	21.37	5.42	-0.22
(0, 20,9.0)	26.02	5.22	-0.78	(50, -10,9.0)	22.09	6.58	-0.44
(10, -20,3.0)	24.96	4.95	-0.98	(50, 0,3.0)	1.27	1.47	-0.65
(10, -20,6.0)	25.81	5.44	-0.89	(50, 0,6.0)	2.45	2.38	-0.80
(10, -20,9.0)	25.86	5.14	-0.96	(50, 0,9.0)	3.23	2.13	0.08
(10, -10,3.0)	26.06	5.37	-0.58	(50, 10,3.0)	20.29	2.21	-0.23
(10, -10,6.0)	26.66	5.79	-0.82	(50, 10,6.0)	21.94	2.77	-0.26
(10, -10,9.0)	26.22	6.38	-0.55	(50, 10,9.0)	22.08	2.58	-0.40
(10, 10,3.0)	26.81	3.80	-0.77	(50, 20,3.0)	20.90	3.36	-0.72
(10, 10,6.0)	27.38	4.39	-0.78	(50, 20,6.0)	21.96	3.82	-0.68
(10, 10,9.0)	27.32	4.58	-0.62	(50, 20,9.0)	22.64	3.83	-0.58
(10, 20,3.0)	26.41	5.20	-0.82	(60, -20,3.0)	20.11	4.25	-0.79
(10, 20,6.0)	26.22	5.05	-0.94	(60, -20,6.0)	21.19	4.17	-0.72
(10, 20,9.0)	26.83	5.12	-0.93	(60, -20,9.0)	21.69	4.05	-0.56
(20, -20,3.0)	24.57	5.00	-0.99	(60, -10,3.0)	19.10	4.18	-0.29
(20, -20,6.0)	25.40	5.36	-0.91	(60, -10,6.0)	20.01	4.45	-0.52
(20, -20,9.0)	25.58	4.89	-0.84	(60, -10,9.0)	20.91	5.63	-0.60
(20, -10,3.0)	25.43	5.41	-0.46	(60, 0,3.0)	9.19	2.99	-1.20
(20, -10,6.0)	25.64	5.77	-0.57	(60, 0,6.0)	11.05	2.38	-1.33
(20, -10,9.0)	25.66	6.59	-0.77	(60, 0,9.0)	12.20	2.79	-0.40
(20, 10,3.0)	26.46	3.16	-1.12	(60, 10,3.0)	18.17	2.86	-0.22
(20, 10,6.0)	27.11	3.70	-1.01	(60, 10,6.0)	20.67	3.05	-0.49
(20, 10,9.0)	27.26	4.34	-0.68	(60, 10,9.0)	20.42	3.18	-0.42
(20, 20,3.0)	25.16	5.00	-0.88	(60, 20,3.0)	19.89	3.46	-0.58
(20, 20,6.0)	25.60	5.16	-0.93	(60, 20,6.0)	21.31	3.77	-0.54
(20, 20,9.0)	26.22	5.21	-0.90	(60, 20,9.0)	21.77	3.81	-0.62
(30, -20,3.0)	23.74	4.96	-0.81	(70, -20,3.0)	18.02	4.17	-0.73
(30, -20,6.0)	24.53	5.55	-0.85	(70, -20,6.0)	19.52	4.28	-0.81
(30, -20,9.0)	24.85	5.00	-0.84	(70, -20,9.0)	20.12	3.60	-0.57
(30, -10,3.0)	25.13	6.04	-0.39	(70, -10,3.0)	18.84	3.60	-0.20
(30, -10,6.0)	24.95	6.39	-0.48	(70, -10,6.0)	19.79	4.62	-0.55
(30, -10,9.0)	25.44	6.97	-0.50	(70, -10,9.0)	20.92	4.96	-0.60
(30, 10,3.0)	24.75	2.57	-0.73	(70, 0,3.0)	13.29	2.96	-1.27
(30, 10,6.0)	25.45	3.01	-0.66	(70, 0,6.0)	15.26	3.26	-1.02
(30, 10,9.0)	25.80	3.16	-0.69	(70, 0,9.0)	15.83	3.16	-0.62
(30, 20,3.0)	23.80	4.11	-0.84	(70, 10,3.0)	18.27	2.56	-0.47
(30, 20,6.0)	24.87	4.21	-0.88	(70, 10,6.0)	20.65	3.63	-0.51
(30, 20,9.0)	25.50	4.34	-0.71	(70, 10,9.0)	21.26	3.67	-0.45
(40, -20,3.0)	22.32	4.94	-0.75	(70, 20,3.0)	18.46	4.05	-0.67
(40, -20,6.0)	23.02	4.58	-0.81	(70, 20,6.0)	20.21	3.85	-0.64
(40, -20,9.0)	23.24	4.49	-0.76	(70, 20,9.0)	20.44	4.11	-0.66

Table D.3: 3D Velocity Components for Experimental Run D3
[Elliptical Island I_1 (b/a=0.15), F_r=0.19,h=15cm]

Coordinates (cm)	Vx (cm/sec)	Vy (cm/sec)	Vz (cm/sec)	Coordinates (cm)	Vx (cm/sec)	Vy (cm/sec)	Vz (cm/sec)
(-50, -20,3.0)	22.62	3.52	-0.94	(-20, 10,3.0)	29.76	6.89	-1.41
(-50, -20,6.0)	23.35	3.62	-1.16	(-20, 10,6.0)	30.95	7.50	-1.79
(-50, -20,9.0)	23.81	3.57	-0.73	(-20, 10,9.0)	31.24	7.38	-1.47
(-50, -10,3.0)	21.85	1.80	-0.77	(-20, 20,3.0)	29.55	6.45	-0.94
(-50, -10,6.0)	23.45	1.95	-1.05	(-20, 20,6.0)	29.67	6.26	-0.77
(-50, -10,9.0)	23.81	1.93	-0.91	(-20, 20,9.0)	30.43	7.14	-0.78
(-50, 0,3.0)	17.17	2.82	-1.24	(-10, -20,3.0)	30.18	5.49	-1.13
(-50, 0,6.0)	18.47	2.68	-1.42	(-10, -20,6.0)	30.94	5.36	-1.34
(-50, 0,9.0)	18.48	2.63	-0.98	(-10, -20,9.0)	31.01	5.25	-1.07
(-50, 10,3.0)	20.99	6.52	-0.69	(-10, -10,3.0)	30.58	5.14	-1.06
(-50, 10,6.0)	22.78	7.40	-0.83	(-10, -10,6.0)	31.83	5.11	-1.44
(-50, 10,9.0)	23.54	7.20	-0.77	(-10, -10,9.0)	32.06	4.88	-1.06
(-50, 20,3.0)	23.82	5.55	-1.03	(-10, 10,3.0)	30.67	6.18	-1.16
(-50, 20,6.0)	24.31	5.19	-1.06	(-10, 10,6.0)	32.13	6.77	-1.48
(-50, 20,9.0)	24.99	5.74	-0.78	(-10, 10,9.0)	31.97	6.35	-1.01
(-40, -20,3.0)	25.28	3.55	-0.12	(-10, 20,3.0)	31.17	6.42	-1.16
(-40, -20,6.0)	26.70	3.70	-0.98	(-10, 20,6.0)	30.71	5.96	-0.94
(-40, -20,9.0)	26.56	3.60	-1.02	(-10, 20,9.0)	31.20	6.41	-0.82
(-40, -10,3.0)	25.74	1.88	-1.05	(0, -20,3.0)	30.55	5.77	-1.40
(-40, -10,6.0)	26.86	1.52	-1.24	(0, -20,6.0)	31.50	5.64	-1.54
(-40, -10,9.0)	27.25	1.80	-1.08	(0, -20,9.0)	31.49	5.84	-1.11
(-40, 10,3.0)	25.38	8.41	-1.11	(0, -10,3.0)	31.01	6.09	-1.03
(-40, 10,6.0)	27.13	9.34	-1.43	(0, -10,6.0)	32.24	6.14	-1.09
(-40, 10,9.0)	27.83	9.05	-1.35	(0, -10,9.0)	32.12	6.00	-0.75
(-40, 20,3.0)	25.67	6.29	-0.98	(0, 10,3.0)	31.42	5.90	-1.54
(-40, 20,6.0)	25.97	6.25	-0.81	(0, 10,6.0)	32.33	6.06	-1.32
(-40, 20,9.0)	26.77	6.89	-0.75	(0, 10,9.0)	31.99	5.66	-0.97
(-30, -20,3.0)	26.75	4.16	-1.08	(0, 20,3.0)	30.80	6.23	-0.83
(-30, -20,6.0)	28.20	4.43	-1.28	(0, 20,6.0)	30.66	5.41	-0.90
(-30, -20,9.0)	27.81	4.18	-0.86	(0, 20,9.0)	31.10	5.90	-0.73
(-30, -10,3.0)	28.12	3.54	-0.85	(10, -20,3.0)	29.06	5.90	-1.11
(-30, -10,6.0)	28.70	3.30	-0.97	(10, -20,6.0)	30.37	5.94	-1.18
(-30, -10,9.0)	29.61	3.42	-0.91	(10, -20,9.0)	30.76	5.94	-0.98
(-30, 10,3.0)	28.51	7.78	-1.31	(10, -10,3.0)	29.99	6.70	-0.86
(-30, 10,6.0)	29.40	8.53	-1.39	(10, -10,6.0)	31.17	7.10	-1.06
(-30, 10,9.0)	29.91	8.23	-1.21	(10, -10,9.0)	31.16	7.17	-0.63
(-30, 20,3.0)	28.35	6.43	-0.83	(10, 10,3.0)	30.85	4.60	-1.24
(-30, 20,6.0)	28.69	6.29	-0.79	(10, 10,6.0)	31.82	4.91	-1.20
(-30, 20,9.0)	29.00	7.10	-0.85	(10, 10,9.0)	32.23	4.65	-0.79
(-20, -20,3.0)	28.83	4.73	-1.21	(10, 20,3.0)	31.43	5.61	-1.08
(-20, -20,6.0)	29.75	4.73	-1.23	(10, 20,6.0)	31.22	4.80	-1.43
(-20, -20,9.0)	29.39	4.68	-0.88	(10, 20,9.0)	31.85	5.48	-1.16
(-20, -10,3.0)	29.31	4.21	-1.04	(20, -20,3.0)	28.79	6.13	-1.18
(-20, -10,6.0)	30.22	3.94	-1.01	(20, -20,6.0)	29.79	6.03	-1.25
(-20, -10,9.0)	30.50	3.86	-0.82	(20, -20,9.0)	29.93	5.92	-0.93

Coordinates (cm)	Vx (cm/sec)	Vy (cm/sec)	Vz (cm/sec)	Coordinates (cm)	Vx (cm/sec)	Vy (cm/sec)	Vz (cm/sec)
(20, -10,3.0)	29.27	7.30	-0.88	(40, -10,3.0)	25.95	8.05	-0.15
(20, -10,6.0)	30.21	7.42	-0.95	(40, -10,6.0)	27.31	7.99	-0.37
(20, -10,9.0)	30.79	7.63	-0.82	(40, -10,9.0)	29.10	8.86	-0.51
(20, 10,3.0)	31.11	3.40	-1.49	(40, 10,3.0)	26.43	1.26	-0.47
(20, 10,6.0)	31.74	3.70	-1.40	(40, 10,6.0)	27.77	1.42	-0.61
(20, 10,9.0)	32.11	3.88	-0.87	(40, 10,9.0)	28.17	1.57	-0.47
(20, 20,3.0)	30.13	5.19	-0.94	(40, 20,3.0)	27.20	4.09	-0.81
(20, 20,6.0)	30.60	4.75	-1.17	(40, 20,6.0)	28.37	3.97	-1.12
(20, 20,9.0)	30.98	5.33	-1.02	(40, 20,9.0)	28.88	4.30	-1.08
(30, -20,3.0)	27.85	6.00	-1.04	(50, -20,3.0)	24.73	5.27	-0.90
(30, -20,6.0)	28.81	6.00	-1.15	(50, -20,6.0)	25.48	5.64	-0.86
(30, -20,9.0)	29.09	5.83	-0.88	(50, -20,9.0)	25.69	5.25	-0.66
(30, -10,3.0)	28.70	8.03	-0.69	(50, -10,3.0)	23.69	6.84	-0.28
(30, -10,6.0)	29.40	7.92	-0.69	(50, -10,6.0)	24.96	6.69	-0.31
(30, -10,9.0)	30.14	8.00	-0.58	(50, -10,9.0)	26.31	7.53	-0.43
(30, 10,3.0)	29.29	2.65	-0.98	(50, 0,3.0)	1.27	1.82	-0.48
(30, 10,6.0)	29.93	2.91	-0.93	(50, 0,6.0)	2.93	3.29	-0.75
(30, 10,9.0)	30.51	2.91	-0.74	(50, 0,9.0)	3.07	2.38	0.16
(30, 20,3.0)	28.53	4.58	-0.88	(50, 10,3.0)	23.73	2.12	-0.31
(30, 20,6.0)	29.71	4.26	-1.10	(50, 10,6.0)	25.78	2.82	-0.51
(30, 20,9.0)	29.80	4.82	-0.96	(50, 10,9.0)	25.99	2.61	-0.45
(40, -20,3.0)	26.40	5.68	-0.89	(50, 20,3.0)	25.10	3.54	-0.80
(40, -20,6.0)	27.22	5.34	-0.95	(50, 20,6.0)	26.24	3.89	-0.82
(40, -20,9.0)	27.34	5.40	-0.73	(50, 20,9.0)	26.46	4.08	-0.82

Table D.4: 3D Velocity Components for Experimental Run D4
[Elliptical Island I_2 (b/a=0.2), F_r=0.14,h=15cm]

Coordinates (cm)	Vx (cm/sec)	Vy (cm/sec)	Vz (cm/sec)	Coordinates (cm)	Vx (cm/sec)	Vy (cm/sec)	Vz (cm/sec)
(-60, -20,3.0)	15.30	3.50	-0.74	(-30, -20,3.0)	17.66	2.57	-0.79
(-60, -20,6.0)	15.66	3.28	-0.77	(-30, -20,6.0)	18.81	2.87	-0.87
(-60, -20,9.0)	16.26	3.31	-0.50	(-30, -20,9.0)	19.33	2.93	-0.76
(-60, -10,3.0)	14.87	3.01	-0.28	(-30, -10,3.0)	17.39	1.01	-0.42
(-60, -10,6.0)	15.88	3.14	-0.44	(-30, -10,6.0)	17.82	0.92	-0.59
(-60, -10,9.0)	16.34	3.27	-0.40	(-30, -10,9.0)	18.86	0.90	-0.48
(-60, 0,3.0)	15.10	3.42	-0.51	(-30, 10,3.0)	18.17	6.33	-0.66
(-60, 0,6.0)	16.43	3.72	-0.60	(-30, 10,6.0)	18.91	6.89	-0.82
(-60, 0,9.0)	16.77	3.79	-0.50	(-30, 10,9.0)	19.58	7.23	-0.85
(-60, 10,3.0)	15.58	3.24	-0.62	(-30, 20,3.0)	19.23	4.68	-0.82
(-60, 10,6.0)	16.23	3.42	-0.65	(-30, 20,6.0)	19.86	5.47	-0.72
(-60, 10,9.0)	16.68	3.88	-0.52	(-30, 20,9.0)	19.69	4.03	-0.74
(-60, 20,3.0)	15.93	3.26	-0.68	(-20, -20,3.0)	18.92	3.15	-0.74
(-60, 20,6.0)	17.25	3.82	-0.80	(-20, -20,6.0)	20.02	3.50	-0.76
(-60, 20,9.0)	17.01	3.79	-0.58	(-20, -20,9.0)	20.22	3.50	-0.66
(-50, -20,3.0)	15.06	3.03	-0.73	(-20, -10,3.0)	20.11	1.88	-0.80
(-50, -20,6.0)	15.79	2.84	-0.80	(-20, -10,6.0)	20.59	1.89	-0.80
(-50, -20,9.0)	16.49	2.87	-0.62	(-20, -10,9.0)	21.58	2.04	-0.78
(-50, -10,3.0)	14.88	2.94	-0.55	(-20, 10,3.0)	20.33	5.67	-0.73
(-50, -10,6.0)	15.57	3.07	-0.86	(-20, 10,6.0)	21.19	6.16	-0.96
(-50, -10,9.0)	16.49	2.81	-0.55	(-20, 10,9.0)	21.78	6.42	-0.84
(-50, 0,3.0)	14.63	3.25	-0.56	(-20, 20,3.0)	20.81	4.94	-0.69
(-50, 0,6.0)	15.83	3.47	-0.77	(-20, 20,6.0)	21.52	5.63	-0.91
(-50, 0,9.0)	16.34	3.36	-0.53	(-20, 20,9.0)	21.18	5.07	-0.45
(-50, 10,3.0)	15.53	3.54	-0.59	(-10, -20,3.0)	20.57	3.87	-0.80
(-50, 10,6.0)	16.15	3.81	-0.64	(-10, -20,6.0)	21.59	4.11	-0.87
(-50, 10,9.0)	16.75	4.15	-0.67	(-10, -20,9.0)	21.84	4.09	-0.74
(-50, 20,3.0)	16.41	3.30	-0.86	(-10, -10,3.0)	21.76	3.87	-0.80
(-50, 20,6.0)	17.33	3.92	-0.87	(-10, -10,6.0)	21.80	4.03	-0.75
(-50, 20,9.0)	17.22	2.91	-0.75	(-10, -10,9.0)	22.37	3.11	-0.67
(-40, -20,3.0)	15.63	2.61	-0.72	(-10, 10,3.0)	21.82	5.29	-1.01
(-40, -20,6.0)	16.78	2.93	-0.84	(-10, 10,6.0)	22.36	5.68	-0.93
(-40, -20,9.0)	17.60	3.12	-0.74	(-10, 10,9.0)	23.12	6.01	-0.85
(-40, -10,3.0)	15.38	1.76	-0.62	(-10, 20,3.0)	22.05	4.69	-0.80
(-40, -10,6.0)	15.78	1.93	-0.46	(-10, 20,6.0)	22.82	5.48	-1.08
(-40, -10,9.0)	17.03	1.79	-0.54	(-10, 20,9.0)	22.57	4.82	-0.61
(-40, 0,3.0)	12.92	2.86	-1.07	(0, -20,3.0)	20.63	4.21	-0.77
(-40, 0,6.0)	13.49	2.76	-1.00	(0, -20,6.0)	21.49	4.32	-0.88
(-40, 0,9.0)	13.85	2.51	-0.80	(0, -20,9.0)	21.78	4.27	-0.73
(-40, 10,3.0)	15.15	4.93	-0.49	(0, -10,3.0)	22.18	4.44	-0.92
(-40, 10,6.0)	15.73	5.37	-0.56	(0, -10,6.0)	21.99	4.70	-0.59
(-40, 10,9.0)	16.46	5.69	-0.74	(0, -10,9.0)	22.55	4.19	-0.65
(-40, 20,3.0)	17.21	3.94	-0.88	(0, 10,3.0)	22.72	4.07	-1.07
(-40, 20,6.0)	17.74	4.74	-0.77	(0, 10,6.0)	22.38	4.29	-0.69
(-40, 20,9.0)	17.76	2.57	-0.79	(0, 10,9.0)	23.27	4.65	-0.67

Coordinates (cm)	Vx (cm/sec)	Vy (cm/sec)	Vz (cm/sec)	Coordinates (cm)	Vx (cm/sec)	Vy (cm/sec)	Vz (cm/sec)
(0,20,3.0)	22.15	4.25	-0.73	(40, -10,3.0)	16.99	5.43	-0.25
(0, 20,6.0)	22.95	5.10	-1.00	(40, -10,6.0)	17.77	5.46	-0.29
(0, 20,9.0)	22.79	4.37	-0.64	(40, -10,9.0)	17.85	4.94	-0.26
(10, -20,3.0)	20.03	4.40	-0.71	(40, 0,3.0)	0.90	1.51	-0.90
(10, -20,6.0)	21.04	4.48	-0.85	(40, 0,6.0)	1.59	1.51	-1.29
(10, -20,9.0)	21.22	4.55	-0.60	(40, 0,9.0)	3.25	1.23	0.23
(10, -10,3.0)	21.35	5.24	-0.74	(40, 10,3.0)	16.20	1.44	0.03
(10, -10,6.0)	21.56	5.08	-0.67	(40, 10,6.0)	17.96	1.89	-0.36
(10, -10,9.0)	21.83	5.00	-0.49	(40, 10,9.0)	18.44	1.93	-0.21
(10, 10,3.0)	21.91	3.00	-0.79	(40, 20,3.0)	18.43	2.96	-0.57
(10, 10,6.0)	22.19	3.31	-0.66	(40, 20,6.0)	19.08	3.37	-0.68
(10, 10,9.0)	22.60	3.43	-0.47	(40, 20,9.0)	18.68	2.82	-0.41
(10, 20,3.0)	21.95	3.96	-0.77	(50, -20,3.0)	16.11	3.62	-0.63
(10, 20,6.0)	22.91	4.78	-1.08	(50, -20,6.0)	17.51	3.89	-0.71
(10, 20,9.0)	22.71	3.92	-0.67	(50, -20,9.0)	17.72	4.06	-0.44
(20, -20,3.0)	19.35	4.64	-0.71	(50, -10,3.0)	15.39	4.13	-0.24
(20, -20,6.0)	20.51	4.70	-0.90	(50, -10,6.0)	16.76	4.02	-0.31
(20, -20,9.0)	20.58	4.89	-0.53	(50, -10,9.0)	17.43	3.91	-0.38
(20, -10,3.0)	21.15	6.31	-0.68	(50, 0,3.0)	8.98	3.08	-1.11
(20, -10,6.0)	21.36	6.41	-0.62	(50, 0,6.0)	10.23	2.98	-0.99
(20, -10,9.0)	21.15	5.23	-0.35	(50, 0,9.0)	11.82	3.04	-0.05
(20, 10,3.0)	21.49	1.97	-0.80	(50, 10,3.0)	15.84	2.15	-0.24
(20, 10,6.0)	22.39	2.37	-0.88	(50, 10,6.0)	17.52	2.57	-0.26
(20, 10,9.0)	22.34	2.25	-0.45	(50, 10,9.0)	18.19	2.67	-0.31
(20, 20,3.0)	21.06	3.49	-0.75	(50, 20,3.0)	17.57	3.21	-0.59
(20, 20,6.0)	22.16	4.25	-1.08	(50, 20,6.0)	18.10	3.40	-0.62
(20, 20,9.0)	21.92	3.29	-0.65	(50, 20,9.0)	17.80	2.86	-0.36
(30, -20,3.0)	18.58	4.43	-0.70	(60, -20,3.0)	15.28	3.23	-0.73
(30, -20,6.0)	19.91	4.55	-0.90	(60, -20,6.0)	16.63	3.60	-0.74
(30, -20,9.0)	20.09	4.85	-0.58	(60, -20,9.0)	16.78	3.54	-0.39
(30, -10,3.0)	18.69	6.38	-0.39	(60, -10,3.0)	14.71	3.77	-0.33
(30, -10,6.0)	18.88	6.17	-0.36	(60, -10,6.0)	16.75	3.87	-0.59
(30, -10,9.0)	19.44	5.81	-0.16	(60, -10,9.0)	17.12	3.31	-0.56
(30, 10,3.0)	18.74	0.96	-0.32	(60, 0,3.0)	12.89	2.77	-1.06
(30, 10,6.0)	20.06	1.20	-0.35	(60, 0,6.0)	14.25	3.10	-0.77
(30, 10,9.0)	20.28	1.18	-0.18	(60, 0,9.0)	13.64	3.15	-0.32
(30, 20,3.0)	19.38	3.14	-0.69	(60, 10,3.0)	15.46	2.58	-0.49
(30, 20,6.0)	20.24	3.71	-0.92	(60, 10,6.0)	17.06	2.92	-0.53
(30, 20,9.0)	19.92	2.97	-0.55	(60, 10,9.0)	17.91	3.07	-0.55
(40, -20,3.0)	16.67	3.92	-0.49	(60, 20,3.0)	17.28	3.49	-0.71
(40, -20,6.0)	18.09	4.09	-0.64	(60, 20,6.0)	17.70	3.46	-0.67
(40, -20,9.0)	18.36	4.48	-0.46	(60, 20,9.0)	17.49	2.93	-0.38

Table D.5: 3D Velocity Components for Experimental Run D5
[Elliptical Island I_2 (b/a=0.2), F_r=0.16,h=15cm]

Coordinates (cm)	Vx (cm/sec)	Vy (cm/sec)	Vz (cm/sec)	Coordinates (cm)	Vx (cm/sec)	Vy (cm/sec)	Vz (cm/sec)
(-60, -20,3.0)	16.16	3.58	-0.66	(-30, -20,3.0)	19.31	3.50	-0.70
(-60, -20,6.0)	16.92	3.43	-0.71	(-30, -20,6.0)	20.17	3.49	-0.80
(-60, -20,9.0)	17.32	3.75	-0.51	(-30, -20,9.0)	20.22	3.66	-0.55
(-60, -10,3.0)	15.40	3.33	-0.23	(-30, -10,3.0)	19.28	1.51	-0.56
(-60, -10,6.0)	17.05	3.50	-0.42	(-30, -10,6.0)	20.30	1.30	-0.46
(-60, -10,9.0)	17.89	3.31	-0.41	(-30, -10,9.0)	20.67	1.11	-0.43
(-60, 0,3.0)	16.32	3.88	-0.39	(-30, 10,3.0)	19.12	7.68	-0.36
(-60, 0,6.0)	17.55	4.22	-0.50	(-30, 10,6.0)	20.03	8.36	-0.51
(-60, 0,9.0)	18.05	4.32	-0.32	(-30, 10,9.0)	20.17	8.13	-0.34
(-60, 10,3.0)	16.93	4.20	-0.40	(-30, 20,3.0)	20.67	6.20	-0.78
(-60, 10,6.0)	17.64	4.30	-0.36	(-30, 20,6.0)	20.82	5.73	-0.91
(-60, 10,9.0)	18.41	4.61	-0.41	(-30, 20,9.0)	21.04	5.61	-0.43
(-60, 20,3.0)	17.52	4.16	-0.88	(-20, -20,3.0)	21.24	3.94	-0.67
(-60, 20,6.0)	17.54	3.81	-0.91	(-20, -20,6.0)	21.97	3.99	-0.74
(-60, 20,9.0)	17.57	4.01	-0.47	(-20, -20,9.0)	21.78	3.95	-0.46
(-50, -20,3.0)	16.70	3.47	-0.72	(-20, -10,3.0)	21.79	3.22	-0.63
(-50, -20,6.0)	17.57	3.36	-0.82	(-20, -10,6.0)	23.08	2.54	-0.80
(-50, -20,9.0)	17.92	3.71	-0.60	(-20, -10,9.0)	23.04	2.21	-0.49
(-50, -10,3.0)	16.18	3.13	-0.59	(-20, 10,3.0)	22.71	7.09	-0.71
(-50, -10,6.0)	17.39	3.08	-0.66	(-20, 10,6.0)	23.60	7.51	-1.00
(-50, -10,9.0)	18.22	2.53	-0.63	(-20, 10,9.0)	23.38	6.98	-0.59
(-50, 0,3.0)	15.82	3.37	-0.57	(-20, 20,3.0)	22.64	6.37	-0.89
(-50, 0,6.0)	17.55	4.52	-0.81	(-20, 20,6.0)	22.66	6.57	-1.08
(-50, 0,9.0)	18.13	4.25	-0.39	(-20, 20,9.0)	22.79	5.74	-0.46
(-50, 10,3.0)	16.66	4.30	-0.40	(-10, -20,3.0)	22.84	4.91	-0.71
(-50, 10,6.0)	17.50	4.65	-0.46	(-10, -20,6.0)	23.64	5.11	-0.84
(-50, 10,9.0)	18.13	4.79	-0.43	(-10, -20,9.0)	23.56	5.20	-0.55
(-50, 20,3.0)	17.88	4.69	-0.90	(-10, -10,3.0)	23.55	4.78	-0.68
(-50, 20,6.0)	18.03	4.47	-0.96	(-10, -10,6.0)	24.25	3.90	-0.66
(-50, 20,9.0)	18.20	4.26	-0.51	(-10, -10,9.0)	24.36	3.64	-0.41
(-40, -20,3.0)	17.29	3.24	-0.67	(-10, 10,3.0)	23.36	6.13	-0.97
(-40, -20,6.0)	18.28	3.17	-0.80	(-10, 10,6.0)	24.21	6.63	-1.29
(-40, -20,9.0)	18.57	3.55	-0.59	(-10, 10,9.0)	24.14	6.40	-0.83
(-40, -10,3.0)	16.39	2.02	-0.58	(-10, 20,3.0)	24.10	5.99	-1.07
(-40, -10,6.0)	17.12	1.99	-0.48	(-10, 20,6.0)	24.12	6.18	-1.30
(-40, -10,9.0)	17.90	1.63	-0.46	(-10, 20,9.0)	24.26	5.40	-0.55
(-40, 0,3.0)	14.14	3.46	-1.06	(0, -20,3.0)	22.83	4.77	-0.70
(-40, 0,6.0)	14.48	3.38	-1.14	(0, -20,6.0)	23.65	5.07	-0.88
(-40, 0,9.0)	15.33	3.29	-0.70	(0, -20,9.0)	23.68	5.27	-0.60
(-40, 10,3.0)	16.92	5.57	-0.40	(0, -10,3.0)	24.21	5.93	-1.05
(-40, 10,6.0)	17.92	6.27	-0.57	(0, -10,6.0)	24.28	4.92	-0.83
(-40, 10,9.0)	18.42	6.42	-0.46	(0, -10,9.0)	24.54	4.76	-0.52
(-40, 20,3.0)	18.70	5.28	-0.85	(0, 10,3.0)	24.25	4.66	-0.78
(-40, 20,6.0)	18.98	5.03	-0.94	(0, 10,6.0)	25.07	5.19	-0.99
(-40, 20,9.0)	19.30	4.80	-0.51	(0, 10,9.0)	25.15	5.28	-0.69

Coordinates (cm)	Vx (cm/sec)	Vy (cm/sec)	Vz (cm/sec)	Coordinates (cm)	Vx (cm/sec)	Vy (cm/sec)	Vz (cm/sec)
(0,20,3.0)	24.43	5.55	-1.03	(40, -10,3.0)	18.10	6.13	-0.09
(0, 20,6.0)	23.80	5.78	-1.39	(40, -10,6.0)	18.74	5.89	-0.06
(0, 20,9.0)	23.98	4.93	-0.58	(40, -10,9.0)	19.54	5.48	-0.08
(10, -20,3.0)	22.21	5.18	-0.66	(40, 0,3.0)	0.52	1.76	-0.77
(10, -20,6.0)	23.19	5.34	-0.82	(40, 0,6.0)	2.25	2.12	-1.01
(10, -20,9.0)	23.11	6.45	-0.54	(40, 0,9.0)	3.08	1.49	0.39
(10, -10,3.0)	23.24	6.57	-0.74	(40, 10,3.0)	17.93	2.04	0.06
(10, -10,6.0)	23.50	5.81	-0.67	(40, 10,6.0)	19.42	2.31	-0.60
(10, -10,9.0)	23.70	5.52	-0.76	(40, 10,9.0)	20.08	2.41	-0.15
(10, 10,3.0)	24.15	3.93	-0.75	(40, 20,3.0)	19.72	3.66	-0.71
(10, 10,6.0)	25.10	4.57	-0.87	(40, 20,6.0)	20.24	3.99	-0.77
(10, 10,9.0)	25.33	4.45	-0.54	(40, 20,9.0)	19.79	3.14	-0.28
(10, 20,3.0)	23.85	4.97	-0.91	(50, -20,3.0)	17.46	4.07	-0.49
(10, 20,6.0)	23.82	5.09	-1.18	(50, -20,6.0)	18.62	4.92	-0.71
(10, 20,9.0)	23.62	4.14	-0.47	(50, -20,9.0)	19.39	4.97	-0.37
(20, -20,3.0)	21.43	5.31	-0.69	(50, -10,3.0)	16.85	4.82	-0.22
(20, -20,6.0)	22.56	5.32	-0.84	(50, -10,6.0)	17.79	4.63	-0.37
(20, -20,9.0)	22.37	7.29	-0.54	(50, -10,9.0)	18.33	4.31	-0.29
(20, -10,3.0)	22.35	7.29	-0.54	(50, 0,3.0)	10.11	3.06	-1.40
(20, -10,6.0)	22.81	6.77	-0.60	(50, 0,6.0)	11.01	2.38	-1.54
(20, -10,9.0)	22.94	6.34	-1.12	(50, 0,9.0)	12.96	3.09	-0.25
(20, 10,3.0)	23.14	2.52	-0.76	(50, 10,3.0)	17.02	2.82	-0.20
(20, 10,6.0)	24.19	3.16	-0.80	(50, 10,6.0)	19.29	3.07	-0.27
(20, 10,9.0)	24.56	2.85	-0.42	(50, 10,9.0)	19.36	3.12	-0.22
(20, 20,3.0)	22.95	4.50	-0.86	(50, 20,3.0)	19.05	3.78	-0.77
(20, 20,6.0)	23.53	4.52	-1.06	(50, 20,6.0)	19.66	3.96	-0.85
(20, 20,9.0)	22.94	3.44	-0.40	(50, 20,9.0)	19.27	3.23	-0.35
(30, -20,3.0)	19.96	5.09	-0.53	(60, -20,3.0)	16.53	3.54	-0.47
(30, -20,6.0)	21.01	5.31	-0.74	(60, -20,6.0)	17.88	4.26	-0.58
(30, -20,9.0)	21.15	6.35	-0.38	(60, -20,9.0)	18.98	4.29	-0.41
(30, -10,3.0)	19.86	7.45	-0.24	(60, -10,3.0)	16.86	4.44	-0.34
(30, -10,6.0)	20.40	7.03	-0.27	(60, -10,6.0)	18.17	4.60	-0.57
(30, -10,9.0)	20.86	6.56	-0.50	(60, -10,9.0)	18.50	3.97	-0.45
(30, 10,3.0)	20.38	1.18	-0.33	(60, 0,3.0)	12.63	3.07	-1.44
(30, 10,6.0)	21.64	1.41	-0.35	(60, 0,6.0)	15.37	3.27	-1.00
(30, 10,9.0)	22.15	1.36	-0.18	(60, 0,9.0)	15.21	3.55	-0.40
(30, 20,3.0)	21.18	3.90	-0.68	(60, 10,3.0)	16.46	3.27	-0.40
(30, 20,6.0)	21.73	4.07	-0.79	(60, 10,6.0)	18.90	3.48	-0.58
(30, 20,9.0)	21.21	3.14	-0.29	(60, 10,9.0)	19.03	3.48	-0.39
(40, -20,3.0)	18.88	4.60	-0.42	(60, 20,3.0)	18.04	4.07	-0.67
(40, -20,6.0)	19.88	5.01	-0.71	(60, 20,6.0)	18.73	4.10	-0.75
(40, -20,9.0)	20.34	5.07	-0.26	(60, 20,9.0)	18.42	3.47	-0.34

Table D.6: 3D Velocity Components for Experimental Run D6
[Elliptical Island I_2 (b/a=0.2), F_r=0.19,h=15cm]

Coordinates (cm)	Vx (cm/sec)	Vy (cm/sec)	Vz (cm/sec)	Coordinates (cm)	Vx (cm/sec)	Vy (cm/sec)	Vz (cm/sec)
(-60, -20,3.0)	21.93	4.50	-0.89	(-30, -20,3.0)	28.11	3.82	-0.95
(-60, -20,6.0)	22.49	4.26	-0.94	(-30, -20,6.0)	28.24	4.02	-1.07
(-60, -20,9.0)	22.90	4.47	-0.64	(-30, -20,9.0)	27.99	4.16	-0.84
(-60, -10,3.0)	22.50	4.02	-0.33	(-30, -10,3.0)	27.27	1.58	-0.62
(-60, -10,6.0)	23.57	4.21	-0.55	(-30, -10,6.0)	27.60	1.40	-0.67
(-60, -10,9.0)	23.94	4.18	-0.51	(-30, -10,9.0)	27.71	1.27	-0.58
(-60, 0,3.0)	24.10	4.62	-0.58	(-30, 10,3.0)	24.32	8.86	-0.66
(-60, 0,6.0)	23.47	5.03	-0.70	(-30, 10,6.0)	27.89	9.64	-0.86
(-60, 0,9.0)	22.84	5.14	-0.53	(-30, 10,9.0)	29.10	9.73	-0.78
(-60, 10,3.0)	20.52	4.69	-0.66	(-30, 20,3.0)	26.62	6.86	-1.02
(-60, 10,6.0)	22.25	4.87	-0.65	(-30, 20,6.0)	26.77	7.11	-1.03
(-60, 10,9.0)	23.28	5.37	-0.60	(-30, 20,9.0)	26.26	6.07	-0.76
(-60, 20,3.0)	21.29	4.68	-0.98	(-20, -20,3.0)	32.38	4.48	-0.90
(-60, 20,6.0)	21.23	4.85	-1.08	(-20, -20,6.0)	31.00	4.74	-0.96
(-60, 20,9.0)	20.85	4.95	-0.67	(-20, -20,9.0)	31.40	4.72	-0.72
(-50, -20,3.0)	22.66	4.12	-0.92	(-20, -10,3.0)	29.91	3.19	-0.92
(-50, -20,6.0)	23.35	3.92	-1.03	(-20, -10,6.0)	31.46	2.79	-1.02
(-50, -20,9.0)	23.69	4.15	-0.78	(-20, -10,9.0)	31.83	2.70	-0.82
(-50, -10,3.0)	23.64	3.85	-0.72	(-20, 10,3.0)	30.39	8.06	-0.92
(-50, -10,6.0)	24.03	3.91	-0.98	(-20, 10,6.0)	30.82	8.64	-1.25
(-50, -10,9.0)	24.38	3.41	-0.75	(-20, 10,9.0)	32.24	8.50	-0.92
(-50, 0,3.0)	23.36	4.21	-0.72	(-20, 20,3.0)	29.42	7.13	-1.00
(-50, 0,6.0)	23.47	5.04	-1.00	(-20, 20,6.0)	28.94	7.72	-1.26
(-50, 0,9.0)	22.94	4.80	-0.59	(-20, 20,9.0)	29.12	6.85	-0.58
(-50, 10,3.0)	20.19	4.96	-0.64	(-10, -20,3.0)	33.41	5.54	-0.96
(-50, 10,6.0)	22.07	5.35	-0.71	(-10, -20,6.0)	32.94	5.82	-1.09
(-50, 10,9.0)	22.93	5.66	-0.71	(-10, -20,9.0)	31.68	5.86	-0.83
(-50, 20,3.0)	21.73	5.02	-1.12	(-10, -10,3.0)	31.46	5.46	-0.95
(-50, 20,6.0)	21.82	5.31	-1.16	(-10, -10,6.0)	32.66	5.05	-0.90
(-50, 20,9.0)	21.60	4.50	-0.81	(-10, -10,9.0)	32.90	4.27	-0.70
(-40, -20,3.0)	24.18	3.69	-0.89	(-10, 10,3.0)	31.12	7.23	-1.26
(-40, -20,6.0)	24.22	3.87	-1.05	(-10, 10,6.0)	32.16	7.79	-1.40
(-40, -20,9.0)	25.00	4.22	-0.85	(-10, 10,9.0)	32.38	7.88	-1.07
(-40, -10,3.0)	24.47	2.39	-0.77	(-10, 20,3.0)	28.14	6.74	-1.18
(-40, -10,6.0)	23.86	2.49	-0.60	(-10, 20,6.0)	29.14	7.39	-1.50
(-40, -10,9.0)	24.72	2.18	-0.64	(-10, 20,9.0)	29.49	6.48	-0.74
(-40, 0,3.0)	19.04	4.00	-1.36	(0, -20,3.0)	30.89	5.69	-0.94
(-40, 0,6.0)	19.08	3.88	-1.36	(0, -20,6.0)	30.33	5.94	-1.12
(-40, 0,9.0)	18.42	3.66	-0.96	(0, -20,9.0)	31.07	6.03	-0.85
(-40, 10,3.0)	20.88	6.65	-0.57	(0, -10,3.0)	28.69	6.53	-1.25
(-40, 10,6.0)	22.69	7.37	-0.72	(0, -10,6.0)	30.47	6.11	-0.89
(-40, 10,9.0)	23.55	7.67	-0.78	(0, -10,9.0)	31.20	5.67	-0.75
(-40, 20,3.0)	22.67	5.81	-1.10	(0, 10,3.0)	27.38	5.53	-1.19
(-40, 20,6.0)	23.07	6.20	-1.08	(0, 10,6.0)	29.23	5.99	-1.06
(-40, 20,9.0)	23.21	4.59	-0.84	(0, 10,9.0)	29.50	6.29	-0.86

Coordinates (cm)	Vx (cm/sec)	Vy (cm/sec)	Vz (cm/sec)	Coordinates (cm)	Vx (cm/sec)	Vy (cm/sec)	Vz (cm/sec)
(0,20,3.0)	26.20	6.18	-1.11	(40, -10,3.0)	20.14	7.32	-0.22
(0, 20,6.0)	27.43	6.89	-1.50	(40, -10,6.0)	29.17	7.20	-0.23
(0, 20,9.0)	28.05	5.89	-0.78	(40, -10,9.0)	32.36	6.61	-0.22
(10, -20,3.0)	30.39	6.06	-0.87	(40, 0,3.0)	11.67	2.07	-1.07
(10, -20,6.0)	30.69	6.21	-1.06	(40, 0,6.0)	13.32	2.28	-1.48
(10, -20,9.0)	30.73	6.11	-1.11	(40, 0,9.0)	20.30	1.72	0.39
(10, -10,3.0)	27.32	7.46	-0.94	(40, 10,3.0)	25.59	2.19	0.06
(10, -10,6.0)	30.87	6.90	-0.85	(40, 10,6.0)	29.66	2.65	-0.60
(10, -10,9.0)	31.26	6.67	-0.78	(40, 10,9.0)	29.13	2.74	-0.23
(10, 10,3.0)	31.03	4.37	-0.98	(40, 20,3.0)	28.89	4.18	-0.81
(10, 10,6.0)	31.86	4.96	-0.96	(40, 20,6.0)	28.94	4.66	-0.92
(10, 10,9.0)	32.14	4.97	-0.64	(40, 20,9.0)	29.18	3.78	-0.44
(10, 20,3.0)	27.09	5.64	-1.06	(50, -20,3.0)	25.81	4.87	-0.72
(10, 20,6.0)	27.85	6.27	-1.43	(50, -20,6.0)	27.76	5.56	-0.90
(10, 20,9.0)	28.06	5.12	-0.73	(50, -20,9.0)	29.28	5.71	-0.52
(20, -20,3.0)	30.67	6.30	-0.89	(50, -10,3.0)	25.83	5.66	-0.29
(20, -20,6.0)	30.08	6.35	-1.11	(50, -10,6.0)	28.88	5.48	-0.43
(20, -20,9.0)	31.58	7.65	-0.68	(50, -10,9.0)	30.03	5.21	-0.43
(20, -10,3.0)	28.93	8.61	-0.78	(50, 0,3.0)	18.15	3.91	-1.58
(20, -10,6.0)	30.79	8.37	-0.78	(50, 0,6.0)	18.84	3.44	-1.59
(20, -10,9.0)	32.13	7.31	-0.90	(50, 0,9.0)	21.38	3.90	-0.18
(20, 10,3.0)	25.00	2.83	-0.99	(50, 10,3.0)	27.12	3.13	-0.28
(20, 10,6.0)	30.33	3.48	-1.07	(50, 10,6.0)	28.54	3.57	-0.34
(20, 10,9.0)	30.72	3.22	-0.55	(50, 10,9.0)	29.00	3.66	-0.34
(20, 20,3.0)	27.19	5.04	-1.02	(50, 20,3.0)	22.42	4.42	-0.86
(20, 20,6.0)	28.06	5.57	-1.36	(50, 20,6.0)	27.67	4.66	-0.93
(20, 20,9.0)	28.54	4.28	-0.68	(50, 20,9.0)	29.47	3.86	-0.45
(30, -20,3.0)	31.50	6.03	-0.79	(60, -20,3.0)	24.43	4.29	-0.77
(30, -20,6.0)	31.62	6.24	-1.05	(60, -20,6.0)	26.66	4.97	-0.85
(30, -20,9.0)	31.66	7.06	-0.62	(60, -20,9.0)	28.66	4.95	-0.51
(30, -10,3.0)	28.80	8.75	-0.41	(60, -10,3.0)	25.84	5.19	-0.43
(30, -10,6.0)	31.06	8.36	-0.40	(60, -10,6.0)	29.50	5.36	-0.74
(30, -10,9.0)	32.77	7.84	-0.41	(60, -10,9.0)	30.31	4.60	-0.65
(30, 10,3.0)	*28.86*	1.35	-0.41	(60, 0,3.0)	22.67	3.70	-1.57
(30, 10,6.0)	30.99	1.65	-0.45	(60, 0,6.0)	26.30	4.05	-1.12
(30, 10,9.0)	31.32	1.61	-0.23	(60, 0,9.0)	25.09	4.25	-0.45
(30, 20,3.0)	26.70	4.45	-0.87	(60, 10,3.0)	26.23	3.69	-0.57
(30, 20,6.0)	28.76	4.93	-1.09	(60, 10,6.0)	27.96	4.05	-0.70
(30, 20,9.0)	28.58	3.88	-0.55	(60, 10,9.0)	28.50	4.15	-0.60
(40, -20,3.0)	32.22	5.39	-0.58	(60, 20,3.0)	21.23	4.78	-0.88
(40, -20,6.0)	32.10	5.75	-0.86	(60, 20,6.0)	26.35	4.78	-0.90
(40, -20,9.0)	32.17	6.05	-0.47	(60, 20,9.0)	28.17	4.05	-0.46

Table D.7: 3D Velocity Components for Experimental Run D7
[Elliptical Island I_3 (b/a=0.3), F_r=0.14,h=15cm]

Coordinates (cm)	Vx (cm/sec)	Vy (cm/sec)	Vz (cm/sec)	Coordinates (cm)	Vx (cm/sec)	Vy (cm/sec)	Vz (cm/sec)
(-55, -20,3.0)	16.16	2.25	-0.62	(-20, -20,3.0)	21.70	1.90	-0.37
(-55, -20,6.0)	16.14	2.85	-0.77	(-20, -20,6.0)	22.42	2.00	-0.70
(-55, -20,9.0)	16.46	2.22	-0.53	(-20, -20,9.0)	22.49	1.79	-0.44
(-55, -10,3.0)	15.13	2.59	-0.40	(-20, -10,3.0)	22.64	-0.62	-0.96
(-55, -10,6.0)	16.44	2.84	-0.48	(-20, -10,6.0)	22.60	-0.17	-1.06
(-55, -10,9.0)	16.32	2.51	-0.35	(-20, -10,9.0)	23.09	-1.59	-1.02
(-55, 0,3.0)	15.20	2.47	-0.36	(-20, 10,3.0)	21.26	8.60	-0.97
(-55, 0,6.0)	16.28	2.54	-0.19	(-20, 10,6.0)	21.62	8.89	-1.05
(-55, 0,9.0)	16.66	3.38	-0.46	(-20, 10,9.0)	22.20	10.26	-0.81
(-55, 10,3.0)	15.66	2.92	-0.17	(-20, 20,3.0)	22.06	5.66	-0.29
(-55, 10,6.0)	16.53	3.64	-0.46	(-20, 20,6.0)	22.48	5.68	-0.24
(-55, 10,9.0)	16.86	3.29	-0.34	(-20, 20,9.0)	22.51	5.83	-0.17
(-55, 20,3.0)	16.45	2.84	-0.55	(-10, -20,3.0)	23.82	3.00	-0.34
(-55, 20,6.0)	16.96	3.35	-0.53	(-10, -20,6.0)	24.79	3.16	-0.64
(-55, 20,9.0)	17.16	2.92	-0.26	(-10, -20,9.0)	24.75	2.33	-0.40
(-45, -20,3.0)	16.44	2.12	-0.52	(-10, -10,3.0)	25.51	2.81	-0.55
(-45, -20,6.0)	16.81	2.88	-0.70	(-10, -10,6.0)	25.58	2.66	-0.79
(-45, -20,9.0)	16.69	1.94	-0.45	(-10, -10,9.0)	25.81	2.38	-0.47
(-45, -10,3.0)	15.18	1.88	-0.36	(-10, 10,3.0)	24.54	6.18	-0.87
(-45, -10,6.0)	16.30	2.06	-0.57	(-10, 10,6.0)	25.04	6.39	-0.94
(-45, -10,9.0)	16.67	1.89	-0.50	(-10, 10,9.0)	25.05	6.71	-0.48
(-45, 0,3.0)	14.60	2.12	-0.36	(-10, 20,3.0)	24.24	5.59	-0.15
(-45, 0,6.0)	15.85	2.56	-0.73	(-10, 20,6.0)	25.31	5.66	-0.41
(-45, 0,9.0)	16.13	2.39	-0.68	(-10, 20,9.0)	24.89	5.79	-0.45
(-45, 10,3.0)	15.27	3.49	-0.43	(0, -20,3.0)	24.66	4.49	-0.20
(-45, 10,6.0)	15.83	4.35	-0.39	(0, -20,6.0)	25.07	4.26	-0.35
(-45, 10,9.0)	16.74	3.49	-0.32	(0, -20,9.0)	25.57	3.16	-0.22
(-45, 20,3.0)	16.94	3.12	-0.50	(0, -10,3.0)	25.54	5.12	-0.81
(-45, 20,6.0)	17.42	3.33	-0.48	(0, -10,6.0)	26.70	4.57	-0.91
(-45, 20,9.0)	17.75	3.34	-0.42	(0, -10,9.0)	26.08	4.17	-0.48
(-35, -20,3.0)	17.23	1.28	-0.41	(0, 10,3.0)	25.59	4.09	-1.07
(-35, -20,6.0)	17.83	1.95	-0.61	(0, 10,6.0)	26.19	4.57	-0.98
(-35, -20,9.0)	18.28	1.65	-0.40	(0, 10,9.0)	26.17	4.96	-0.54
(-35, -10,3.0)	16.85	-0.35	-0.32	(0,20,3.0)	25.22	4.92	0.04
(-35, -10,6.0)	16.76	0.07	-0.66	(0, 20,6.0)	26.39	4.94	-0.22
(-35, -10,9.0)	17.38	-0.16	-0.38	(0, 20,9.0)	25.65	5.19	-0.55
(-35, 0,3.0)	12.15	1.57	-0.92	(10, -20,3.0)	24.13	5.12	-0.21
(-35, 0,6.0)	12.32	2.17	-1.09	(10, -20,6.0)	24.34	4.86	-0.71
(-35, 0,9.0)	12.54	1.62	-0.76	(10, -20,9.0)	24.64	4.18	-0.16
(-35, 10,3.0)	14.95	5.00	-0.19	(10, -10,3.0)	25.13	7.26	-0.46
(-35, 10,6.0)	15.14	5.21	-0.28	(10, -10,6.0)	25.08	6.14	-0.78
(-35, 10,9.0)	16.01	5.39	-0.38	(10, -10,9.0)	24.73	6.25	-0.38
(-35, 20,3.0)	17.77	4.06	-0.36	(10, 10,3.0)	25.12	1.18	-1.18
(-35, 20,6.0)	18.53	4.03	-0.36	(10, 10,6.0)	26.05	1.55	-1.11
(-35, 20,9.0)	18.37	4.28	-0.42	(10, 10,9.0)	25.98	1.49	-0.60

Coordinates (cm)	Vx (cm/sec)	Vy (cm/sec)	Vz (cm/sec)	Coordinates (cm)	Vx (cm/sec)	Vy (cm/sec)	Vz (cm/sec)
(10, 20,3.0)	25.01	3.37	-0.25	(45, -20,3.0)	18.41	3.90	-0.10
(10, 20,6.0)	25.88	3.34	-0.25	(45, -20,6.0)	18.34	3.74	-0.13
(10, 20,9.0)	25.31	3.96	-0.70	(45, -20,9.0)	19.16	3.56	-0.09
(20, -20,3.0)	22.21	5.35	-0.16	(45, -10,3.0)	17.59	5.21	0.08
(20, -20,6.0)	22.57	5.08	-0.45	(45, -10,6.0)	18.21	5.33	0.04
(20, -20,9.0)	22.74	4.30	-0.13	(45, -10,9.0)	18.65	5.88	0.00
(20, -10,3.0)	22.00	8.02	-0.55	(45, 0,3.0)	4.49	1.55	-0.88
(20, -10,6.0)	23.32	8.11	-0.17	(45, 0,6.0)	6.01	0.92	-2.02
(20, -10,9.0)	23.07	8.27	-0.10	(45, 0,9.0)	7.99	2.19	-2.33
(20, 10,3.0)	22.03	-0.49	-1.01	(45, 10,3.0)	16.59	1.09	-0.18
(20, 10,6.0)	23.30	-0.26	-0.89	(45, 10,6.0)	18.81	0.86	-0.25
(20, 10,9.0)	23.60	-0.20	-0.72	(45, 10,9.0)	19.81	0.99	-0.30
(20, 20,3.0)	22.28	2.81	-0.04	(45, 20,3.0)	17.82	2.57	0.24
(20, 20,6.0)	23.66	2.77	-0.16	(45, 20,6.0)	19.56	2.33	0.19
(20, 20,9.0)	23.84	3.17	-0.50	(45, 20,9.0)	19.66	2.86	-0.11
(35, -20,3.0)	19.19	4.57	0.06	(55, -20,3.0)	16.55	3.52	-0.30
(35, -20,6.0)	19.79	4.38	-0.20	(55, -20,6.0)	17.86	3.69	-0.31
(35, -20,9.0)	20.20	4.08	0.08	(55, -20,9.0)	18.47	2.95	-0.02
(35, -10,3.0)	18.57	6.25	0.21	(55, -10,3.0)	14.94	3.93	0.02
(35, -10,6.0)	19.57	7.52	-0.08	(55, -10,6.0)	17.81	5.02	-0.31
(35, -10,9.0)	19.64	7.04	0.26	(55, -10,9.0)	18.29	4.94	-0.21
(35, 0,3.0)	-3.25	-0.03	-0.19	(55, 0,3.0)	9.84	0.73	-1.73
(35, 0,6.0)	0.06	0.82	-1.49	(55, 0,6.0)	12.30	2.48	-1.53
(35, 0,9.0)	0.91	1.86	-1.86	(55, 0,9.0)	14.02	3.14	-1.55
(35, 10,3.0)	18.15	1.01	-0.29	(55, 10,3.0)	16.18	1.54	-0.50
(35, 10,6.0)	20.33	0.70	-0.26	(55, 10,6.0)	18.10	1.21	-0.41
(35, 10,9.0)	20.74	-0.32	-0.74	(55, 10,9.0)	19.29	1.68	-0.51
(35, 20,3.0)	19.76	2.40	0.01	(55, 20,3.0)	16.75	2.65	-0.07
(35, 20,6.0)	20.46	2.33	0.06	(55, 20,6.0)	18.65	2.25	-0.07
(35, 20,9.0)	20.67	2.88	-0.20	(55, 20,9.0)	18.62	2.66	-0.08

Table D.8: 3D Velocity Components for Experimental Run D8
[Elliptical Island I_3 (b/a=0.3), F_r=0.16,h=15cm]

Coordinates (cm)	Vx (cm/sec)	Vy (cm/sec)	Vz (cm/sec)	Coordinates (cm)	Vx (cm/sec)	Vy (cm/sec)	Vz (cm/sec)
(-55, -20,3.0)	17.48	3.84	-0.94	(-20, -20,3.0)	24.61	3.47	-0.67
(-55, -20,6.0)	19.40	3.24	-0.79	(-20, -20,6.0)	25.26	3.49	-0.71
(-55, -20,9.0)	19.17	3.50	-0.49	(-20, -20,9.0)	25.41	3.58	-0.80
(-55, -10,3.0)	17.52	2.90	-0.41	(-20, -10,3.0)	24.91	0.88	-1.08
(-55, -10,6.0)	18.98	3.46	-0.61	(-20, -10,6.0)	25.72	0.09	-1.01
(-55, -10,9.0)	19.27	2.97	-0.30	(-20, -10,9.0)	26.82	-0.15	-0.92
(-55, 0,3.0)	17.24	3.18	-0.56	(-20, 10,3.0)	24.01	8.93	-1.33
(-55, 0,6.0)	18.70	3.22	-0.73	(-20, 10,6.0)	24.70	9.19	-1.30
(-55, 0,9.0)	19.80	3.37	-0.48	(-20, 10,9.0)	26.14	9.73	-0.91
(-55, 10,3.0)	16.61	3.15	-0.52	(-20, 20,3.0)	24.16	6.53	-0.68
(-55, 10,6.0)	18.48	3.71	-0.56	(-20, 20,6.0)	24.62	6.63	-0.83
(-55, 10,9.0)	18.88	3.91	-0.43	(-20, 20,9.0)	24.75	7.03	-0.46
(-55, 20,3.0)	18.38	3.63	-0.79	(-10, -20,3.0)	27.25	4.55	-0.62
(-55, 20,6.0)	19.21	3.83	-0.86	(-10, -20,6.0)	27.97	4.52	-0.94
(-55, 20,9.0)	18.16	4.02	-0.52	(-10, -20,9.0)	27.79	5.09	-0.70
(-45, -20,3.0)	17.78	3.48	-1.01	(-10, -10,3.0)	28.71	4.37	-1.16
(-45, -20,6.0)	19.55	2.90	-0.97	(-10, -10,6.0)	29.07	4.26	-1.18
(-45, -20,9.0)	19.32	3.17	-0.59	(-10, -10,9.0)	28.72	3.67	-0.89
(-45, -10,3.0)	17.21	2.19	-0.43	(-10, 10,3.0)	27.63	7.43	-1.15
(-45, -10,6.0)	18.47	2.69	-0.58	(-10, 10,6.0)	28.43	7.62	-1.11
(-45, -10,9.0)	19.19	2.47	-0.43	(-10, 10,9.0)	28.91	7.31	-0.60
(-45, 0,3.0)	15.94	2.89	-0.68	(-10, 20,3.0)	27.07	6.28	-0.60
(-45, 0,6.0)	18.54	2.90	-0.83	(-10, 20,6.0)	27.86	6.96	-0.86
(-45, 0,9.0)	18.57	3.03	-0.41	(-10, 20,9.0)	27.76	6.63	-0.43
(-45, 10,3.0)	17.45	3.74	-0.66	(0, -20,3.0)	28.01	5.17	-0.70
(-45, 10,6.0)	18.46	3.72	-0.51	(0, -20,6.0)	27.75	5.12	-0.82
(-45, 10,9.0)	18.98	4.18	-0.48	(0, -20,9.0)	28.58	5.73	-0.58
(-45, 20,3.0)	18.17	3.82	-0.91	(0, -10,3.0)	29.46	6.38	-1.05
(-45, 20,6.0)	18.61	4.24	-0.84	(0, -10,6.0)	30.23	5.87	-1.19
(-45, 20,9.0)	19.11	4.48	-0.61	(0, -10,9.0)	29.94	5.71	-0.51
(-35, -20,3.0)	19.32	3.08	-0.68	(0, 10,3.0)	29.08	4.86	-0.94
(-35, -20,6.0)	21.07	2.71	-0.63	(0, 10,6.0)	29.92	5.58	-0.82
(-35, -20,9.0)	21.09	2.95	-0.74	(0, 10,9.0)	30.46	5.42	-0.34
(-35, -10,3.0)	18.26	1.10	-0.60	(0,20,3.0)	28.25	5.66	-0.36
(-35, -10,6.0)	19.43	0.60	-0.55	(0, 20,6.0)	28.87	6.09	-0.89
(-35, -10,9.0)	19.42	0.66	-0.53	(0, 20,9.0)	29.20	5.72	-0.52
(-35, 0,3.0)	13.66	1.53	-0.97	(10, -20,3.0)	27.39	6.16	-0.70
(-35, 0,6.0)	15.47	1.34	-1.07	(10, -20,6.0)	28.41	5.47	-0.95
(-35, 0,9.0)	15.32	1.35	-0.73	(10, -20,9.0)	28.32	5.67	-0.67
(-35, 10,3.0)	16.86	5.68	-0.55	(10, -10,3.0)	29.15	7.39	-1.04
(-35, 10,6.0)	18.84	5.86	-0.38	(10, -10,6.0)	29.75	6.94	-0.97
(-35, 10,9.0)	18.79	6.09	-0.38	(10, -10,9.0)	30.14	6.68	-0.71
(-35, 20,3.0)	19.30	4.99	-0.66	(10, 10,3.0)	29.28	2.09	-0.98
(-35, 20,6.0)	19.39	5.54	-0.74	(10, 10,6.0)	29.78	3.57	-0.99
(-35, 20,9.0)	20.29	5.54	-0.55	(10, 10,9.0)	29.40	3.28	-0.65

Coordinates (cm)	Vx (cm/sec)	Vy (cm/sec)	Vz (cm/sec)	Coordinates (cm)	Vx (cm/sec)	Vy (cm/sec)	Vz (cm/sec)
(10, 20,3.0)	28.40	4.37	-0.58	(45, -20,3.0)	19.88	4.76	-0.50
(10, 20,6.0)	28.83	4.88	-0.95	(45, -20,6.0)	21.09	4.35	-0.50
(10, 20,9.0)	29.46	4.28	-0.47	(45, -20,9.0)	21.91	4.84	-0.35
(20, -20,3.0)	25.75	6.03	-0.56	(45, -10,3.0)	19.42	5.39	-0.16
(20, -20,6.0)	26.71	5.77	-0.75	(45, -10,6.0)	21.22	5.67	-0.04
(20, -20,9.0)	26.08	6.01	-0.54	(45, -10,9.0)	21.67	5.79	-0.07
(20, -10,3.0)	24.94	8.28	-0.23	(45, 0,3.0)	3.44	2.03	-0.80
(20, -10,6.0)	26.16	8.58	-0.69	(45, 0,6.0)	4.05	3.11	-1.69
(20, -10,9.0)	26.20	8.13	-0.03	(45, 0,9.0)	7.63	2.73	-1.27
(20, 10,3.0)	24.90	0.95	-0.53	(45, 10,3.0)	19.45	2.56	-0.01
(20, 10,6.0)	25.32	2.27	-0.53	(45, 10,6.0)	20.57	2.58	-0.14
(20, 10,9.0)	25.95	2.28	-0.42	(45, 10,9.0)	21.71	3.02	-0.42
(20, 20,3.0)	25.87	3.46	-0.56	(45, 20,3.0)	20.32	3.36	-0.20
(20, 20,6.0)	26.26	3.76	-0.91	(45, 20,6.0)	21.43	3.51	-0.38
(20, 20,9.0)	27.20	3.62	-0.35	(45, 20,9.0)	22.37	3.56	-0.35
(35, -20,3.0)	21.30	5.02	-0.35	(55, -20,3.0)	19.60	4.12	-0.41
(35, -20,6.0)	23.01	5.09	-0.53	(55, -20,6.0)	20.39	3.91	-0.48
(35, -20,9.0)	23.39	5.42	-0.49	(55, -20,9.0)	20.51	4.66	-0.49
(35, -10,3.0)	21.31	6.38	0.04	(55, -10,3.0)	16.82	3.93	-0.14
(35, -10,6.0)	23.18	6.87	-0.07	(55, -10,6.0)	20.70	4.84	-0.30
(35, -10,9.0)	23.18	6.94	0.13	(55, -10,9.0)	21.43	4.63	-0.31
(35, 0,3.0)	-3.19	-1.33	-0.42	(55, 0,3.0)	10.30	3.45	-1.34
(35, 0,6.0)	-1.37	2.33	-0.78	(55, 0,6.0)	13.73	3.33	-1.18
(35, 0,9.0)	-0.54	1.08	-0.83	(55, 0,9.0)	15.74	3.71	-0.90
(35, 10,3.0)	21.89	1.67	-0.05	(55, 10,3.0)	18.69	2.75	-0.28
(35, 10,6.0)	23.15	2.25	-0.30	(55, 10,6.0)	21.91	2.76	-0.38
(35, 10,9.0)	25.69	2.71	-0.15	(55, 10,9.0)	20.98	3.48	-0.39
(35, 20,3.0)	22.20	3.71	-0.27	(55, 20,3.0)	18.90	3.46	-0.30
(35, 20,6.0)	22.90	3.65	-0.49	(55, 20,6.0)	20.44	3.70	-0.50
(35, 20,9.0)	23.83	3.50	-0.22	(55, 20,9.0)	21.06	3.51	-0.29

Table D.9: 3D Velocity Components for Experimental Run D9
[Elliptical Island I_3 (b/a=0.3), F_r=0.19,h=15cm]

Coordinates (cm)	Vx (cm/sec)	Vy (cm/sec)	Vz (cm/sec)	Coordinates (cm)	Vx (cm/sec)	Vy (cm/sec)	Vz (cm/sec)
(-55, -20,3.0)	22.73	3.81	-0.98	(-20, -20,3.0)	32.73	3.35	-0.65
(-55, -20,6.0)	25.79	3.86	-0.99	(-20, -20,6.0)	34.67	3.43	-0.90
(-55, -20,9.0)	26.12	3.58	-0.65	(-20, -20,9.0)	33.98	3.34	-0.77
(-55, -10,3.0)	22.86	3.48	-0.51	(-20, -10,3.0)	31.86	0.10	-1.29
(-55, -10,6.0)	23.83	3.98	-0.69	(-20, -10,6.0)	32.27	-0.06	-1.32
(-55, -10,9.0)	23.97	3.47	-0.42	(-20, -10,9.0)	33.23	-1.17	-1.24
(-55, 0,3.0)	22.98	3.56	-0.58	(-20, 10,3.0)	26.34	11.14	-1.45
(-55, 0,6.0)	25.06	3.64	-0.56	(-20, 10,6.0)	28.41	11.29	-1.43
(-55, 0,9.0)	26.67	4.29	-0.60	(-20, 10,9.0)	28.76	12.74	-1.09
(-55, 10,3.0)	20.18	3.85	-0.42	(-20, 20,3.0)	25.39	7.72	-0.60
(-55, 10,6.0)	21.70	4.67	-0.64	(-20, 20,6.0)	25.44	7.78	-0.69
(-55, 10,9.0)	22.16	4.55	-0.49	(-20, 20,9.0)	27.38	8.13	-0.39
(-55, 20,3.0)	20.54	4.08	-0.84	(-10, -20,3.0)	32.76	4.74	-0.60
(-55, 20,6.0)	20.81	4.55	-0.87	(-10, -20,6.0)	34.70	4.83	-0.99
(-55, 20,9.0)	21.04	4.37	-0.49	(-10, -20,9.0)	34.75	4.60	-0.69
(-45, -20,3.0)	25.33	3.50	-0.95	(-10, -10,3.0)	33.49	4.50	-1.06
(-45, -20,6.0)	27.02	3.68	-1.05	(-10, -10,6.0)	34.71	4.33	-1.24
(-45, -20,9.0)	25.37	3.20	-0.66	(-10, -10,9.0)	34.92	3.79	-0.85
(-45, -10,3.0)	22.87	2.58	-0.50	(-10, 10,3.0)	29.36	8.61	-1.27
(-45, -10,6.0)	24.10	3.00	-0.73	(-10, 10,6.0)	30.10	8.86	-1.30
(-45, -10,9.0)	24.46	2.75	-0.59	(-10, 10,9.0)	31.60	8.89	-0.68
(-45, 0,3.0)	21.46	3.15	-0.65	(-10, 20,3.0)	22.78	7.52	-0.46
(-45, 0,6.0)	21.72	3.46	-0.99	(-10, 20,6.0)	27.92	7.97	-0.79
(-45, 0,9.0)	21.46	3.42	-0.70	(-10, 20,9.0)	28.14	7.87	-0.56
(-45, 10,3.0)	20.34	4.59	-0.68	(0, -20,3.0)	32.10	6.12	-0.55
(-45, 10,6.0)	23.23	5.16	-0.57	(0, -20,6.0)	34.24	5.93	-0.72
(-45, 10,9.0)	22.80	4.85	-0.50	(0, -20,9.0)	31.28	5.55	-0.49
(-45, 20,3.0)	22.06	4.39	-0.88	(0, -10,3.0)	33.42	7.26	-1.17
(-45, 20,6.0)	22.21	4.78	-0.82	(0, -10,6.0)	33.45	6.59	-1.32
(-45, 20,9.0)	22.98	4.93	-0.65	(0, -10,9.0)	34.49	6.22	-0.63
(-35, -20,3.0)	27.52	2.70	-0.68	(0, 10,3.0)	27.84	5.66	-1.28
(-35, -20,6.0)	29.12	2.93	-0.79	(0, 10,6.0)	29.40	6.41	-1.15
(-35, -20,9.0)	27.69	2.87	-0.71	(0, 10,9.0)	30.30	6.58	-0.57
(-35, -10,3.0)	24.26	0.42	-0.57	(0,20,3.0)	30.29	6.70	-0.19
(-35, -10,6.0)	25.35	0.40	-0.77	(0, 20,6.0)	30.84	6.97	-0.68
(-35, -10,9.0)	24.75	0.28	-0.57	(0, 20,9.0)	31.26	6.92	-0.68
(-35, 0,3.0)	18.39	1.97	-1.20	(10, -20,3.0)	30.43	7.13	-0.56
(-35, 0,6.0)	18.12	2.27	-1.37	(10, -20,6.0)	34.38	6.55	-1.05
(-35, 0,9.0)	17.70	1.90	-0.95	(10, -20,9.0)	34.47	6.20	-0.51
(-35, 10,3.0)	19.65	6.77	-0.46	(10, -10,3.0)	31.95	9.31	-0.93
(-35, 10,6.0)	23.71	7.01	-0.42	(10, -10,6.0)	33.27	8.29	-1.11
(-35, 10,9.0)	22.57	7.27	-0.48	(10, -10,9.0)	33.52	8.21	-0.68
(-35, 20,3.0)	23.43	5.72	-0.64	(10, 10,3.0)	23.48	2.04	-1.38
(-35, 20,6.0)	23.14	6.02	-0.68	(10, 10,6.0)	28.67	3.17	-1.34
(-35, 20,9.0)	24.40	6.19	-0.61	(10, 10,9.0)	28.50	2.96	-0.79

Coordinates (cm)	Vx (cm/sec)	Vy (cm/sec)	Vz (cm/sec)	Coordinates (cm)	Vx (cm/sec)	Vy (cm/sec)	Vz (cm/sec)
(10, 20,3.0)	27.73	4.88	-0.51	(45, -20,3.0)	24.98	5.47	-0.36
(10, 20,6.0)	28.30	5.16	-0.73	(45, -20,6.0)	27.96	5.12	-0.39
(10, 20,9.0)	28.46	5.23	-0.75	(45, -20,9.0)	28.72	5.29	-0.27
(20, -20,3.0)	27.48	7.21	-0.44	(45, -10,3.0)	25.50	6.74	-0.04
(20, -20,6.0)	32.67	6.87	-0.75	(45, -10,6.0)	29.85	6.98	0.00
(20, -20,9.0)	31.46	6.49	-0.41	(45, -10,9.0)	31.09	7.43	-0.04
(20, -10,3.0)	30.25	10.36	-0.51	(45, 0,3.0)	13.22	2.26	-1.07
(20, -10,6.0)	33.02	10.60	-0.53	(45, 0,6.0)	13.87	2.47	-2.37
(20, -10,9.0)	33.37	10.44	-0.09	(45, 0,9.0)	16.35	3.11	-2.34
(20, 10,3.0)	19.85	0.23	-1.00	(45, 10,3.0)	29.31	2.26	-0.13
(20, 10,6.0)	20.31	1.17	-0.92	(45, 10,6.0)	30.28	2.12	-0.25
(20, 10,9.0)	19.70	1.22	-0.74	(45, 10,9.0)	29.42	2.46	-0.45
(20, 20,3.0)	27.04	3.96	-0.36	(45, 20,3.0)	29.17	3.74	0.04
(20, 20,6.0)	29.11	4.11	-0.65	(45, 20,6.0)	29.53	3.67	-0.10
(20, 20,9.0)	30.06	4.30	-0.55	(45, 20,9.0)	31.35	4.05	-0.28
(35, -20,3.0)	26.76	6.08	-0.17	(55, -20,3.0)	26.10	4.83	-0.45
(35, -20,6.0)	30.50	5.99	-0.45	(55, -20,6.0)	24.50	4.83	-0.50
(35, -20,9.0)	30.66	5.99	-0.24	(55, -20,9.0)	26.13	4.77	-0.30
(35, -10,3.0)	27.98	8.03	0.17	(55, -10,3.0)	23.75	5.00	-0.07
(35, -10,6.0)	32.61	9.18	-0.10	(55, -10,6.0)	29.51	6.28	-0.39
(35, -10,9.0)	33.26	8.90	0.25	(55, -10,9.0)	27.94	6.10	-0.33
(35, 0,3.0)	2.67	-0.81	-0.38	(55, 0,3.0)	17.42	2.54	-1.97
(35, 0,6.0)	5.82	1.94	-1.47	(55, 0,6.0)	18.49	3.66	-1.74
(35, 0,9.0)	6.11	1.90	-1.75	(55, 0,9.0)	17.32	4.33	-1.59
(35, 10,3.0)	32.98	1.68	-0.23	(55, 10,3.0)	27.92	2.68	-0.51
(35, 10,6.0)	34.08	1.81	-0.35	(55, 10,6.0)	29.68	2.46	-0.50
(35, 10,9.0)	34.81	1.39	-0.59	(55, 10,9.0)	29.71	3.21	-0.58
(35, 20,3.0)	31.87	3.83	-0.15	(55, 20,3.0)	25.43	3.85	-0.23
(35, 20,6.0)	31.56	3.75	-0.25	(55, 20,6.0)	27.31	3.72	-0.34
(35, 20,9.0)	33.40	4.03	-0.27	(55, 20,9.0)	27.67	3.89	-0.23

Table D.10: 3D Velocity Components for Experimental Run D10
[Elliptical Island I_4 (b/a=0.4), F_r=0.14,h=15cm]

Coordinates (cm)	Vx (cm/sec)	Vy (cm/sec)	Vz (cm/sec)	Coordinates (cm)	Vx (cm/sec)	Vy (cm/sec)	Vz (cm/sec)
(-40, -20,3.0)	15.66	3.15	-0.79	(-10, -20,3.0)	20.69	3.23	-0.55
(-40, -20,6.0)	16.28	3.16	-0.71	(-10, -20,6.0)	21.86	3.47	-0.53
(-40, -20,9.0)	16.29	3.10	-0.37	(-10, -20,9.0)	21.09	2.99	-0.31
(-40, -10,3.0)	14.05	2.20	-0.33	(-10, -10,3.0)	22.56	-0.04	-0.64
(-40, -10,6.0)	16.54	3.42	-0.55	(-10, -10,6.0)	23.68	0.89	-1.05
(-40, -10,9.0)	19.96	3.24	-0.48	(-10, -10,9.0)	23.90	0.72	-0.80
(-40, 0,3.0)	14.06	3.03	-0.47	(-10, 10,3.0)	21.13	8.17	-0.73
(-40, 0,6.0)	15.83	3.55	-0.66	(-10, 10,6.0)	22.15	8.66	-0.92
(-40, 0,9.0)	16.63	3.45	-0.39	(-10, 10,9.0)	22.55	9.33	-0.75
(-40, 10,3.0)	15.18	3.65	-0.31	(-10, 20,3.0)	20.45	5.87	-0.20
(-40, 10,6.0)	16.18	4.13	-0.26	(-10, 20,6.0)	21.09	5.83	-0.22
(-40, 10,9.0)	17.11	4.28	-0.21	(-10, 20,9.0)	21.13	6.09	-0.24
(-40, 20,3.0)	16.35	3.35	-0.58	(0, -20,3.0)	22.62	5.09	-0.49
(-40, 20,6.0)	16.16	3.22	-0.42	(0, -20,6.0)	23.01	4.96	-0.69
(-40, 20,9.0)	17.99	4.25	-0.29	(0, -20,9.0)	22.39	3.73	-0.19
(-30, -20,3.0)	16.04	2.79	-0.52	(0, -10,3.0)	24.74	6.01	-0.97
(-30, -20,6.0)	16.81	2.50	-0.52	(0, -10,6.0)	25.47	5.90	-0.99
(-30, -20,9.0)	17.13	2.62	-0.34	(0, -10,9.0)	25.21	5.30	-0.47
(-30, -10,3.0)	14.82	1.53	-0.21	(0, 10,3.0)	23.86	4.70	-0.72
(-30, -10,6.0)	16.34	2.18	-0.36	(0, 10,6.0)	24.44	5.08	-0.92
(-30, -10,9.0)	17.02	2.11	-0.37	(0, 10,9.0)	24.14	4.92	-0.50
(-30, 0,3.0)	13.41	3.12	-0.61	(0, 20,3.0)	21.32	4.90	-0.11
(-30, 0,6.0)	15.54	3.37	-0.96	(0, 20,6.0)	22.22	4.75	-0.34
(-30, 0,9.0)	15.11	2.86	-0.27	(0, 20,9.0)	22.27	5.36	-0.23
(-30, 10,3.0)	14.89	4.36	-0.07	(10, -20,3.0)	21.84	5.75	-0.67
(-30, 10,6.0)	16.02	4.68	-0.13	(10, -20,6.0)	22.43	5.82	-0.82
(-30, 10,9.0)	16.80	5.20	-0.05	(10, -20,9.0)	21.07	4.36	-0.07
(-30, 20,3.0)	17.04	4.22	-0.38	(10, -10,3.0)	23.42	9.15	-0.93
(-30, 20,6.0)	17.29	4.19	-0.24	(10, -10,6.0)	23.00	8.34	-0.67
(-30, 20,9.0)	17.18	4.54	-0.26	(10, -10,9.0)	22.94	7.86	-0.06
(-20, -20,3.0)	17.82	2.46	-0.54	(10, 10,3.0)	21.28	1.28	-0.76
(-20, -20,6.0)	18.80	2.72	-0.54	(10, 10,6.0)	22.09	1.41	-0.78
(-20, -20,9.0)	18.64	2.27	-0.26	(10, 10,9.0)	22.59	1.99	-0.48
(-20, -10,3.0)	16.01	-1.20	-0.35	(10, 20,3.0)	21.13	3.40	-0.23
(-20, -10,6.0)	17.45	0.58	-0.62	(10, 20,6.0)	22.03	3.29	-0.28
(-20, -10,9.0)	17.80	-0.30	-0.43	(10, 20,9.0)	22.04	4.19	-0.30
(-20, 0,3.0)	10.85	2.40	-1.14	(20, -20,3.0)	19.19	5.25	-0.37
(-20, 0,6.0)	10.20	1.52	-0.90	(20, -20,6.0)	20.22	5.47	-0.56
(-20, 0,9.0)	11.26	1.67	-0.80	(20, -20,9.0)	19.66	4.25	-0.05
(-20, 10,3.0)	15.62	7.42	-0.26	(20, -10,3.0)	18.54	7.93	-0.08
(-20, 10,6.0)	16.95	7.76	-0.31	(20, -10,6.0)	19.58	8.08	0.04
(-20, 10,9.0)	17.87	7.69	-0.59	(20, -10,9.0)	19.97	7.15	0.16
(-20, 20,3.0)	17.69	4.73	-0.38	(20, 0,3.0)	-2.86	-1.27	0.83
(-20, 20,6.0)	18.39	4.81	-0.20	(20, 0,6.0)	-1.89	0.08	0.52
(-20, 20,9.0)	18.74	5.44	-0.23	(20, 0,9.0)	-0.97	-0.82	0.18

Coordinates (cm)	Vx (cm/sec)	Vy (cm/sec)	Vz (cm/sec)	Coordinates (cm)	Vx (cm/sec)	Vy (cm/sec)	Vz (cm/sec)
(20,10,3.0)	19.18	1.07	-0.17	(30, 20,3.0)	17.84	3.02	-0.21
(20, 10,6.0)	20.23	1.27	-0.37	(30, 20,6.0)	18.54	2.92	-0.37
(20, 10,9.0)	20.64	2.00	-0.34	(30, 20,9.0)	19.51	3.49	-0.24
(20,20,3.0)	19.47	3.14	-0.18	(40, -20,3.0)	16.54	4.17	-0.22
(20,20,6.0)	20.31	3.04	-0.31	(40, -20,6.0)	17.90	4.21	-0.43
(20,20,9.0)	20.89	3.67	-0.35	(40, -20,9.0)	17.25	3.13	-0.08
(30, -20,3.0)	17.54	4.82	-0.31	(40, -10,3.0)	15.18	4.68	0.12
(30, -20,6.0)	18.72	4.78	-0.42	(40, -10,6.0)	17.38	5.40	0.01
(30, -20,9.0)	18.14	3.70	-0.14	(40, -10,9.0)	17.71	4.59	0.01
(30, -10,3.0)	16.24	5.96	0.09	(40, 0,3.0)	11.07	2.58	0.36
(30, -10,6.0)	17.71	6.53	0.07	(40, 0,6.0)	11.28	3.31	0.06
(30, -10,9.0)	18.35	5.90	-0.08	(40, 0,9.0)	12.14	3.08	0.79
(30, 0,3.0)	2.85	0.11	-0.14	(40, 10,3.0)	15.37	2.00	-0.17
(30, 0,6.0)	4.98	1.50	1.04	(40, 10,6.0)	17.20	2.40	-0.31
(30, 0,9.0)	4.88	1.84	1.56	(40, 10,9.0)	17.36	2.79	-0.55
(30, 10,3.0)	16.73	1.39	-0.05	(40, 20,3.0)	17.30	3.27	-0.26
(30, 10,6.0)	18.18	1.66	-0.10	(40, 20,6.0)	17.91	3.16	-0.11
(30, 10,9.0)	18.74	1.99	-0.26	(40, 20,9.0)	18.38	3.43	-0.28

Table D.11: 3D Velocity Components for Experimental Run D11
[Elliptical Island I_4 (b/a=0.4), F_r=0.16,h=15cm]

Coordinates (cm)	Vx (cm/sec)	Vy (cm/sec)	Vz (cm/sec)	Coordinates (cm)	Vx (cm/sec)	Vy (cm/sec)	Vz (cm/sec)
(-40, -20,3.0)	18.58	3.55	-0.72	(-10, -20,3.0)	24.61	4.18	-0.50
(-40, -20,6.0)	20.20	3.87	-1.02	(-10, -20,6.0)	26.24	3.56	-0.60
(-40, -20,9.0)	20.10	3.47	-0.55	(-10, -20,9.0)	25.30	2.34	-0.16
(-40, -10,3.0)	17.47	2.00	-0.55	(-10, -10,3.0)	27.43	-0.81	-1.35
(-40, -10,6.0)	19.73	3.29	-1.01	(-10, -10,6.0)	27.41	0.98	-1.61
(-40, -10,9.0)	19.21	3.47	-0.49	(-10, -10,9.0)	28.23	0.39	-1.04
(-40, 0,3.0)	17.67	4.13	-0.58	(-10, 10,3.0)	25.32	9.98	-0.96
(-40, 0,6.0)	18.39	4.08	-0.38	(-10, 10,6.0)	23.96	10.08	-0.94
(-40, 0,9.0)	18.87	3.41	-0.17	(-10, 10,9.0)	14.41	10.33	-0.76
(-40, 10,3.0)	17.44	4.26	-0.27	(-10, 20,3.0)	23.91	6.30	-0.40
(-40, 10,6.0)	18.80	5.07	-0.47	(-10, 20,6.0)	23.61	6.03	-0.31
(-40, 10,9.0)	18.75	4.76	-0.21	(-10, 20,9.0)	14.13	6.35	-0.21
(-40, 20,3.0)	17.71	3.59	-0.54	(0, -20,3.0)	27.44	6.10	-0.84
(-40, 20,6.0)	18.74	3.86	-0.47	(0, -20,6.0)	27.39	5.27	-0.81
(-40, 20,9.0)	18.85	4.15	-0.36	(0, -20,9.0)	27.06	4.19	-0.10
(-30, -20,3.0)	19.16	2.94	-0.58	(0, -10,3.0)	29.59	7.09	-1.27
(-30, -20,6.0)	20.34	3.12	-0.64	(0, -10,6.0)	30.36	7.51	-1.49
(-30, -20,9.0)	20.41	3.21	-0.34	(0, -10,9.0)	29.99	6.86	-0.69
(-30, -10,3.0)	17.18	0.56	-0.22	(0, 10,3.0)	27.55	5.19	-0.79
(-30, -10,6.0)	18.85	2.44	-0.53	(0, 10,6.0)	27.76	5.76	-0.73
(-30, -10,9.0)	20.03	2.56	-0.58	(0, 10,9.0)	27.81	5.41	-0.34
(-30, 0,3.0)	15.93	3.54	-0.44	(0, 20,3.0)	25.04	5.65	-0.34
(-30, 0,6.0)	17.51	3.82	-0.62	(0, 20,6.0)	24.81	4.78	-0.31
(-30, 0,9.0)	17.73	2.57	-0.09	(0, 20,9.0)	25.40	5.53	-0.12
(-30, 10,3.0)	17.36	5.08	-0.20	(10, -20,3.0)	26.03	6.90	-0.66
(-30, 10,6.0)	18.03	5.26	-0.24	(10, -20,6.0)	26.40	6.50	-0.77
(-30, 10,9.0)	18.48	5.34	-0.12	(10, -20,9.0)	25.34	4.81	0.00
(-30, 20,3.0)	18.44	4.60	-0.37	(10, -10,3.0)	26.69	9.58	-0.91
(-30, 20,6.0)	19.45	4.61	-0.41	(10, -10,6.0)	27.91	10.09	-1.00
(-30, 20,9.0)	19.64	4.61	-0.13	(10, -10,9.0)	27.11	8.84	-0.23
(-20, -20,3.0)	22.20	3.13	-0.64	(10, 10,3.0)	24.74	1.32	-1.04
(-20, -20,6.0)	22.18	2.72	-0.54	(10, 10,6.0)	25.80	2.18	-0.98
(-20, -20,9.0)	22.30	2.29	-0.30	(10, 10,9.0)	25.96	2.17	-0.57
(-20, -10,3.0)	19.67	-1.65	-0.56	(10, 20,3.0)	24.39	4.45	-0.28
(-20, -10,6.0)	20.28	-1.02	-0.95	(10, 20,6.0)	24.57	3.75	-0.40
(-20, -10,9.0)	21.15	-0.57	-0.77	(10, 20,9.0)	25.05	3.80	-0.15
(-20, 0,3.0)	12.97	3.32	-1.17	(20, -20,3.0)	23.59	6.29	-0.48
(-20, 0,6.0)	14.36	3.08	-1.18	(20, -20,6.0)	24.19	6.44	-0.61
(-20, 0,9.0)	14.08	1.91	-0.59	(20, -20,9.0)	23.59	4.75	0.04
(-20, 10,3.0)	18.70	8.54	-0.32	(20, -10,3.0)	21.23	8.52	0.07
(-20, 10,6.0)	19.90	9.05	-0.65	(20, -10,6.0)	23.27	8.68	-0.31
(-20, 10,9.0)	19.75	8.44	-0.48	(20, -10,9.0)	23.41	8.56	-0.09
(-20, 20,3.0)	20.36	5.43	-0.45	(20, 0,3.0)	-2.94	-0.48	1.13
(-20, 20,6.0)	20.92	5.44	-0.42	(20, 0,6.0)	-1.68	-0.60	0.72
(-20, 20,9.0)	21.11	5.60	-0.12	(20, 0,9.0)	-2.12	-1.94	0.13

Coordinates (cm)	Vx (cm/sec)	Vy (cm/sec)	Vz (cm/sec)	Coordinates (cm)	Vx (cm/sec)	Vy (cm/sec)	Vz (cm/sec)
(20,10,3.0)	21.87	1.09	-0.29	(30, 20,3.0)	21.03	3.81	-0.35
(20, 10,6.0)	23.09	1.31	-0.35	(30, 20,6.0)	21.99	3.35	-0.21
(20, 10,9.0)	24.17	2.03	-0.78	(30, 20,9.0)	21.25	3.14	0.03
(20,20,3.0)	22.36	3.65	-0.22	(40, -20,3.0)	19.79	4.65	-0.28
(20,20,6.0)	23.53	3.32	-0.40	(40, -20,6.0)	20.65	4.90	-0.30
(20,20,9.0)	23.29	3.31	0.03	(40, -20,9.0)	20.49	3.47	0.05
(30, -20,3.0)	21.19	5.40	-0.42	(40, -10,3.0)	17.44	4.92	0.18
(30, -20,6.0)	22.21	5.70	-0.54	(40, -10,6.0)	20.10	5.75	-0.12
(30, -20,9.0)	21.52	4.22	0.09	(40, -10,9.0)	20.37	5.55	-0.11
(30, -10,3.0)	17.90	5.92	0.17	(40, 0,3.0)	13.02	2.23	0.09
(30, -10,6.0)	21.11	7.38	-0.20	(40, 0,6.0)	14.45	3.50	0.64
(30, -10,9.0)	21.36	7.23	-0.16	(40, 0,9.0)	14.61	3.22	1.62
(30, 0,3.0)	5.83	1.56	0.26	(40, 10,3.0)	17.59	2.20	-0.19
(30, 0,6.0)	3.70	2.70	1.32	(40, 10,6.0)	20.19	2.66	-0.41
(30, 0,9.0)	6.67	2.30	2.08	(40, 10,9.0)	20.78	3.90	-0.48
(30, 10,3.0)	19.34	1.67	-0.07	(40, 20,3.0)	19.25	3.79	-0.14
(30, 10,6.0)	21.42	2.03	-0.28	(40, 20,6.0)	20.39	3.38	-0.11
(30, 10,9.0)	21.69	2.68	-0.47	(40, 20,9.0)	20.77	3.04	0.04

Table D.12: 3D Velocity Components for Experimental Run D12
[Elliptical Island I_4 (b/a=0.4), F_r=0.19,h=15cm]

Coordinates (cm)	Vx (cm/sec)	Vy (cm/sec)	Vz (cm/sec)	Coordinates (cm)	Vx (cm/sec)	Vy (cm/sec)	Vz (cm/sec)
(-40, -20,3.0)	21.88	4.25	-0.96	(-10, -20,3.0)	29.60	4.67	-0.67
(-40, -20,6.0)	22.17	4.44	-1.09	(-10, -20,6.0)	31.14	4.47	-0.72
(-40, -20,9.0)	22.93	4.16	-0.58	(-10, -20,9.0)	30.25	3.42	-0.31
(-40, -10,3.0)	22.48	2.68	-0.55	(-10, -10,3.0)	30.12	-0.51	-1.24
(-40, -10,6.0)	21.93	4.27	-0.97	(-10, -10,6.0)	30.91	1.19	-1.67
(-40, -10,9.0)	21.96	4.26	-0.62	(-10, -10,9.0)	30.23	0.72	-1.16
(-40, 0,3.0)	19.00	4.51	-0.66	(-10, 10,3.0)	24.97	11.47	-1.07
(-40, 0,6.0)	21.26	4.83	-0.67	(-10, 10,6.0)	25.71	11.86	-1.18
(-40, 0,9.0)	21.59	4.37	-0.37	(-10, 10,9.0)	26.46	12.46	-0.96
(-40, 10,3.0)	17.93	5.01	-0.37	(-10, 20,3.0)	24.69	7.72	-0.37
(-40, 10,6.0)	19.75	5.81	-0.46	(-10, 20,6.0)	25.52	7.54	-0.33
(-40, 10,9.0)	20.33	5.73	-0.27	(-10, 20,9.0)	24.94	7.90	-0.29
(-40, 20,3.0)	18.93	4.40	-0.71	(0, -20,3.0)	31.71	7.08	-0.83
(-40, 20,6.0)	20.24	4.48	-0.56	(0, -20,6.0)	32.41	6.49	-0.95
(-40, 20,9.0)	20.29	5.35	-0.41	(0, -20,9.0)	31.37	5.02	-0.19
(-30, -20,3.0)	23.21	3.64	-0.70	(0, -10,3.0)	32.35	8.29	-1.41
(-30, -20,6.0)	24.33	3.55	-0.73	(0, -10,6.0)	33.99	8.46	-1.56
(-30, -20,9.0)	23.97	3.68	-0.43	(0, -10,9.0)	33.96	7.67	-0.73
(-30, -10,3.0)	22.65	1.37	-0.27	(0, 10,3.0)	25.97	6.27	-0.96
(-30, -10,6.0)	22.80	2.93	-0.56	(0, 10,6.0)	28.12	6.87	-1.06
(-30, -10,9.0)	22.43	2.95	-0.60	(0, 10,9.0)	28.46	6.55	-0.54
(-30, 0,3.0)	18.25	4.22	-0.68	(0, 20,3.0)	23.84	6.68	-0.28
(-30, 0,6.0)	20.04	4.55	-1.02	(0, 20,6.0)	25.20	6.06	-0.41
(-30, 0,9.0)	20.13	3.47	-0.24	(0, 20,9.0)	26.27	6.92	-0.23
(-30, 10,3.0)	18.65	5.97	-0.17	(10, -20,3.0)	29.54	8.00	-0.85
(-30, 10,6.0)	19.19	6.30	-0.23	(10, -20,6.0)	31.82	7.81	-1.01
(-30, 10,9.0)	20.57	6.70	-0.11	(10, -20,9.0)	29.79	5.81	-0.05
(-30, 20,3.0)	19.46	5.59	-0.48	(10, -10,3.0)	30.14	11.90	-1.17
(-30, 20,6.0)	20.91	5.58	-0.41	(10, -10,6.0)	31.02	11.65	-1.05
(-30, 20,9.0)	21.36	5.82	-0.25	(10, -10,9.0)	31.77	10.58	-0.18
(-20, -20,3.0)	25.55	3.53	-0.75	(10, 10,3.0)	25.38	1.65	-1.13
(-20, -20,6.0)	27.03	3.46	-0.69	(10, 10,6.0)	26.37	2.25	-1.11
(-20, -20,9.0)	26.57	2.90	-0.35	(10, 10,9.0)	27.96	2.64	-0.66
(-20, -10,3.0)	23.95	-1.79	-0.57	(10, 20,3.0)	23.55	4.95	-0.32
(-20, -10,6.0)	24.41	-0.21	-0.98	(10, 20,6.0)	25.83	4.46	-0.43
(-20, -10,9.0)	23.80	-0.54	-0.75	(10, 20,9.0)	25.49	5.10	-0.29
(-20, 0,3.0)	14.90	3.60	-1.47	(20, -20,3.0)	25.73	7.30	-0.54
(-20, 0,6.0)	16.08	2.86	-1.31	(20, -20,6.0)	28.69	7.54	-0.74
(-20, 0,9.0)	15.72	2.27	-0.89	(20, -20,9.0)	27.94	5.70	-0.01
(-20, 10,3.0)	19.09	10.11	-0.37	(20, -10,3.0)	23.65	10.44	-0.01
(-20, 10,6.0)	20.25	10.64	-0.60	(20, -10,6.0)	26.52	10.64	-0.16
(-20, 10,9.0)	20.58	10.23	-0.69	(20, -10,9.0)	27.73	9.93	0.06
(-20, 20,3.0)	22.34	6.43	-0.53	(20, 0,3.0)	1.01	-1.15	1.23
(-20, 20,6.0)	23.15	6.49	-0.39	(20, 0,6.0)	2.57	-0.30	0.78
(-20, 20,9.0)	22.85	7.02	-0.23	(20, 0,9.0)	2.04	-1.71	0.20

Coordinates (cm)	Vx (cm/sec)	Vy (cm/sec)	Vz (cm/sec)	Coordinates (cm)	Vx (cm/sec)	Vy (cm/sec)	Vz (cm/sec)
(20,10,3.0)	18.68	1.37	-0.29	(30, 20,3.0)	23.48	4.31	-0.35
(20, 10,6.0)	26.62	1.64	-0.46	(30, 20,6.0)	25.73	3.97	-0.38
(20, 10,9.0)	25.87	2.56	-0.69	(30, 20,9.0)	26.90	4.23	-0.15
(20,20,3.0)	21.99	4.30	-0.25	(40, -20,3.0)	24.58	5.59	-0.32
(20,20,6.0)	24.72	4.03	-0.45	(40, -20,6.0)	24.67	5.77	-0.47
(20,20,9.0)	24.82	4.46	-0.22	(40, -20,9.0)	25.05	4.18	-0.02
(30, -20,3.0)	24.05	6.48	-0.46	(40, -10,3.0)	19.07	6.10	0.19
(30, -20,6.0)	28.82	6.63	-0.61	(40, -10,6.0)	22.08	7.08	-0.06
(30, -20,9.0)	27.98	5.02	-0.04	(40, -10,9.0)	22.76	6.41	-0.06
(30, -10,3.0)	19.87	7.56	0.16	(40, 0,3.0)	13.05	3.07	0.30
(30, -10,6.0)	24.79	8.81	-0.07	(40, 0,6.0)	16.98	4.32	0.42
(30, -10,9.0)	26.53	8.30	-0.15	(40, 0,9.0)	17.25	4.00	1.50
(30, 0,3.0)	8.70	1.00	0.06	(40, 10,3.0)	17.06	2.66	-0.23
(30, 0,6.0)	15.90	2.62	1.49	(40, 10,6.0)	20.89	3.21	-0.45
(30, 0,9.0)	11.75	2.61	2.29	(40, 10,9.0)	23.98	4.21	-0.66
(30, 10,3.0)	23.52	1.93	-0.08	(40, 20,3.0)	24.68	4.47	-0.26
(30, 10,6.0)	26.95	2.33	-0.23	(40, 20,6.0)	22.86	4.15	-0.14
(30, 10,9.0)	27.93	2.94	-0.46	(40, 20,9.0)	24.21	4.13	-0.17

Table D.13: 3D Velocity Components for Experimental Run D13
[Elliptical Island I_5 (b/a=0.6), F_r=0.14,h=15cm]

Coordinates (cm)	Vx (cm/sec)	Vy (cm/sec)	Vz (cm/sec)	Coordinates (cm)	Vx (cm/sec)	Vy (cm/sec)	Vz (cm/sec)
(-40, -20,3.0)	14.28	3.44	-0.57	(-10, -20,3.0)	19.48	3.77	-0.55
(-40, -20,6.0)	15.51	3.62	-0.70	(-10, -20,6.0)	20.10	3.75	-0.61
(-40, -20,9.0)	15.83	3.61	-0.45	(-10, -20,9.0)	19.24	2.68	-0.14
(-40, -10,3.0)	14.99	3.69	-0.44	(-10, -10,3.0)	19.36	0.11	-0.38
(-40, -10,6.0)	16.25	3.52	-0.60	(-10, -10,6.0)	20.40	0.57	-0.63
(-40, -10,9.0)	16.58	3.48	-0.38	(-10, -10,9.0)	20.49	-0.10	-0.43
(-40, 0,3.0)	14.03	3.46	-0.21	(-10, 10,3.0)	16.95	9.14	-0.50
(-40, 0,6.0)	16.08	3.81	-0.51	(-10, 10,6.0)	17.77	9.56	-0.91
(-40, 0,9.0)	16.02	3.46	-0.04	(-10, 10,9.0)	17.94	9.77	-0.34
(-40, 10,3.0)	14.11	3.72	-0.19	(-10, 20,3.0)	17.93	6.15	-0.42
(-40, 10,6.0)	15.88	4.05	-0.44	(-10, 20,6.0)	19.35	6.34	-0.61
(-40, 10,9.0)	16.87	4.78	-0.37	(-10, 20,9.0)	19.25	6.24	-0.33
(-40, 20,3.0)	15.35	3.86	-0.61	(0, -20,3.0)	20.82	4.83	-0.42
(-40, 20,6.0)	16.75	4.26	-0.56	(0, -20,6.0)	21.90	4.97	-0.51
(-40, 20,9.0)	16.73	4.23	-0.33	(0, -20,9.0)	20.74	3.28	-0.15
(-30, -20,3.0)	16.17	3.54	-0.71	(0, -10,3.0)	24.74	5.38	-1.10
(-30, -20,6.0)	16.00	3.57	-0.52	(0, -10,6.0)	25.37	4.76	-1.25
(-30, -20,9.0)	16.34	3.20	-0.33	(0, -10,9.0)	25.05	4.87	-0.22
(-30, -10,3.0)	14.53	2.84	-0.24	(0, 10,3.0)	21.92	5.46	-0.66
(-30, -10,6.0)	16.10	3.22	-0.33	(0, 10,6.0)	22.84	7.37	-0.68
(-30, -10,9.0)	16.83	3.19	-0.26	(0, 10,9.0)	22.82	6.81	-0.35
(-30, 0,3.0)	14.91	3.89	-0.40	(0, 20,3.0)	20.74	6.31	-0.41
(-30, 0,6.0)	15.82	3.49	-0.47	(0, 20,6.0)	21.33	5.84	-0.74
(-30, 0,9.0)	15.78	3.21	-0.03	(0, 20,9.0)	21.28	5.78	-0.14
(-30, 10,3.0)	14.62	4.30	-0.19	(10, -20,3.0)	21.09	5.92	-0.55
(-30, 10,6.0)	16.01	4.51	-0.35	(10, -20,6.0)	21.60	6.29	-0.73
(-30, 10,9.0)	16.06	4.12	-0.13	(10, -20,9.0)	20.05	3.78	-0.03
(-30, 20,3.0)	15.91	4.45	-0.46	(10, -10,3.0)	21.38	8.10	-0.46
(-30, 20,6.0)	16.65	4.53	-0.47	(10, -10,6.0)	22.34	8.15	-0.49
(-30, 20,9.0)	16.75	4.58	-0.18	(10, -10,9.0)	22.99	7.96	-0.18
(-20, -20,3.0)	16.91	3.39	-0.55	(10, 10,3.0)	21.61	3.34	-0.58
(-20, -20,6.0)	17.41	3.11	-0.54	(10, 10,6.0)	22.15	3.57	-0.38
(-20, -20,9.0)	17.38	3.02	-0.35	(10, 10,9.0)	22.66	4.08	-0.83
(-20, -10,3.0)	15.31	1.56	-0.22	(10, 20,3.0)	21.09	5.21	-0.35
(-20, -10,6.0)	16.50	1.95	-0.29	(10, 20,6.0)	22.14	5.10	-0.66
(-20, -10,9.0)	16.38	1.54	-0.22	(10, 20,9.0)	21.88	4.79	-0.22
(-20, 0,3.0)	12.75	3.44	-0.86	(20, -20,3.0)	19.45	5.77	-0.50
(-20, 0,6.0)	14.00	3.04	-0.78	(20, -20,6.0)	20.55	5.72	-0.63
(-20, 0,9.0)	13.86	2.69	-0.17	(20, -20,9.0)	19.33	3.54	0.11
(-20, 10,3.0)	14.83	5.38	-0.20	(20, -10,3.0)	19.23	8.05	-0.18
(-20, 10,6.0)	15.88	5.73	-0.32	(20, -10,6.0)	20.95	8.26	-0.55
(-20, 10,9.0)	15.94	5.66	-0.23	(20, -10,9.0)	21.15	7.47	-0.21
(-20, 20,3.0)	16.12	5.14	-0.44	(20, 0,3.0)	-2.63	-1.58	1.04
(-20, 20,6.0)	17.43	5.12	-0.45	(20, 0,6.0)	-3.85	-0.69	0.42
(-20, 20,9.0)	17.49	5.17	-0.19	(20, 0,9.0)	-2.56	0.62	0.75

Coordinates (cm)	Vx (cm/sec)	Vy (cm/sec)	Vz (cm/sec)	Coordinates (cm)	Vx (cm/sec)	Vy (cm/sec)	Vz (cm/sec)
(20,10,3.0)	19.71	1.61	-0.45	(30, 20,3.0)	18.71	4.26	-0.41
(20, 10,6.0)	21.41	2.43	-0.75	(30, 20,6.0)	19.39	4.29	-0.37
(20, 10,9.0)	20.91	2.96	-0.88	(30, 20,9.0)	19.68	3.79	-0.14
(20,20,3.0)	20.19	4.81	-0.31	(40, -20,3.0)	17.40	4.66	-0.41
(20,20,6.0)	21.37	4.59	-0.51	(40, -20,6.0)	17.86	4.98	-0.43
(20,20,9.0)	20.68	3.73	-0.15	(40, -20,9.0)	16.70	2.81	-0.03
(30, -20,3.0)	17.95	4.92	-0.31	(40, -10,3.0)	16.13	5.20	0.03
(30, -20,6.0)	18.65	5.33	-0.58	(40, -10,6.0)	17.15	5.75	-0.10
(30, -20,9.0)	18.39	3.49	-0.01	(40, -10,9.0)	17.92	5.50	-0.18
(30, -10,3.0)	17.38	6.81	-0.03	(40, 0,3.0)	10.85	3.46	0.57
(30, -10,6.0)	18.08	7.38	-0.05	(40, 0,6.0)	9.59	2.93	0.71
(30, -10,9.0)	18.79	7.05	-0.33	(40, 0,9.0)	11.31	3.56	0.58
(30, 0,3.0)	4.52	1.69	0.22	(40, 10,3.0)	15.50	2.67	-0.03
(30, 0,6.0)	4.62	1.26	0.60	(40, 10,6.0)	16.78	3.21	-0.35
(30, 0,9.0)	5.77	2.94	1.17	(40, 10,9.0)	16.92	3.44	-0.28
(30, 10,3.0)	17.34	1.39	-0.18	(40, 20,3.0)	18.21	4.48	-0.35
(30, 10,6.0)	18.60	2.46	-0.31	(40, 20,6.0)	19.47	4.57	-0.32
(30, 10,9.0)	17.32	2.83	-1.01	(40, 20,9.0)	18.69	3.79	-0.14

Table D.14: 3D Velocity Components for Experimental Run D14
[Elliptical Island I_5 (b/a=0.6), F_r=0.16,h=15cm]

Coordinates (cm)	Vx (cm/sec)	Vy (cm/sec)	Vz (cm/sec)	Coordinates (cm)	Vx (cm/sec)	Vy (cm/sec)	Vz (cm/sec)
(-40, -20,3.0)	17.33	3.86	-0.77	(-10, -20,3.0)	21.14	2.99	-0.67
(-40, -20,6.0)	18.48	3.99	-0.80	(-10, -20,6.0)	21.44	3.10	-0.78
(-40, -20,9.0)	18.47	4.33	-0.56	(-10, -20,9.0)	21.48	3.40	-0.53
(-40, -10,3.0)	17.99	4.21	-0.60	(-10, -10,3.0)	18.90	0.00	-0.24
(-40, -10,6.0)	17.96	4.41	-0.39	(-10, -10,6.0)	20.94	0.02	-0.75
(-40, -10,9.0)	18.66	3.32	-0.27	(-10, -10,9.0)	19.91	-2.23	-0.22
(-40, 0,3.0)	17.86	4.29	-0.89	(-10, 10,3.0)	22.21	11.50	-0.43
(-40, 0,6.0)	18.55	4.18	-0.62	(-10, 10,6.0)	22.90	11.79	-0.82
(-40, 0,9.0)	18.55	3.47	-0.33	(-10, 10,9.0)	23.47	12.00	-0.75
(-40, 10,3.0)	16.86	3.56	-0.37	(-10, 20,3.0)	22.48	6.17	-0.05
(-40, 10,6.0)	18.57	4.18	-0.32	(-10, 20,6.0)	23.48	6.46	-0.18
(-40, 10,9.0)	19.53	4.69	-0.13	(-10, 20,9.0)	23.23	4.59	0.08
(-40, 20,3.0)	18.15	3.66	-0.56	(0, -20,3.0)	23.26	4.03	-0.75
(-40, 20,6.0)	18.95	3.90	-0.59	(0, -20,6.0)	23.91	4.40	-0.67
(-40, 20,9.0)	19.16	3.70	-0.22	(0, -20,9.0)	24.10	4.40	-0.56
(-30, -20,3.0)	17.70	3.58	-0.70	(0, -10,3.0)	25.59	4.90	-1.27
(-30, -20,6.0)	18.64	3.96	-0.66	(0, -10,6.0)	26.36	4.03	-1.27
(-30, -20,9.0)	18.88	3.65	-0.48	(0, -10,9.0)	24.72	-0.07	-0.11
(-30, -10,3.0)	16.70	3.68	-0.22	(0, 10,3.0)	28.28	4.62	-1.02
(-30, -10,6.0)	18.59	3.98	-0.49	(0, 10,6.0)	28.02	5.05	-1.47
(-30, -10,9.0)	18.06	2.31	0.05	(0, 10,9.0)	28.69	6.01	-1.74
(-30, 0,3.0)	16.99	4.18	-0.47	(0, 20,3.0)	25.82	5.28	-0.33
(-30, 0,6.0)	18.25	4.62	-0.70	(0, 20,6.0)	26.60	5.50	-0.34
(-30, 0,9.0)	18.04	3.02	-0.22	(0, 20,9.0)	24.56	2.52	0.56
(-30, 10,3.0)	17.27	4.35	-0.10	(10, -20,3.0)	23.23	5.40	-0.56
(-30, 10,6.0)	17.96	4.50	-0.16	(10, -20,6.0)	24.28	5.82	-0.81
(-30, 10,9.0)	19.35	5.31	-0.17	(10, -20,9.0)	23.94	5.44	-0.58
(-30, 20,3.0)	18.46	4.01	-0.30	(10, -10,3.0)	24.73	7.99	-0.85
(-30, 20,6.0)	18.74	4.18	-0.38	(10, -10,6.0)	25.38	6.78	-0.69
(-30, 20,9.0)	19.22	3.59	-0.03	(10, -10,9.0)	23.84	2.90	0.03
(-20, -20,3.0)	18.57	2.79	-0.62	(10, 10,3.0)	25.17	1.54	-0.35
(-20, -20,6.0)	19.42	3.35	-0.69	(10, 10,6.0)	26.92	1.48	-0.51
(-20, -20,9.0)	19.70	3.50	-0.48	(10, 10,9.0)	27.13	0.71	-0.56
(-20, -10,3.0)	16.94	2.17	-0.30	(10, 20,3.0)	24.94	3.86	-0.23
(-20, -10,6.0)	17.26	2.01	-0.21	(10, 20,6.0)	26.08	4.00	-0.43
(-20, -10,9.0)	16.87	0.78	0.07	(10, 20,9.0)	24.64	1.19	0.34
(-20, 0,3.0)	15.16	3.71	-1.05	(20, -20,3.0)	22.96	5.92	-0.56
(-20, 0,6.0)	16.23	4.37	-1.15	(20, -20,6.0)	23.41	5.89	-0.83
(-20, 0,9.0)	15.09	3.05	-0.46	(20, -20,9.0)	23.45	5.97	-0.47
(-20, 10,3.0)	16.99	6.30	-0.02	(20, -10,3.0)	23.36	9.12	-0.68
(-20, 10,6.0)	18.74	6.52	-0.30	(20, -10,6.0)	23.71	8.37	-0.40
(-20, 10,9.0)	19.66	7.28	-0.26	(20, -10,9.0)	22.06	4.25	0.24
(-20, 20,3.0)	19.71	5.08	-0.24	(20, 0,3.0)	-4.48	-1.16	0.95
(-20, 20,6.0)	21.14	5.46	-0.31	(20, 0,6.0)	-4.52	-0.62	0.56
(-20, 20,9.0)	19.72	3.96	0.26	(20, 0,9.0)	-4.17	-0.05	-0.20

Coordinates (cm)	Vx (cm/sec)	Vy (cm/sec)	Vz (cm/sec)	Coordinates (cm)	Vx (cm/sec)	Vy (cm/sec)	Vz (cm/sec)
(20,10,3.0)	22.50	0.28	-0.34	(30, 20,3.0)	21.42	3.77	-0.09
(20, 10,6.0)	23.81	1.24	-0.08	(30, 20,6.0)	22.28	3.77	-0.14
(20, 10,9.0)	24.81	1.20	-0.09	(30, 20,9.0)	20.99	1.05	0.57
(20,20,3.0)	23.86	3.77	-0.24	(40, -20,3.0)	19.69	4.90	-0.39
(20,20,6.0)	24.08	3.84	-0.32	(40, -20,6.0)	21.29	5.25	-0.72
(20,20,9.0)	22.39	0.89	0.68	(40, -20,9.0)	21.22	5.09	-0.47
(30, -20,3.0)	21.27	5.72	-0.58	(40, -10,3.0)	18.44	6.59	-0.53
(30, -20,6.0)	21.99	5.64	-0.81	(40, -10,6.0)	19.52	5.83	-0.58
(30, -20,9.0)	23.32	5.61	-0.40	(40, -10,9.0)	18.21	2.58	-0.04
(30, -10,3.0)	20.70	8.34	-0.39	(40, 0,3.0)	12.39	2.83	-0.11
(30, -10,6.0)	20.73	7.11	-0.33	(40, 0,6.0)	14.50	2.95	0.46
(30, -10,9.0)	19.57	4.03	0.10	(40, 0,9.0)	14.31	2.40	0.71
(30, 0,3.0)	4.93	0.99	0.16	(40, 10,3.0)	17.87	2.00	-0.13
(30, 0,6.0)	6.02	1.04	1.85	(40, 10,6.0)	20.31	1.93	-0.47
(30, 0,9.0)	6.19	0.88	0.52	(40, 10,9.0)	20.81	2.03	-0.08
(30, 10,3.0)	19.50	1.44	0.13	(40, 20,3.0)	19.73	3.65	0.10
(30, 10,6.0)	21.32	1.73	0.12	(40, 20,6.0)	21.09	3.46	-0.01
(30, 10,9.0)	21.94	1.16	-0.16	(40, 20,9.0)	19.53	1.24	0.51

Table D.15: 3D Velocity Components for Experimental Run D15
[Elliptical Island I_5 (b/a=0.6), F_r=0.19,h=15cm]

Coordinates (cm)	Vx (cm/sec)	Vy (cm/sec)	Vz (cm/sec)	Coordinates (cm)	Vx (cm/sec)	Vy (cm/sec)	Vz (cm/sec)
(-40, -20,3.0)	21.94	4.63	-0.84	(-10, -20,3.0)	24.67	4.33	-0.77
(-40, -20,6.0)	21.65	4.83	-0.95	(-10, -20,6.0)	24.86	4.39	-0.88
(-40, -20,9.0)	21.58	5.02	-0.64	(-10, -20,9.0)	25.03	3.84	-0.41
(-40, -10,3.0)	23.52	5.00	-0.65	(-10, -10,3.0)	23.72	0.07	-0.40
(-40, -10,6.0)	21.72	5.01	-0.64	(-10, -10,6.0)	24.79	0.40	-0.87
(-40, -10,9.0)	23.12	4.33	-0.42	(-10, -10,9.0)	24.88	-1.39	-0.42
(-40, 0,3.0)	21.01	4.90	-0.67	(-10, 10,3.0)	22.32	13.03	-0.59
(-40, 0,6.0)	20.58	5.07	-0.71	(-10, 10,6.0)	24.96	13.49	-1.10
(-40, 0,9.0)	21.83	4.41	-0.22	(-10, 10,9.0)	25.22	13.75	-0.68
(-40, 10,3.0)	19.60	4.64	-0.35	(-10, 20,3.0)	24.22	7.84	-0.31
(-40, 10,6.0)	21.85	5.23	-0.49	(-10, 20,6.0)	24.36	8.14	-0.52
(-40, 10,9.0)	22.01	6.03	-0.33	(-10, 20,9.0)	25.00	6.96	-0.18
(-40, 20,3.0)	20.16	4.79	-0.75	(0, -20,3.0)	26.32	5.67	-0.73
(-40, 20,6.0)	22.04	5.21	-0.73	(0, -20,6.0)	26.96	5.99	-0.74
(-40, 20,9.0)	21.93	5.07	-0.35	(0, -20,9.0)	27.25	4.84	-0.43
(-30, -20,3.0)	22.41	4.53	-0.90	(0, -10,3.0)	29.62	6.56	-1.50
(-30, -20,6.0)	21.84	4.77	-0.74	(0, -10,6.0)	30.53	5.62	-1.60
(-30, -20,9.0)	22.06	4.34	-0.51	(0, -10,9.0)	31.62	3.26	-0.21
(-30, -10,3.0)	21.83	4.11	-0.29	(0, 10,3.0)	29.53	6.45	-1.05
(-30, -10,6.0)	22.48	4.55	-0.51	(0, 10,6.0)	31.34	8.00	-1.33
(-30, -10,9.0)	22.38	3.54	-0.15	(0, 10,9.0)	30.29	8.19	-1.27
(-30, 0,3.0)	19.99	5.12	-0.55	(0, 20,3.0)	25.16	7.42	-0.47
(-30, 0,6.0)	20.25	5.11	-0.73	(0, 20,6.0)	25.95	7.23	-0.70
(-30, 0,9.0)	21.23	3.97	-0.15	(0, 20,9.0)	27.15	5.42	0.24
(-30, 10,3.0)	20.08	5.50	-0.19	(10, -20,3.0)	26.75	7.22	-0.71
(-30, 10,6.0)	21.13	5.73	-0.33	(10, -20,6.0)	27.62	7.72	-0.98
(-30, 10,9.0)	21.81	5.95	-0.19	(10, -20,9.0)	26.87	5.80	-0.36
(-30, 20,3.0)	20.50	5.40	-0.49	(10, -10,3.0)	25.02	10.24	-0.82
(-30, 20,6.0)	21.80	5.56	-0.54	(10, -10,6.0)	28.71	9.56	-0.74
(-30, 20,9.0)	22.00	5.24	-0.14	(10, -10,9.0)	29.38	7.12	-0.10
(-20, -20,3.0)	22.68	3.96	-0.74	(10, 10,3.0)	26.97	3.18	-0.60
(-20, -20,6.0)	23.16	4.10	-0.78	(10, 10,6.0)	28.79	3.30	-0.56
(-20, -20,9.0)	23.22	4.13	-0.52	(10, 10,9.0)	28.81	3.19	-0.90
(-20, -10,3.0)	21.95	2.35	-0.33	(10, 20,3.0)	24.45	5.83	-0.37
(-20, -10,6.0)	22.17	2.52	-0.32	(10, 20,6.0)	26.13	5.84	-0.70
(-20, -10,9.0)	22.20	1.51	-0.11	(10, 20,9.0)	26.70	3.96	0.05
(-20, 0,3.0)	18.52	4.54	-1.21	(20, -20,3.0)	24.82	7.43	-0.67
(-20, 0,6.0)	28.38	4.66	-1.21	(20, -20,6.0)	25.97	7.38	-0.92
(-20, 0,9.0)	18.92	3.64	-0.39	(20, -20,9.0)	26.55	5.95	-0.20
(-20, 10,3.0)	19.09	7.39	-0.15	(20, -10,3.0)	16.22	10.88	-0.53
(-20, 10,6.0)	20.75	7.76	-0.40	(20, -10,6.0)	26.28	10.57	-0.61
(-20, 10,9.0)	21.16	8.16	-0.31	(20, -10,9.0)	27.20	7.59	0.00
(-20, 20,3.0)	21.22	6.50	-0.44	(20, 0,3.0)	6.13	-1.76	1.27
(-20, 20,6.0)	22.20	6.72	-0.49	(20, 0,6.0)	10.55	-0.84	0.62
(-20, 20,9.0)	22.78	5.86	0.03	(20, 0,9.0)	16.47	0.39	0.39

Coordinates (cm)	Vx (cm/sec)	Vy (cm/sec)	Vz (cm/sec)	Coordinates (cm)	Vx (cm/sec)	Vy (cm/sec)	Vz (cm/sec)
(20,10,3.0)	22.38	1.26	-0.51	(30, 20,3.0)	22.34	5.13	-0.33
(20, 10,6.0)	25.31	2.39	-0.56	(30, 20,6.0)	24.25	5.15	-0.33
(20, 10,9.0)	26.40	2.72	-0.65	(30, 20,9.0)	26.04	3.20	0.24
(20,20,3.0)	22.00	5.50	-0.35	(40, -20,3.0)	23.76	6.07	-0.51
(20,20,6.0)	25.40	5.39	-0.54	(40, -20,6.0)	25.90	6.50	-0.72
(20,20,9.0)	26.15	3.06	0.30	(40, -20,9.0)	23.19	4.93	-0.30
(30, -20,3.0)	25.67	6.73	-0.55	(40, -10,3.0)	18.45	7.44	-0.29
(30, -20,6.0)	26.75	6.97	-0.87	(40, -10,6.0)	22.74	7.36	-0.41
(30, -20,9.0)	25.49	5.70	-0.24	(40, -10,9.0)	25.20	5.26	-0.15
(30, -10,3.0)	20.71	9.57	-0.25	(40, 0,3.0)	17.27	4.03	0.32
(30, -10,6.0)	24.15	9.23	-0.23	(40, 0,6.0)	20.18	3.74	0.75
(30, -10,9.0)	27.08	7.18	-0.16	(40, 0,9.0)	21.05	3.84	0.82
(30, 0,3.0)	15.55	1.73	0.24	(40, 10,3.0)	19.78	3.00	-0.10
(30, 0,6.0)	16.55	1.47	1.51	(40, 10,6.0)	22.99	3.32	-0.52
(30, 0,9.0)	20.29	2.52	1.10	(40, 10,9.0)	24.15	3.54	-0.24
(30, 10,3.0)	21.58	1.80	-0.04	(40, 20,3.0)	20.58	5.21	-0.18
(30, 10,6.0)	24.13	2.70	-0.14	(40, 20,6.0)	22.94	5.16	-0.22
(30, 10,9.0)	25.46	2.61	-0.78	(40, 20,9.0)	24.23	3.31	0.21

Table D.16: 3D Velocity Components for Experimental Run D16
[Circular Island I_6 (d=15cm), F_r=0.14,h=15cm]

Coordinates (cm)	Vx (cm/sec)	Vy (cm/sec)	Vz (cm/sec)	Coordinates (cm)	Vx (cm/sec)	Vy (cm/sec)	Vz (cm/sec)
(-30, -20,3.0)	15.48	2.66	-0.77	(-10,20,6.0)	19.86	4.42	-0.74
(-30, -20,6.0)	16.07	2.96	-0.74	(-10, 20,9.0)	20.00	4.17	-0.76
(-30, -20,9.0)	16.42	3.17	-0.62	(-5, -20,3.0)	22.14	2.36	-1.09
(-30, -10,3.0)	14.61	2.86	-0.67	(-5, -20,6.0)	22.16	2.31	-1.15
(-30, -10,6.0)	16.37	2.80	-0.99	(-5, -20,9.0)	22.08	1.40	-1.01
(-30, -10,9.0)	16.46	2.93	-0.93	(-5, -10,3.0)	22.91	-2.52	-1.31
(-30, 0,3.0)	15.01	3.21	-0.88	(-5, -10,6.0)	22.48	-2.87	-1.27
(-30, 0,6.0)	16.19	3.48	-1.09	(-5, -10,9.0)	20.66	-4.85	-0.80
(-30, 0,9.0)	16.23	3.33	-0.84	(-5, 10,3.0)	20.35	8.81	-2.65
(-30, 10,3.0)	15.00	3.86	-0.28	(-5, 10,6.0)	21.01	8.79	-2.04
(-30, 10,6.0)	16.47	4.29	-0.60	(-5, 10,9.0)	20.91	9.14	-1.31
(-30, 10,9.0)	16.76	4.21	-0.38	(-5, 20,3.0)	20.45	4.59	-0.80
(-30, 20,3.0)	15.40	3.73	-0.77	(-5, 20,6.0)	20.94	4.85	-0.64
(-30, 20,6.0)	15.91	3.61	-0.85	(-5, 20,9.0)	21.26	4.34	-0.59
(-30, 20,9.0)	15.64	3.60	-0.55	(0, -20,3.0)	20.82	3.31	-0.72
(-20, -20,3.0)	18.44	2.24	-0.64	(0, -20,6.0)	21.33	3.90	-0.84
(-20, -20,6.0)	19.27	1.99	-0.67	(0, -20,9.0)	21.99	3.95	-0.78
(-20, -20,9.0)	18.63	1.65	-0.46	(0, -10,3.0)	25.34	4.63	-2.46
(-20, -10,3.0)	18.33	1.57	-0.72	(0, -10,6.0)	25.22	2.73	-2.21
(-20, -10,6.0)	18.09	1.55	-0.55	(0, -10,9.0)	25.86	3.07	-1.88
(-20, -10,9.0)	17.23	0.81	-0.78	(0, 10,3.0)	23.54	7.46	-1.01
(-20, 0,3.0)	16.65	3.57	-0.83	(0, 10,6.0)	23.95	8.43	-1.16
(-20, 0,6.0)	16.46	2.92	-0.92	(0, 10,9.0)	24.17	9.56	-1.17
(-20, 0,9.0)	16.18	1.39	-0.34	(0, 20,3.0)	21.64	5.78	-0.76
(-20, 10,3.0)	16.34	4.52	-0.72	(0, 20,6.0)	21.68	5.65	-0.86
(-20, 10,6.0)	18.27	4.87	-0.90	(0, 20,9.0)	21.61	5.25	-0.79
(-20, 10,9.0)	17.44	3.98	-0.49	(5, -20,3.0)	24.06	4.33	-1.04
(-20, 20,3.0)	18.67	3.95	-0.46	(5, -20,6.0)	24.36	3.07	-1.35
(-20, 20,6.0)	18.81	3.46	-0.61	(5, -20,9.0)	24.11	3.07	-1.35
(-20, 20,9.0)	18.77	3.50	-0.58	(5, -10,3.0)	27.60	3.32	-3.14
(-10, -20,3.0)	19.98	1.66	-0.81	(5, -10,6.0)	27.00	2.53	-1.76
(-10, -20,6.0)	21.04	2.13	-1.00	(5, -10,9.0)	27.23	2.56	-1.70
(-10, -20,9.0)	20.78	1.21	-0.99	(5, 10,3.0)	26.78	2.06	-1.44
(-10, -10,3.0)	19.07	-1.96	-0.91	(5, 10,6.0)	26.17	3.76	-1.67
(-10, -10,6.0)	18.18	-2.18	-0.88	(5, 10,9.0)	26.46	4.81	-2.33
(-10, -10,9.0)	17.65	-3.29	-0.70	(5, 20,3.0)	23.04	5.95	-0.38
(-10, 0,3.0)	11.86	4.06	-2.39	(5, 20,6.0)	23.25	4.20	-0.56
(-10, 0,6.0)	11.38	2.39	-1.52	(5, 20,9.0)	23.79	4.64	-0.90
(-10, 0,9.0)	10.05	0.30	-0.82	(10, -20,3.0)	21.56	5.03	-0.83
(-10, 10,3.0)	17.69	7.67	-1.60	(10, -20,6.0)	22.50	5.26	-0.85
(-10, 10,6.0)	18.67	8.19	-1.68	(10, -20,9.0)	23.02	5.70	-0.74
(-10, 10,9.0)	17.84	7.15	-0.85	(10, -10,3.0)	21.83	8.41	-1.87
(-10,20,3.0)	19.89	4.71	-0.60	(10, -10,6.0)	23.48	7.89	-1.99

Coordinates (cm)	Vx (cm/sec)	Vy (cm/sec)	Vz (cm/sec)	Coordinates (cm)	Vx (cm/sec)	Vy (cm/sec)	Vz (cm/sec)
(10, -10,9.0)	23.72	7.79	-1.59	(20, -10,3.0)	24.27	9.20	3.10
(10, 0,3.0)	-3.17	-0.98	-0.58	(20, -10,6.0)	24.79	8.87	0.19
(10, 0,6.0)	-3.15	-1.31	0.58	(20, -10,9.0)	25.25	9.30	-1.25
(10, 0,9.0)	-3.10	-0.81	1.20	(20, 0,3.0)	5.64	3.74	7.88
(10, 10,3.0)	23.64	1.72	-1.15	(20, 0,6.0)	5.76	3.36	8.50
(10, 10,6.0)	25.22	3.52	-1.17	(20, 0,9.0)	4.38	1.14	9.34
(10, 10,9.0)	25.24	4.04	-0.94	(20, 10,3.0)	17.97	1.35	2.87
(10,20,3.0)	21.70	4.13	-0.56	(20, 10,6.0)	25.49	-0.16	0.43
(10,20,6.0)	22.37	3.96	-0.99	(20, 10,9.0)	23.65	0.09	-0.17
(10, 20,9.0)	22.13	3.96	-0.86	(20, 20,3.0)	23.58	1.70	-0.10
(20, -20,3.0)	25.70	5.17	-0.40	(20, 20,6.0)	23.61	2.53	-0.62
(20, -20,6.0)	25.76	5.30	-1.05	(20, 20,9.0)	24.44	2.81	-0.83
(20, -20,9.0)	25.99	5.54	-1.27				

Table D.17: 3D Velocity Components for Experimental Run D17
[Circular Island I_6 (d=15cm), F_r=0.16,h=15cm]

Coordinates (cm)	Vx (cm/sec)	Vy (cm/sec)	Vz (cm/sec)	Coordinates (cm)	Vx (cm/sec)	Vy (cm/sec)	Vz (cm/sec)
(-30, -20,3.0)	18.12	3.32	-0.98	(-10,20,6.0)	21.03	6.41	-0.75
(-30, -20,6.0)	19.13	3.61	-0.96	(-10, 20,9.0)	20.24	6.25	-0.73
(-30, -20,9.0)	18.99	3.34	-0.59	(-5, -20,3.0)	22.65	3.50	-1.62
(-30, -10,3.0)	17.92	3.00	-0.90	(-5, -20,6.0)	23.28	4.60	-1.43
(-30, -10,6.0)	18.79	3.08	-0.85	(-5, -20,9.0)	23.26	4.18	-1.31
(-30, -10,9.0)	19.33	3.34	-0.75	(-5, -10,3.0)	22.42	-1.31	-2.93
(-30, 0,3.0)	17.88	3.51	-1.09	(-5, -10,6.0)	22.88	-2.74	-2.12
(-30, 0,6.0)	19.34	4.32	-1.19	(-5, -10,9.0)	23.16	-2.81	-1.27
(-30, 0,9.0)	18.96	4.02	-0.93	(-5, 10,3.0)	21.01	9.37	-3.24
(-30, 10,3.0)	17.54	3.99	-0.86	(-5, 10,6.0)	21.63	10.57	-2.60
(-30, 10,6.0)	19.47	4.71	-1.30	(-5, 10,9.0)	21.47	11.31	-2.02
(-30, 10,9.0)	19.39	4.53	-1.08	(-5, 20,3.0)	20.53	6.14	-0.65
(-30, 20,3.0)	18.46	3.94	-0.70	(-5, 20,6.0)	21.54	6.59	-0.85
(-30, 20,6.0)	18.44	3.81	-0.58	(-5, 20,9.0)	21.36	6.36	-0.71
(-30, 20,9.0)	18.86	4.16	-0.39	(0, -20,3.0)	24.69	4.02	-1.09
(-20, -20,3.0)	19.83	3.89	-0.64	(0, -20,6.0)	25.56	4.34	-1.25
(-20, -20,6.0)	20.88	4.63	-0.91	(0, -20,9.0)	25.59	4.00	-0.85
(-20, -20,9.0)	19.93	4.37	-0.77	(0, -10,3.0)	29.36	4.75	-2.46
(-20, -10,3.0)	18.66	3.94	-0.65	(0, -10,6.0)	29.89	3.92	-2.45
(-20, -10,6.0)	19.01	3.17	-0.91	(0, -10,9.0)	30.06	3.33	-2.00
(-20, -10,9.0)	18.79	2.93	-0.95	(0, 10,3.0)	28.75	6.30	-2.55
(-20, 0,3.0)	17.59	4.15	-1.33	(0, 10,6.0)	29.29	7.97	-2.50
(-20, 0,6.0)	17.31	3.81	-1.24	(0, 10,9.0)	29.19	7.77	-1.99
(-20, 0,9.0)	17.18	3.38	-0.79	(0, 20,3.0)	24.66	6.60	-0.56
(-20, 10,3.0)	17.00	6.00	-0.71	(0, 20,6.0)	25.41	6.31	-0.66
(-20, 10,6.0)	17.56	5.65	-0.58	(0, 20,9.0)	25.12	5.78	-0.41
(-20, 10,9.0)	18.32	6.09	-0.86	(5, -20,3.0)	25.25	5.51	0.12
(-20, 20,3.0)	18.23	4.98	-0.55	(5, -20,6.0)	25.10	6.18	-0.68
(-20, 20,6.0)	19.23	5.34	-0.55	(5, -20,9.0)	25.22	6.00	-1.14
(-20, 20,9.0)	18.62	5.05	-0.65	(5, -10,3.0)	26.49	9.51	-1.76
(-10, -20,3.0)	21.26	3.29	-0.91	(5, -10,6.0)	26.64	7.81	-2.85
(-10, -20,6.0)	22.39	4.56	-1.33	(5, -10,9.0)	25.69	3.14	-1.85
(-10, -20,9.0)	21.31	3.70	-0.83	(5, 10,3.0)	25.23	4.20	-1.69
(-10, -10,3.0)	19.24	0.36	-1.88	(5, 10,6.0)	26.12	5.86	-2.24
(-10, -10,6.0)	19.12	-1.12	-1.62	(5, 10,9.0)	26.48	6.31	-2.69
(-10, -10,9.0)	18.37	-1.94	-1.37	(5, 20,3.0)	22.52	6.85	-0.38
(-10, 0,3.0)	12.00	3.88	-2.85	(5, 20,6.0)	23.64	6.18	-0.63
(-10, 0,6.0)	11.57	3.08	-2.40	(5, 20,9.0)	23.40	5.99	-0.76
(-10, 0,9.0)	11.79	2.42	-1.37	(10, -20,3.0)	24.89	6.35	-1.04
(-10, 10,3.0)	18.75	8.22	-2.38	(10, -20,6.0)	25.11	5.36	-1.12
(-10, 10,6.0)	18.81	8.82	-1.77	(10, -20,9.0)	26.38	5.33	-0.81
(-10, 10,9.0)	19.39	9.70	-1.51	(10, -10,3.0)	27.02	10.16	-2.28
(-10,20,3.0)	18.99	6.02	-0.46	(10, -10,6.0)	27.98	8.73	-1.98

Coordinates (cm)	Vx (cm/sec)	Vy (cm/sec)	Vz (cm/sec)	Coordinates (cm)	Vx (cm/sec)	Vy (cm/sec)	Vz (cm/sec)
(10, -10,9.0)	28.28	8.42	-1.55	(20, -10,3.0)	22.36	9.49	1.80
(10, 0,3.0)	-3.77	-1.87	-0.59	(20, -10,6.0)	23.17	9.92	0.05
(10, 0,6.0)	-4.05	-2.47	0.49	(20, -10,9.0)	19.99	7.41	-2.09
(10, 0,9.0)	-4.96	-2.33	-0.26	(20, 0,3.0)	12.89	-2.49	1.22
(10, 10,3.0)	22.57	-0.04	-2.08	(20, 0,6.0)	13.16	0.24	7.65
(10, 10,6.0)	24.80	2.23	-2.60	(20, 0,9.0)	6.57	4.90	8.51
(10, 10,9.0)	23.29	1.52	-2.02	(20, 10,3.0)	24.52	7.46	2.70
(10,20,3.0)	26.66	5.24	-0.60	(20, 10,6.0)	25.25	3.16	0.07
(10,20,6.0)	26.82	4.74	-0.92	(20, 10,9.0)	23.43	2.36	-2.02
(10, 20,9.0)	25.82	3.56	-0.29	(20, 20,3.0)	24.34	5.66	-0.22
(20, -20,3.0)	25.71	5.29	-0.52	(20, 20,6.0)	24.60	4.62	-1.00
(20, -20,6.0)	25.60	7.94	-1.16	(20, 20,9.0)	25.53	4.50	-0.68
(20, -20,9.0)	25.45	7.51	-1.00				

APPENDIX-E

EXPERIMENTAL DATA RELATING TO SCOUR PATTERN AROUND CIRCULAR ISLAND WITH V-SHAPED DEFLECTOR

Table E.1: Scour Pattern for Experimental Run E1
[Circular Island (d=15cm) with V-shaped deflector (3cm length) at F_r=0.16, h=15cm, L=11.25cm, θ=84°]

x(cm)	y(cm)	z(cm)	x(cm)	y(cm)	z(cm)	x(cm)	y(cm)	z(cm)
-16.5	-10	0	-3	-12.5	-2.20	12	-7.5	-3.04
-16.5	-5	0	-3	-9.5	-3.83	12	-3.5	-1.55
-16.5	0	0	-3	-7.5	-4.98	12	0.5	0.12
-16.5	5	0	-3	8.5	-4.50	12	4.5	-1.20
-16.5	10	0	-3	11.5	-3.00	12	8.5	-2.50
-15	-4.5	0	-3	14.5	-1.50	12	12.5	-2.77
-15	-1.5	-0.72	-3	16.5	-0.05	12	16.5	-2.70
-15	1.5	-0.95	0	-16	-0.30	12	20.5	-2.10
-15	4.5	-0.30	0	-13.5	-1.92	17	-19.5	-2.80
-15	5.9	0	0	-10.5	-3.78	17	-14.5	-2.44
-12	-9	-0.05	0	-8	-4.80	17	-9.5	-1.50
-12	-6.5	-1.14	0	9	-4.70	17	-4.5	-0.21
-12	-3.5	-1.76	0	11.5	-3.65	17	0.5	1.13
-12	-0.5	-2.75	0	14.5	-1.90	17	5.5	-0.92
-12	2.5	-2.43	0	17.2	-0.10	17	10.5	-2.50
-12	5.5	-1.40	4	-17	-0.35	17	15.5	-2.15
-12	8.5	-0.65	4	-13.5	-1.66	17	20.5	-2.08
-12	10.5	0.10	4	-9.5	-4.15	22	-19.5	-2.05
-9	-12	-0.15	4	-6.9	-4.36	22	-14.5	-1.64
-9	-9.5	-1.47	4	7.7	-4.28	22	-9.5	-0.47
-9	-6.5	-2.37	4	11.5	-3.80	22	-4.5	0.77
-9	-3.5	-3.04	4	15.5	-1.30	22	0.5	2.40
-9	-1	-3.13	4	18.6	-0.15	22	5.5	1.12
-9	3.5	-3.00	8	-17.6	-0.45	22	10.5	-0.25
-9	6.5	-2.55	8	-14.5	-1.90	22	15.5	-1.46
-9	9.5	-1.55	8	-10.5	-2.50	22	20.5	-1.63
-9	13.5	0	8	-6.5	-3.86	27	-19.5	-2.82
-6	-14.2	-0.16	8	-2.5	-1.90	27	-14.5	-0.56
-6	-11.5	-1.90	8	3	-1.40	27	-9.5	-0.46
-6	-8.5	-3.15	8	6.5	-3.23	27	-4.5	1.53
-6	-5.5	-4.35	8	9.5	-4.80	27	0.5	2.40
-6	6	-3.71	8	13.5	-2.70	27	5.5	1.90
-6	8.5	-3.40	8	17.5	-1.80	27	10.5	0.50
-6	11.5	-2.00	8	20.5	-0.83	27	15.5	-0.32
-6	14.5	-0.55	12	-19.5	-0.55	27	20.5	-2.15
-6	15.5	0	12	-15.5	-1.10			
-3	-15.3	-0.25	12	-11.5	-2.25			

Table E.2: Scour Pattern for Experimental Run E2
[Circular Island (d=15cm) with V-shaped deflector (3cm length) at F_r=0.16, h=15cm, L=15cm, θ=60°]

x(cm)	y(cm)	z(cm)	x(cm)	y(cm)	z(cm)	x(cm)	y(cm)	z(cm)
-17	-10	0	-4	11	-1.75	11	-3.5	0.50
-17	0	0	-4	14.1	0.15	11	-0.5	1.50
-17	10	0	-1	-14	0.10	11	2.5	-0.50
-16	-1.9	0	-1	-11	-1.65	11	4.5	-1.20
-16	0	-0.45	-1	-8	-2.95	11	8.5	0.10
-16	1.7	0	-1	9	-3.20	11	12.5	1.00
-13	-6.7	-0.10	-1	12	-1.30	11	16.5	-0.90
-13	-4	-0.70	-1	13.5	-0.30	11	20.5	0.20
-13	-2	-0.90	-1	15	0.15	15	-19.5	-1.37
-13	0	-0.43	3	-14.8	0.05	15	-15.5	-2.40
-13	3.5	-1.05	3	-14	0.20	15	-11.5	-0.53
-13	7	-0.10	3	-11	-1.20	15	-7.5	-0.35
-10	-10.1	-0.10	3	-9	-1.80	15	-3.5	0.45
-10	-7	-1.52	3	-7.5	-2.00	15	-0.5	2.00
-10	-4	-2.38	3	8.5	-2.48	15	2.5	0.70
-10	-1.5	-1.20	3	11.5	-0.95	15	6.5	0.05
-10	1.5	-2.22	3	14.5	0.40	15	10.5	1.05
-10	4.5	-2.35	3	15.5	0.05	15	14.5	-0.87
-10	7.5	-1.20	7	-15.5	0	15	18.5	-1.76
-10	10.5	-0.10	7	-15	-0.20	15	20.5	-1.03
-7	-12	-0.10	7	-13.5	0.55	19	-19.5	-1.71
-7	-9	-1.56	7	-10.5	-0.25	19	-15.5	-2.38
-7	-6	-2.70	7	-7.5	-0.80	19	-11.5	-1.00
-7	-4	-2.40	7	-4.5	0.50	19	-7.5	0.70
-7	5.1	-4.00	7	5.5	-1.30	19	-3.5	2.24
-7	8	-2.65	7	8.5	-1.25	19	-1	3.20
-7	11	-0.87	7	11.5	0.25	19	2.5	2.30
-7	12.5	-0.05	7	14.5	0.60	19	6.5	0.65
-4	-13.3	0	7	16	-0.20	19	10.5	0.20
-4	-10.5	-1.60	11	-19.5	0.05	19	14.5	-1.90
-4	-8.5	-2.57	11	-15.5	-1.30	19	18.5	-2.06
-4	-6.7	-3.10	11	-11.5	0.25	19	20.5	-1.45
-4	8	-3.58	11	-7.5	-0.35			

Table E.3: Scour Pattern for Experimental Run E3
[Circular Island (d=15cm) with V-shaped deflector (3cm length) at F_r=0.16, h=15cm, L=22.55cm, θ=40°]

x(cm)	y(cm)	z(cm)	x(cm)	y(cm)	z(cm)	x(cm)	y(cm)	z(cm)
-24	-10	0	-7	10.5	-2.05	7	17.5	-0.01
-24	0	0	-7	13.5	-1.10	7	19.5	0.15
-24	10	0.10	-7	15	0.10	11	-18.5	0.10
-23	-1.5	0.10	-4	-15	-0.10	11	-14.5	-0.70
-23	0	-0.45	-4	-12.5	-1.30	11	-10.5	-0.62
-23	1.5	0.05	-4	-9.5	-2.95	11	-6.5	-0.12
-19	-3	0.15	-4	-6.5	-4.35	11	-2.5	1.35
-19	0	0.57	-4	8	-4.45	11	1.5	1.67
-19	3	0.15	-4	10.5	-2.97	11	5.5	-0.45
-16	-5	0	-4	13.5	-1.30	11	9.5	-1.05
-16	-2.5	-0.85	-4	16.5	0.15	11	13.5	-0.97
-16	0	-0.25	-1	-16	0	11	17.5	-1.02
-16	3	-0.90	-1	-13.5	-1.11	11	20.5	-0.59
-16	-5.1	-0.10	-1	-10.5	-2.70	15	-19.5	-0.43
-13	-8.3	-0.10	-1	-8	-4.18	15	-15.5	-1.55
-13	-5.5	-0.95	-1	9	-4.05	15	-11.5	-1.05
-13	-2.5	-0.45	-1	11.5	-2.65	15	-7.5	-0.20
-13	0.5	-0.70	-1	14.5	-0.83	15	-3.5	1.21
-13	3.5	-1.00	-1	17	0.15	15	0.5	2.25
-13	6.5	-0.70	3	-16.7	0.030	15	4.5	1.05
-13	10	0	3	-14.5	-0.55	15	8.5	0.31
-10	-11.7	-0.10	3	-11.5	-1.55	15	12.5	0.21
-10	-9.5	-1.20	3	-8.5	-3.10	15	16.5	-0.32
-10	-6.5	-2.05	3	-7.6	-3.34	15	20.5	-1.45
-10	-3.5	-2.20	3	8.5	-3.05	20	-19.5	-0.15
-10	-0.5	-2.45	3	11.5	-2.20	20	-15.5	0.43
-10	2.5	-2.93	3	14.5	-0.45	20	-11.5	0.08
-10	5.5	-2.75	3	18	0.20	20	-7.5	1.09
-10	8.5	-1.75	7	-17.5	0.08	20	-3.5	1.80
-10	11.5	-1.10	7	-14.5	-0.20	20	0.5	2.55
-10	13.8	0.10	7	-11.5	-0.45	20	4.5	1.30
-7	-13.5	-0.10	7	-8.5	-1.31	20	8.5	0.20
-7	-10.5	-1.50	7	-5.5	-0.91	20	12.5	0.45
-7	-7.5	-2.85	7	5	-0.76	20	16.5	-0.55
-7	-4.1	-3.85	7	8.5	-1.95	20	20.5	-1.05
-7	4.8	-4.05	7	11.5	-0.90			
-7	7.5	-3.60	7	14.5	-0.31			

Table E.4: Scour Pattern for Experimental Run E4
[Circular Island (d=15cm) with V-shaped deflector (3cm length) at F_r=0.16, h=15cm, L=30cm, θ=30°]

x(cm)	y(cm)	z(cm)	x(cm)	y(cm)	z(cm)	x(cm)	y(cm)	z(cm)
-31.5	-10	0	-10	11.5	-1.00	7	-4.5	0.20
-31.5	0	0	-10	13.5	0.10	7	5.1	-0.85
-31.5	10	0	-7	-14.2	-0.10	7	8.5	-2.00
-31	-1.5	0	-7	-11.5	-1.57	7	12.5	-0.70
-31	0	-0.25	-7	-8.5	-2.75	7	16.5	-0.80
-31	1.5	0	-7	-5.5	-4.21	7	20.5	0.40
-28	-3	0.15	-7	-4	-4.30	11	-19.5	0.22
-28	-1.5	-0.45	-7	5	-5.00	11	-15.5	-0.15
-28	2	-0.25	-7	7.5	-4.20	11	-11.5	0.55
-28	2.8	0.15	-7	10.5	-2.65	11	-7.5	0.61
-25	-3	0	-7	13.5	-1.10	11	-3.5	1.15
-25	0	-0.60	-7	15.5	0.10	11	0.5	1.55
-25	2.5	0.10	-4	-15.5	-1.00	11	4.5	-0.12
-22	-4.3	0	-4	-12.5	-1.70	11	8.5	-0.75
-22	-3	-0.35	-4	-9.5	-2.95	11	12.5	-1.03
-22	0	-0.05	-4	-6.9	-4.35	11	16.5	-0.18
-22	2.5	-0.25	-4	8.3	-4.75	11	20.5	0.45
-22	3.7	0	-4	11.5	-2.75	15	-19.5	-0.90
-19	-5.5	-0.10	-4	14.5	-0.80	15	-15.5	0.25
-19	-3	0.05	-4	16.5	0.15	15	-11.5	1.35
-19	0	0.75	-1	-16	0.05	15	-7.5	1.85
-19	4	0.05	-1	-12.5	-1.55	15	-3.5	1.60
-15	-7.5	-0.05	-1	-9.5	-3.20	15	0.5	1.45
-15	0	0.35	-1	-8	-4.03	15	4.5	1.05
-15	7.5	-0.05	-1	9	-4.40	15	8.5	0.40
-13	-8.5	0	-1	11.5	-2.85	15	12.5	0.25
-13	-5.5	-1.15	-1	14.5	-0.85	15	16.5	-0.55
-13	-2.5	-1.60	-1	17	0.25	15	20.5	-0.18
-13	0.5	-1.85	3	-16.3	0.10	19	-19.5	-1.50
-13	3.5	-1.87	3	-13.5	-0.80	19	-15.5	-0.35
-13	6.5	-1.18	3	-10.5	-1.75	19	-11.5	0.85
-13	10	0	3	-7.5	-2.90	19	-7.5	1.48
-10	-12	0	3	8.5	-3.30	19	-3.5	1.55
-10	-9.5	-1.33	3	11.5	-2.00	19	0.5	1.95
-10	-6.5	-2.45	3	14.5	-0.31	19	4.5	2.10
-10	-3.5	-3.38	3	18	0.10	19	8.5	0.15
-10	-0.5	-3.70	7	-17.5	0.10	19	12.5	0.19
-10	2.5	-3.80	7	-13.5	0.05	19	16.5	-0.98
-10	5.5	-3.23	7	-9.5	-0.50	19	20.5	-1.05
-10	8.5	-2.35	7	-6.5	-0.90			

Table E.5: Scour Pattern for Experimental Run E5
[Circular Island (d=15cm) with V-shaped deflector (3cm length) at F_r=0.19, h=15cm, L=11.25cm, θ=84°]

x(cm)	y(cm)	z(cm)	x(cm)	y(cm)	z(cm)	x(cm)	y(cm)	z(cm)
-19	-10	0	-6	6	-5.03	8	20.5	-1.13
-19	-5	0	-6	8.5	-4.61	12	-19.5	-0.75
-19	0	0	-6	11.5	-2.71	12	-15.5	-1.49
-19	5	0	-6	14.5	-0.75	12	-11.5	-3.05
-19	10	0	-6	15.5	0	12	-7.5	-4.13
-17	-2.6	0	-3	-15.3	-0.34	12	-3.5	-2.10
-17	0	-0.56	-3	-12.5	-2.99	12	0.5	0.16
-17	2.1	0	-3	-9.5	-5.20	12	4.5	-1.63
-16.5	-3.2	0	-3	-7.5	-6.76	12	8.5	-3.39
-16.5	-1.5	-0.48	-3	8.5	-6.11	12	12.5	-3.76
-16.5	0	-1.05	-3	11.5	-4.07	12	16.5	-3.66
-16.5	1.5	-0.35	-3	14.5	-2.04	12	20.5	-2.85
-16.5	3.8	0	-3	16.5	-0.07	17	-19.5	-3.80
-15	-4.5	0	0	-16	-0.41	17	-14.5	-3.31
-15	-1.5	-0.98	0	-13.5	-2.61	17	-9.5	-2.04
-15	1.5	-1.29	0	-10.5	-5.13	17	-4.5	-0.28
-15	4.5	-0.41	0	-8	-6.51	17	0.5	1.53
-15	5.9	0	0	9	-6.38	17	5.5	-1.25
-12	-9	-0.07	0	11.5	-4.95	17	10.5	-3.39
-12	-6.5	-1.55	0	14.5	-2.58	17	15.5	-2.92
-12	-3.5	-2.39	0	17.2	-0.14	17	20.5	-2.82
-12	-0.5	-3.73	4	-17	-0.47	22	-19.5	-2.78
-12	2.5	-3.30	4	-13.5	-2.25	22	-14.5	-2.23
-12	5.5	-1.90	4	-9.5	-5.63	22	-9.5	-0.64
-12	8.5	-0.88	4	-6.9	-5.92	22	-4.5	1.04
-12	10.5	0.14	4	7.7	-5.81	22	0.5	3.26
-9	-12	-0.20	4	11.5	-5.16	22	5.5	1.52
-9	-9.5	-1.99	4	15.5	-1.76	22	10.5	-0.34
-9	-6.5	-3.35	4	18.6	-0.20	22	15.5	-1.98
-9	-3.5	-4.13	8	-17.6	-0.61	22	20.5	-2.21
-9	-1	-4.25	8	-14.5	-2.58	27	-19.5	-2.12
-9	3.5	-4.07	8	-10.5	-3.39	27	-14.5	-0.76
-9	6.5	-3.46	8	-6.5	-5.24	27	-9.5	-0.62
-9	9.5	-2.10	8	-2.5	-2.58	27	-4.5	2.08
-9	13.5	0	8	3	-1.90	27	0.5	3.30
-6	-14.2	-0.22	8	6.5	-4.38	27	5.5	2.58
-6	-11.5	-2.58	8	9.5	-6.51	27	10.5	0.68
-6	-8.5	-4.27	8	13.5	-3.56	27	15.5	-0.43
-6	-5.5	-5.78	8	17.5	-2.44	27	20.5	-2.92

Table E.6: Scour Pattern for Experimental Run E6
[Circular Island (d=15cm) with V-shaped deflector (3cm length) at F_r=0.19, h=15cm, L=15cm, θ=60°]

x(cm)	y(cm)	z(cm)	x(cm)	y(cm)	z(cm)	x(cm)	y(cm)	z(cm)
-20	-10	0	-7	-4.1	-5.40	11	-19.5	-3.00
-20	-5	0	-7	4.8	-6.15	11	-15.5	-4.20
-20	0	0	-7	8.5	-4.63	11	-11.5	-2.49
-20	5	0	-7	12.5	-2.45	11	-7.5	-1.42
-20	10	0	-7	16.5	-1.30	11	-3.5	0.42
-18	-7.2	0	-7	19.3	0.10	11	0.5	0.55
-18	-4.5	-0.33	-4	-19.5	-0.42	11	4.5	-1.51
-18	-1.5	-1.55	-4	-15.5	-1.94	11	8.5	-3.21
-18	1.5	-1.63	-4	-11.5	-2.91	11	12.5	-2.35
-18	4.5	-0.85	-4	-7.5	-5.40	11	16.5	-2.89
-18	6.3	0	-4	7.7	-5.99	11	20.5	-1.33
-16	-10.9	-0.05	-4	11.5	-4.01	15	-19.5	-1.73
-16	-8.5	-1.00	-4	15.5	-2.05	15	-15.5	-2.82
-16	-5.5	-1.33	-4	18.5	-0.75	15	-11.5	-2.10
-16	-2.5	-2.60	-4	19.7	0.12	15	-7.5	-0.82
-16	0.5	-3.15	-1	-19.5	-1.42	15	-3.5	0.83
-16	3.5	-2.39	-1	-15.5	-2.15	15	0.5	1.00
-16	6.5	-1.03	-1	-11.5	-3.13	15	4.5	-0.97
-16	8.5	0.10	-1	-7.5	-5.00	15	8.5	-1.94
-13	-14.1	-0.20	-1	9	-5.65	15	12.5	-2.44
-13	-12.5	-0.97	-1	12.5	-4.12	15	16.5	-0.75
-13	-8.5	-2.00	-1	16.5	-1.70	15	20.5	-1.12
-13	-4.5	-3.27	-1	20.5	0.12	19	-19.5	-2.45
-13	0	-4.03	3	-19.5	-2.18	19	-14.5	-1.23
-13	3.5	-3.84	3	-15.5	-2.35	19	-9.5	0.32
-13	7.5	-1.87	3	-11.5	-2.79	19	-4.5	1.47
-13	9.5	-1.29	3	-7.5	-3.18	19	0.5	1.70
-13	12.1	0.15	3	8.1	-4.55	19	5.5	-0.43
-10	-16.3	-0.35	3	11.5	-4.05	19	10.5	-2.11
-10	-13.5	-1.32	3	15.5	-2.32	19	15.5	-0.79
-10	-9.5	-2.30	3	18.5	-1.32	19	20.5	-1.45
-10	-5.5	-3.80	3	20.5	-0.43	23	-19.5	-2.60
-10	-1.5	-3.95	7	-19.5	-3.92	23	-14.5	0.15
-10	2.5	-4.77	7	-15.5	-3.42	23	-9.5	1.85
-10	6.5	-3.93	7	-11.5	-2.16	23	-4.5	2.42
-10	10.5	-2.16	7	-7.5	-1.60	23	0.5	2.06
-10	13.5	-0.70	7	-4.5	-0.05	23	5.5	-0.53
-10	16.3	0.10	7	4.5	-2.02	23	10.5	-1.48
-7	-18	-0.35	7	8.5	-3.68	23	15.5	-0.38
-7	-15.5	-1.57	7	12.5	-2.43	23	20.5	-1.48
-7	-11.5	-2.19	7	16.5	-2.39			
-7	-7.5	-4.33	7	20.5	-1.32			

Table E.7: Scour Pattern for Experimental Run E7
[Circular Island (d=15cm) with V-shaped deflector (3cm length) at F_r=0.19, h=15cm, L=22.5cm, θ=40°]

x(cm)	y(cm)	z(cm)	x(cm)	y(cm)	z(cm)	x(cm)	y(cm)	z(cm)
-28	-10	0	-11	-17.7	-0.05	-2	16.5	-3.70
-28	-5	0	-11	-14.5	-2.20	-2	20.5	-2.48
-28	0	0	-11	-10.5	-2.85	1	-19.5	-1.68
-28	5	0	-11	-6.5	-4.50	1	-15.5	-2.68
-28	10	0	-11	7.5	-5.30	1	-11.5	-4.67
-27	-3.2	0	-11	1.5	-4.70	1	-8	-5.17
-27	0	-0.65	-11	5.5	-5.08	1	8.5	-5.94
-27	3.3	0	-11	9.5	-4.00	1	12.5	-5.30
-24	-5.5	0	-11	13.5	-2.22	1	16.5	-4.50
-24	-3	-1.85	-11	17.5	-1.20	1	20.5	-3.30
-24	0	-2.80	-11	19.5	0.14	5	-19.5	-2.96
-24	3	-1.66	-8	-18.7	-0.10	5	-15.5	-2.46
-24	6	0.10	-8	-15.5	-2.08	5	-11.5	-3.65
-20	-7.6	0	-8	-11.5	-3.62	5	-7.5	-3.25
-20	-5.5	-1.90	-8	-7.5	-5.40	5	7	-3.40
-20	-2	-4.27	-8	-5	-5.90	5	10.5	-4.28
-20	2.3	-3.22	-8	-2.3	-6.00	5	14.5	-4.77
-20	5.5	-1.53	-8	3	-6.40	5	17.5	-4.79
-20	8.5	-0.70	-8	6.5	-6.08	5	20.5	-3.40
-20	11.9	0	-8	10.5	-4.78	9	-19.5	-3.30
-17	-10.2	-0.05	-8	14.5	-2.60	9	-15.5	-2.13
-17	-7.5	-1.25	-8	16.5	-1.75	9	-11.5	-2.51
-17	-3.5	-3.58	-8	18	-2.18	9	-7.5	-2.09
-17	-0.8	-3.98	-8	20.5	-0.80	9	-3.5	-0.56
-17	0.7	-3.15	-5	-19.5	-0.30	9	0.5	0.28
-17	2	-3.40	-5	-16.5	-1.55	9	4.5	-1.65
-17	5.5	-2.52	-5	-12.5	-3.80	9	8.5	-2.40
-17	9.5	-1.95	-5	-9.5	-5.20	9	12.5	-4.04
-17	12.5	-1.05	-5	-6.2	-6.48	9	16.5	-4.63
-17	14.3	0	-5	7	-6.98	9	20.5	-2.98
-14	-15.9	-0.05	-5	10.5	-5.90	13	-19.5	-2.64
-14	-13.5	-1.55	-5	14.5	-3.62	13	-15.5	-2.40
-14	-9.5	-1.70	-5	17.5	-2.95	13	-11.5	-1.67
-14	-5.5	-3.35	-5	20.5	-1.78	13	-7.5	-1.03
-14	-1.5	-4.26	-2	-19.5	-1.14	13	-3.5	-0.28
-14	2.5	-3.75	-2	-15.5	-2.76	13	0.5	-0.54
-14	6.5	-3.18	-2	-11.5	-4.85	13	4.5	-1.00
-14	10.5	-2.70	-2	-7.5	-6.10	13	8.5	-2.15
-14	13.5	-1.28	-2	8.5	-6.80	13	12.5	-3.19
-14	16.5	0	-2	12.5	-5.45	13	16.5	-3.00

x(cm)	y(cm)	z(cm)	x(cm)	y(cm)	z(cm)	x(cm)	y(cm)	z(cm)
13	20.5	-2.13	17	10.5	-1.93	21	0.5	-0.22
17	-19.5	-1.97	17	15.5	-2.30	21	5.5	-0.87
17	-14.5	-1.57	17	20.5	-2.10	21	10.5	-1.95
17	-9.5	-0.76	21	-19.5	-1.07	21	15.5	-2.60
17	-4.5	0	21	-14.5	-0.10	21	20.5	-1.82
17	0.5	-0.73	21	-9.5	0.15			
17	5.5	-0.71	21	-4.5	-0.10			

Table E.8: Scour Pattern for Experimental Run E8
[Circular Island (d=15cm) with V-shaped deflector (3cm length) at F_r=0.19, h=15cm, L=30cm, θ=30°]

x(cm)	y(cm)	z(cm)	x(cm)	y(cm)	z(cm)	x(cm)	y(cm)	z(cm)
-33	-10	0	-11	-15.3	-0.15	1	-16.5	-2.95
-33	0	0	-11	-11.5	-2.65	1	-12.5	-4.20
-33	10	0	-11	-7.5	-3.75	1	-9.5	-6.10
-31	-3.3	0	-11	-3.5	-4.70	1	-8.1	-6.35
-31	0	-2.10	-11	0.5	-4.90	1	9	-6.40
-31	3.1	0.10	-11	4.5	-5.30	1	12.5	-4.52
-28	-5.5	0	-11	8.5	-4.55	1	16.5	-2.25
-28	-2.5	-2.10	-11	12.5	-3.05	1	20.5	-1.25
-28	2.5	-1.90	-11	15.5	-1.35	5	-19.5	-1.35
-28	4.9	0.10	-11	17	0.10	5	-15.5	-2.20
-25	-5.4	0	-8	-17.4	-0.15	5	-11.5	-3.80
-25	-2.5	-1.66	-8	-14.5	-1.10	5	-8.5	-4.90
-25	0	-2.26	-8	-10.5	-3.90	5	-6.5	-4.80
-25	2.5	-1.70	-8	-6.5	-5.25	5	7.5	-4.90
-25	5.5	0	-8	-2.5	-5.40	5	11.5	-4.40
-22	-5.1	0.10	-8	2.5	-5.75	5	15.5	-2.60
-22	-2	-0.75	-8	6.5	-6.00	5	18.5	-2.00
-22	0	-0.90	-8	10.5	-4.75	5	20.5	-1.80
-22	2.5	-0.70	-8	14.5	-2.75	9	-19.5	-1.00
-22	5.7	0.10	-8	18.5	0.10	9	-15.5	-1.56
-19.5	-10	-0.15	-5	-19	-0.15	9	-11.5	-2.55
-19.5	-5.1	0.35	-5	-15.5	-2.50	9	-7.5	-3.15
-19.5	0	-0.25	-5	-11.5	-4.60	9	-3.5	-2.05
-19.5	5.7	0.20	-5	-8.5	-6.00	9	0.5	-2.30
-19.5	0	0	-5	-6.1	-6.25	9	2	-1.70
-17	-8.5	0	-5	7.2	-6.60	9	5.5	-3.68
-17	-4.5	-1.35	-5	10.5	-5.70	9	9.5	-4.20
-17	-0.5	-2.15	-5	14.5	-3.10	9	13.5	-3.10
-17	3.5	-2.20	-5	17.5	-1.45	9	17.5	-1.40
-17	7.5	-1.75	-5	19.7	0.10	9	20.5	-1.25
-17	10.5	-1.30	-2	-19.8	-0.15	13	-19.5	-0.50
-17	12.6	0	-2	-16.5	-2.85	13	-15.5	-0.50
-14	-12.3	-0.15	-2	-12.5	-4.45	13	-11.5	-1.70
-14	-8.5	-2.25	-2	-9.5	-6.40	13	-7.5	-2.70
-14	-4.5	-2.88	-2	-7.8	-6.90	13	-3.5	-2.65
-14	-0.5	-3.75	-2	9	-6.85	13	0.5	-3.35
-14	3.5	-3.50	-2	12.5	-4.75	13	2.7	-2.45
-14	7.5	-3.45	-2	16.5	-2.35	13	6.5	-3.10
-14	11.5	-2.60	-2	20.5	-0.10	13	10.5	-2.70
-14	15.7	0	1	-19.5	-0.90	13	14.5	-1.28

x(cm)	y(cm)	z(cm)	x(cm)	y(cm)	z(cm)	x(cm)	y(cm)	z(cm)
13	17.5	-0.62	17	7.5	-0.85	21	-5.5	0.40
13	20.5	-1.50	17	11.5	-1.25	21	-2.5	-1.20
17	-19.5	-0.30	17	14.5	-0.78	21	-0.5	-1.90
17	-16	0.90	17	17.5	-0.35	21	3.5	-0.40
17	-12.5	-0.02	17	20.5	-0.65	21	7.5	0.15
17	-8.5	-1.60	21	-19.5	-0.30	21	11.5	0.65
17	-4.5	-1.80	21	-15.5	1.40	21	14.5	0.75
17	-0.5	-2.90	21	-13	2.10	21	17.5	-0.40
17	3.5	-1.60	21	-9.5	1.20	21	20.5	-0.75

Table E.9: Scour Pattern for Experimental Run E9
[Circular Island (d=15cm) with V-shaped deflector (4.5cm length) at F_r=0.16, h=15cm, L=15cm, θ=60°]

x(cm)	y(cm)	z(cm)	x(cm)	y(cm)	z(cm)	x(cm)	y(cm)	z(cm)
-18.5	-10	0	-4	-14.5	0	11	-19.5	-0.30
-18.5	-5	0	-4	-11.5	-1.62	11	-15.5	-0.90
-18.5	-0.1	0.10	-4	-8.5	-3.55	11	-11.5	0.15
-18.5	5	0.10	-4	-6.9	-4.10	11	-7.5	-0.40
-18.5	10	0.10	-4	7.9	-2.20	11	-3.5	-1.05
-16	-4.7	0.10	-4	10.5	-1.45	11	0.5	0.02
-16	-2	-0.85	-4	13.5	-0.25	11	4.5	0.10
-16	0	-1.57	-4	16.7	0.30	11	8.5	0.80
-16	3	-0.72	-1	-15.5	-0.05	11	12.5	1.15
-16	5.7	0.28	-1	-12.5	-1.15	11	16.5	-0.33
-13	-7.3	0	-1	-9.5	-3.20	11	20.5	-1.25
-13	-4.5	-0.97	-1	-8	-3.80	15	-19.5	-1.77
-13	-1.5	-1.65	-1	9	-1.70	15	-15.5	-2.37
-13	0.5	-0.08	-1	11.5	-1.02	15	-11.5	-0.53
-13	3.5	-1.15	-1	14.5	0.22	15	-7.5	0.30
-13	6.5	-0.25	-1	17.5	0.30	15	-3.5	-1.05
-13	8.1	0.25	3	-16.5	-0.10	15	0.5	0.57
-10	-10	0	3	-13.5	-0.50	15	2.5	1.40
-10	-7.5	-1.00	3	-10.5	-1.83	15	6.5	0.31
-10	-4.5	-2.35	3	-7.5	-2.92	15	10.5	0.75
-10	-1.5	-1.92	3	8.4	-0.48	15	14.5	-0.93
-10	1.5	-0.80	3	10.5	-0.70	15	18.5	-2.30
-10	4.5	-1.48	3	13.5	0.35	15	20.5	-2.53
-10	7.5	-0.87	3	16.5	0.67	19	-19.5	-2.55
-10	10.5	-0.52	3	18.5	0.30	19	-15.5	-3.05
-10	14	0.30	7	-17.5	-0.23	19	-11.5	-1.60
-7	-12.8	0	7	-13.5	-0.30	19	-7.5	0
-7	-10.5	-1.15	7	-9.5	-0.96	19	-3.5	0.28
-7	-7.5	-2.72	7	-5.5	-1.90	19	0.5	1.87
-7	-4	-3.80	7	-4.5	-1.63	19	2	2.35
-7	5	-1.68	7	5.3	0.17	19	4.5	1.00
-7	7.5	-2.20	7	8.5	0.47	19	8.5	0
-7	10.5	-1.05	7	12.5	0.60	19	12.5	-0.70
-7	13.5	-0.78	7	16.5	0.55	19	16.5	-2.45
-7	16.1	0.30	7	19	0.07	19	20.5	-3.15

Table E.10: Scour Pattern for Experimental Run E10
[Circular Island (d=15cm) with V-shaped deflector (4.5cm length) at F_r=0.16, h=15cm, L=18.75cm, θ=48°]

x(cm)	y(cm)	z(cm)	x(cm)	y(cm)	z(cm)	x(cm)	y(cm)	z(cm)
-20.5	-10	0	-6	-12.1	-0.05	8	11.5	0.20
-20.5	-5	0	-6	-9.5	-1.40	8	15.5	-0.43
-20.5	0	0	-6	-6.5	-2.83	8	17.5	-0.15
-20.5	5	0	-6	-5.1	-3.10	12	-19.5	-0.45
-20.5	10	0	-6	6.1	-3.85	12	-15.5	-1.15
-19.5	-1.5	0	-6	8.5	-2.91	12	-11.5	0.50
-19.5	0	-0.55	-6	11.5	-0.95	12	-7.5	0.75
-19.5	2	0	-6	13.1	0	12	-3.5	0.02
-16	-2.9	0.17	-3	-13.2	-0.10	12	1	1.47
-16	-1.7	-0.05	-3	-10.5	-1.55	12	4.5	-0.58
-16	0	0.27	-3	-8	-3.15	12	8.5	0.15
-16	2.5	-0.22	-3	-7.3	-3.60	12	12.5	0.55
-16	3.9	0.10	-3	8.5	-3.69	12	16.5	-1.52
-14	-5.3	0.05	-3	11.5	-1.48	12	20.5	-0.55
-14	-2.7	0	-3	14	-0.05	17	-19.5	-2.12
-14	0	0.25	0	-14	-0.15	17	-14.5	-1.35
-14	3.5	-0.37	0	-11.5	-1.15	17	-9.5	0.63
-14	6.1	0	0	-8.5	-2.83	17	-4.5	0.20
-12	-8.3	0	0	9	-3.00	17	1.5	2.10
-12	-5.5	-1.25	0	11.5	-1.53	17	6.5	0.22
-12	-2.5	-0.53	0	14.5	-0.02	17	10.5	0.10
-12	0.5	0.13	4	-15	-0.20	17	15.5	-1.87
-12	3.5	-1.10	4	-11.5	-0.45	17	20.5	-2.05
-12	6.5	-1.20	4	-8.5	-1.40	22	-19.5	-2.75
-12	9.3	-0.05	4	-7.5	-1.75	22	-14.5	-3.07
-9	-10.8	-0.05	4	8.5	-1.48	22	-9.5	-1.45
-9	-8.5	-1.07	4	12.5	-0.38	22	-4.5	0.25
-9	-5.5	-1.83	4	15.5	-0.17	22	0.5	2.00
-9	-2.5	-1.65	8	-15.5	-0.30	22	5.5	2.55
-9	0.5	-1.95	8	-11.5	0.15	22	10.5	-0.75
-9	3.5	-2.35	8	-7.5	-0.05	22	15.5	-2.80
-9	6.5	-2.50	8	-3.5	0.44	22	20.5	-2.25
-9	9.5	-1.20	8	3.5	-0.45			
-9	11.9	0.05	8	7.5	-0.45			

Table E.11: Scour Pattern for Experimental Run E11
[Circular Island (d=15cm) with V-shaped deflector (4.5cm length) at F_r=0.16, h=15cm, L=22.5cm, θ=40°]

x(cm)	y(cm)	z(cm)	x(cm)	y(cm)	z(cm)	x(cm)	y(cm)	z(cm)
-24.5	-10	0	-5	-11.5	-1.48	9	-5.5	0.35
-24.5	-5	0	-5	-8.5	-2.78	9	-1.5	1.33
-24.5	0	0	-5	-6.2	-4.02	9	2.5	-0.03
-24.5	5	0	-5	7.1	-4.88	9	6.5	-0.65
-24.5	10	0	-5	9.5	-3.55	9	10.5	-0.25
-17	-5.8	0	-5	12.5	-2.05	9	14.5	-0.08
-17	-2.5	-0.58	-5	15.5	-0.25	9	18.5	-0.60
-17	0.5	0.15	-5	16.5	0.15	9	20.5	-0.46
-17	3.5	-0.60	-2	-13.9	0	13	-19.5	-1
-17	6.3	0.10	-2	-11.5	-1.78	13	-15.5	0.45
-14	-7.4	0	-2	-8.5	-3.35	13	-11.5	1.20
-14	-4.5	-1.48	-2	-7.8	-3.80	13	-7.5	1.55
-14	-1.5	-0.25	-2	8.9	-4.50	13	-3.5	1.50
-14	1.5	-0.45	-2	11.5	-2.90	13	0.5	1.30
-14	4.5	-1.70	-2	14.5	-1.08	13	4.5	0.12
-14	7.5	-0.68	-2	17.1	0.20	13	8.5	0.64
-14	9.5	0.10	1	-16	-0.10	13	12.5	0.80
-11	-9.5	0.02	1	-14.5	-0.22	13	16.5	-0.97
-11	-6.5	-1.05	1	-11.5	-1.43	13	20.5	-2.05
-11	-3.5	-1.72	1	-8.5	-3.10	17	-19.5	-2.30
-11	-0.5	-1.97	1	-8	-3.18	17	-14.5	-0.15
-11	2.5	-2.30	1	8.5	-3.88	17	-9.5	0.80
-11	5.5	-2.48	1	11.5	-2.65	17	-4.5	1.20
-11	8.5	-1.55	1	14.5	-1.14	17	0.5	2.53
-11	11.5	-0.38	1	17.5	0.10	17	5.5	1.08
-11	12.8	0.14	5	-16.3	-0.18	17	10.5	1.45
-8	-12.5	0.05	5	-12.5	-0.33	17	15.5	-1.35
-8	-9.5	-1.32	5	-8.5	-1.64	17	20.5	-2.25
-8	-6.5	-2.55	5	-6.7	-1.35	21	-19.5	-3.00
-8	-3.5	-3.25	5	7	-1.90	21	-14.5	-1.20
-8	-2	-3.20	5	10.5	-1.60	21	-9.5	-0.45
-8	3.7	-4.35	5	14.5	-0.64	21	-4.5	0.56
-8	6.5	-3.88	5	18.5	-0.25	21	0.5	2.50
-8	9.5	-2.70	5	20	0.17	21	5.5	1.40
-8	12.5	-1.18	9	-17.5	-0.27	21	10.5	0.93
-8	15.3	0.25	9	-13.5	0.46	21	15.5	-1.73
-5	-14	0	9	-9.5	0.64	21	20.5	-1.47

Table E.12: Scour Pattern for Experimental Run E12
[Circular Island (d=15cm) with V-shaped deflector (4.5cm length) at F_r=0.16, h=15cm, L=30cm, θ=30°]

x(cm)	y(cm)	z(cm)	x(cm)	y(cm)	z(cm)	x(cm)	y(cm)	z(cm)
-32	-10	0	-10	13.5	-0.53	7	-4.5	-0.62
-32	-5	0	-10	15.3	0.25	7	5.5	-1.28
-32	0	0	-7	-15.1	0.10	7	9.5	-2.68
-32	5	0	-7	-11.5	-1.90	7	13.5	-1.40
-32	10	0	-7	-7.5	-3.63	7	17.5	-0.45
-31	-2.3	0	-7	-4	-4.77	7	20.5	-1.05
-31	0	-0.90	-7	4.9	-5.10	11	-19.5	-0.65
-31	2.2	0	-7	8.5	-3.90	11	-15.5	-0.59
-28	-3.7	0.05	-7	12.5	-2.15	11	-11.5	0.40
-28	-1.6	-1.05	-7	15.5	-0.63	11	-7.5	0.08
-28	1.7	-0.50	-4	-16	0.03	11	-3.5	0.48
-28	3	0.15	-4	-12.5	-1.85	11	0.5	1.17
-25	-4.1	0.15	-4	-8.5	-4.15	11	4.5	-0.79
-25	-1.8	-0.75	-4	-6.7	-5.00	11	8.5	-1.75
-25	0	0.05	-4	8	-5.25	11	12.5	-1.44
-25	3.1	0.43	-4	11.5	-3.15	11	16.5	-1.90
-20	-5.2	0.15	-4	15.5	-0.90	11	20.5	-0.51
-20	-1.5	0.15	-4	18.2	0.25	15	-19.5	-1.22
-20	2.5	-0.82	-1	-17	0.10	15	-15.5	0
-20	6.9	0.12	-1	-13.5	-1.53	15	-11.5	0.69
-14.5	-6.9	0.20	-1	-9.5	-3.92	15	-7.5	0.45
-14.5	-3.5	-0.60	-1	-8	-4.73	15	-3.5	1.50
-14.5	0.5	-0.83	-1	9	-5.00	15	0.5	0.83
-14.5	4.5	-0.97	-1	12.5	-2.93	15	4.5	0.19
-14.5	9.9	0.25	-1	16.5	-0.85	15	8.5	-0.65
-13	-9.2	0	-1	19.7	0.20	15	12.5	-0.13
-13	-5.5	-0.95	3	-17.9	0.15	15	16.5	-0.26
-13	-1.5	-1.65	3	-15.9	0.07	15	20.5	-1.18
-13	2.5	-1.75	3	-12.5	-1.37	20	-19.5	-1.80
-13	6.5	-1.30	3	-9.5	-3.05	20	-15.5	-1.59
-13	10.5	-0.63	3	-7.5	-3.55	20	-11.5	-0.55
-13	12.8	0.25	3	8.7	-4.13	20	-7.5	0.55
-10	-13.2	0.10	3	12.5	-2.55	20	-3.5	1.38
-10	-9.5	-1.57	3	16.5	-1.33	20	0.5	0.78
-10	-5.5	-2.83	3	20.5	-0.02	20	4.5	1.31
-10	-1.5	-3.55	7	-18.5	0.02	20	8.5	1.40
-10	2.5	-3.70	7	-14.5	-0.15	20	12.5	0.36
-10	6.5	-3.05	7	-10.5	-0.96	20	16.5	-0.55
-10	10.5	-1.92	7	-6.5	-1.58	20	20.5	-0.17

Table E.13: Scour Pattern for Experimental Run E13
[Circular Island (d=15cm) with V-shaped deflector (4.5cm length) at F_r=0.19, h=15cm, L=15cm, θ=60°]

x(cm)	y(cm)	z(cm)	x(cm)	y(cm)	z(cm)	x(cm)	y(cm)	z(cm)
-21	-10	0	-10	15.3	0.05	3	16.5	-1.88
-21	-5	0	-7	-18.5	-0.20	3	20.5	-1.25
-21	0	0	-7	-15.5	-1.50	7	-19.5	-2.65
-21	5	0	-7	-13.3	-2.55	7	-15.5	-4.10
-21	10	0	-7	-11.1	-2.18	7	-11.5	-3.00
-19	-5	0	-7	-7.5	-3.63	7	-7.5	-3.25
-19	-2.5	-1.20	-7	-4.2	-4.55	7	-4.7	-1.38
-19	0.5	-1.70	-7	5	-6.30	7	5.1	-1.40
-19	3.5	-0.82	-7	7.5	-5.35	7	8.5	-2.85
-19	6.1	0	-7	10.5	-3.60	7	12.5	-2.78
-16	-12.7	-0.05	-7	13.5	-2.08	7	16.5	-2.00
-16	-10.5	-0.65	-7	15.5	-0.82	7	20.5	-1.55
-16	-8.2	-0.20	-7	17.1	0.05	11	-19.5	-1.25
-16	-5.5	-1.55	-4	-19.3	-0.20	11	-15.5	-3.58
-16	-2.5	-2.80	-4	-16.5	-1.40	11	-11.5	-3.20
-16	0.5	-3.50	-4	-13.5	-2.58	11	-7.5	-2.65
-16	3.5	-2.60	-4	-10.5	-3.08	11	-3.5	-0.15
-16	6.5	-1.37	-4	-7.5	-4.80	11	0.5	0.97
-16	8.7	0.05	-4	-6.9	-4.88	11	4.5	-0.50
-13	-15.2	-0.15	-4	8.1	-6.10	11	8.5	-2.40
-13	-11.5	-2.15	-4	11.5	-3.90	11	12.5	-2.88
-13	-8.9	-1.30	-4	14.5	-2.22	11	16.5	-2.57
-13	-6.5	-2.08	-4	18.5	0.05	11	20.5	-1.35
-13	-2.5	-3.95	-1	-19.5	-0.70	15	-19.5	-0.92
-13	0	-2.65	-1	-16.5	-1.68	15	-14.5	-2.12
-13	3.5	-4.10	-1	-13.5	-2.65	15	-9.5	-1.47
-13	6.5	-2.60	-1	-10.5	-3.50	15	-4.5	-0.70
-13	9.5	-1.28	-1	-7.9	-4.90	15	0.5	1.05
-13	12.5	0.05	-1	9	-5.55	15	5.5	0.55
-10	-17.4	-0.15	-1	11.5	-4.20	15	10.5	-0.75
-10	-14.5	-1.37	-1	14.5	-2.58	15	15.5	-1.98
-10	-12.5	-2.40	-1	17.5	-0.95	15	20.5	-1.80
-10	-9.5	-1.65	-1	20.5	-0.10	19	-19.5	-0.50
-10	-6.5	-3.00	3	-19.5	-1.87	19	-14.5	-1.80
-10	-3.5	-4.05	3	-15.5	-2.95	19	-9.5	0.75
-10	-0.5	-3.18	3	-12.5	-2.55	19	-4.5	1.10
-10	2.5	-4.35	3	-9.5	-3.85	19	0.5	1.50
-10	5.5	-4.45	3	-7.5	-4.30	19	5.5	0.55
-10	8.5	-3.29	3	8.6	-4.45	19	10.5	-0.35
-10	11.5	-1.64	3	12.5	-3.50	19	15.5	-1.55

x(cm)	y(cm)	z(cm)	x(cm)	y(cm)	z(cm)	x(cm)	y(cm)	z(cm)
19	20.5	-1.55	23	-4.5	2.50	23	15.5	-1.00
23	-19.5	-0.05	23	0.5	0.90	23	20.5	-0.37
23	-14.5	0.35	23	5.5	1.00			
23	-9.5	2.42	23	10.5	-1.00			

Table E.14: Scour Pattern for Experimental Run E14
[Circular Island (d=15cm) with V-shaped deflector (4.5cm length) at F_r=0.19, h=18.75cm, L=15cm, θ=48°]

x(cm)	y(cm)	z(cm)	x(cm)	y(cm)	z(cm)	x(cm)	y(cm)	z(cm)
-22.5	-10	0	-6	-12.1	-0.06	8	11.5	0.26
-22.5	-5	0	-6	-9.5	-1.80	8	15.5	-0.55
-22.5	0	0	-6	-6.5	-3.64	8	17.5	-0.19
-22.5	5	0	-6	-5.1	-3.98	12	-19.5	-0.58
-22.5	10	0	-6	6.1	-4.95	12	-15.5	-1.48
-20	-1.5	0	-6	8.5	-3.74	12	-11.5	0.64
-20	0	-0.71	-6	11.5	-1.22	12	-7.5	0.96
-20	2	0	-6	13.1	0	12	-3.5	0.03
-17	-2.9	0.22	-3	-13.2	-0.13	12	1	1.89
-17	-1.7	-0.06	-3	-10.5	-1.99	12	4.5	-0.75
-17	0	0.35	-3	-8	-4.05	12	8.5	0.19
-17	2.5	-0.28	-3	-7.3	-4.63	12	12.5	0.71
-17	3.9	0.13	-3	8.5	-4.74	12	16.5	-1.95
-14	-5.3	0.06	-3	11.5	-1.90	12	20.5	-0.71
-14	-2.7	0	-3	14	-0.06	17	-19.5	-2.72
-14	0	0.32	0	-14	-0.19	17	-14.5	-1.69
-14	3.5	-0.55	0	-11.5	-1.48	17	-9.5	0.81
-14	6.1	0	0	-8.5	-3.64	17	-4.5	0.26
-12	-8.3	0	0	9	-3.86	17	1.5	2.70
-12	-5.5	-1.61	0	11.5	-1.97	17	6.5	0.28
-12	-2.5	-0.68	0	14.5	-0.03	17	10.5	0.13
-12	0.5	0.17	4	-15	-0.26	17	15.5	-2.40
-12	3.5	-1.48	4	-11.5	-0.58	17	20.5	-2.63
-12	6.5	-1.54	4	-8.5	-1.80	22	-19.5	-3.53
-12	9.3	-0.06	4	-7.5	-2.25	22	-14.5	-3.98
-9	-10.8	-0.06	4	8.5	-1.90	22	-9.5	-1.86
-9	-8.5	-1.37	4	12.5	-0.49	22	-4.5	0.32
-9	-5.5	-2.35	4	15.5	-0.26	22	0.5	2.57
-9	-2.5	-2.10	8	-15.5	-0.39	22	5.5	3.28
-9	0.5	-2.51	8	-11.5	0.19	22	10.5	-0.96
-9	3.5	-3.02	8	-7.5	-0.06	22	15.5	-3.60
-9	6.5	-3.21	8	-3.5	0.57	22	20.5	-2.76
-9	9.5	-1.54	8	3.5	-0.58			
-9	11.9	0.06	8	7.5	-0.58			

Table E.15: Scour Pattern for Experimental Run E15
[Circular Island (d=15cm) with V-shaped deflector (4.5cm length) at F_r=0.19, h=15cm, L=22.5cm, θ=40°]

x(cm)	y(cm)	z(cm)	x(cm)	y(cm)	z(cm)	x(cm)	y(cm)	z(cm)
-25	-10	0	-8	5.5	-4.00	5	14.5	-2.20
-25	-5	0	-8	8.5	-3.18	5	18.5	0.06
-25	0	0	-8	11.5	-1.82	9	-19.5	-0.65
-25	5	0	-8	13.5	-1.02	9	-15.5	-0.60
-25	10	0	-8	15.5	0.05	9	-11.5	-1.07
-23	-2.3	0	-5	-15	-0.30	9	-7.5	-0.86
-23	0	-1.25	-5	-12.5	-1.68	9	-3.5	0.38
-23	2.9	0	-5	-9.5	-3.05	9	0.5	1.73
-20	-3.7	0	-5	-6.1	-5.05	9	4.5	-0.17
-20	-1.5	-0.68	-5	7.2	-5.10	9	8.5	-0.68
-20	0	0.20	-5	9.5	-3.72	9	12.5	-0.78
-20	2.3	-0.55	-5	12.5	-2.60	9	16.5	-0.20
-20	3.9	0.05	-5	15.5	-0.88	9	20.5	-0.26
-17	-6.2	0	-5	16.9	0	13	-19.5	-0.86
-17	-3.5	-0.80	-2	-16.7	-0.35	13	-14.5	-0.88
-17	0	0.15	-2	-14.5	-1.50	13	-9.5	-0.42
-17	3.5	-0.40	-2	-11.5	-2.60	13	-4.5	0.36
-17	5.9	0	-2	-8.5	-4.20	13	0.5	1.00
-14	-8.5	-0.10	-2	-7.5	-4.70	13	5.5	0.35
-14	-5.5	-1.98	-2	8.8	-4.78	13	10.5	-0.77
-14	-2.5	-1.42	-2	11.5	-3.30	13	15.5	-0.04
-14	0.5	-1.18	-2	14.5	-2.18	13	20.5	-0.25
-14	3.5	-1.18	-2	17.5	-0.10	17	-19.5	-0.94
-14	6.5	-1.55	1	-19.5	-0.44	17	-14.5	-0.04
-14	9.3	0.05	1	-16.5	-1.76	17	-9.5	1.03
-11	-11	-0.15	1	-13.5	-2.15	17	-4.5	1.75
-11	-8.5	-1.45	1	-10.5	-2.85	17	0.5	1.14
-11	-5.5	-2.48	1	-7.9	-4.09	17	5.5	1.86
-11	-2.5	-3.15	1	8.5	-4.15	17	10.5	0.85
-11	0.5	-2.92	1	11.5	-3.00	17	15.5	0.84
-11	3.5	-1.52	1	14.5	-2.45	17	20.5	-0.66
-11	6.5	-2.30	1	17.5	-0.45	21	-19.5	-1.27
-11	9.5	-1.35	1	18.5	-0.14	21	-14.5	0.16
-11	12.8	0.10	5	-19.5	-1.57	21	-9.5	1.16
-8	-13.2	-0.30	5	-15.5	-1.38	21	-4.5	2.33
-8	-10.5	-1.60	5	-11.5	-2.04	21	0.5	1.44
-8	-7.5	-3.05	5	-7.5	-2.70	21	5.5	1.27
-8	-4.5	-4.22	5	-6.5	-2.28	21	10.5	0.84
-8	-2	-4.35	5	6.5	-2.24	21	15.5	-0.4
-8	2.7	-4.42	5	10.5	-2.04	21	20.5	-1.97

Table E.16: Scour Pattern for Experimental Run E16
[Circular Island (d=15cm) with V-shaped deflector (4.5cm length) at F_r=0.19, h=15cm, L=30cm, θ=30°]

x(cm)	y(cm)	z(cm)	x(cm)	y(cm)	z(cm)	x(cm)	y(cm)	z(cm)
-32	-10	0	-9	13.5	-0.65	7	-4.5	-0.76
-32	-5	0	-9	15.3	0.31	7	5.5	-1.57
-32	0	0	-6	-15.1	0.12	7	9.5	-3.28
-32	5	0	-6	-11.5	-2.32	7	13.5	-1.71
-32	10	0	-6	-7.5	-4.44	7	17.5	-0.55
-31	-2.3	0	-6	-4	-5.83	7	20.5	-1.28
-31	0	-1.10	-6	4.9	-6.24	11	-19.5	-0.79
-31	2.2	0	-6	8.5	-4.77	11	-15.5	-0.72
-28	-3.7	0.06	-6	12.5	-2.63	11	-11.5	0.49
-28	-1.6	-1.28	-6	15.5	-0.77	11	-7.5	0.10
-28	1.7	-0.61	-3	-16	0.04	11	-3.5	0.59
-28	3	0.18	-3	-12.5	-2.26	11	0.5	1.43
-25	-4.1	0.18	-3	-8.5	-5.08	11	4.5	-0.97
-25	-1.8	-0.92	-3	-6.7	-6.12	11	8.5	-2.14
-25	0	0.06	-3	8	-6.42	11	12.5	-1.76
-25	3.1	0.53	-3	11.5	-3.85	11	16.5	-2.32
-20	-5.2	-0.18	-3	15.5	-1.10	11	20.5	-0.62
-20	-1.5	-0.92	-3	18.2	0.18	15	-19.5	-1.49
-20	2.5	-1.00	0	-17	-0.35	15	-15.5	0
-20	6.9	0.15	0	-13.5	-1.87	15	-11.5	0.84
-16	-6.9	0.10	0	-9.5	-4.79	15	-7.5	0.67
-16	-3.5	-0.73	0	-8	-5.78	15	-3.5	1.83
-16	0.5	-1.02	0	9	-6.12	15	0.5	1.02
-16	4.5	-1.19	0	12.5	-3.58	15	4.5	0.23
-16	9.9	0.00	0	16.5	-1.04	15	8.5	-0.79
-12	-9.2	0	0	19.7	0.24	15	12.5	-0.16
-12	-5.5	-1.16	3	-17.9	0.18	15	16.5	-0.32
-12	-1.5	-2.02	3	-15.9	0.09	15	20.5	-1.44
-12	2.5	-2.14	3	-12.5	-1.68	20	-19.5	-2.20
-12	6.5	-1.59	3	-9.5	-3.56	20	-15.5	-1.94
-12	10.5	-0.77	3	-7.5	-4.76	20	-11.5	-0.67
-12	12.8	-0.31	3	8.7	-5.05	20	-7.5	0.67
-9	-13.2	0.12	3	12.5	-3.12	20	-3.5	1.69
-9	-9.5	-1.92	3	16.5	-2.05	20	0.5	0.95
-9	-5.5	-3.46	3	20.5	-0.02	20	4.5	1.60
-9	-1.5	-4.34	7	-18.5	0.02	20	8.5	1.71
-9	2.5	-4.53	7	-14.5	-0.18	20	12.5	0.44
-9	6.5	-3.73	7	-10.5	-1.17	20	16.5	-0.67
-9	10.5	-2.35	7	-6.5	-1.93	20	20.5	-0.21